SUMMARY REPORT ON THE PRELIMINARY DESIGN STUDIES OF AN ADVANCED GENERAL AVIATION AIRCRAFT

PREPARED FOR: NASA USRA ADVANCED DESIGN PROGRAM

PREPARED BY: RON BARRETT
                     SHANE DEMOSS
                     AB DIRKZWAGER
                     DARRYL EVANS
                     CHARLES GOMER
                     JERRY KEITER
                     DARREN KNIPP
                     GLEN SEIER
                     STEVE SMITH
                     ED WENNINGER

                     THE UNIVERSITY OF KANSAS
                     MAY 1991

TEAM LEADER: CHARLES GOMER

FACULTY ADVISOR: JAN ROSKAM

NASA ADVISOR: JACK MORRIS

ABSTRACT

The purpose of this report is to present the preliminary design results of the advanced aircraft design project at the University of Kansas. The goal of the project is to take a revolutionary look into the design of a general aviation aircraft. This project was conducted as a graduate level design class under the auspices of the KU/NASA/USRA Advanced Design Program in Aeronautics. The class is open to aerospace and electrical engineering seniors and first level graduate students.

Phase I of the design procedure (fall semester 1990) included the preliminary design of two configurations, a pusher and a tractor. The references listed in Section 1.1 of this report document this preliminary airframe design as well as other (more detailed) design studies, such as a pilot workload study, an advanced guidance and display study, a market survey, structural layout and manufacturing, and others.

Phase II (spring semester 1991) included the selection of only one configuration for further study. The pusher configuration was selected on the basis of performance characteristics, cabin noise considerations, natural laminar flow considerations, and system layouts. The design was then iterated to achieve higher levels of performance. Several of the more detailed studies were also continued through Phase II. Section 1.2 of this report contains a listing of all reports documenting the work completed in Phase II design.

This report specifically deals with the Phase II design studies. Reference 1.1.17 is a summary report on the Phase I design studies.

TABLE OF CONTENTS

LIST OF SYMBOLS

	Definition	Unit
A	Aspect Ratio	-----
B	Number of blades	-----
Cd	Airfoil drag coefficient	-----
Cl_{max}	Maximum lift coefficient	-----
Cp	Pressure coefficient	-----
Cp^*	Critical pressure coefficient	-----
C	Chord	ft/Inch
C_f	Flap Chord	-----
c_a	Aileron Chord	in
c_{ha_0}	Aileron Zero Lift Hinge Moment Coefficient	-----
$c_{ha_{\delta a}}$	Aileron Hinge Moment Coefficient due to a Aileron Deflection	-----
$c_{ha_{\delta t}}$	Aileron Hinge Moment Coefficient due to a Tab Deflection	-----
$c_{ha_{\alpha w}}$	Aileron Hinge Moment Coefficient due to wing Angle of Attack	-----
c_l	Lift Coefficient	-----
c_t	Tab Chord	in
c_{ht_0}	Tab Zero Lift Hinge Moment Coefficient	-----
$c_{ht_{\delta a}}$	Tab Hinge Moment Coefficient due to an Aileron Deflection	-----

$c_{h_t \delta_t}$	Tab Hinge Moment Coefficient due to a Tab Deflection	-----
$c_{h_t \alpha_w}$	Tab Hinge Moment Coefficient Due to Wing Angle of Attack	-----
D	Diameter	in
E	Endurance	hr
f	equivalent skin friction coefficient	
h	wave height	in
h_{crit}	gap length	in
H	Altitude	ft
$HM_{aActuator}$	Actuator Hinge Moment for the Aileron	-----
$HM_{tActuator}$	Actuator Hinge Moment for the Tab	-----
I	Angle of incidence	deg
I_{oa}	Aileron zero-lift Moment of Inertia	lb-s²-in
I_{ot}	Tab Zero-Lift Moment of Inertia	lb-s²-in
K	Boost Factor	-----
$K_{\delta_a spring}$	Spring Constant due to an Aileron Deflection	lb/in
$K_{\delta_t spring}$	Spring Constant for a Tab Deflection	lb/in
M	Mach Number	-----
M_{DR}	Drag Rise Mach number	-----

M_{CR}	Critical Mach number	-----
n,N	Rotational Speed	rpm
P	Power	hp
q	Dynamic Pressure	psf
R'	Unit Reynold's number	1/ft
R_{hcrit}	Critical height Reynold's number	-----
Re	Chord Reynolds number	-----
R_n	Reynold's number	-----
s_t	surface length to transition	in
S	Surface Area	ft^2
S	Wing Area	ft^2
S_{wf}	Flapped Wing Area	ft^2
t/c	Thickness to chord ratio	-----
V	Velocity	Kts or ft/sec
W	Weight	lbs
X	Distance between Spring	in
$(x/c)_{tr}$	X-position of transition relative to the chord	-----
$(x/c)_{sep}$	X-position of separation relative to the chord	-----
Y	Distance to Spring Setting	in
Y	Y-coordinate	Inch

Greek	Definition	Units
α	Angle of Attack	deg
δ	Deflection	deg
δ_a	Aileron Deflection	deg
δ_f	Flap deflection angle	deg
δ_t	Tab Deflection	deg
η_i	Inboard Flap position relative to Wing Half Span	-----
η_o	Outboard Flap position Relative to Wing Half Span	-----
ρ	Density	lb/ft^3
Θ	Linkage Angle	deg
μ	Friction Coefficient	-----
λ	wave length	in
Λ_{LE}	Wing leading edge sweep	deg
λ	Frequency	Hz or rad/sec

Subscripts	Definition
a	Aileron
ACQ	acquisition
c,C	canard
d,D	drag
DISP	disposal
e,E	elevator
E	Empty
F	Fuel
h,H	horizontal tail
l,L	lift
LE	leading edge
MAN	manufacturing
o	Zero-lift
OPS	operations

PL	Payload
r,R	rudder
t	Tab
TO	Takeoff
v,V	vertical tail
w	Wing
wet	wetted

Abbreviation	Description
ABT	Automatic Bus Transfer
AC	alternating current
ADF	Automatic Direction Finder
AE	Aerospace Engineer
AEO	All Engines Operating
AIM	Airman's Information Manual
APT	Advanced Personal Transport
Arall	Aramid-aluminum
ARTCC	Air Route Traffic Control Center
ATC	Air Traffic Control
AWG	American Wire Gauge
BITE	Built-in Test
C/A	Coarse/Acquisition
CAD	Computer Aided Drafting
CAT	Category
CG	Center of Gravity
CRT	Cathode Ray-Tube
DC	direct current
DEU	Drive Electronics Unit
DFAD	Digital Feature Analysis Data
DLMS	Digital Landmass Data
DME	Distance Measuring Equipment
DTED	Digital Terrain Elevation Data
EE	Electrical Engineer
ELT	Emergency Locator Transmitter
EMI	Electromagnetic Interference
ETE	Estimated Time Enroute
FAA	Federal Aviation Administration
FAR	Federal Aviation Regulations
FBL	Fly By Light
FBW	Fly By Wire
FEA	Finite Element Analysis
FOD	Foreign Object Damage
FS	Fuselage Station
FSS	Flight Service Station

FSW	Forward Swept Wing
GA	General Aviation
GCU	Generator Control Unit
GMU	Glareshield Mount Unit
GPS	Global Positioning System
HERF	High Energy Radio Frequencies
HOE	Holographic Optical Element
HSNLF	High Speed Natural Laminar Flow
HSNLF-3012	HSNLF Airfoil with Cl_{design} = 0.3 and t/c = 12%
HUD	Head-Up Display
IFR	Instrument Flight Rules
IGG	Imagined GPS/GLONASS
ILS	Instrument Landing System
INS	Inertial Navigation System
KU	University of Kansas
LCC	Life Cycle Cost
LCD	Liquid Crystal Display
LED	Light Emitting Diode
MAC	Mean Aerodynamic Chord
MTBF	Mean Time Between Failure
NAS	National Airspace System
NASA	National Aeronautics and Space Administration
NC-PVC	Non-contaminating Polyvinyl Chloride
NDB	Non-Directional Beacon
NLF	Natural Laminar Flow
OEI	One Engine Inoperative
PCA	Power, Control and Avionics
PCFS	Primary Flight Control System
RDTE	Research, Development, Testing, and Evaluation
SCR	silicon-controlled rectifier
SSSA	Separate Surface Stability Augmentation
TO	Takeoff
USRA	Universities Space Research Association
VFR	Visual Flight Rules
VOR	VHF Omnidirectional Ranging

STABILITY DERIVATIVES

Symbol	Definition	Dimension
C_{Du}	$\partial C_D/\partial(u/U_1)$	-
C_{Lu}	$\partial C_L/\partial(u/U_1)$	-
C_{mu}	$\partial C_m/\partial(u/U_1)$	-
C_{Txu}	$\partial C_{Tx}/\partial(u/U_1)$	-
C_{mTu}	$\partial C_{mT}/\partial(u/U_1)$	-
$C_{D\alpha}$	$\partial C_D/\partial\alpha$	rad^{-1}
$C_{L\alpha}$	$\partial C_L/\partial\alpha$	rad^{-1}
$C_{m\alpha}$	$\partial C_m/\partial\alpha$	rad^{-1}
$C_{mT\alpha}$	$\partial C_{mT}/\partial\alpha$	rad^{-1}
$C_{D\dot\alpha}$	$\partial C_D/\partial(\dot\alpha\ c/2\ U_1)$	rad^{-1}
$C_{L\dot\alpha}$	$\partial C_L/\partial(\dot\alpha\ c/2\ U_1)$	rad^{-1}
$C_{m\dot\alpha}$	$\partial C_m/\partial(\dot\alpha\ c/2\ U_1)$	rad^{-1}
$C_{Y\beta}$	$\partial C_Y/\partial\beta$	rad^{-1}
$C_{l\beta}$	$\partial C_l/\partial\beta$	rad^{-1}
$C_{n\beta}$	$\partial C_n/\partial\beta$	rad^{-1}
$C_{nT\beta}$	$\partial C_{nT}/\partial\beta$	rad^{-1}
$C_{Y\dot\beta}$	$\partial C_Y/\partial(\dot\beta\ b/2\ U_1)$	rad^{-1}
$C_{l\dot\beta}$	$\partial C_l/\partial(\dot\beta\ b/2\ U_1)$	rad^{-1}
$C_{n\dot\beta}$	$\partial C_n/\partial(\dot\beta\ b/2\ U_1)$	rad^{-1}
C_{Yp}	$\partial C_Y/\partial(p\ b/2\ U_1)$	rad^{-1}
C_{lp}	$\partial C_l/\partial(p\ b/2\ U_1)$	rad^{-1}
C_{np}	$\partial C_n/\partial(p\ b/2\ U_1)$	rad^{-1}
C_{Dq}	$\partial C_D/\partial(q\ c/2\ U_1)$	rad^{-1}
C_{Lq}	$\partial C_L/\partial(q\ c/2\ U_1)$	rad^{-1}
C_{mq}	$\partial C_m/\partial(q\ c/2\ U_1)$	rad^{-1}
C_{Yr}	$\partial C_Y/\partial(r\ b/2\ U_1)$	rad^{-1}
C_{lr}	$\partial C_l/\partial(r\ b/2\ U_1)$	rad^{-1}
C_{nr}	$\partial C_n/\partial(r\ b/2\ U_1)$	rad^{-1}

CONTROL DERIVATIVES

Symbol	Definition	Dimension
$C_{D\delta e}$	$\partial C_D/\partial\delta e$	rad^{-1}
$C_{L\delta e}$	$\partial C_L/\partial\delta e$	rad^{-1}
$C_{m\delta e}$	$\partial C_m/\partial\delta e$	rad^{-1}
$C_{D\delta c}$	$\partial C_D/\partial\delta c$	rad^{-1}
$C_{L\delta c}$	$\partial C_L/\partial\delta c$	rad^{-1}
$C_{m\delta c}$	$\partial C_m/\partial\delta c$	rad^{-1}
$C_{Y\delta a}$	$\partial C_Y/\partial\delta a$	rad^{-1}
$C_{l\delta a}$	$\partial C_l/\partial\delta a$	rad^{-1}
$C_{n\delta a}$	$\partial C_n/\partial\delta a$	rad^{-1}
$C_{Y\delta r}$	$\partial C_Y/\partial\delta r$	rad^{-1}
$C_{l\delta r}$	$\partial C_l/\partial\delta r$	rad^{-1}
$C_{n\delta r}$	$\partial C_n/\partial\delta r$	rad^{-1}

1. INTRODUCTION

The purpose of this report is to document the Phase II design studies of the Advanced Personal Transport (APT) pusher configuration. This project was conducted at The University of Kansas under the auspices of the KU/NASA/USRA Advanced Design Program in Aeronautics. The design process was broken into two phases:

Phase I - AE 621 (fall semester 1990)
>   pilot workload study
>   market survey
>   determination of mission specifications
>   preliminary design of two configurations, a pusher and a tractor.
>   design of natural laminar flow (NLF) airfoils
>   preliminary design of a fly-by-wire, decoupled response flight control
>   system
>   aircraft system layouts
>   advanced guidance and display study
>   structural layout and manufacturing of the wing and fuselage
>   investigation into smart structures
>   maintenance and repairability
>   design, construction, and testing of an iron bird

Phase II - AE 622 (spring semester 1991)
>   selection of one configuration and reiteration of airframe design
>   continued research and study in the following areas:
>>   advanced guidance and display
>>   primary flight control system design
>>   iron bird
>>   electrical system design considerations
>>   maintenance and repairability
>>   manufacturing and cost
>>   structural analysis

All of the reports documenting the work completed in Phase I are shown in Section 1.1, and a similar list for Phase II is shown in Section II.

This report contains a brief summary of the Phase I configuration designs and a summary of the Phase II design studies.

1.1 Reference List of Phase I Design Reports

This section contains a listing of all reports documenting Phase I design work.

1.1.1   Burgstahler, Huffman, Ryan, _Market Survey Report for the Advanced Personal Transport_, The University of Kansas, 11 September 1990.

1.1.2 Axmann, Knipp, Roper, Wenninger, <u>Pilot Work Load Study</u>, The University of Kansas, 20 September 1990.

1.1.3 Hoffmann, Rodkey, Roper, <u>Advanced Guidance and Display Study</u>, The University of Kansas, 30 November 1990.

1.1.4 Axmann, Knipp, <u>Equipment List for Typical Aircraft and Proposed APT</u>, The University of Kansas, 4 October 1990.

1.1.5 Burgstahler, Huffman, <u>Mission Specification for the Advanced Personal Transport</u>, The University of Kansas, 20 September 1990.

1.1.6 Barrett, et. all., <u>Preliminary Design of Two Configurations</u>, The University of Kansas, 15 December 1990.

1.1.7 Anderson, Jackson, <u>Loads Analysis of the Advanced Personal Transport</u>, The University of Kansas, 4 December 1990.

1.1.8 Chronister, Jackson, <u>Fuselage Design and Manufacturing Study</u>, The University of Kansas, 4 December 1990.

1.1.9 Bauguess, Weiss, <u>Wing Layout, Design and Manufacturing Tolerances of the Advanced Personal Transport</u>, The University of Kansas, 12 December 1990.

1.1.10 Hoffmann, Wu, <u>Electrical System Design Considerations for the Advanced Personal Transport</u>, The University of Kansas, 20 November 1990.

1.1.11 Dreiling, Weiss, <u>Results of Investigation into the Use of Smart Structures for the Advanced Personal Transport</u>, The University of Kansas, 4 December 1990.

1.1.12 Shumate, Woolpert, <u>Primary Flight Control System Study</u>, The University of Kansas, December 1990.

1.1.13 Axmann, Knipp, <u>System Layouts for the Advanced Personal Transport</u>, The University of Kansas, 30 November 1990.

1.1.14 Bauguess, Lawson, Woolpert, <u>Maintenance and Repairability Study</u>, The University of Kansas, 13 November 1990.

1.1.15 Dirkzwager, Schlatter, <u>Natural Laminar Flow Airfoil Design for the Advanced Personal Transport</u>, The University of Kansas, 9 November 1990.

1.1.16 Barrett, Chronister, <u>Design, Construction, and Test of the Iron Bird</u>, The University of Kansas, 11 December 1990.

1.1.17 Gomer, et. al., <u>Preliminary Design Studies of an Advanced General Aviation Aircraft</u>, The University of Kansas, 21 December 1990.

<u>1.2 Reference List of Phase II Design Reports</u>

This section contains a listing of all reports documenting Phase II design work.

1.2.1 Evans, Demoss, <u>Electrical System Report for the Advanced Personal Transport</u>, The University of Kansas, April 1991.

1.2.2 Knipp, Dirkzwager, <u>Manufacturing Plan and Cost Analysis for the Advanced Personal Transport Pusher Configuration</u>, The University of Kansas, May 1991.

1.2.3 Dirkzwager, <u>Structural Design of the Advanced Personal Transport Pusher Configuration</u>, The University of Kansas, May 1991.

1.2.4 Knipp, Keiter, Demoss, <u>Advanced Guidance and Display Study for the Advanced Personal Transport</u>, The University of Kansas, April 1991.

1.2.5 Barrett, et. al., <u>Design, Construction, Test and Evaluation of an Aileron-Servotab Iron Bird</u>, The University of Kansas, May 1991.

1.2.6 Barrett, et. al., <u>Preliminary Airframe Design for the Advanced Personal Transport Pusher Configuration</u>, The University of Kansas, May 1991.

1.2.7 Wenninger, et.al., <u>Preliminary Airframe Design for the Advanced Personal Transport</u>, The University of Kansas, May 1991.

1.2.8 Evans, Smith, Wenninger, <u>Maintenance and Repairability Study for the Advanced Personal Transport</u>, The University of Kansas, May 1991.

2. PRESENTATION OF PHASE I DESIGNS

The purpose of this chapter is to discuss the configuration selection and final Phase I layouts of the APT pusher and tractor configurations. This section provides a general summary of the material discussed in Reference 2.1.

2.1 DESCRIPTION OF THE PUSHER APT CONFIGURATION

A twin boom three surface configuration was selected for the pusher APT layout. Some of the advantages of this configuration include:

* Provides a high degree of structural synergism by allowing the aft pressure bulkhead, wing carry-through mount, and main landing gear mount to form one integral fail-safe unit.

* Recent research (References 2.2 and 2.3) has shown that, for the same basic geometry, three surface configurations typically have a higher trimmed L/D than either conventional or canard configurations. The research has also shown that three surface layouts can have lower trim drag over a wider center of gravity range than do two surface layouts.

* Flap-induced pitching moments can be automatically trimmed by incorporating a flap on the canard that is "geared" to wing flap deflection.

A three-view and table of geometry of the final Phase I design is shown in Figure 2.1 and the fuselage layout is shown in Figure 2.2. One of the primary features of this layout is that it was designed to attain a high extent of natural laminar flow (NLF). All flying surfaces utilize NLF airfoils, and the fuselage features a pusher propeller and smooth NLF forward fuselage. The wing is swept forward 15° (measured at the leading edge), and features a mid-wing location to decrease fuselage interference drag. A strake is incorporated at the wing root for the following reasons:

* To stiffen the wing root against the high torsional loads inherent with forward swept wings.

* Provide local strengthening for tail boom support.

* Increase available fuel volume.

The horizontal tail was located at the top of the vertical tails to place it above the propeller slipstream, which reduces structural noise and fatigue and should allow attainment of NLF on the tail surface. Ventral fins mounted on the tail booms insure against prop strikes if the airplane is over-rotated.

Engine air is provided by twin inlets located on each side of the airplane underneath the wing, with each inlet independently feeding one engine. This arrangement provides an essential

Table of Geometry of the Pusher APT Configuration

	Wing	Horiz. Tail	Canard	Vert. Tail
Area	156.9 ft²	31.7 ft²	8.0 ft²	38.6 ft²
Span	43.4 ft	11.9 ft	7.8 ft	6.5 ft
Aspect Ratio	12.0	4.5	3.8	1.1
Sweep Angle	-15° (@ L.E.)	0°	0° (@ 0.10c)	40° (@ L.E.)
M.A.C.	4.00 ft	2.6 ft	1.00 ft	4.2 ft
Taper Ratio	0.35	1.0	0.70	0.40
Dihedral Angle	3°	0°	-5°	90°
Incidence Angle	1.0°	0°	3.0°	0°
Twist Angle	0°	0°	0°	0°
Airfoil	Custom NLF Section	"	"	"
Thickness Ratio	0.13	0.09	0.11	0.09
Control Surf. Chord Ratio	0.25	0.30	N/A	0.32
Control Surf. Span Ratio	0.72 - 1.00	0 - .98	N/A	0.20 - 0.85
Flap Chord Ratio	0.25	N/A	0.35	N/A
Flap Span Ratio	0.19 - 0.72	N/A	0.21 - 1.00	N/A

	Cabin	Fuselage	Overall
Length	11.17 ft	29.33 ft	34.75 ft
Max. Height	4.67 ft	5.42 ft	9.92 ft
Max. Width	4.58 ft	4.92 ft	43.40 ft
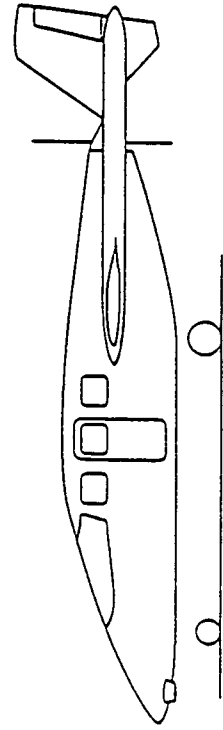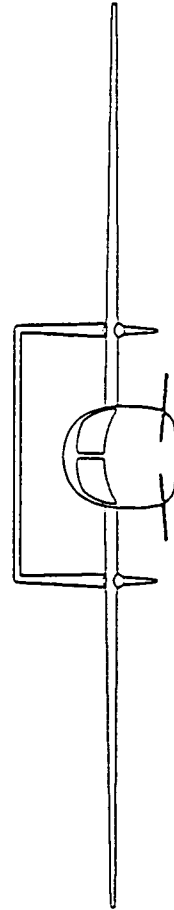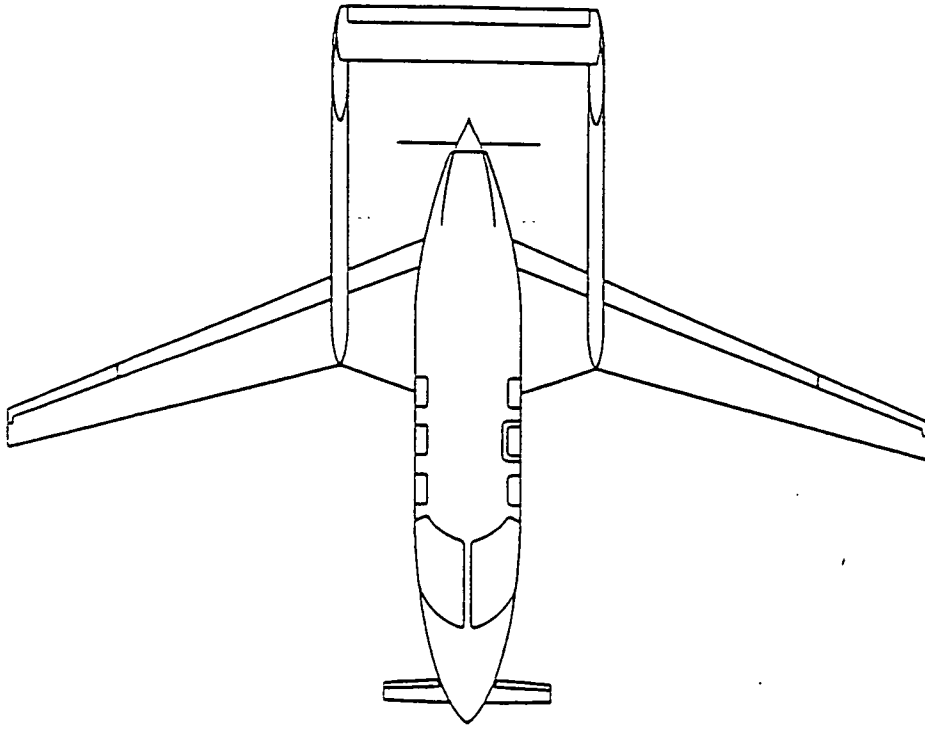
Figure 2.1: Phase I Pusher APT Configuration

SCALE: 1/100

EMERGENCY EXIT

A.C.

CABIN DOOR

INLETS

CANARD TORQUE BOX

WING TORQUE BOX

ENGINE EXHAUST
(ALSO PROP. DE-ICE)

AFT WING MOUNT/
FIREWALL

AFT PRESSURE
BULKHEAD

FORWARD PRESSURE
BULKHEAD

WEATHER RADAR
(12 IN. DISH)

AIRSTAIR DOOR
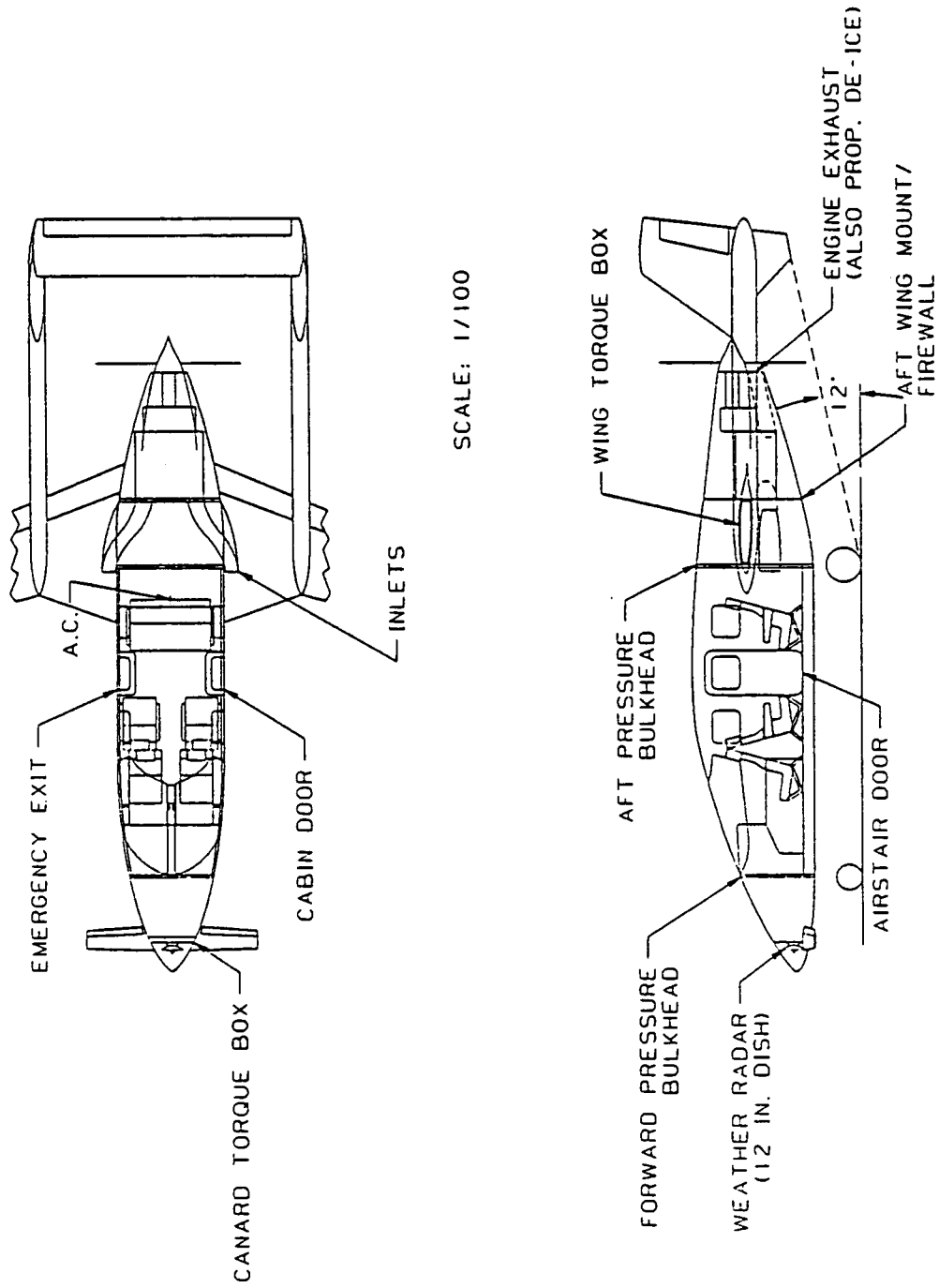
Figure 2.2: Fuselage Layout of the Phase I Pusher APT Configuration

6

measure of redundancy, since if a bird or piece of ice is ingested by one inlet, it will only affect one engine and not both. A combined single exhaust is directed straight aft, which offers the advantage that the hot exhaust gases can provide simple propeller de-icing. A standard retractable tricycle landing gear arrangement was selected, with the nose gear retracting forward into the nose and the fuselage-mounted main gear retracting aft into the area underneath the wing and inlets. Cabin access is provided by an air-stair door on the left fuselage, which is a convenient feature usually found only on larger turboprops and business jets.

2.2 DESCRIPTION OF THE TRACTOR APT CONFIGURATION

A conventional configuration was selected for the tractor APT layout. Some of the advantages of this layout include:

* Good balance and flexible wing placement.

* Low development costs due to the extensive database of similar airplanes.

A three-view and table of geometry of the final Phase I design is shown in Figure 2.3 and the fuselage layout is shown in Figure 2.4. As can be seen, the layout is rather conventional and is similar to many popular general aviation airplanes.

To allow a fair comparison with the pusher APT configuration, the tractor configuration utilizes the same cabin layout and wing geometry. A low wing arrangement was selected to allow the wing carry-through structure to pass under the cabin and to allow simple wing-mounted landing gear. A T-tail arrangement was used to remove the horizontal tail from the turbulence of the fuselage and propwash, which can allow a small reduction in tail area and should allow attainment of NLF on the tail surface. A standard retractable tricycle landing gear arrangement was selected, with the nose gear retracting underneath the engine and the main gear retracting into the wing. Cabin access is achieved by first stepping up onto the wing and then entering a side-hinged door located on the left side of the fuselage.

Unlike the pusher configuration, there was no practical place in the fuselage of the tractor configuration to mount the weather radar. Consequently, the radar was mounted in a pod on the left wing, similar in arrangement to that of the Cessna P-210 Centurion.

2.3 CABIN LAYOUT

The cabin layout of the APT was sized by comparison with similar current general aviation airplanes, and the final layout is shown in Figure 2.5. The cabin dimensions selected for the APT are relatively large compared to similar airplanes for the following reasons:

* Current small general aviation airplanes are not known for cabin comfort. To improve marketability, the cabin of the APT was designed to ease this problem as much as practical, without causing undue weight or drag penalties.

7

Table of Geometry of the Tractor APT Configuration

	Wing	Horiz. Tail	Vert. Tail
Area	151.7 ft²	36.4 ft²	27.3 ft²
Span	42.7 ft	12.8 ft	5.6 ft
Aspect Ratio	12.0	4.5	1.2
Sweep Angle	-15° (@ L.E.)	9° (@ L.E.)	40° (@ L.E.)
M. A. C.	3.89 ft	2.87 ft	5.7 ft
Taper Ratio	0.35	0.7	0.40
Dihedral Angle	3°	0°	90°
Incidence Angle	1.0°	0°	0°
Twist Angle	0°	0°	0°
Airfoil	Custom NLF Section	"	"
Thickness Ratio	0.13	0.09	0.09
Control Surf. Chord Ratio	0.25	0.30	0.32
Control Surf. Span Ratio	0.72 - 1.00	0 - .98	0.20 - 0.85
Flap Chord Ratio	0.25	N/A	N/A
Flap Span Ratio	0.19 - 0.72	N/A	N/A

	Cabin	Fuselage	Overall
Length	11.17 ft	29.33 ft	34.75 ft
Max. Height	4.67 ft	5.42 ft	9.92 ft
Max. Width	4.58 ft	4.92 ft	43.40 ft

Figure 2.3: Phase I Tractor APT Configuration

8

A.C.

EMERGENCY EXIT

CABIN DOOR

INLET DUCTS

EXHAUST

WEATHER RADAR POD

SCALE: 1/100

AVIONICS/ELECTRONICS BAY
(REQ'D FOR BALANCE)

AFT PRESSURE
BULKHEAD

FORWARD PRESSURE
BULKHEAD

15'
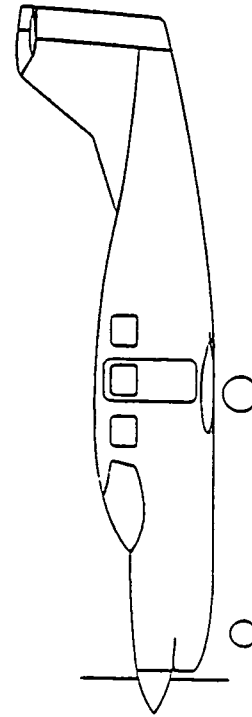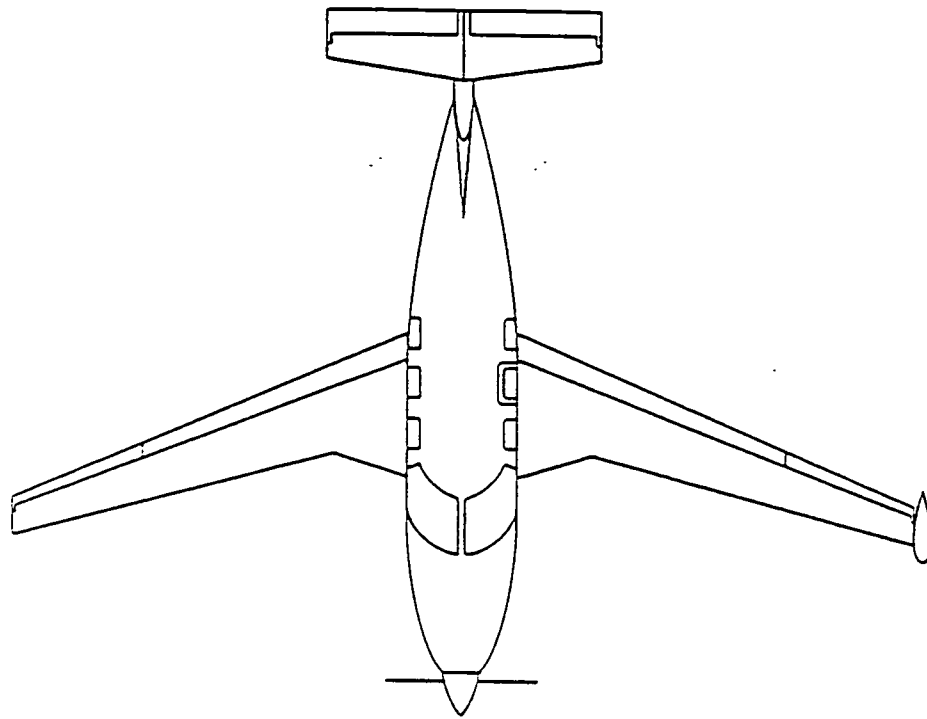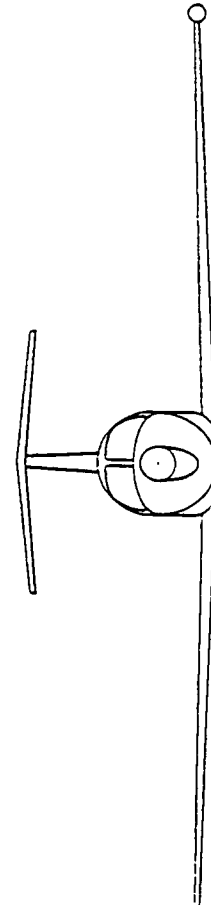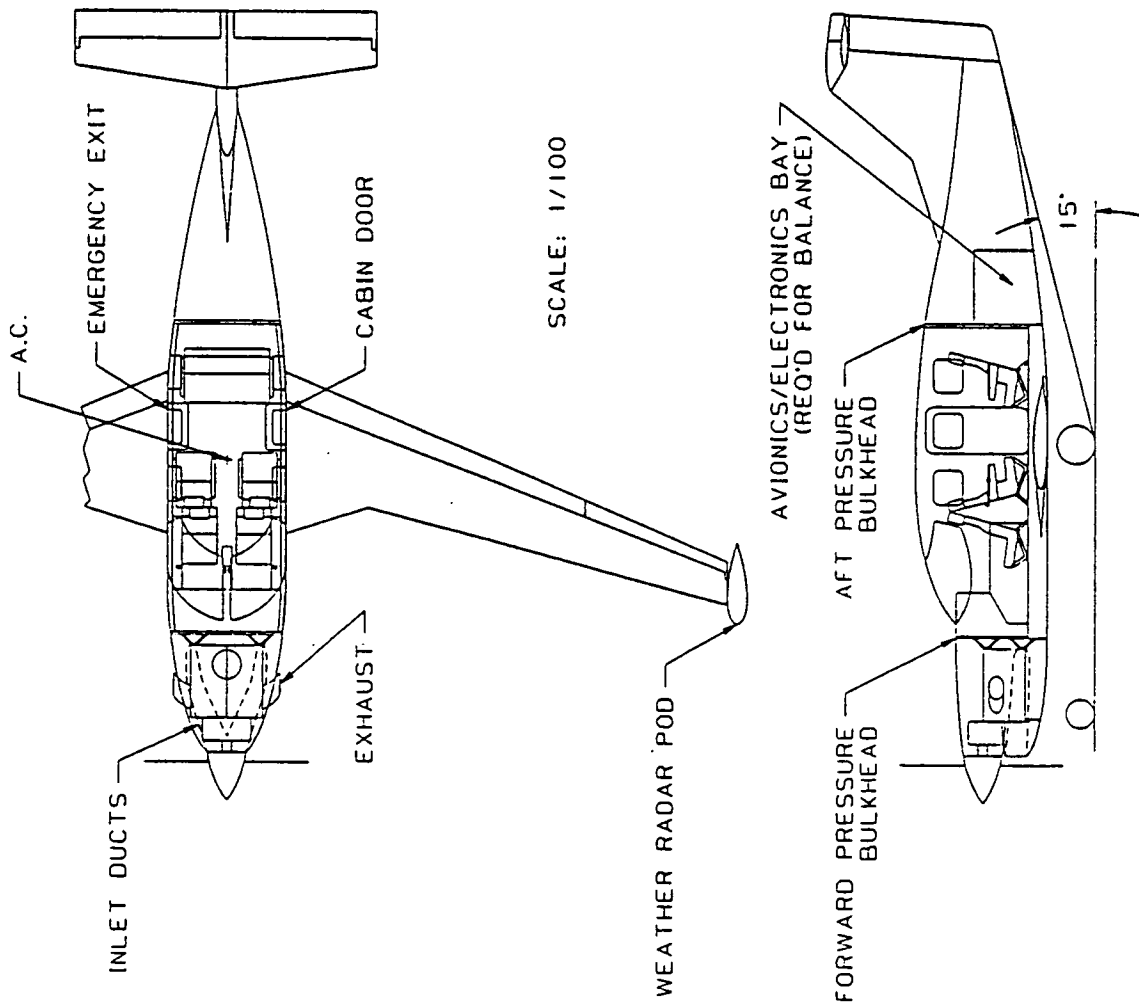
Figure 2.4: Fuselage Layout of the Phase I Tractor APT Configuration

9
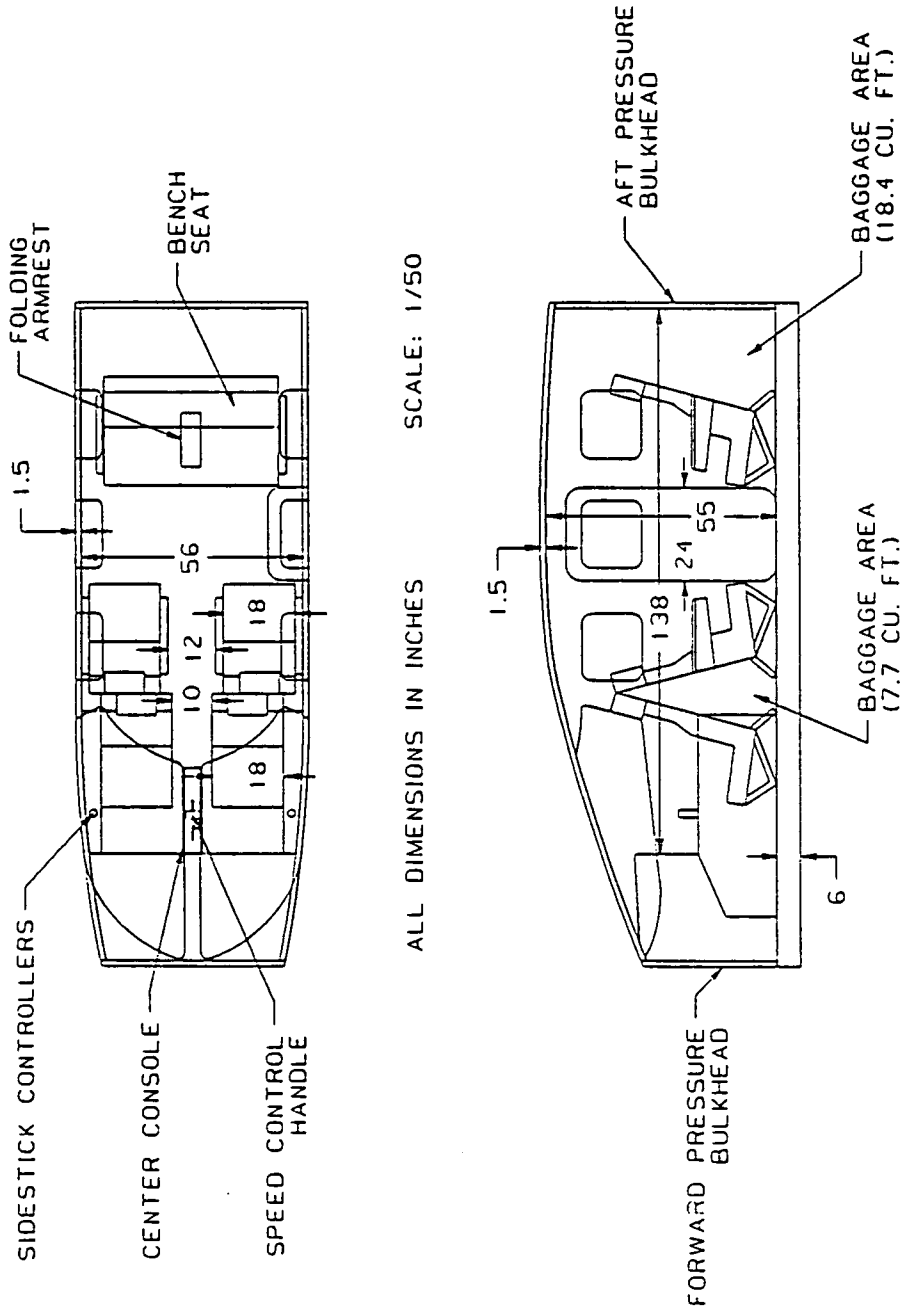
Figure 2.5: APT Cabin Layout

SCALE: 1/50

ALL DIMENSIONS IN INCHES

10

* The rather long range specified in the mission requirements results in long flight times, and a comfortable cabin is very desirable for long flights.

The fuselage cross section of the APT is shown in Figure 2.6, and features a circular upper and a rounded square lower cross section. This arrangement was selected as being a compromise between the structural efficiency of a fully circular cross section and the low wetted area and volume penalties of a fully square cross section.

A pictoral illustration of the proposed APT cockpit layout is shown in Figure 2.7. The layout features two sidestick controllers, one on each side of the cabin, and a center console containing the speed control handle. Due to the high degree of automation in the flight control system, neither rudder pedals, brake pedals, flap handles, or landing gear handles are required (Reference 2.4). The layout features a HUD (heads up display) projected directly onto the windshield and a single CRT (cathode ray tube) touch screen. The CRT will display all required systems information and will also be used for data entry, hence no other instruments or separate data entry devices are required in the cockpit. One interesting feature of this cockpit arrangement is that it allows incorporation of a sliding table or tray, which can be slid out from under the control panel to hold aeronautical charts, maps, or even drinks.

2.4 PERFORMANCE

The performance capabilities of both configurations of the APT are shown in Table 2.1. Table 2.1 also compares the APT configurations with the primary competitors: the Piaggio P-180, the TBM-700, and the Beech Starship. The APT meets or nearly meets all of the requirements defined in the mission specification, except for the cruise speed and maximum range. This could demand the resizing of the entire aircraft. The APT configurations compare favorably with the competitors in Table 2.1.

2.5 REFERENCES FOR CHAPTER 2

2.1 Barrett, et. al., Preliminary Design of Two Configurations, The University of Kansas, December 1990.

2.2 Kendall, E.R., The Minimum Induce Drag, Longitudinal Trim and Static Longitudinal Stability of Two-Surface and Three-Surface Airplanes, AIAA Report 84-2164.

2.3 Selberg, B.P., Analytical Study of Three-Surface Lifting Systems, NASA TN 850866.

2.4 Shumate, Woolpert, Primary Flight Control System Study, The University of Kansas, December 1990.

11

55 IN.
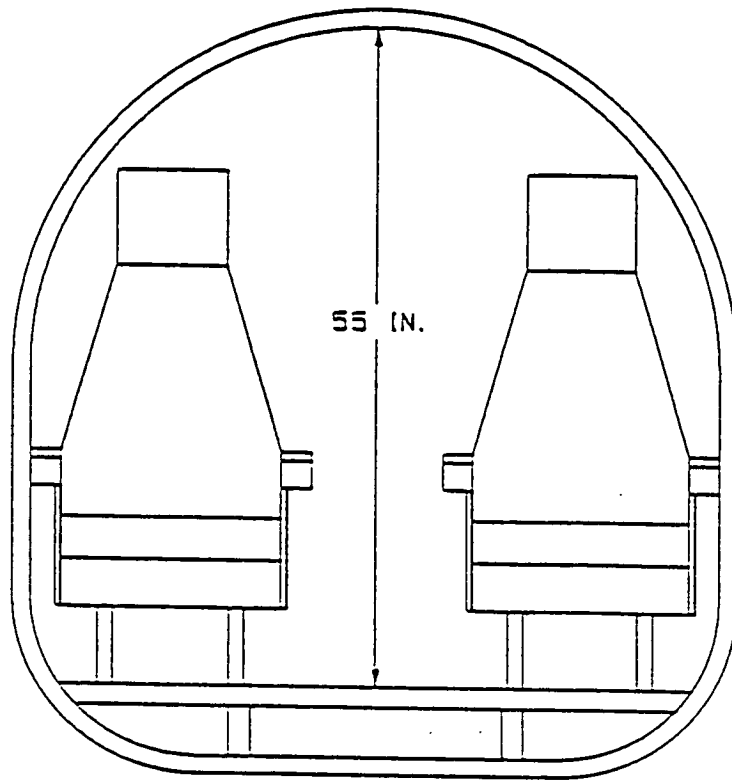
Figure 2.6: Cabin Cross Section

NOT TO SCALE

HEADS UP DISPLAY

CRT/TOUCH SCREEN

AVIONICS ACCESS PANELS

SIDESTICK CONTROLLERS
(BOTH SIDES)

SLIDING TABLE
(BOTH SIDES)

MASTER START W/KEY

OPTICAL DISK DRIVES (2)

TURN HOLD SWITCH

CLIMB HOLD
SWITCH

SPEED CONTROL
HANDLE

APT
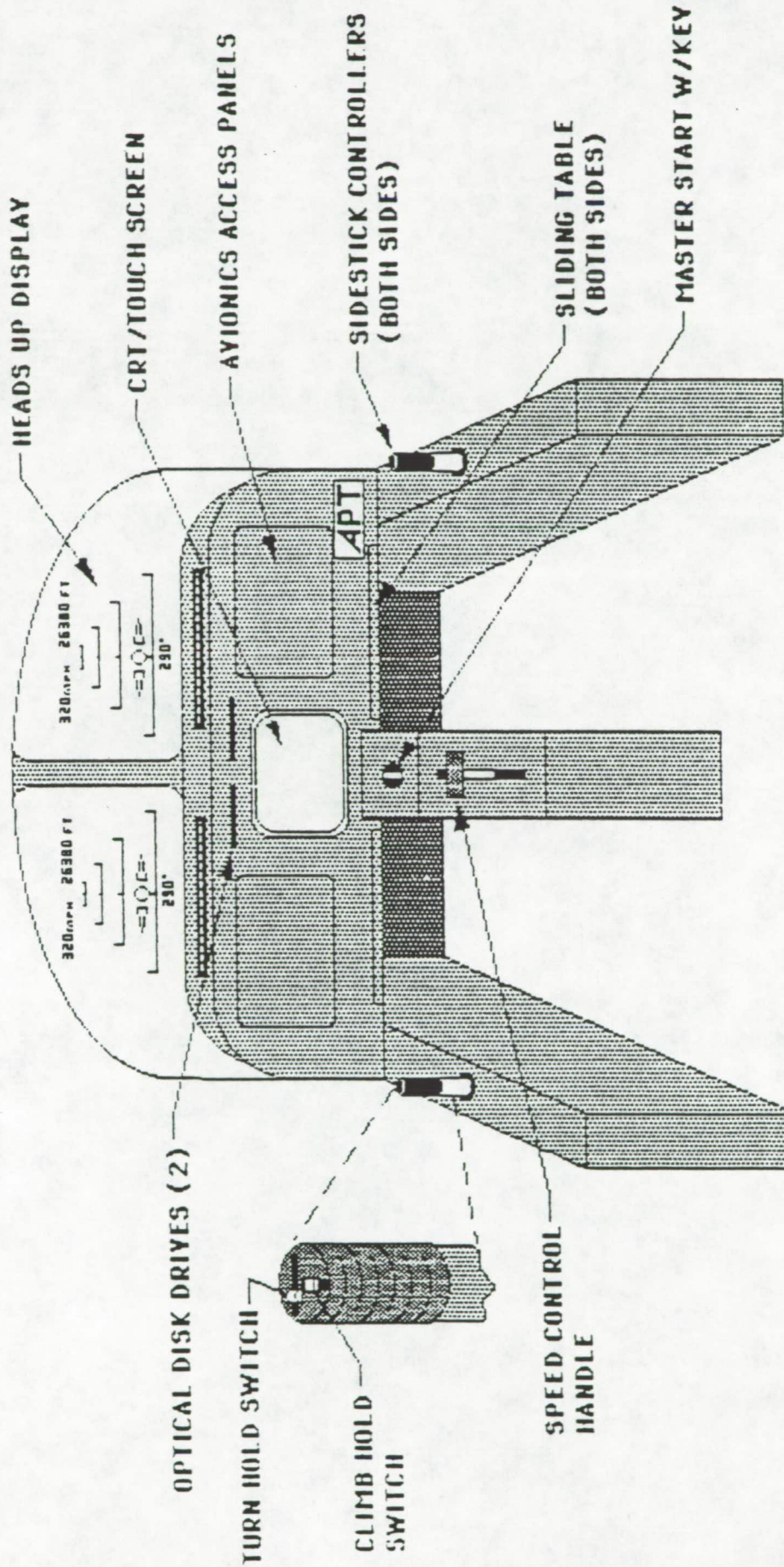
Figure 2.7: Proposed APT Cockpit Layout

13

Table 2.1 Comparison of the APT with the Competition

	APT PUSHER	APT TRACTOR	Socata/Mooney TBM-700	BEECH STARSHIP	PIAGGIO P - 180
WEIGHTS					
Maximum Takeoff wt. (lbs)	6325	6250	6510	14400	10510
Standard empty wt.(lbs)	3760	3660	3637	10320	6700
Maximum useful load (lbs)	2800	2800	2646	4280	3810
Maximum wing loading (psf)	40.3	41.2	32.2	51.3	61.95
PERFORMANCE					
T.O. Fieldlength (ft) [sls,isa]	1870	2050	1936	3280	2415
Maximum climb rate (fpm)	4300	4650	2380	3100	3650
Best climb rate speed (kts)	260	243	123	180	160
Clean stall speed (kts)	76	77	75	99	105
Landing stall speed (kts)	60	63	61	84	82
Service ceiling (ft)	45000	44000	30000	41000	41000
Normal cruise speed (kts)	310	300	282	270	320
at altitude of (ft)	45000	44000	30000	35000	41000
High speed cruise (kts)	360	350	300	335	400
at altitude of (ft)	25000	25000	26000	22000	27000
Fuel flow for:					
Normal cruise (lbs/hr)	323	330	312	---	460
High speed cruise (lbs/hr)	708	700	320	984	860
Maximum range (nm)	945	930	1000	1450	1800

3. PHASE I DESIGN DIFFICULTIES

The purpose of this chapter is to discuss the design difficulties encountered in Phase I design. The discussion will be limited to those aspects that pertain specifically to the airframe design of the pusher configuration. The design difficulties are summarized in the following list.

* The APT does not meet the maximum speed and range requirements. A possible solution is the reiteration of the design at a higher wing loading and a resized powerplant installation.

* Early in the design process, a twin inlet arrangement was selected for the pusher APT configuration, with one inlet located under each wing root. Later propulsion integration studies suggested an arrangement using a single inlet mounted on the top of the fuselage. The top mounted inlet would also be advantageous from a foreign object damage (FOD) perspective.

* The aft end of the fuselage needs to grow to accommodate the dual Garrett engine and Soloy Twin Pack configuration.

* In Phase I design of the fuselage, the shaping of the forward fuselage for laminar flow was only estimated by comparison with similar designs.

* The APT does not fulfill all of the Level 1 flying quality requirements.

* The APT is too stable in the spiral mode for the power approach flight condition.

* The dutch roll in cruise flight does not satisfy the requirements for Level 1 flight. By increasing the vertical tail area slightly the APT will satisfy this requirement.

* It is a concern that the wing will not allow adequate volume for complete fuel storage. This needs to be verified.

* Further research needs to be done in the area of de-/anti-icing, specifically maintenance considerations.

4. ADVANCED GUIDANCE AND DISPLAY

This chapter documents the design considerations for the guidance and display system in an Advanced Personal Transport. The chapter begins with an in depth look into possible navigation systems. The types looked at are the Global Positioning System (GPS), differential GPS, Inertial Navigation Systems (INS), and an integrated system combining all of these. The advantages and disadvantages of each system are studied, with the most appropriate system being chosen in the end.

The HUD will be introduced in the next section. What the HUD is and its justification are discussed. The following section will show what is on the HUD and the display screen during flight. Both normal flight and emergency flight situations will be shown.

4.1 NAVIGATION

The purpose of this section is to discuss the navigation system that will be used in the APT Pusher. The systems that will be studied are the Global Positioning System (GPS), differential GPS, Inertial Navigation Systems (INS), and an integrated GPS/INS system. It will be shown that an integrated system would be most appropriate for the APT.

4.1.1 Global Positioning System

The Global Positioning System consists of a constellation of 21 satellites. Each satellite transmits two kinds of data, almanac and ephemeris. Almanac data describes were each satellite should be at any given moment. Ephemeris data provides precise orbital correction factors to account for the gravitational tug of war exerted on the satellite by the earth, sun, and moon. Data is transmitted at a rate of 50 bits/sec over channel L1, which is 1575.42 MHz. The GPS receiver decodes these signals and can compute the aircrafts latitude, longitude, and altitude.

Although GPS is a potentially lightweight and accurate navigation system, there are some problems that make it inappropriate for sole means of navigation. These problems are listed and will be discussed below.

1. Satellite clock synchronization errors
2. Error introduced in ionosphere
3. Satellite lock in time error
4. Blockage by terrain or fuselage
5. Spatiotemporal gaps in coverage.

GPS operates on the satellite ranging principle, which uses time as a measure of distance. The GPS receiver decodes the satellite signals and computes the aircrafts latitude, longitude, and altitude, based on the assumption that its clock is exactly synchronized with the clock of the satellite. The clocks; however, are generally not synchronized exactly. This error in time leads to a distance error of approximately 1.5 meters.

The ionosphere is the part of the earth's atmosphere that extends from about 25 miles out to about 250 miles. It contains free electrically charged particles. As the satellite signal passes through the ionosphere, a position error of approximately 4 meters occurs.

As a vehicle equipped with GPS travels, some satellites will drop out of sight as others move into sight. The receiver will drop a disappearing satellite and lock on to the one coming into sight. At the instant that a satellite is locked, there is a noise error that is approximately 1 meter. This error is reduced by the square root of t, were t is time in seconds. For example, after 100 seconds of maintaining a lock on a satellite, the error is reduced by 10. A 1 meter error is then reduced to .1 meter. The noise reduction then further improves with time.

Blockage by terrain is mainly a problem when the receiver is locked on to a satellite that is close to the horizon and a mountain obscures its reception. The more troublesome problem is blockage by the fuselage during a turn. If the aircraft experiences a 30 degree bank turn, 3-D coverage could be obscured up to a minute. When the satellites are recovered the error discussed in the previous section, lock in error, will be present.

Even after GPS is fully operational, there will still be times of the day where areas of the world are not in the line of sight of four satellites. A minimum of four satellites are required for the receiver to compute latitude, longitude, and altitude. Although this loss of 3-D coverage may not be critical in cruise, if 3-D coverage was lost during the landing phase of flight it would cause serious problems.

4.1.2 Differential GPS

Differential GPS is a system designed to enhance GPS by eliminating some of the errors associated with GPS. The base station, which is at a known position on the ground, receives the broadcasted data from the satellites. It then computes the satellite orbital estimation errors and clock synchronization errors. These corrections are then sent to the aircraft's GPS receiver for more accurate position determination. With the corrections sent by the base station, the GPS receiver can calculate position to within 1-2 meters.

GPS problems 1 and 2, (satellite clock synchronization errors and errors introduced in ionosphere) are eliminated by differential GPS. However; problems 3-5 (lock in time error, blockage by terrain or fuselage, and spatiotemporal gaps in coverage) are not effected by differential GPS. Since these problems cannot be corrected by differential GPS, another means of navigation must be found.

4.1.3 Inertial Navigation System

Inertial navigation is a dead reckoning method of navigation based on the integration of acceleration to determine velocity and the integration of velocity to obtain position. Three orthogonally mounted accelerometers measure the acceleration and three orthogonally mounted gyroscopes measure the aircrafts angular velocity. The INS does not require external commun-

ications or inputs during the measurement process, thus it is referred to as a self contained system.

Various instrument errors, initial state errors, and inaccuracies in the gravity field lead to relative position errors in the integration. For INS instrumentation presently available, these position errors are of the order of several centimeters after integration intervals of several minutes and grow to hundreds of meters for integration intervals of several hours.

The advantages of INS is that it is totally self contained, therefore it is not dependant on outside sources, and it can offer a full navigation solution (i.e. position, velocity, heading, pitch and roll). The major limitation of the system is that it has a high intrinsic error that increases to an unacceptable level with time. Therefore, INS is good for short term navigation but is unacceptable for long term navigation.

4.1.4 Integrated Differential GPS/Inertial Navigation System

Global Positioning Systems and inertial navigation systems have been discussed in the previous sections. Both have been shown to have disadvantages that make them unacceptable for sole means of navigation. The navigation system that would be appropriate for the APT would be an integrated differential GPS/INS system. This integrated system maintains the advantages of both navigation systems without many of the limitations of either.

4.1.5 Gyroscope Types

It has been shown that an integrated differential GPS/INS navigation system is most appropriate for the APT. A decision must now be made on what type of gyroscope to use in the INS. The three possible choices are:

1. Tuned Rotor Gyro (TRG)
2. Ring Laser Gyro (RLG)
3. Interferometric Fiber Optic Gyro (IFOG).

The tuned rotor gyro is the most common type of mechanical gyroscope. It is the oldest type of gyro and is becoming obsolete. Its weight, power, volume, and cost make it impractical for the APT.

The second type of gyro considered is the ring laser gyro (RLG). This is now a rather mature technology with many units in production. It uses an optical cavity that supports two counter rotating beams of laser light. These beams are recombined after transversing the cavity and the resulting beat frequency of the recombination is proportional to the angular velocity. The specifications are reasonable; however, there are some disadvantages associated with RLG's. These problems are that it is not amenable to employing integrated optics and a high voltage discharge is needed to excite lasers.

The final type of gyro considered is the interferometric fiber optic gyro. IFOG's are a new technology and are not on the market yet; however, they are projected to be on the market by 1992. It works on the same concept as the ring laser gyro, but light waves in a fiber optic cable are used instead of lasers. IFOG's can employ integrated optics and do not need a high voltage, thus eliminating the problems associated with the ring laser gyro. IFOGs have the most desirable specifications in every aspect; weight, power, size, cost, and reliability. Thus, the Interferometric fiber optic gyro would be best suited for the navigation system.

4.2 HEADS UP DISPLAY

The HUD is a display positioned between the pilot and the outside world. The display contains two types of information, symbology and aircraft data. Symbology, such as horizon lines and runway markers, are overlaid on the outside world. Many different types of aircraft data could be displayed, including attitude, air speed, altitude, course, and acceleration. The HUD eliminates the need for the pilot to cross check instruments with the outside world because the information is right in front of him. This yields the following advantages:

1. Increased pilot confidence
2. Reduced pilot workload
3. Increased safety
4. More accurate flying in low visibility

The first two advantages, increase pilot confidence and reduced pilot workload are nice; but the more substantial advantages are the last two, increased safety and more accurate flying in low visibility. Increased safety is most evident during the most critical phase of flight, the landing. The vast majority of aircraft accidents occur during landing. This is partly because the pilot has to often cross check the outside world with inside instruments because position is changing rapidly. This is what some pilots refer to as "chasing the needles" and results in a very high pilot workload. With a HUD the pilot can keep his eyes focused on the real world and still read situational data, since the display is right in front of him.

4.3 ADVANCED DISPLAY

The purpose of this chapter is to present the proposed HUD/Multifunction Display interaction during a typical flight in the Advanced Personal Transport. In addition, a sample emergency profile will be outlined.

Section 4.1 will present the typical mission, and section 4.2 will present the emergency mission profile. Section 4.3 will cover the Multifunction Display as it could be used by the pilot during a normal mission.

4.3.1 Advanced Personal Transport: Standard Mission

The purpose of this section is to conduct a step by step analysis of how flight critical information is to be displayed to the pilot during a standard mission.

The first information presented to the pilot upon entering the APT is from the Multi-Function Display (MFD). This display is called Power On.

```
 _____
|                Power On                  |
|  _____     |
|                                          |
|  System Initialization in Progress       |
|                                          |
|  .............                           |
|        Done                              |
|                                          |
|                                          |
|  Self Test & Check List in Progress      |
|                                          |
|  ...............                         |
|        Done                              |
|_____|
```
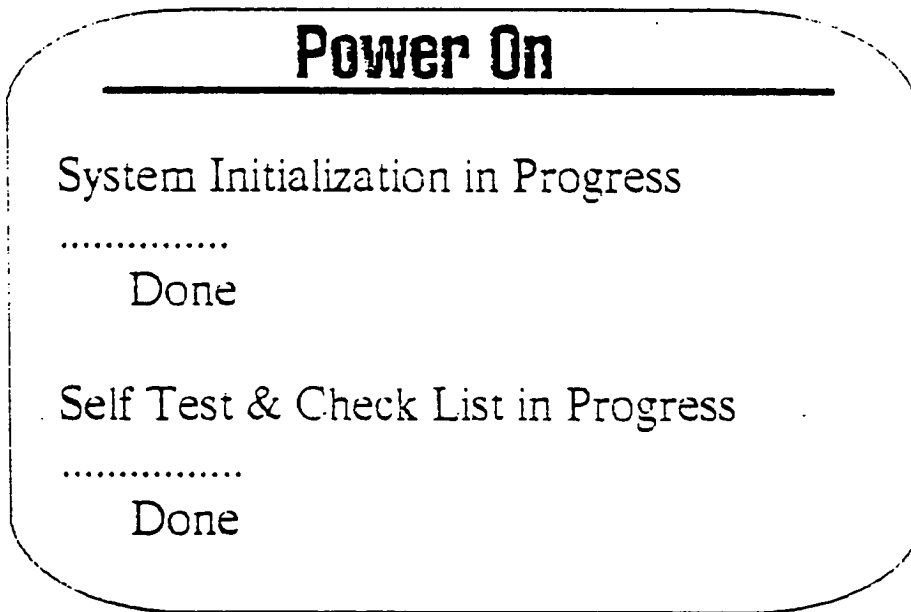
Figure 4.1 Power On (MFD)

This display informs the pilot that the system initialization is in progress, and that the self-test is also complete. The system initialization would include things such as turning on the communications equipment and other avionics systems required for flight. The self-test is a series of diagnostic tests performed by the computer on different systems throughout the aircraft.

The next display that the pilot would see is called Flight Plan Information.

Flight Plan Information

If flight information not encoded press the button to enter data.

Data Entry

Departure: Dallas/Fort Worth

Destination: Kansas City/International

Waypoints: Oklahoma City

Wichita

Lawrence
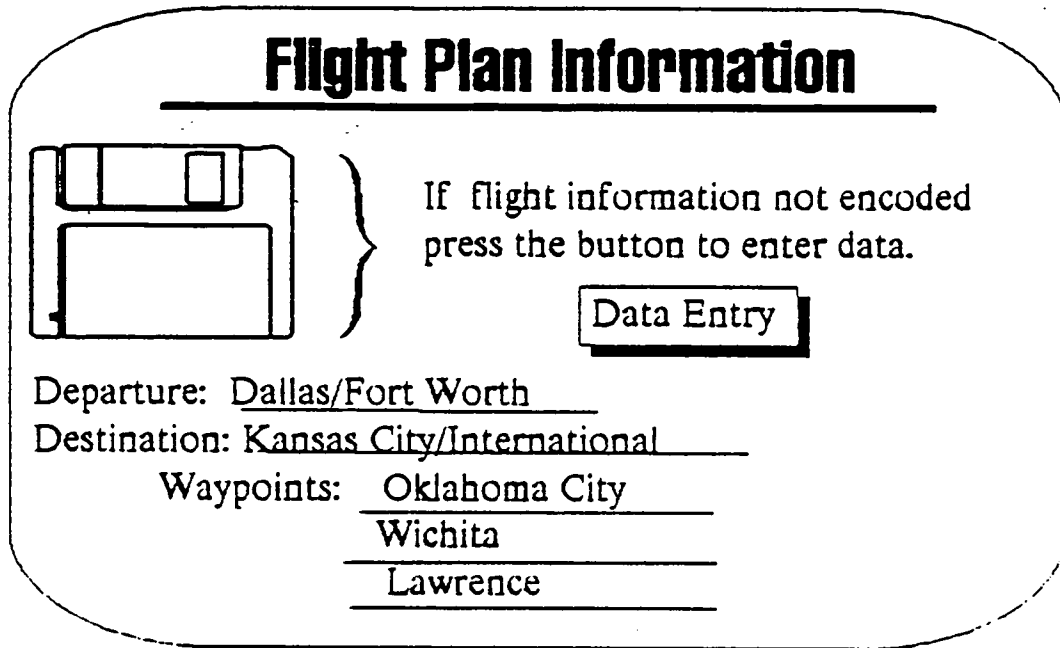
Figure 4.2 Flight Plan Information (MFD)

This display informs the pilot that if he is not using a computer encoded flight plan, then he could enter the data manually by pressing the Data Entry button which would result in a series of different menus being displayed. For this mission it is assumed that the flight plan was encoded and the pertinent information for the flight is shown on the display.

The next display that the pilot would see is called Clearance.

Clearance

Awaiting Departure Clearance to:

1st Destination: Kansas City/International

....

Flight Approved -- Taxi to Runway 27
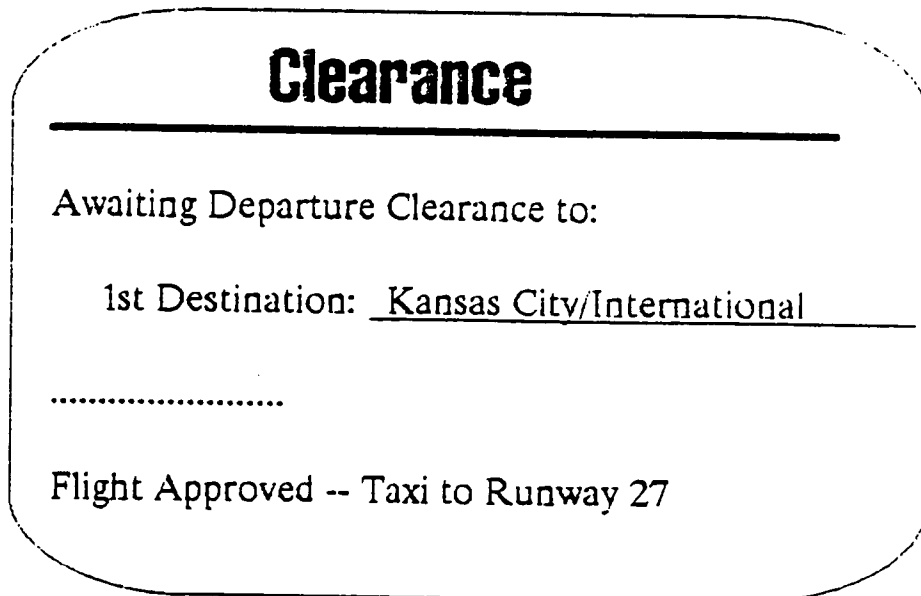
Figure 4.3 Clearance (MFD)

21

This display informs the pilot that clearance for the flight has been requested and that it has been approved. It is assumed that a Mode-S equipped communications system will allow the ATC and APT computers to communicate without intervention by humans being necessary. The display also informs the pilot that he has been cleared to taxi.

The next display is a representation of what the pilot would see when he looked through the HUD. The proposed HUD system will be incorporated into the windshield. The display is called Taxi.
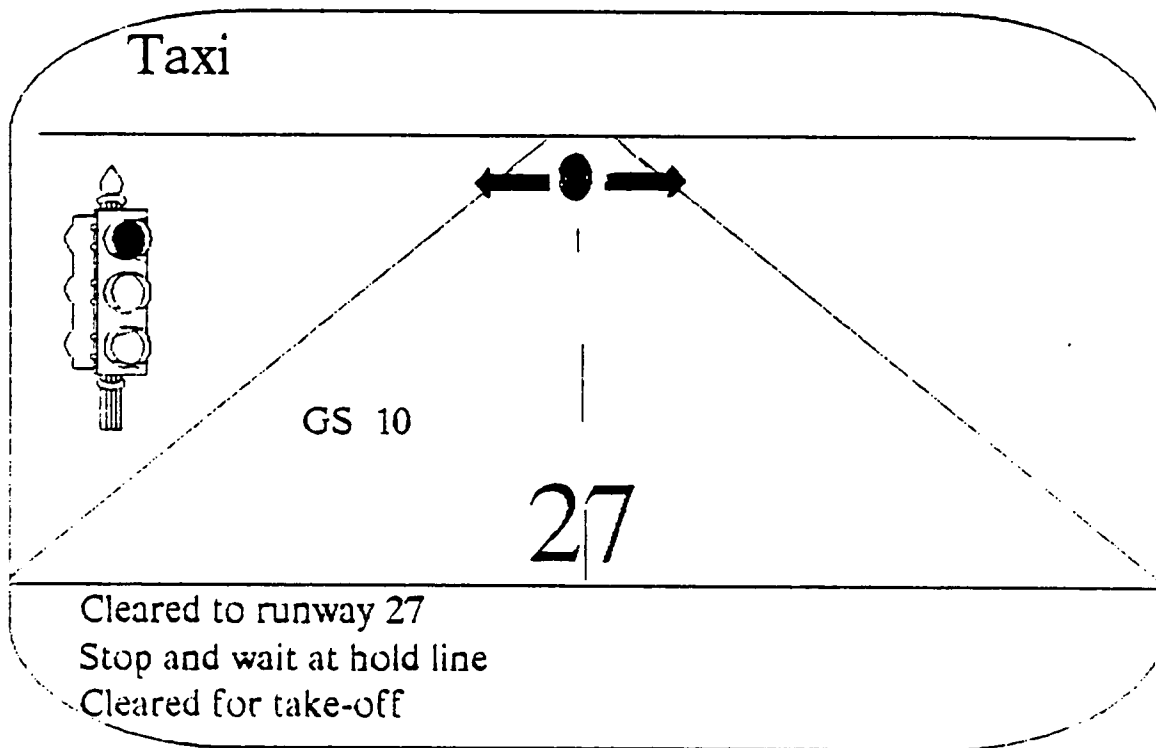
Figur 4.4 Taxi (HUD)

The Taxi display portrays what the pilot would see while looking through the windshield of the APT. Flight crucial information is shown on the HUD in consistent locations so the pilot does not have to search for it. The stoplight alerts the pilot that he needs to stop at the hold short line. Using the stoplight is an attempt to make navigating the plane on the ground no more difficult than driving a car.

The next HUD display is a representation of what the pilot would see during take-off.

270

TAS 110

GS 100
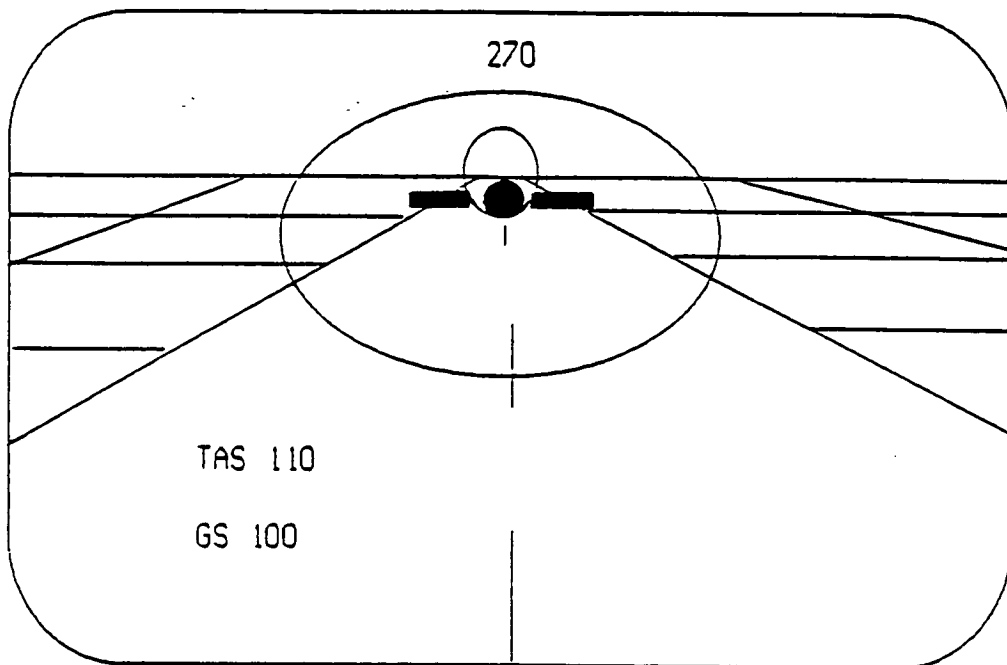
Figure 4.5 Take Off (HUD)

The HUD portrays a normal takeoff. The hoops show the pilot the direction he needs to travel. As long as he keeps the circle (A/C) and horizontal bars (wings) in the hoops then he is on course. As the plane passes through the hoops they get larger.

The next figure displays what the pilot would see during normal cruise flight.

210

740 MSL

TAS 325

GS 320
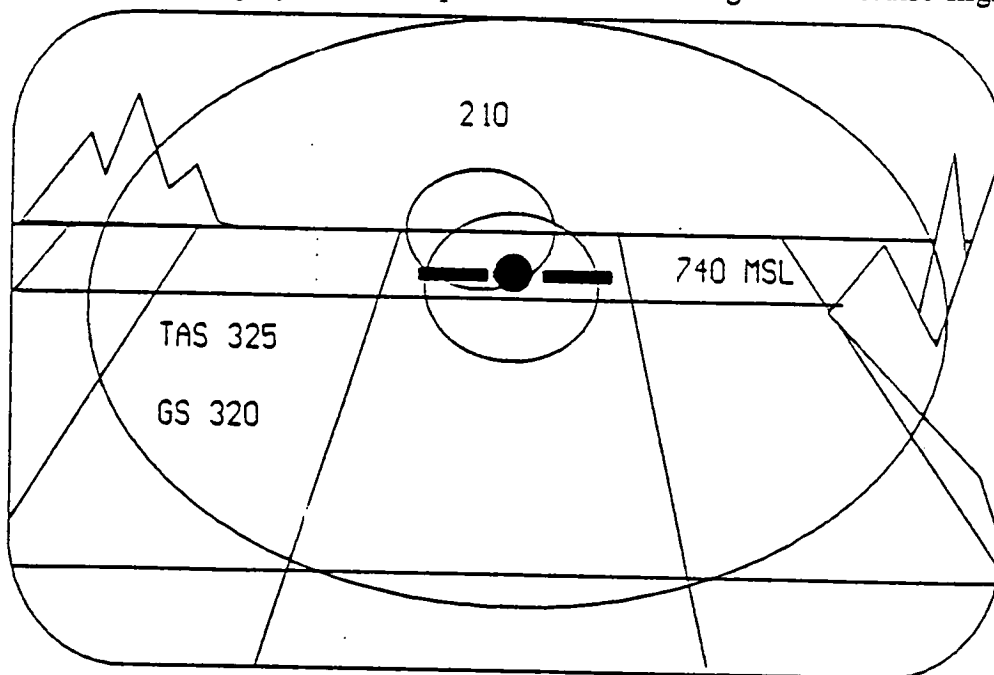
Figure 4.6 Flight (HUD)

Again, this figure shows the flight crucial information that is required by the pilot. The final phase of the flight is to land the aircraft.

360

TAS 100

GS 90

36

50 AGL
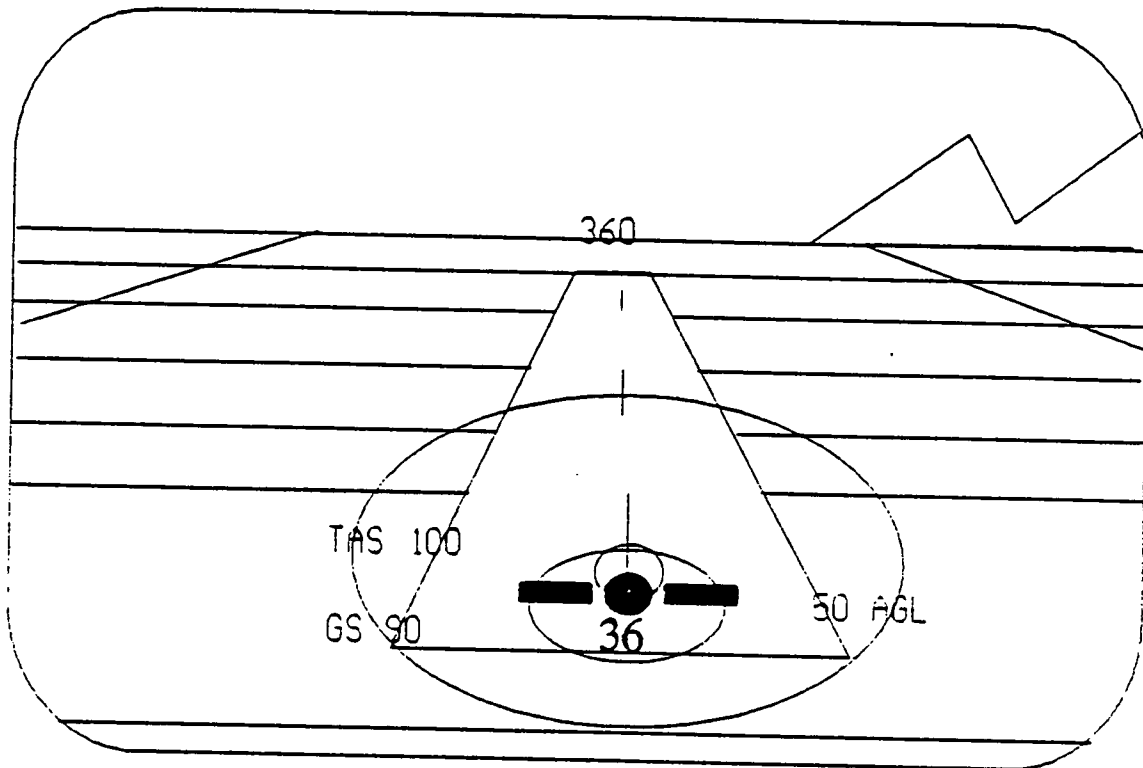
Figure 4.7 Landing (HUD)

The HUD depicts how the outline of the runway would appear during landing. Also, the elevation is now given in reference to ground level instead of sea level since this information is critical during landing.

Assuming the pilot lands safely and taxis to the hangar the next information he would see would be the Shutdown MFD.

System ShutDown

System Shutdown in Progress

....

    Done

Please Remove the Key

Have a Nice Day!
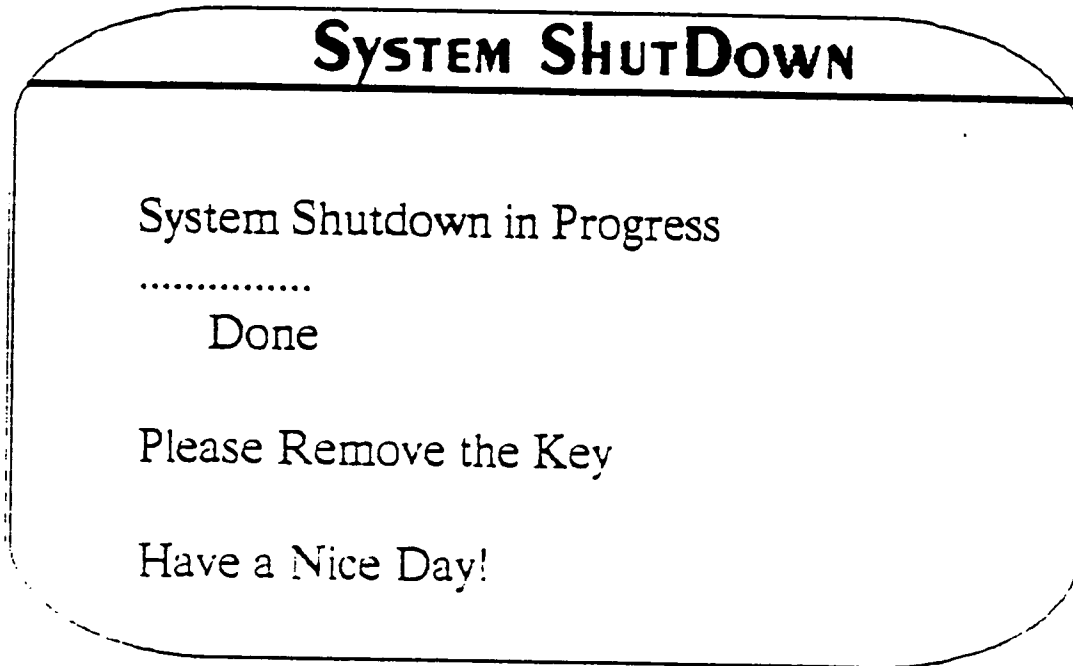
Figure 4.9 Shutdown (MFD)

The MFD informs the pilot that the systems are being shutdown. All that is left is to remove the key.

4.3.2 Advanced Personal Transport: Emergency Situation

The purpose of this section is to present the guidance and display system for the APT in an emergency situation. One of the primary objectives of the display system is to inform the pilot what to do, because that is really all he needs to know.

This section assumes the pilot has taken off safely and is in the flight cruise mode.

Figure 4.10 shows what the pilot would see as he was flying along if an emergency situation arose.
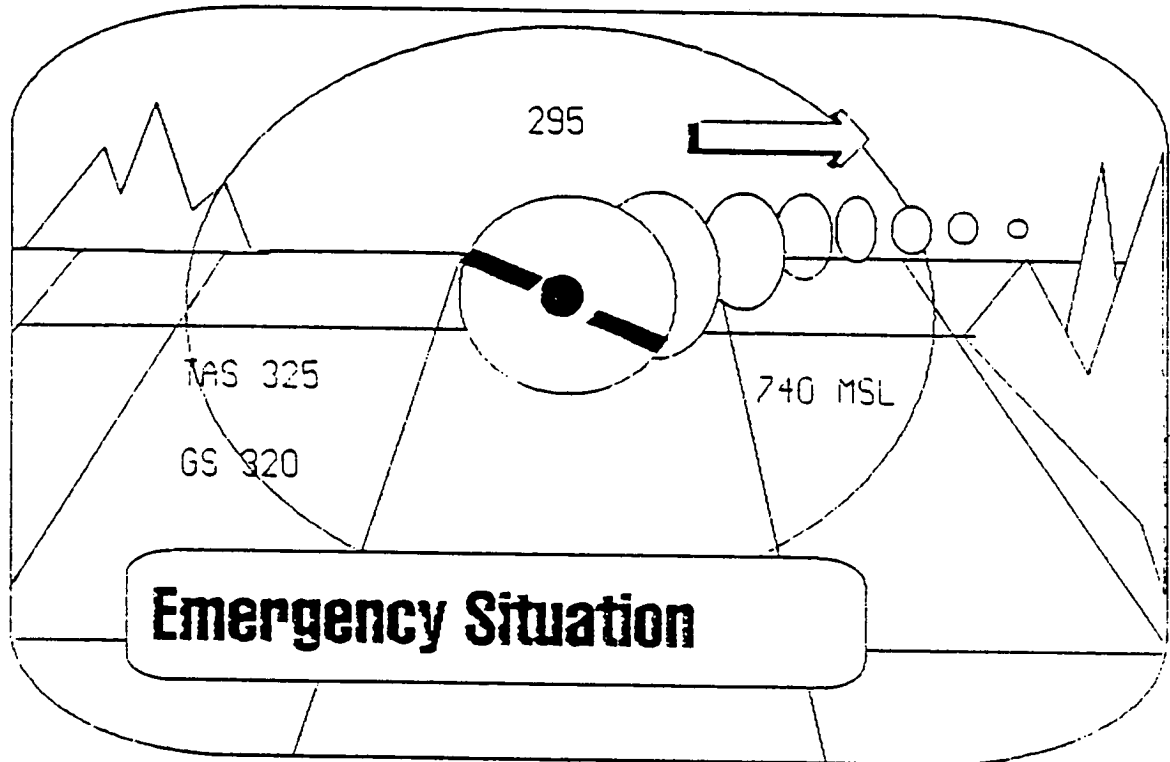
Figure 4.10 Emergency Flight HUD

The emergency situation block would be outlined in red and so would the hoops during an emergency situation. This color scheme would remain throughout the flight or until the emergency situation had ceased. Notice that the pilot does not know what the emergency situation is yet, but all he has to do is look at the MFD and this is what he would see.

Emergency Situation

Left Wing Fuel Boost Pump Failure

Follow Directions on the Screen:

1). Turn Right to Heading 080
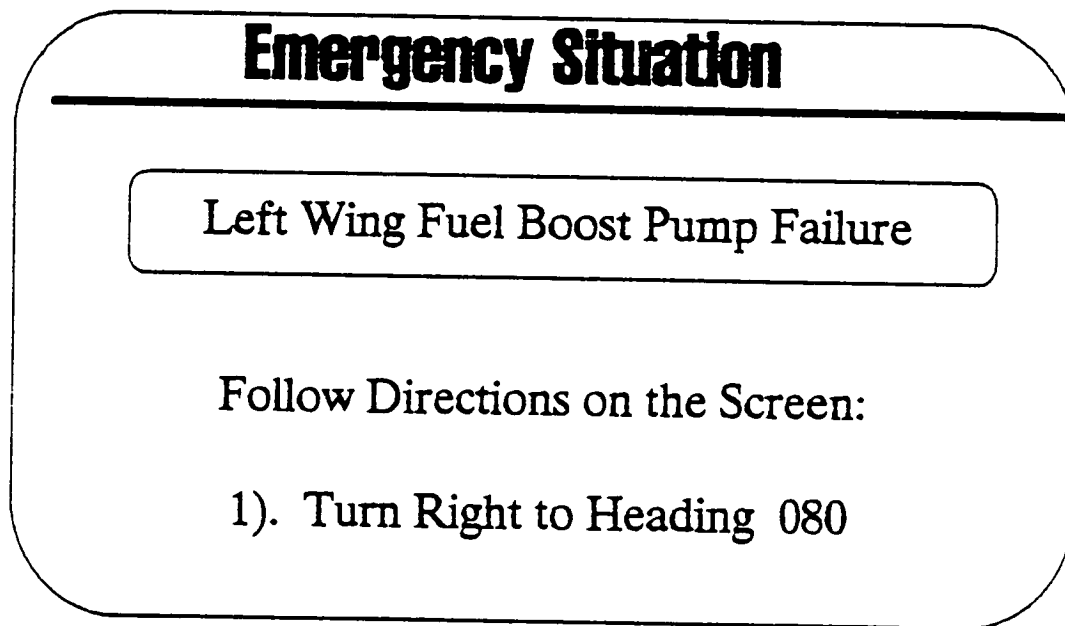
Figure 4.11 EMFD #1

The display shows the pilot what the malfunction is and primarily what he should do about it. In this scenario, the left wing fuel boost pump has failed. The APT can fly on only one boost pump because the engine driven pumps can increase their output to compensate for the loss. However, the loss of the left pump could be due to some type of material getting in the pump, and it is better to land the plane safely than to let another pump be damaged by the same material. The computer has determined where the nearest airport is and is instructing the pilot to turn to a desired heading. The pilot only has to read and follow the instructions provided.

Figure 4.12 displays what the pilot would see on the HUD corresponding to the message on the MFD.
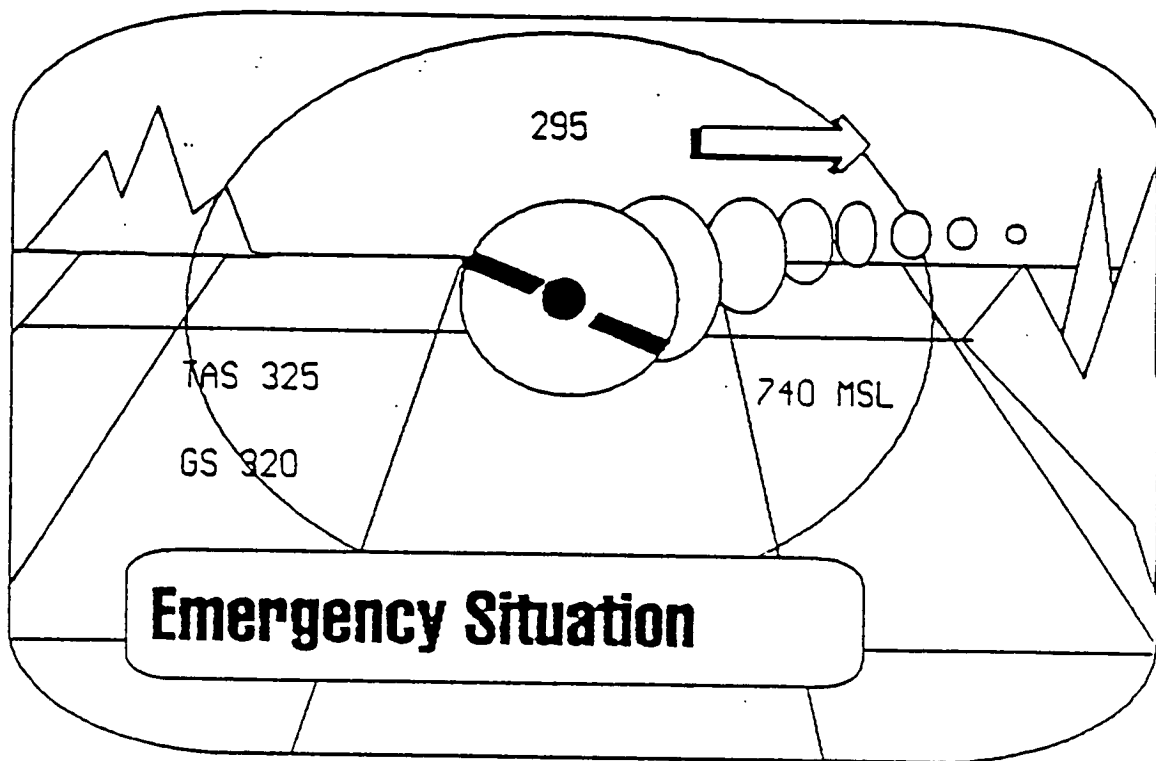
Figure 4.12 Emergency Turn (HUD)

The hoops show the pilot where he needs to turn, and the arrow will be displayed until the desired heading of 080 degrees has been achieved. Again, the hoops would be red as would the emergency situation flag throughout the entire emergency situation.

Figure 4.13 is the next MFD that would be displayed to the pilot during the emergency situation.

Emergency Situation

Left Wing Fuel Boost Pump Failure

2) Continue Flying the Plane
Diverting to the nearest airport
-- Salina/Municipal
-- ETE 20 minutes
Left Wing Boost Pump Shutdown
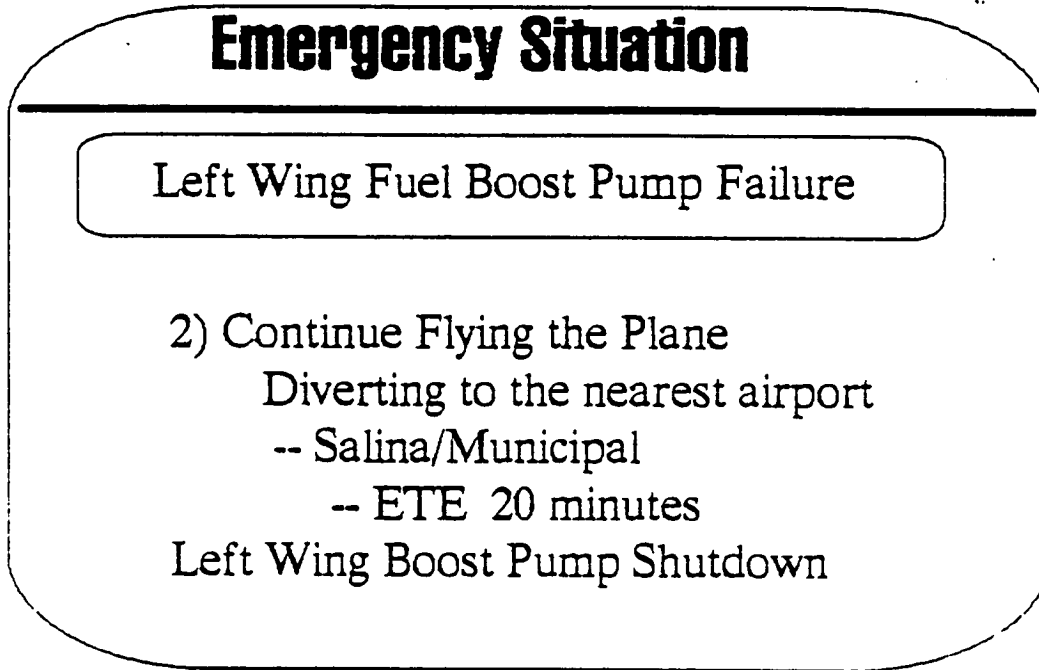
Figure 4.13 EMFD #2

This MFD tells the pilot to remain calm. In many emergencies, fatalities could be avoided if the pilot would just continue flying the plane instead of worrying about doing so many other things. The sophistication of the APT should eliminate this problem since the computer manages a large share of the tasks normally performed by the pilot. Figure 4.13 also tells the pilot what is happening and what has been done with the faulty pump.

The following HUD figure represents what the pilot would see during the landing phase of the emergency situation. It is basically the same as a normal landing except that the hoops would be red as would the emergency situation flag.
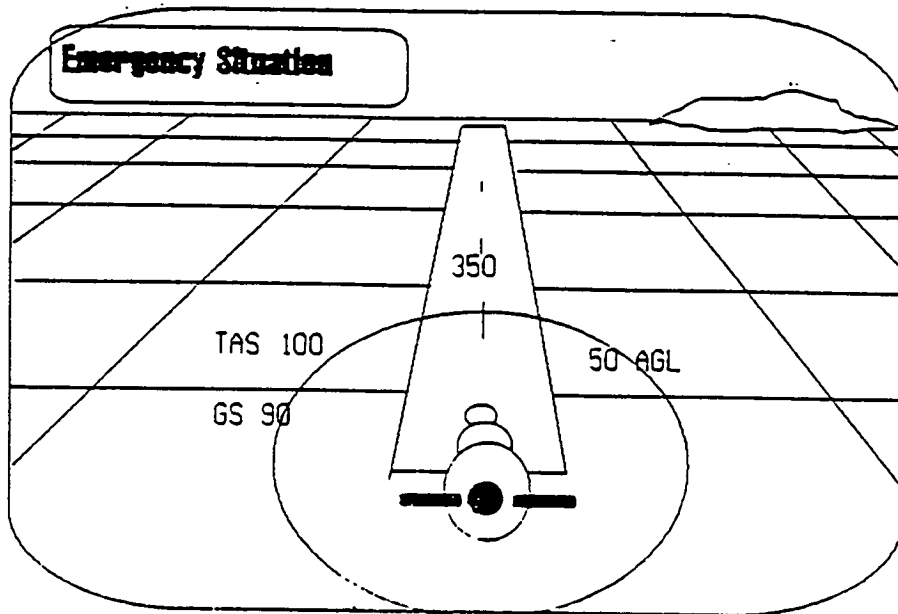
Figure 4.14 Emergency Landing (HUD)

At the same time as Figure 4.14 is on the windscreen the following figure is on the MFD.

Figure 4.15 EMFD #3

Figure 4.15 tells the pilot to land as normal and where to taxi since it is likely he has never been to this airport before. The display also informs the pilot that the boost pump has been marked for maintenance. The maintenance personnel can plug into the computer and access the maintainablity data, thus increasing their efficiency in correcting the problem since it is already known what caused the emergency.

The final display that the pilot would see after taxing to the appropriate hangar is the System Shutdown MFD shown in Figure 4.9.

4.3.3 Multifunction Display Interaction

The purpose of this section is to present the Multi- Function Display (MFD) as it would be used by the pilot during a typical mission. In most instances the pilot will not have to worry about the MFD. However, in case of emergency, or even curiosity, the basics of the MFD are explained.

The MFD is a multi-color, touch sensitive Liquid Crystal Display (LCD) through which the pilot accesses pertinent information on the many systems in the APT.

The program menu in Figure 4.16 provides the pilot with an easy method to access information and control certain systems.

Program Menu

Preflight

Airport Information

Fuel System

Environment

Systems
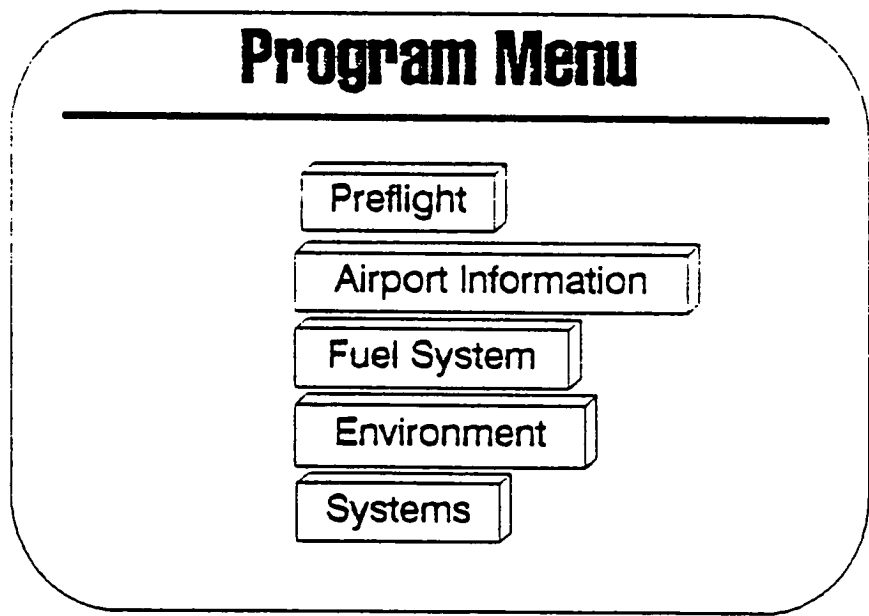
Figure 4.16 Program Menu

Assuming the pilot presses the the preflight button, the first display he would see is shown in Figure 4.17

Preflight

Weight & Balance :

Current C.G. location is

<u>Acceptable</u>

If C.G. location is unacceptable then follow instructions on display.

| Exit | Continue |
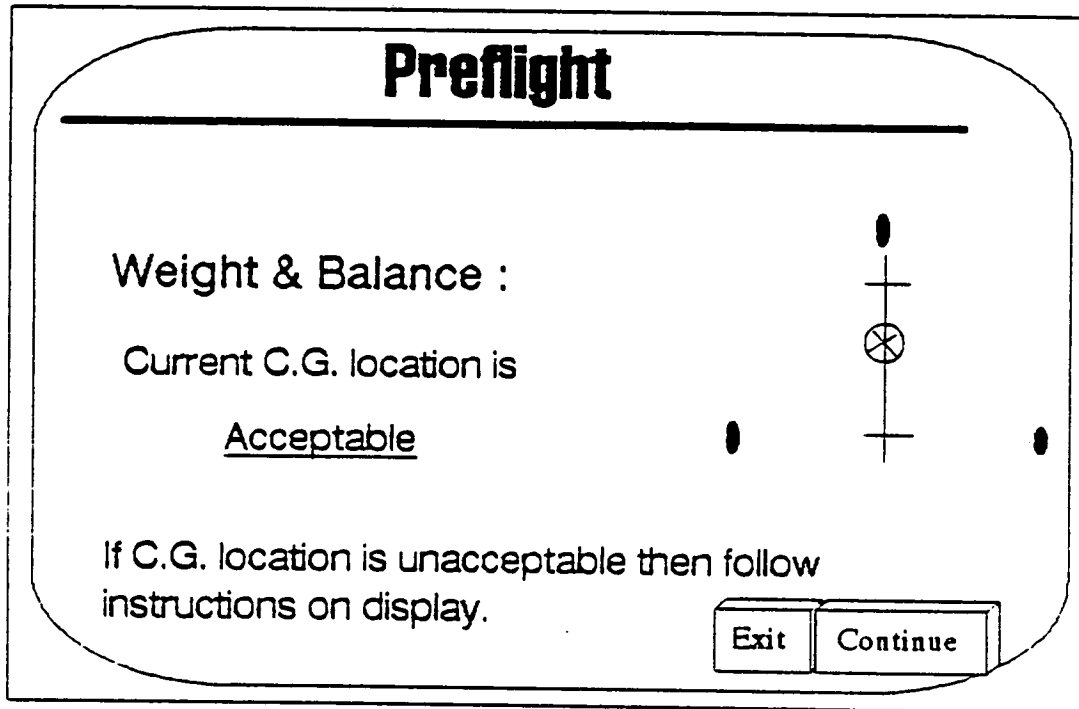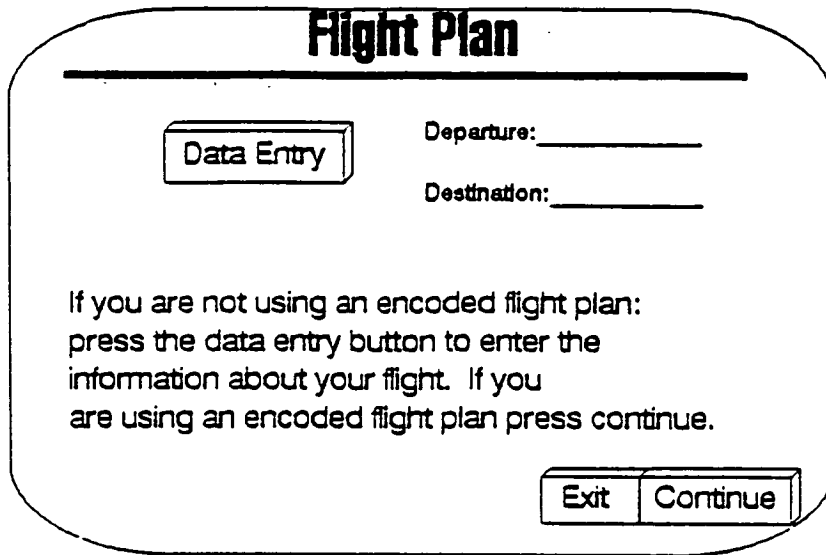
<u>Figure 4.17 Weight and Balance</u>

Figure 4.17 informs the pilot whether or not the currennt loading condition is acceptable in terms of center of gravity location. Load sensors on the landing gear could be used to determine the aircraft C.G. If the plane is loaded such that there is an unacceptable C.G. location then the computer will tell the pilot via the MFD what should be done to correct the situation. The exit and continue buttons allow the pilot to continue with preflight operations or return to the main menu shown in Figure 4.16.

32

If the pilot presses the continue button the following display appears.
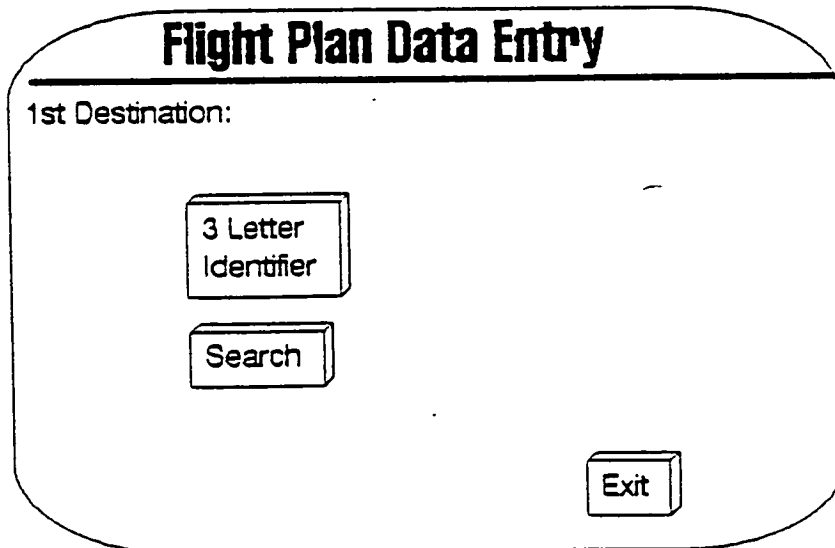
Flight Plan

Data Entry

Departure:_____

Destination:_____

If you are not using an encoded flight plan:
press the data entry button to enter the
information about your flight. If you
are using an encoded flight plan press continue.

Exit | Continue

Figure 4.18 Flight Plan

The flight plan MFD tells the pilot that he is not using an encoded flight plan then he can enter the destination manually. The APT already knows where it is based on data from the last flight. This is the capability that was discussed in the mission scenario where it was assumed that the flight plan was encoded. In this section it is assumed that the flight plan is not encoded and a description is given of the process.

If the Data Entry button is pressed then the Flight Plan Data Entry dispaly appears.

Flight Plan Data Entry

1st Destination:

3 Letter
Identifier

Search

Exit

Figure 4.19 Flight Plan Data Entry

This display gives the pilot the option of entering the three letter identifier for the first destination or doing a search. If the pilot knows the three letter identifier he would push that button. Figure 4.20 displays the MFD that the pilot would see if 3 Letter Identifier button were pressed.

3 Letter Identifier

1st Destination:

Please enter the three letter indentifier
for the 1st destination airport:

| Up | Down | ___ MCI ___

| Enter | | Exit | Continue |
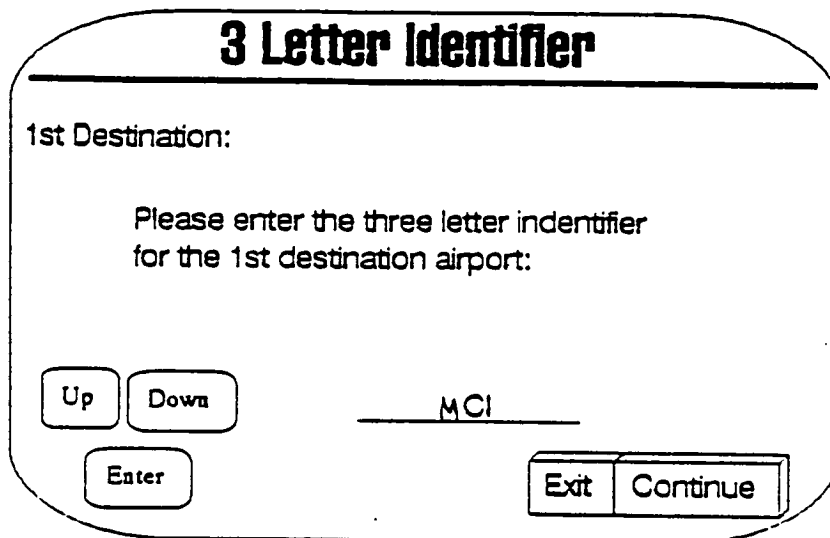
Figure 4.20 3 Letter Identifier

The pilot can use the up, down, and enter buttons to enter the appropriate identifier for the first destination. Pressing exit returns one to Figure 4.19 in case the three letter identifier is forgotten. Pressing continue causes the next display to appear.

Flight Plan

Selected Flight Plan Information:

1st Destination: ___ Kansas City/International ___
2nd Destination: ___

The computer automatically determines the waypoints, for the flight. However, if you would like to enter specific waypoints push the WP button. | WP |

| Return to Program Menu | Continue |
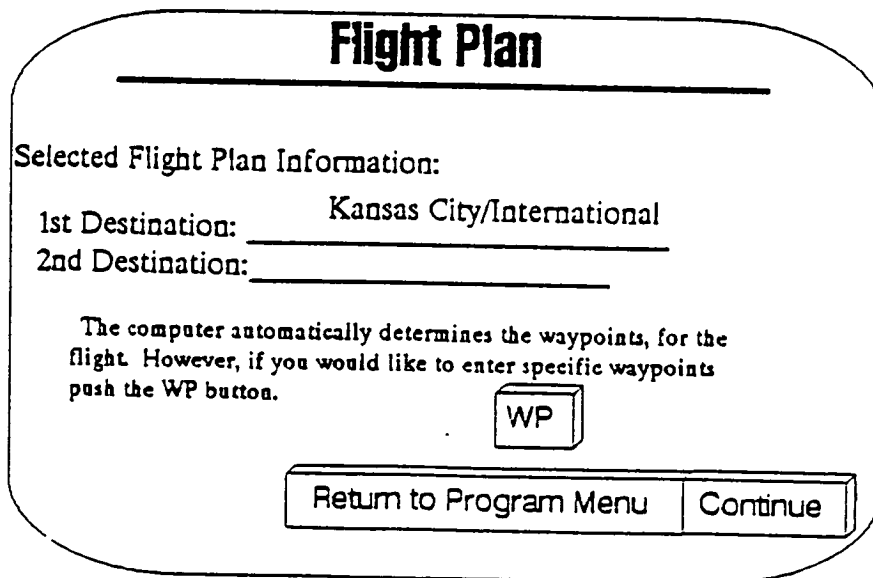
Figure 4.21 Flight Plan

34

This display informs the pilot what the computer assigns as the fir
st destination so this can be verified with what the pilot desired to be the first destination. If there is an error the pilot can press continue. Continue takes the pilot to Figure 4.18. so that data can be reentered or to input data for a second destination. In addition, the waypoint button allows the pilot see what the computer selected as waypoints for the flight. The Waypoint MFD can be seen in Figure 4.22.

Waypoints

Flight from Dallas to Kansas City International:
Waypoints: Oklahoma City
                Wichita
                Lawrence

To change the Waypoints, use the search command modified for waypoint selection.
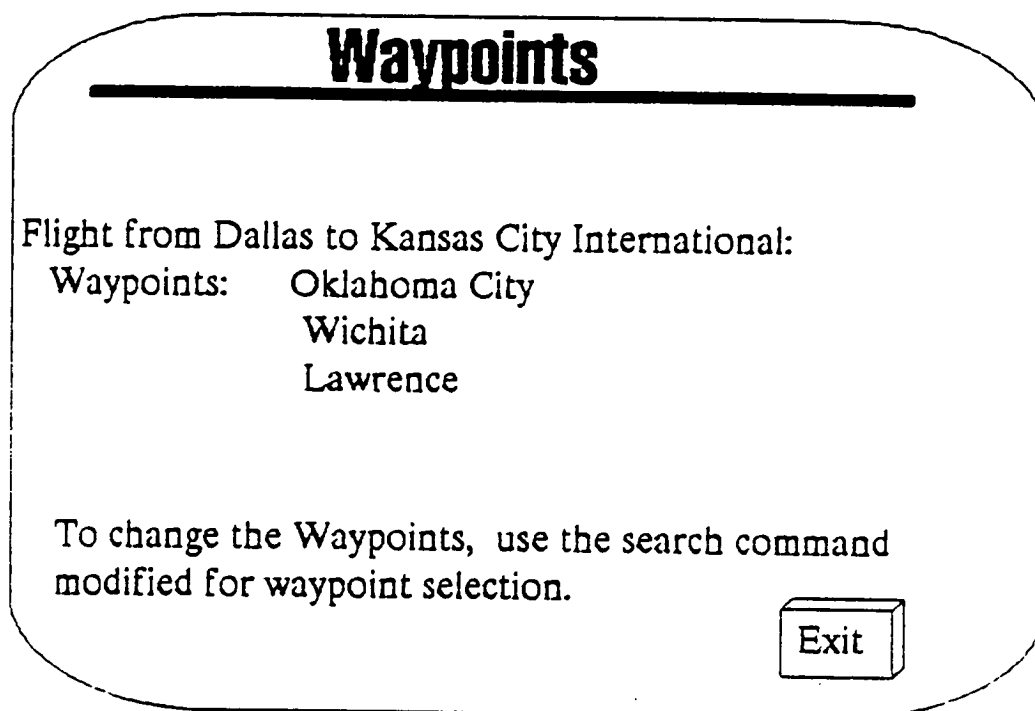
Exit

Figure 4.22 Waypoints MFD

As the display points out the pilot can change the waypoints as desired. This feature is not covered, but could easily be incorporated in the final design. Pressing exit returns the pilot to Figure 4.21 and from there he could return to the Program Menu shown in Figure 4.16.

The method for enter data using the search command is essentially the same as the 3 Letter Identifier method just covered, however, a few words of explanation are required. Assuming the pilot is looking at Figure 4.19 and presses the Search button this is what would be displayed.

Flight Plan Search

Range Capability

Up   Down

Up   Down

1st Destination:

1st Destination:

State: _____ Missouri

State: _____ Missouri

City/Airport:

Depress

Enter

Kansas City/International

Enter when both are complete

Exit | Continue

Figure 4.23 Flight Plan Search

This display allows the pilot to enter the destination airport using a search procedure that would start at the state level. Assuming the destination airport is in Missouri the pilot would use the up and down keys to scroll through the states until Missouri appeared on the state line. This search command could be extended to an international level but for now it is assumed to be strictly U.S. capable. After Missouri has been selected the pilot would then use the up and down buttons to select the destination City/Airport. This function is extremely vital since many cities have more than one airport. When both state and airport are correct the pilot presses the enter button and the information is processed. If the pilot pressed continue, Figure 4.21 would appear and the same options described previously for that figure would be available. Pressing the Range Capability button causes the following display to appear.

Range Information

The circle shows the range for the aircraft from the selected departure point. If this circle is exceeded you will be required to re-enter the flight coordinates.

Exit
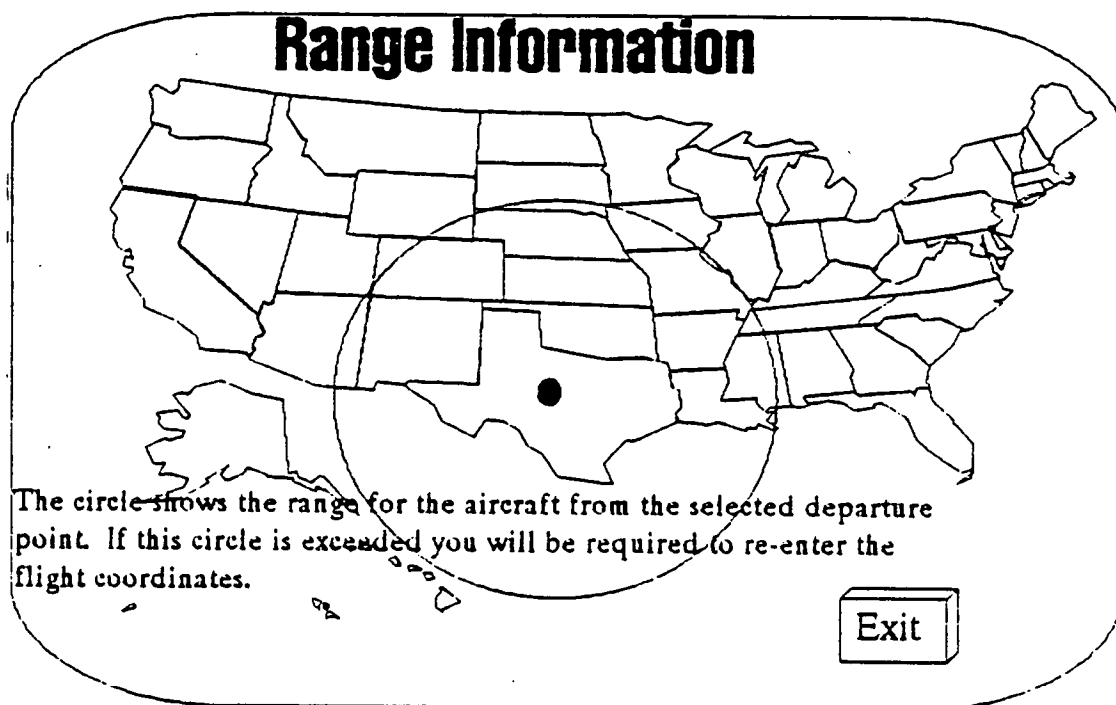
Figure 4.24 Range Information

As explained on the display, the circle shows the available range of the APT from the destination airport based on the amount of fuel onboard. If the chosen destination exceeds this range the pilot will be required to reenter it. More than likely the pilot would look at Figure 4.24 before entering the destination just to make sure there is adequate range.

Assuming the pilot presses the exit button on the Range Information display and the continue button on the Flight Plan Search display, he will now see Figure 4.21. From here the Return to Program Menu is pressed and the Preflight Menu appears.

Pressing the Airport Information button causes the following information to appear.

Airport Information

Nearest Waypoint Information: R/W 36 in use

Altimeter: _29.90_ ATIS: _119.2_
Approach: _118.0_ Departure: _119.0_
Tower: _118.3_ Ground: 121.9
VOR: _115.3_

Destination Information: R/W 34 in use

Altimeter: _28.70_ ATIS: _119.9_
Approach: _116.0_ Departure: _116.5_
Tower: _117.1_ Ground: _121.3_
VOR: _114.5_ | Exit |

Figure 4.25 Airport Information

    This display is a listing of the current information on the nearest waypoint and destination airport. The waypoint information changes automatically as the nearest waypoint changes and the destination information changes after departure from the destination. This type of information is useful when the pilot needs to communicate with someone. In the case of an emergency in which the the capabilities of the APT to manage the situation are diminished, it essential for the pilot to be able to perform these functions.

Pressing Exit returns the pilot to the the Program Menu. Assuming the Fuel System button is pressed the following information is displayed.

Fuel System

Amount of Fuel Required: <u>1000 lbs</u>

Amount of Fuel Remaining: <u>1200 lbs</u>

Left Fuel Tank:

88 %

Right Fuel Tank:

88 %

Exit
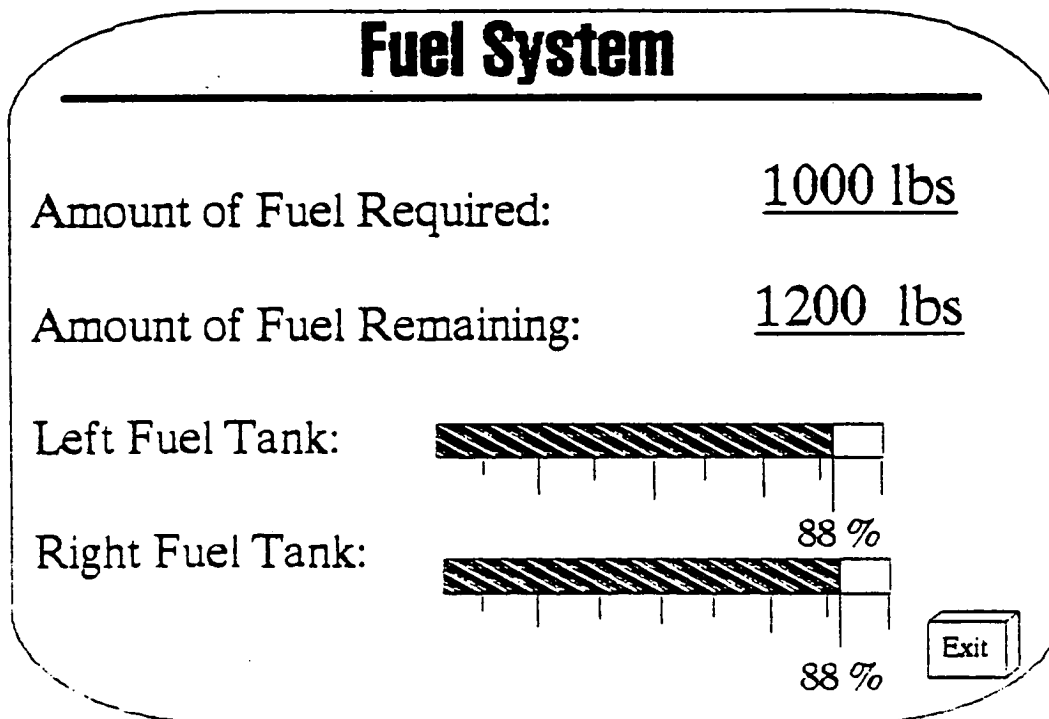
Figure 4.26 Fuel System

The display informs the pilot how much fuel is required for the mission and the amount of fuel remaining. In addition, the display presents the percentage of fuel in relation to maximum left in each tank. The pilot does not need to worry about units, but only how much is left compared to how much the tanks are capable of holding. Pressing exit returns the pilot to the Program Menu display.

If the Environment button is pushed the following information will appear on the MFD.

Environmental Systems

Current Cabin Temperature: _____ 72 (F)

Ambient Temperature: _____ 40 (F)

Heat/Cooling

Oxygen

Exit
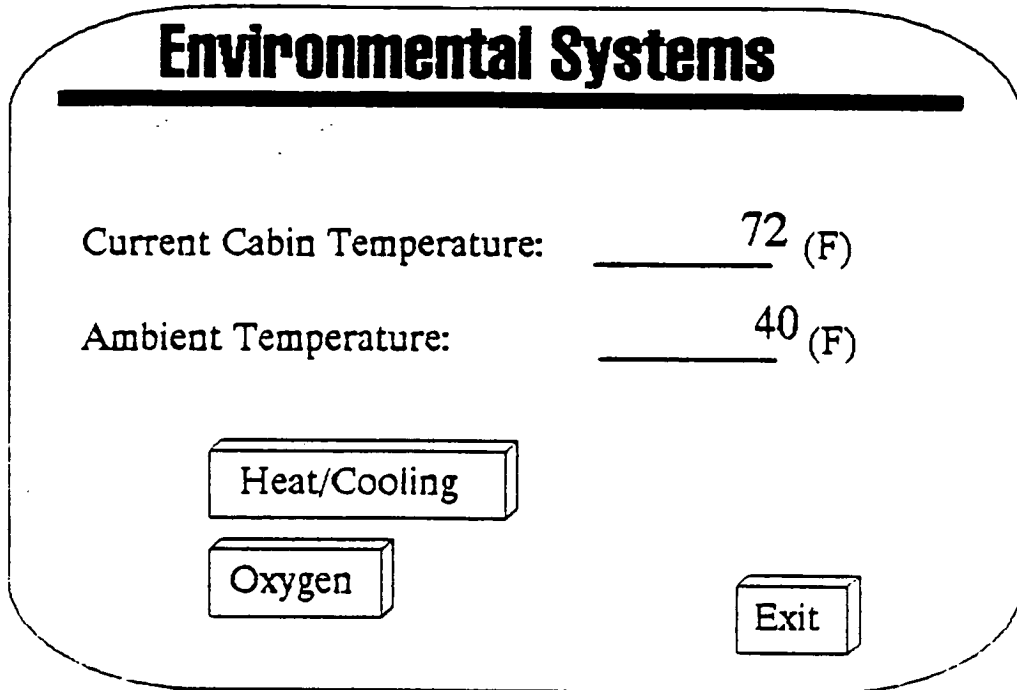
Figure 4.27 Enviormental Systems

The informatin on the Environmental Systems display lets the pilot immediately see the temperature for the cabin and ambient temperature. Pressing the Heat/Cooling button causes the following display to appear.

Heating/Cooling Control

Temperature Control Bar

60   72   85

Down   Up

Exit | Return to Environment Menu
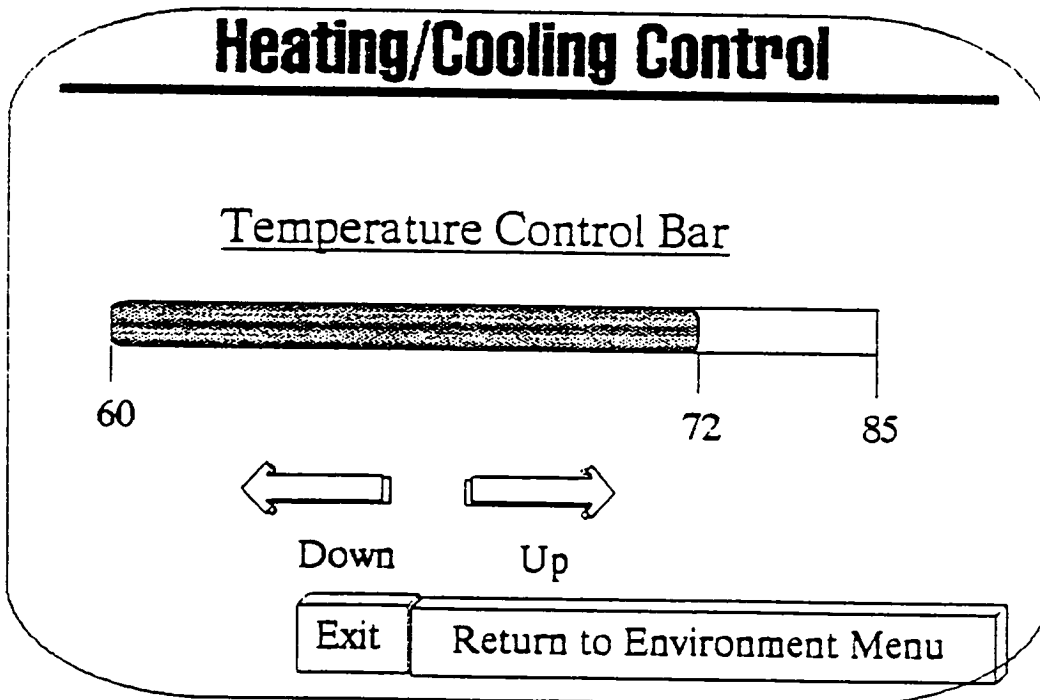
Figure 4.28 Heat/Cooling Control

The up and down buttons can be used to manually control the cabin temperature. The current temperature is also shown. Assuming Figure 4.27 is displayed on the MFD, pressing the oxygen button results in Figure 4.29 appearing.

Oxygen System Information

Status: 72%

100 %

50 %

0 %

⊠ Mark for Maintenance

| Exit | Return to Environment Menu |
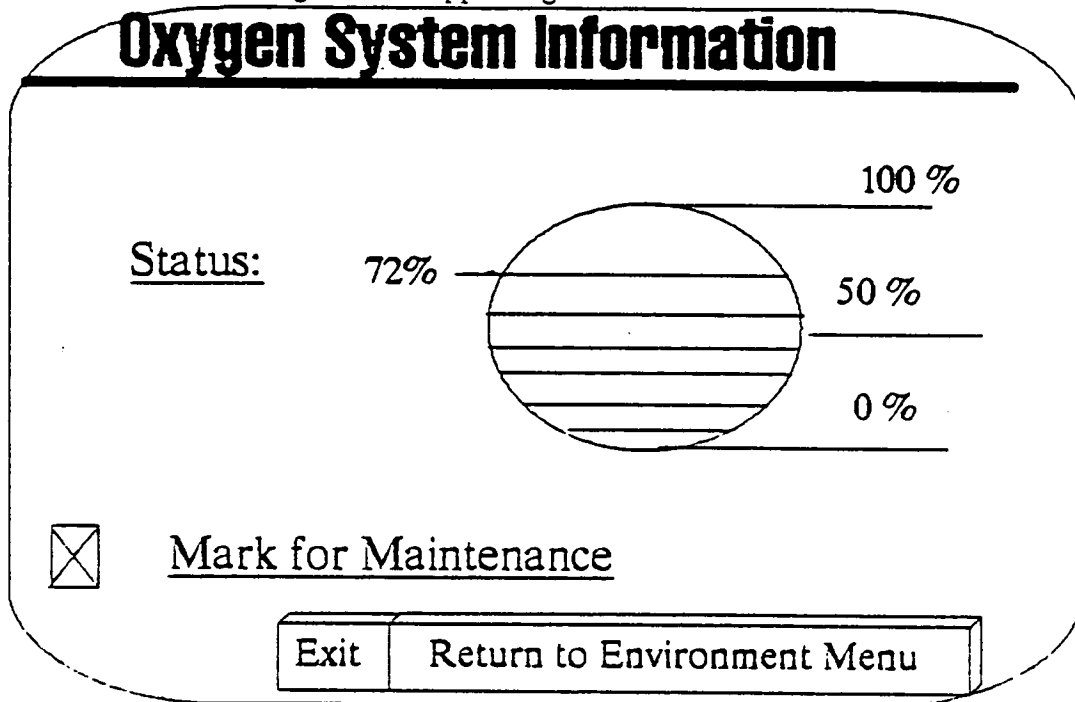
Figure 4.29 Oxygen System

The purpose of this display is to not only show the status of the oxygen system onboard the APT, but, to also show how a system can be marked for maintenance by pressing a button on the MFD. If the Exit button is pressed the pilot is returned to the Program Menu.

If the Systems button is pressed the following display appears.

Systems

APT Systems

Powerplant

Ice Protection

Exit
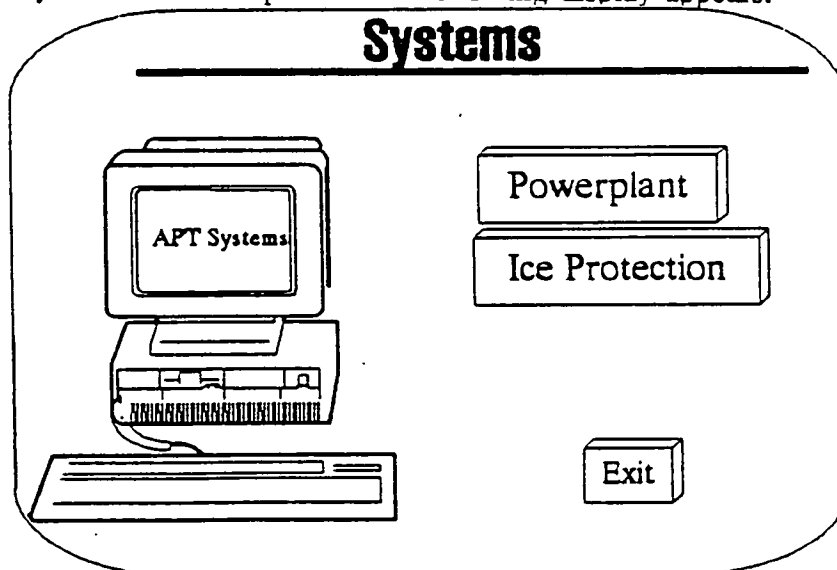
Figure 4.30 Systems

The systems display could be augmented with many more systems, however, there are only two for demonstration purposes. Pressing the Powerplant button causes Figure 4.31 to appear.
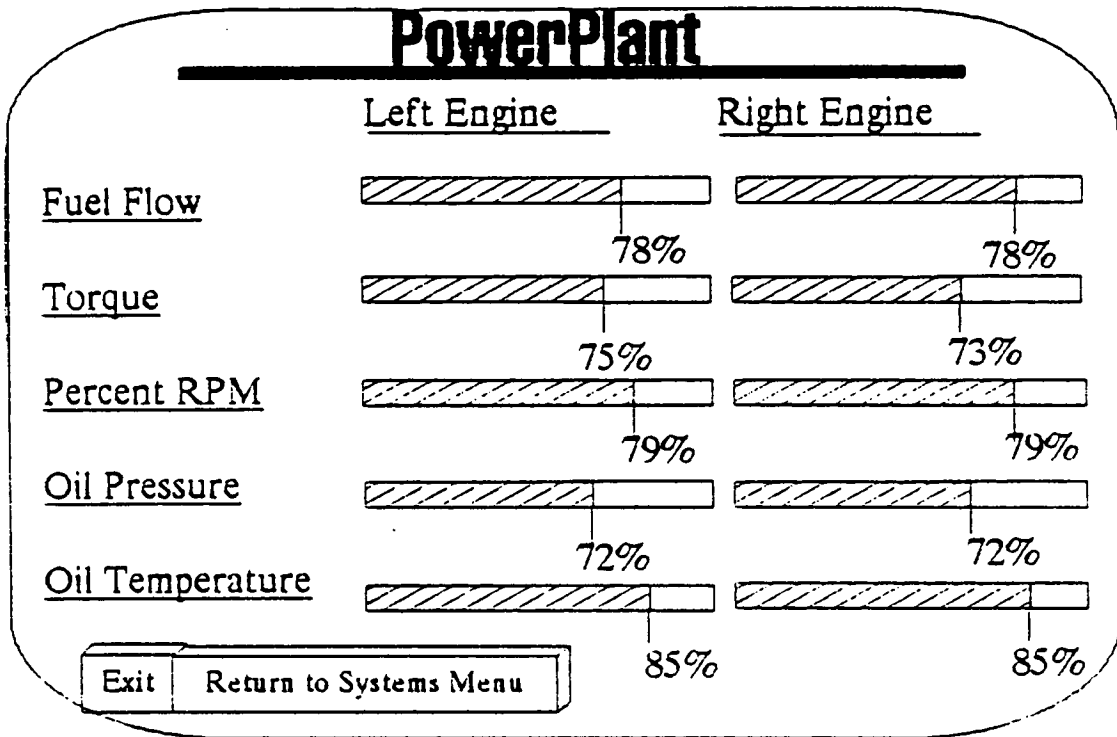
Figure 4.31 Powerplant

The important parameters of the engine are displayed in a manner which is easy to read and understand. There are no units just percentages of maximum for each parameter. This reduces the time required for the pilot to correlate the data.

If the Return to Systems Menu is pressed Figure 4.30 is displayed. Pressing the Ice Protection button causes the following information to appear.

Ice-Protection

Engine Inlet

Left Wing De/Ice

Right Wing De/Ice

Windshield

Vertical Fin De/Ice

Horizontal Tail De/Ice

Increase ➡ Impulse Frequency Control
Decrease ⬅

75%

Exit | Return to Systems Menu

Ice-Protection is Automatic,
if you want to turn a systemon/off press the button.
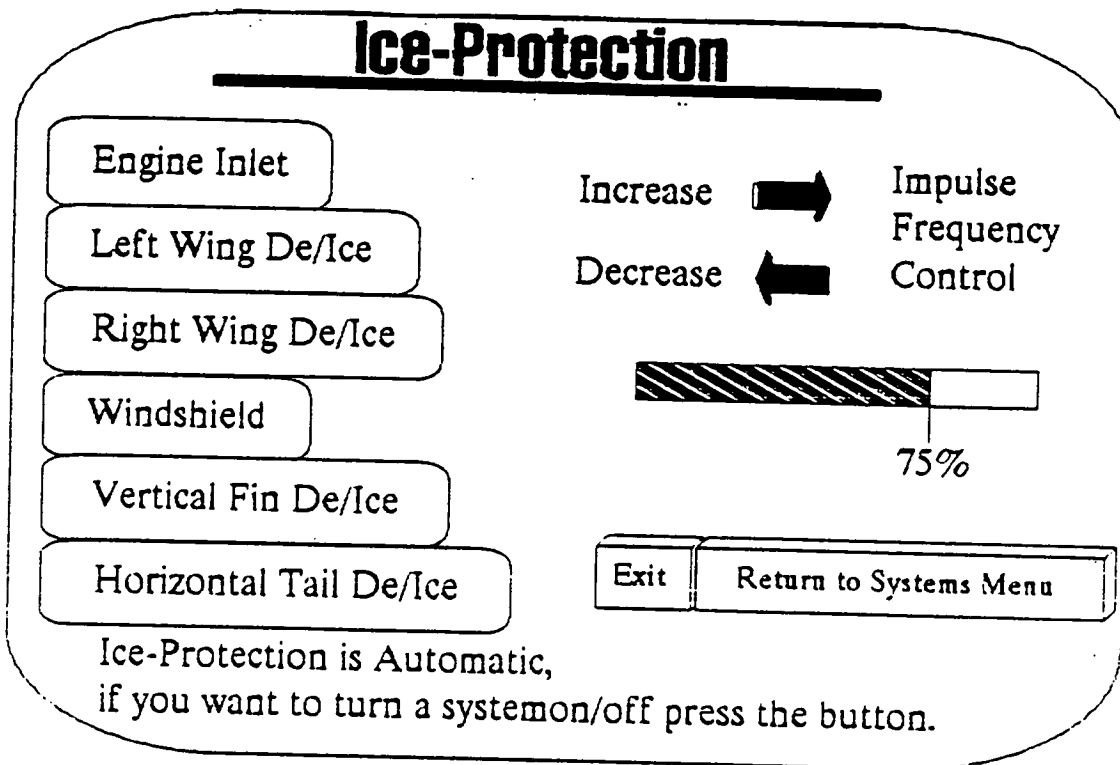
Figure 4.32 Ice Protection

The ice protection system is automatic, however, the pilot can press the buttons to turn a system on or off depending on circumstances. In addition, the Impulse Frequency control adjusts how many times the Electro-Impulse Coils are energized in a given time period. These type of options enable the pilot to have some sort of control over the systems on the APT.

5. DESIGN, CONSTRUCTION AND TESTING OF AN IRON BIRD

Current methods of achieving automatic roll control in general aviation aircraft involve the use of large aileron actuator devices or heavy mechanical systems. Such mechanical or electro-mechanical actuators are generally heavy, consume considerable amounts of power and are relatively expensive. Push-rod and cable systems are heavy, penetrate structural members and are difficult to inspect and maintenance. This chapter will outline the procedures that were used to evaluate the performance of small, lightweight servoactuators. These servoactuators would drive servotabs on control surfaces to achieve flight control.

5.1. OVERVIEW OF SERVOTAB ACTUATION CONCEPT

For an advanced general aviation aircraft, it may be desirable to employ a multitude of low-cost, efficient, light weight servoactuators for roll control instead of heavy mechanical systems. Such servos would be used to drive separate servotabs on the ailerons as shown below.
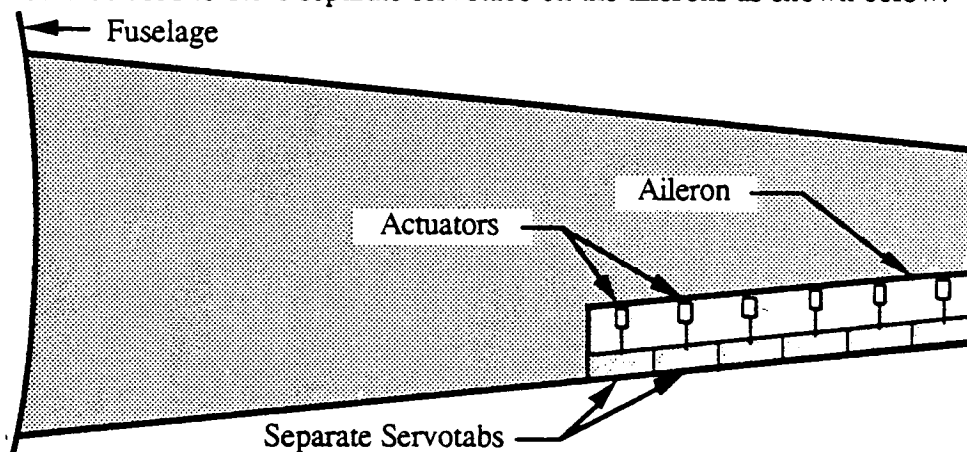
Figure 5.1: Servotab-Aileron-Wing Arrangement

It is the purpose of this investigation to determine the feasibility of using these light-weight servoactuators in this capacity through testing on an iron-bird model.

5.1.1 Goals of Iron Bird Design, Construction and Testing

This investigation will be composed of several stages of analysis and development. The first analysis stage is to accurately model the forces and moments that are involved with the motions of the aileron and servotab. Forces and moments arising from both steady and unsteady aerodynamic and structural forces will be taken into account. Upon determining the magnitude and nature of forces involved, the equations will be assembled in matrix form as functions of aileron and servotab deflections, their velocities and accelerations.

Using the force and moment models, a configuration for the hardware of the proof-of-concept/iron-bird model will be selected. The forces and moments determined from the aerodynamic analysis will be simulated by a set of springs. Conclusions on the feasibility of such a system will be drawn from all aspects of this investigation including weight, power consumption, frequency response, maintainability, and reliability.

5.1.2 Instrumentation, Testing and Manpower Schedule

The testing of the iron bird will involve the use of several sensors, a data acquisition network and driving network. The initial phase of Iron Bird instrumentation and testing is underway. More than 38 hours of testing has shown no failures or performance degradation in the servoactuator system. This Phase 1 testing was constructed as a preliminary test set-up as the automatic test network that was planned is still under development. Phase 2 testing will involve the automatic testing of the Iron Bird which is monitored by a 286 based microprocessor. Phase 2 testing will actuate the servotab at scheduled rates, under various flight conditions automatically (without the presence of a monitoring technician).
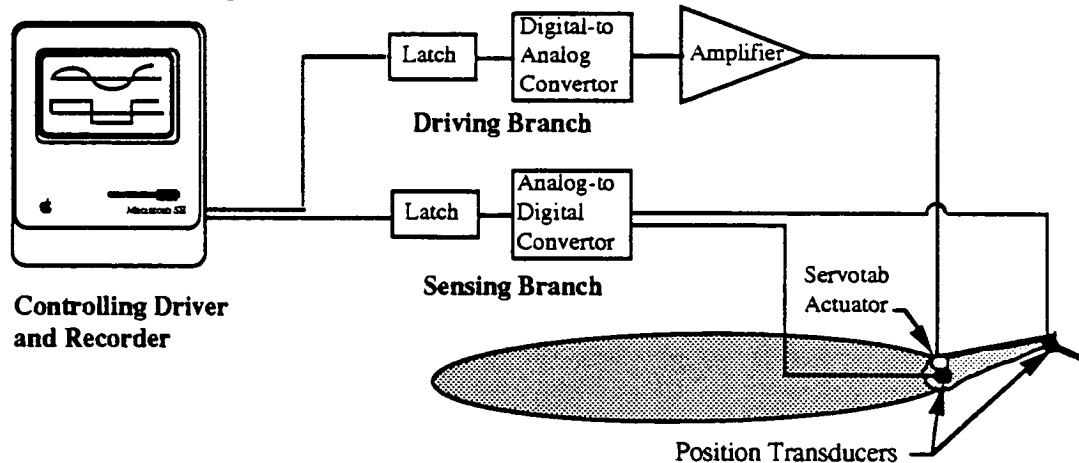
Figure 5.2 Iron Bird Driving and Data Acquisition Network

Testing of the controlling network and software will take place prior to the data acquisition network and software calibration. Upon completion of the calibration procedures, endurance runs will be performed over a span of weeks. Since one of the purposes is to determine the reliability of the system, it will be tested continuously during the endurance runs at all deflection amplitudes typical of each flight condition. The test and project schedule is shown below and includes completed activities (✓) and the number and type of students that have been assigned to each task .

Table 5.1 Iron Bird Schedule of Activities

Activity	1990 9 10 11 12	1991 1 2 3 4 5 6 7 8 9	Manpower
Literature Search	✓		2AE, 1EE
Derivation of Aileron and Servotab Equations of Motion	✓		2AE
Selection of Iron Bird Configuration		✓	2AE, 1EE
Construction of Iron Bird and Force Simulation System		✓	1AE
Design & Construction of Phase 1 Data Acquisition Network		✓	1AE
Design & Construction of Phase 1 Driving Network		✓	1AE
Calibration and Testing of Phase 1 Networks		✓	1AE
Endurance and Performance Test Runs using Phase 1 System			1AE
Data Reduction from Phase 1 Testing			1AE
Design & Construction of Phase 2 Data Acquisition Network			4EE
Design & Construction of Phase 2 Data Driving Network			4EE
Calibration and Testing of Phase 2 Networks			4EE
Endurance and Performance Test Runs using Phase 2 System			1AE, 4EE
Data Reduction from Phase 2 Testing			1AE, 4EE
Author Final Report for Ae 622			1AE, 4EE

45

The manpower that has been devoted to this project has been far less than required for completely successful conclusion of the above tasks within the required time. This is highlighted by the inability of the EE team to complete an automatic test system (Phase 2 data acquisition and driving network). In its place, a test system that requires a technician for operation was constructed (Phase 1 data acquisition and driving network). The Phase 1 test system successfully gathered the 38 hours of test data that is currently available.

The testing of the iron bird should provide a valuable set of data to the aerospace industry. If successful, this investigation will demonstrate a less expensive, more reliable, light-weight low power actuator system for use in general aviation aircraft.

5.2. SUMMARY OF IRON BIRD FORCE MODELING

There are four sources of forces and moments that act on the aileron and the servotab: aerodynamics, mass, structural and actuator. Their characteristics are outlined below and determined by using the procedures outlined in Ref.'s 5.1 and 5.2.

Several variables should be taken into account when determining the forces that affect the aerodynamic moments that act on the aileron and servotab.

    a. deflections of aileron and servotab

    b. wing angle of attack

    c. unsteady aerodynamic damping during rapid deflections

Mass and moments of inertia, friction and effective or actual spring forces and moments are generated and included in the model, as follows:

    a. mass-moment of inertia

    b. structural damping: bearing/support friction, Coulomb damping

    c. spring forcing: flexible members, actual springs included in system

    d. motion limiting at the stops of the aileron and the servotab

Actuators that drive the aileron and/or the servotab can generate static and/or dynamic forces that are position, force or rate dependent.

The sign convention that a positive rolling moment is generated by a positive aileron deflection will be used. A schematic of the right wing, aileron and servotab is shown below.
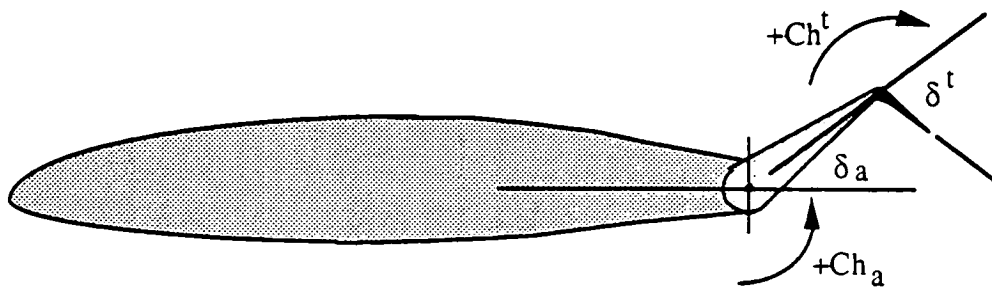
Figure 5.3: Sign Conventions of Aileron and Servotab

By considering the mass, moment of inertia, damping, spring rate and external forces, a matrix equation can be assembled as follows:

$$[I_o]\{\ddot{\delta}\} + [C]\{\dot{\delta}\} + [K]\{\delta\} = [F]$$

(eq. 5.1)

Expanding equation 5.1 details the components of each term.

46

$$\begin{bmatrix} I_{o_a} & 0 \\ -I_{o_t} & I_{o_t} \end{bmatrix} \begin{Bmatrix} \ddot{\delta}_a \\ \ddot{\delta}_t \end{Bmatrix} + \begin{bmatrix} C_{\dot{\delta}_a} & 0 \\ -C^t_{\dot{\delta}_a} & -C^t_{\dot{\delta}_t} \end{bmatrix} \begin{Bmatrix} \dot{\delta}_a \\ \dot{\delta}_t \end{Bmatrix} + \begin{bmatrix} K_{\delta_{a_{spring}}} - \bar{q}S_a\bar{c}_aC_{h_{a_{\delta a}}} & -\bar{q}S_a\bar{c}_aC_{h_{a_{\delta t}}} \\ -\bar{q}S_t\bar{c}_tC^t_{h_{\delta a}} & K_{\delta_{t_{spring}}} - \bar{q}S_t\bar{c}_tC^t_{h_{\delta t}} \end{bmatrix} \begin{Bmatrix} \delta_a \\ \delta_t \end{Bmatrix}$$

$$= \begin{bmatrix} HM_{a_{actuator}} + \bar{q}S_a\bar{c}_a\left(C_{h_{a_0}} + C_{h_{a_{\alpha w}}}\alpha w\right) + I_{o_a}\dot{Q} \\ HM^t_{actuator} + \bar{q}S_t\bar{c}_t\left(C^t_{h_0} + C^t_{h_{\alpha w}}\alpha w\right) - I_{o_t}\dot{Q} \end{bmatrix}$$

(eq. 5.2)

5.3 AILERON/SERVOTAB SYSTEM DESIGN

This section will outline the characteristics of the servotab driven aileron that will be used on the APT. This section will outline the procedures that were used to size the deflections required as a function of flight condition. The various modes of possible failure are also outlined as well as the systems designed to counter such failures along with a reliability and maintainability analysis. The flight hardware will be designed as well as the electronics that are required to be in each actuator for sensing and countering the various failures. Finally, a comparison of this system will be made to the systems that are used on conventional aircraft in terms of weight, internal volume, power, dynamic response, and reliability and maintainability. This section should provide the general overview of system viability and will be supported by the test data in the chapters to follow. The procedures used to obtain these results are detailed in Ref. 5.1.

5.3.1 Aileron/Servotab Sizing

The sizing of the aileron and servotab is an iterative process, the procedure that was followed was to start with the geometric constraints that are given by the rear spar, the flap, and the outline of the wing. Then, using the procedures outlined in Ref. 5.2, the rolling moments that were required to meet Level I and Level II flying qualities were determined. The deflections of the servotab corresponding to these rolling moments were determined. If the deflections were beyond $\pm30°$, then a recommendation would be made to enlarge the aileron so as to enhance the effectiveness of the aileron, and provide more roll control.Since both the aileron and servotab deflections required for Level I and Level II flight are less than $\pm30°$ of deflection, another iteration in the design process is not needed. Accordingly, the flaps and rear spar do not need to be moved to accommodate a larger aileron. This is shown in Table 5.2 and taken from Ref. 5.1.

Table 5.2 Required Aileron and Servotab Deflections

	Level I, δ_a	Level I, δ_t	Level II, δ_a	Level II, δ_t
Take-Off and Landing	$\pm19.7°$	$\pm23.8°$	$\pm9.85°$	$\pm11.9°$
Climb and Descent	$\pm8.70°$	$\pm10.8°$	±4.35	$\pm5.42°$
Cruise	$\pm4.79°$	$\pm7.96°$	$\pm2.40°$	$\pm3.98°$

5.3.2 Servotab Flight Hardware Considerations

Many different considerations were taken into account during the design of the flight hardware. Among these considerations were maintainability, reliability, cost, failure modes and

systems for countering failures, weight, internal volume and frequency response. Figure 5.4 details the arrangement of the servoactuator failure protection systems.

1. Strain gaged gear staging deck for loading verification

2. Mechanical microswitches within servo at mechanical limits

3. Thermistor on motor for cut-off

Actuator Arrangement

4. Ground resettable low amperage fuse
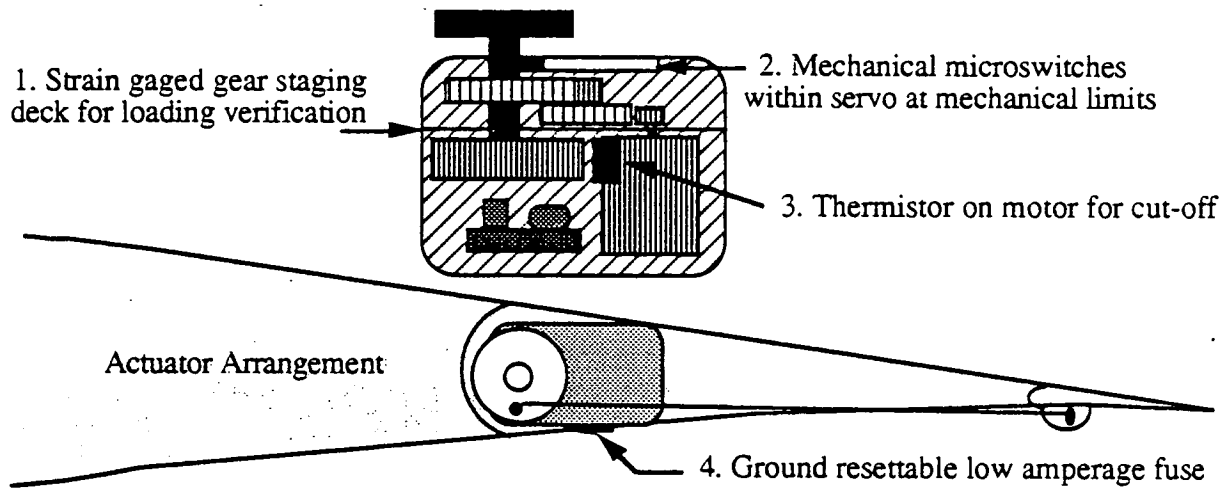
Figure 5.4 Servotab Actuator Arrangement within Aileron

The four system protections should provide protection for the aircraft so that the proper failure rates can be met. Again, there is very little data on the reliabilities of each subsystem because only 38 hours of testing has been documented on the Iron Bird. It should be noted that all 38 hours have been free of failure of any of the servoactuator, linkages, internal electronics and the servoactuator performance has not been degraded from the original performance. At this point, the reader is asked to refer to Chapter 5 of the APT Maintenance and Repairability Report under the Reliability Analysis of Servotab System and the Maintainability of Servotab Actuation System for further information on the considerations that governed the design of the aileron and servotab.

5.3.3 Design of Servotab Flight Hardware

The hardware that was designed for the aileron section uses Kraft Systems KPS-24 servoactuators. Figure 5.5 shows the KPS-24 servoactuators as they are integrated into the aileron at the root and tip. Note that the push-rod is on the pressure surface so that the upper surface flow will not be disturbed. If it were on the upper surface, then the laminar flow properties would be altered along with the possible triggering of trailing-edge stall. Reference 5.1 contains more information on the integration of the servoactuators into the aileron and servotabs of the APT.

For the integration of the servoactuators into the aileron structure, the hinge moment that each servoactuator was determined and the corresponding chordwise section of aileron was determined, with a safety factor of 2. This procedure was laid out in Ref. 5.1 and it was found that a 10" section of aileron is the maximum span that can be driven by a single actuator.

48

aileron section at root η = 0.76

push-rod

mounting plate

depleted uranium counterbalance

aileron section at tip η = 1.0

mounting plate

push-rod
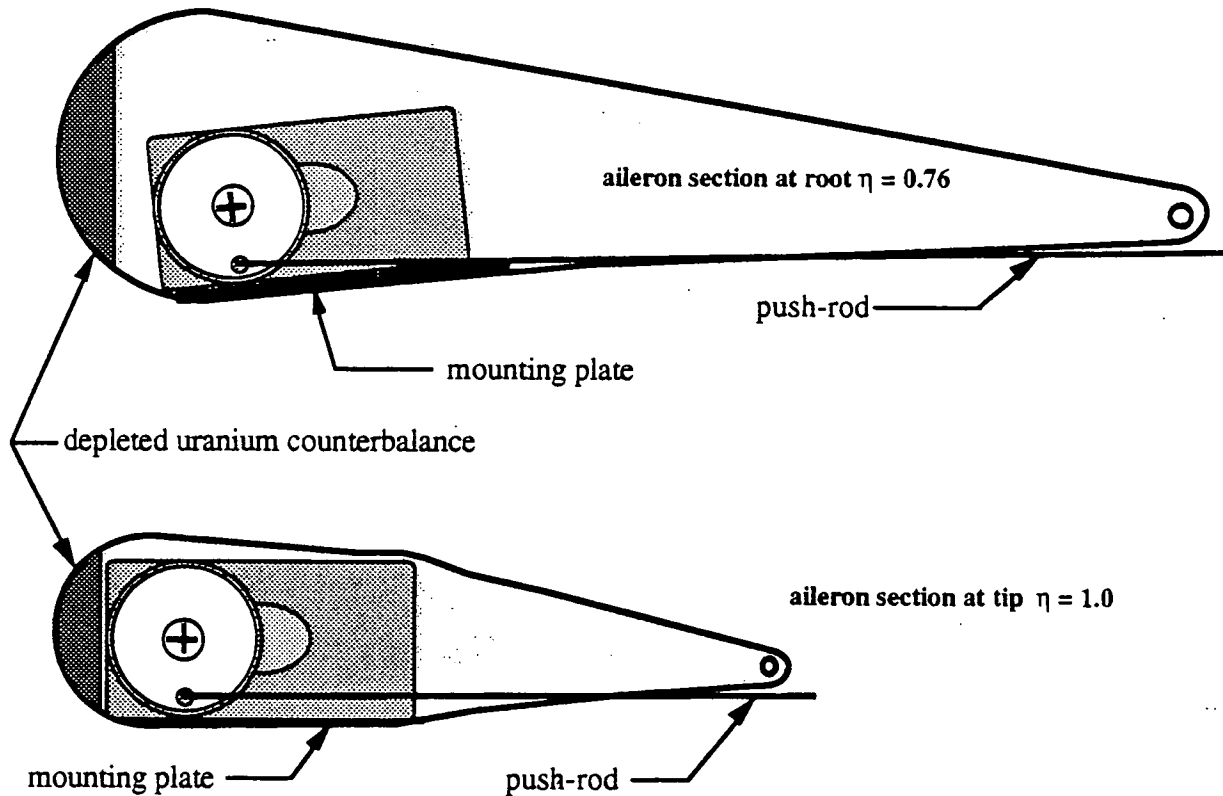
Figure 5.5: Arrangement of the KPS-24 Servo in the Aileron Structure (full scale)

The actuators towards the tip will drive still smaller loads (approximately 63% of the load at the root). These are the steady state loads and do not take into account any of the complex aerodynamic phenomena that occur at the tip. The tip vortices and more unsteady flow will cyclically load the servoactuators more than those at the root. Accordingly, they should carry less static loading. Figure 3.8 shows the integration of the servoactuators into a single aileron surface along with the access panels and linkages.

This concludes the design of the flight hardware for the aileron, servotab and actuation system. Still more detailed design is needed for production and is clearly beyond the scope of this investigation. For more information, the reader is asked to refer to Reference 5.1.

5.3.4 Comparison of Servotab System to Conventional Flight Control System

Table 5.2 summarizes the characteristics of the conventional flight control system using conventional servoactuators and the flight control system used on the APT which uses KPS-24 servoactuators. The data for Table 5.3 was obtained from Ref. 5.1.

Table 5.3 Comparison of Servoactuators and Flight Control Systems

	Conventional Flight Control System (King Radio KSA 470)	APT Flight Control System (Kraft Systems KPS-24)
Flight Control System Weights	263 lb	66.3 lb
Flight Control Internal Volume Required	7.5 ft^3	0.30 ft^3
Cruise Power Consumption	48 Watts	12.8 Watts
Servoactuator Unloaded Break Frequencies	19.5 Rad/s	10.2 Rad/s
Servoactuator Mean Time Between Failure	1500 Hours	1200-1400 hours
Annual Maintenance Time for Servoactuators	5.5 hours	2.3 hours (est.)
Acquisition Cost for Lateral Control System	$1650	$1900
Annual Maintenance and Replacement Costs	$1279	$1405

Table 5.3 shows the comparison of the two servoactuator systems. Comparable acquisition costs, dynamic response and maintenance times are overshadowed by the drastic reduction in control system weight, power consumption and internal volume required. Overall, the flight control system of the APT which uses the KPS-24 servoactuators will allow for significant gains over a conventional flight control system.

5.4. DESIGN, CONSTRUCTION AND TESTING OF THE IRON BIRD TEST APPARATUS

5.4.1 Spring-Forcing System

The procedures used to arrive at the spring-forcing system configuration are detailed in Ref. 1. Figure 5.6 shows the spring network mounted to the side of the aileron during testing.
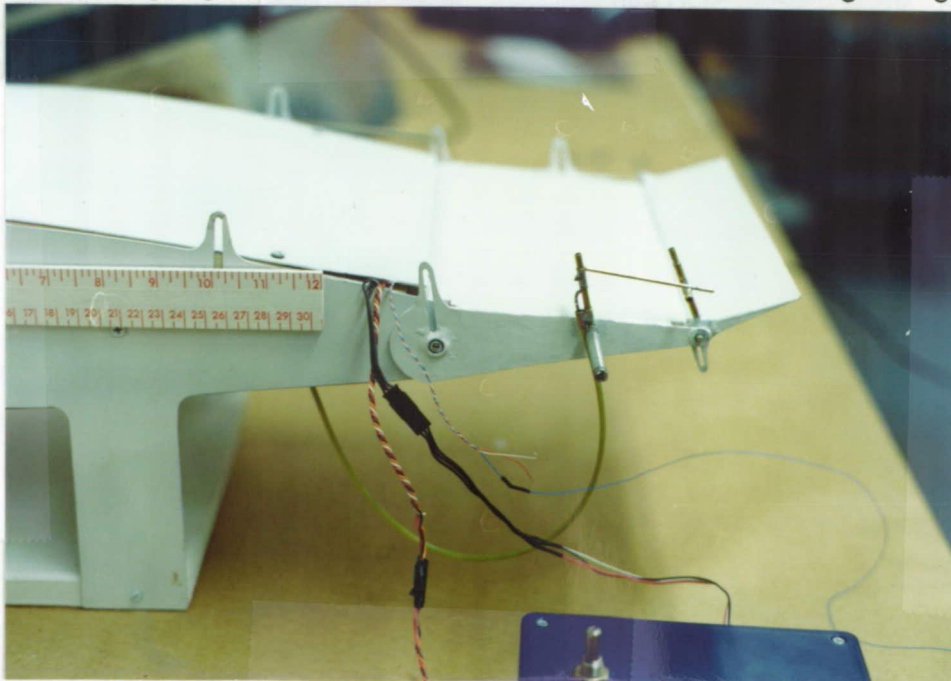

Figure 5.6: Configuration of Spring-Forcing Network on the Iron Bird

50

The full-scale figure in Appendix D of Ref. 5.1 shows the location and orientation of the rotary spring and linkages in greater detail.

5.4.2 Servoactuator System

The KPS-24 servoactuator that was integrated into the structure of the Iron Bird and was connected to the core with a 0.032 in. mounting plate. The push rod that drove the servotab penetrated the upper surface and was attached to a short horn on the upper surface. This arrangement was primarily made so that the actuator, linkage and supports could be observed constantly during the test process. If a failure were to occur in the linkage and it were not visible to the technician, then the results might go unnoticed for some time. This linkage along with the mirror that was used for deflection measurement with a laser and the rotary spring are shown in Figure 5.7.
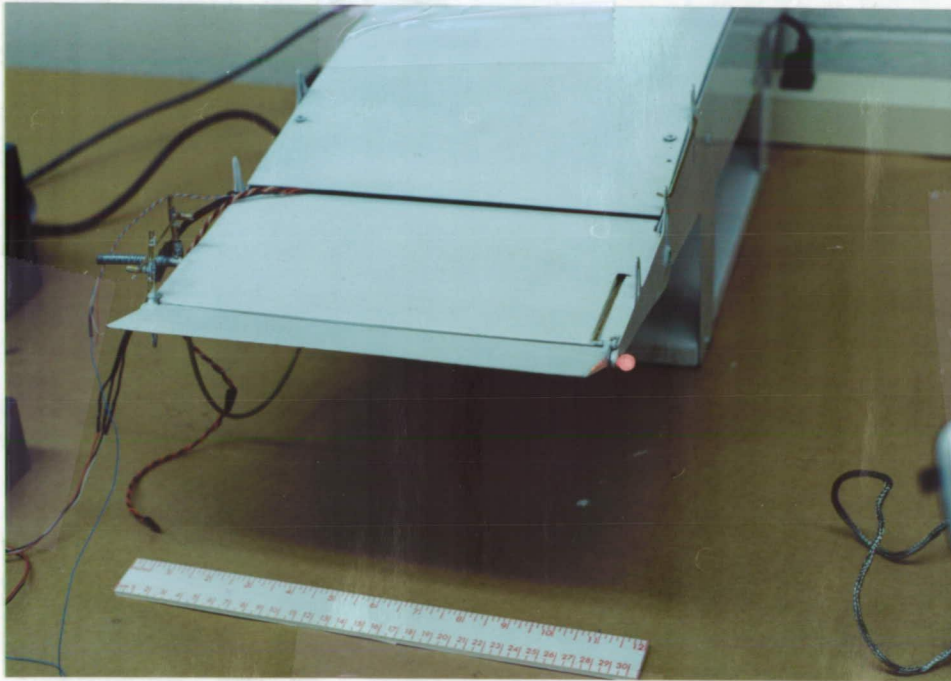
Figure 5.7 Iron Bird Apparatus Showing Mechanical Test Systems

5.4.3 Electronic Test Equipment

This equipment was designed and constructed with the goal of obtaining a usable test network that could drive the servoactuator and record the voltage history of the signals within the servoactuator itself. This is detailed in Ref. 5.1. The test network provided several different types of signals that corresponded to varying amplitudes of

The driver network utilized a TL555 timer chip integrated into an astable circuit. To use this chip in the network as designed, the amplitudes and frequencies that are desired must be known.

Mr. Dan Rogers of King Radio Corporation was asked to provide typical amplitudes and frequencies for aileron deflections under various flight conditions for a typical general aviation aircraft like the APT. Mr. Rogers provided data that corresponded to the Beech C-12F (King Air) that was modified by King Radio sponsored under a U.S. Army program. Table 5.4 delivers these frequencies and amplitudes.

Table 5.4 Lateral Surface Deflections as a Function of Flight Condition

Flight Condition	Deflection Amplitude	Characteristic Frequencies
Take-off and Landing	±85% max	1.5, 2.0 Hz
Climb and Descent	±30% max	0.5, 1.5 Hz
Cruise	±10% max	0.1, 1.5 Hz

It should be noted that there are two typical frequencies superimposed upon each other. The first frequency is due to deflections characteristic of the human pilot. These deflections are in response to maneuvers or gusts. The second frequency is that generated by the flight control system which constantly works to overcome the effects of gust perturbations. Both of these frequencies and the maximum amplitudes must be simulated by the driver network.

5.4.4 Test Procedures for Simulation of Flight Conditions

Several stages of preparation were conducted prior to the actual test runs. These stages included set-up of the measuring apparatus, positioning of the laser and connection of the servoactuators to the driver network.

Figure 5.8 shows all of the equipment that was used to drive the Iron Bird and record the voltage traces. The equipment on the left are the power supply and signal generator. The Metrologic Hard-Seal Helium-Neon laser (0.50 mW) is positioned on the tripod and is pointing at the deflection measurement mirror. This mirror is rigidly connected to the shaft of the servotab and moves the beam up and down on a recording sheet which is used for calibration.
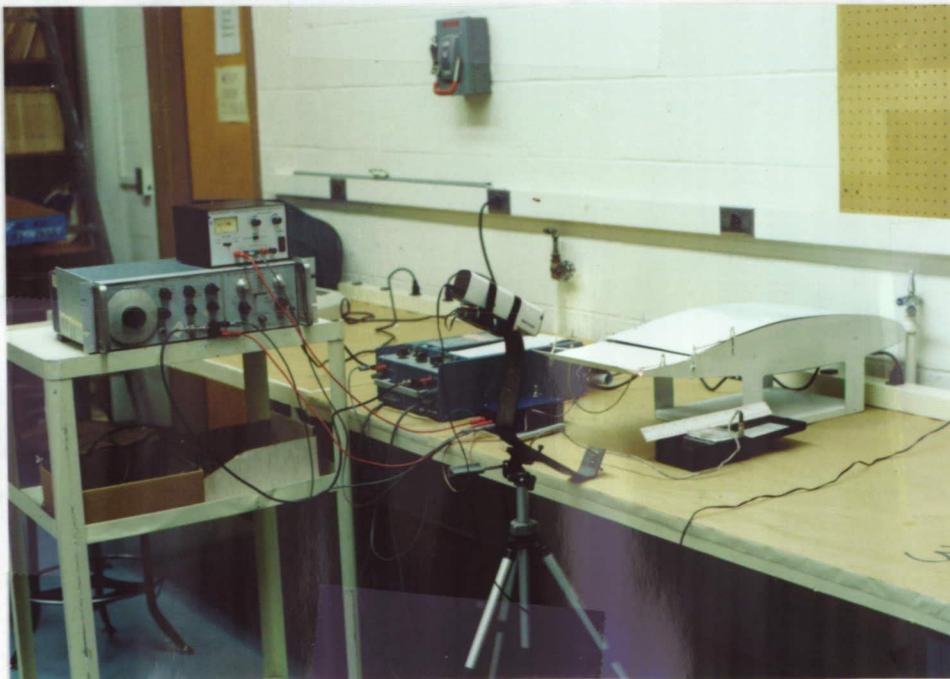

Figure 5.8 Laboratory Test Set-Up

After the test equipment was set-up in the proper position, the calibration of the servotab deflections was performed. First, a sweep of the maximum range was commanded to the servotab and can be seen in Figure 4.6 of Ref. 5.1. The maximum rate was commanded by the controller during this process. This was done by using square wave inputs at 0.10 Hz through the signal generator. These square wave inputs allowed the servotab position to be held for 10 seconds as its position was noted. Following this step, the voltage on the trim potentiometers was adjusted up or down corresponding to the angle of deflection desired. Figure 5.9 shows the trace of the laser beam deflection on the calibration sheet. The deflection commanded by the control system was checked against this actual deflection and adjustments to the trim potentiometers were made to compensate for any errors. When the trace was within ±5% of the commanded deflection, the calibration process was ended. The measuring board was placed 8 feet away from the mirror and the accuracy of the system is approximately ±0.05°. Dispersion in the laser beam (0.17 mrad) caused the beam diameter to be approximately 0.25" in diameter at the recording board. However, the accuracy required for the testing was far less than the accuracy that could be provided by the laser beam deflection measurements.
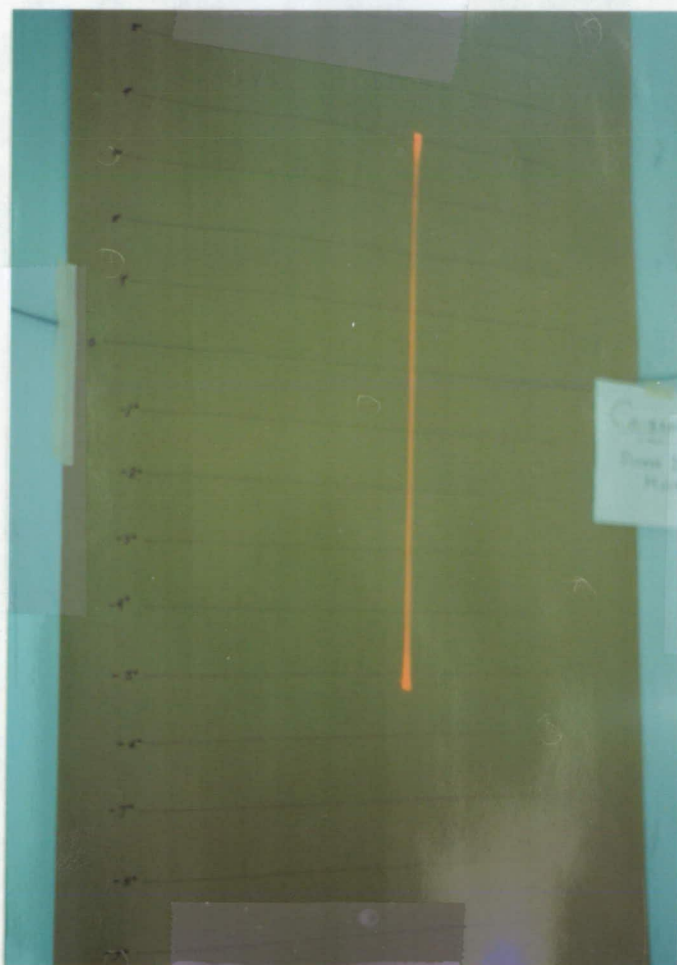

Figure 5.9 Laser Beam Trace on Measurement Board Due to Servotab Deflection

The single method that was available for recording deflection history was to use a two channel recorder. The two channel recorder recorded the amplitude and frequency of the input signal to the driver TL555 chip on one channel. The other channel was connected to the wiper arm on the servoactuator feedback potentiometer. This wiper arm channel recorded the transient voltages that were present in the potentiometer as it swept through its range. These voltages are not directly proportional to the deflection of the servoactuator. Instead, these voltages are an indication of failure within the servoactuator as any failure of any component within the servoactuator will show up as either a dead region or a spike. Since the purpose of this testing is not to obtain the dynamic response (which has already been obtained), the state of health of the servoactuator can be determined by analysis of the traces of the data. Appendix G of Ref. 5.1 delivers several sample traces from "flight" data taken during test runs. Both channels of the Gulton Industries TR-722 Two-Channel recorder were calibrated according to the input voltages that were delivered.

The ultimate goal of the experimental investigation is to test the servoactuator under simulated flight conditions. These conditions were simulated according to the schedule delivered by Mr. Rogers and deviated as little as possible. Because of the limitations of the test network that was devised, the steady frequency (low frequency) oscillations were limited to 0.3 Hz. This is not thought to pose much of a problem as the higher frequencies were the ones that challenged the servoactuator, not the low frequencies. From Table 5.4, considering maximum deflections at 30°, the deflections are scheduled as shown in Table 5.5.

Table 5.5 Servotab Deflections as a Function of Flight Condition for Iron Bird Testing

Flight Condition	Deflection Amplitude	Characteristic Frequencies
Take-off and Landing	±25.5°	1.5, 2.0 Hz
Climb and Descent	±9.0°	0.5, 1.5 Hz
Cruise	±3.0°	0.3, 1.5 Hz

From the mission specifications, the time schedule for each flight is shown in Table 5.6. The testing was conducted with the operator present at all times. In the future, an automated test network will be used and is outlined in Chapter 5 of Ref. 5.1.

Table 5.6 Test Time for Each Flight Phase

Flight Condition	Deflections	Frequencies	Time
Pre-Flight	±30.0° check twice	n/a	10 minutes
Take-off	±25.5°	1.5, 2.0 Hz	10 minutes
Climb	±9.0°	0.5, 1.5 Hz	20 minutes
Cruise	±3.0°	0.3, 1.5 Hz	4 hours
Descent	±9.0°	0.5, 1.5 Hz	20 minutes
Landing	±25.5°	1.5, 2.0 Hz	10 minutes
Taxi and Post Flight	no deflection	no deflection	10 minutes
Total Time for Flight Test			5 Hours 20 Minutes

A total of six simulated flights have been performed at the time of this report's authoring. Each flight was observed by the technician and the major events and observations are delivered in Table 5.7. One will notice the servoactuator internal temperature. This is from the thermistor that was placed beside the drive motor and can be seen in Figure 5.4.

Table 5.7 Summary of Major Test Results from Flight Testing

Flight	Servoactuator Failure(s) or Performance Decrease	Servoactuator Peak Internal Temperature	Observations and Remarks
1	none measured	158°F	all systems worked well
2	none measured	144°F	all systems worked well
3	none measured	165°F	2° calibration slip at test end, cause unknown
4	none measured	152°F	one driver chip (TL555) failed, 5 minute delay during replacement (no effect on actuator)
5	none measured	149°F	all systems worked well
6	none measured	147°F	all systems worked well

The servotab is seen during a flight test in Figure 5.10. This shows all systems functioning properly. The red glow near the servotab hinge is caused by the laser beam reflecting off of the mirror which is also visible. The linkages and rotary spring post are also in motion.
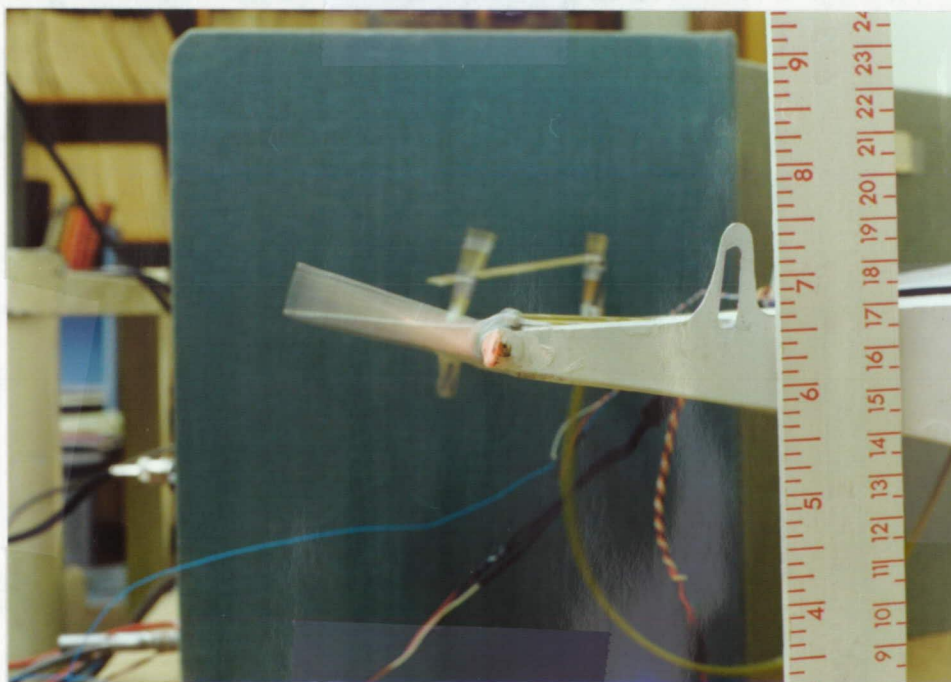

Figure 5.10: Servotab Undergoing Deflections During Flight Test Number 4

The final testing that was performed on the Iron Bird was a simple frequency response test. This test was conducted at the conclusion of each flight, after the servoactuator had cooled for 30 minutes. The results of the frequency response tests were nearly identical and are shown in Figure 5.11. This is surprising, considering the different flight conditions and wear on the actuators.

Servotab Actuation Frequency, Ω (Rad/s)
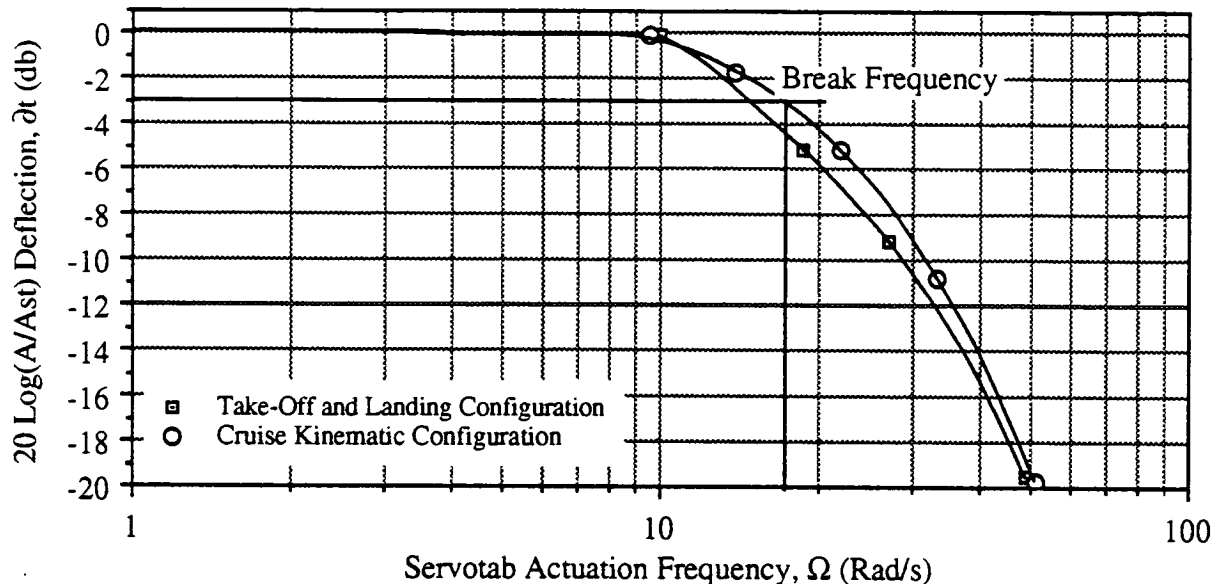
Figure 5.11: Loaded Frequency Response of Iron Bird

5.5. CONCLUSIONS OF IRON BIRD TESTING

From this investigation, conclusions on three major areas can be drawn.

*From data generated on the full-sacle APT flight control system, the KPS-24 servoactuator-servotab system exhibits drastic reductions in weight (75%reduction), power consumption (73% reduction) and internal volume (96% reduction) over conventional systems. The reliability, frequency response, and cost parameters are similar to those found in conventional flight control systems.

* The Iron Bird which was constructed for this investigation is adequate for evaluating the performance of the servoactuators under investigation.

* The performance of the Kraft Systems KPS-24 servoactuators has been error free. Through 6 simulated flights and more than 38 hours of testing at temperatures up to 165°F, the servoactuators have exhibited no failures or performance decrements.

5.6 REFERENCES FOR CHAPTER 5

5.1 Barrett, Ronald et al.,"Design, Construction, Test and Evaluation of an Aileron-Servotab Iron Bird," Report prepared for the NASA/USRA Advanced Design Program, University of Kansas, Lawrence, Kansas, 1991.

5.2. Roskam, Jan, "Airplane Flight Dynamics," Roskam Aviation and Engineering Corporation, Ottawa, Kansas 1982.

5.3. "Report on the Advanced Personal Transport," class project for Ae 621, University of Kansas, Lawrence, Kansas 1990.

5.4. Roskam, Jan,"Airplane Design, Part VI: Preliminary Calculation of Aerodynamic, Thrust and Power Characteristics," Roskam Aviation and Engineering Corporation, Ottawa, Kansas 1987.

5.5. Barrett, Ron, Cronister, Phil, and Rodkey, Brian, "Design, Construction and Test of an Iron Bird," Final Report prepared for Ae 621, Prof. Jan Roskam advising, University of Kansas, Lawrence, Kansas, 1990.

6. PROPULSION SYSTEM INTEGRATION AND RESIZING

This section will outline the procedures that were used for integrating the propulsion system into the airframe of the Advanced Personal Transport (APT). For efficiency throughout the flight envelope, a turboprop powerplant and propeller were selected as the propulsion system of the APT. This chapter will discuss the major design factors and the integration techniques that were used to choose the propeller and integrate the Garrett TPE331-15 turboprop engines into the airframe. Maintainability of the powerplants and drive system, engine installation and removal as well as ducting and external flow considerations will be addressed. The major conclusions of this section are that a 5 bladed Hartzell HC-E5N-3L/L8218 propeller was mounted to a Garrett TPE331-15 in a twin pac configuration.

6.1 PROPELLER SELECTION AND PERFORMANCE EVALUATION

A survey of several manufacturers was conducted to determine the pool of propeller candidates that may be used on the APT. Several major propeller manufacturers were contacted for this candidate propeller search. Ratier-Figeac, McCauley, Hartzell, and Hamilton-Standard were contacted. All manufacturers except for Hamilton-Standard responded with propeller data.

6.1.1 Manufacturers Survey of Propellers

Several candidate propellers were selected for consideration. The propellers were generally used on aircraft of the 8,000 to 12,500 lb MGWTO category. The typical powerplants that were used with these propellers were of 700 to 1000 shp.

Table 6.1 Summary of Manufacturers Propeller Data

Propeller	D (in)	B	AF	C_{Li}	Wt (lb)	P (hp)	N (RPM)	Vmax (kts)	Aircraft
McCauley 4HFR34C754	94	4	114	0.419	154	850	2000	317	USAF C12F
Ratier-Figeac 23LF-379	100	3	154	0.533	132	965	1900	405	FMA Pucará
Hartzell HC-B3TN-T10282-2.5	100	3	118	0.329	152	715	2200	282	Beech C99
Hartzell HC-E5N-3L/L8218	85	5	164	0.583	198	800	1885	420	Piaggio P-180

From conversations with manufacturers and examination of the propeller data, the superior propeller for the APT is the Hartzell HC-E5N-3L/8218. This 5 bladed propeller was specifically designed to the type of flight conditions that the APT will operate in. One difficulty with the propeller is that its small diameter severely limits the amount of shaft power that the propeller can make use of. A search of considerably larger diameter propellers (greater than 120 in. dia.) was not conducted because the configuration of the pusher APT. Rotation considerations and empennage interference concerns of the APT configuration were the primary diameter limiting factors. Accordingly, the power range of this diameter propeller fell between 700 and 1000 hp as outlined above. The sizing method that was used to determine the propeller diameter calls upon tip Mach considerations and power coefficient limitations.

6.1.2 Propeller Resizing Procedure

Due to the larger powerplant (twin pac), the Hartzell HC-E5N-3L/8218 will not be able to accept all of the power available at its original diameter. In conversations with the manufacturer, it was determined that changing two of the propeller characteristics will yield the maximum benefit. The propeller operational speed and diameter could be changed to accept a higher power level. This change in diameter would not significantly change the performance maps of the propeller until the propeller grew to more than 120% of its original diameter. It was thought that a greater number of blades may be one solution to the greater power acceptance, but the sizing criterion of Cp < 0.90

would not be affected by a change in number of blades and therefore would not affect the performance of the propeller significantly at the design conditions.

The critical flight condition for the APT with respect to propulsion system performance is the high altitude, high speed cruise. At 45,000 ft, 400 kts, most propellers and engines must be tailored very precisely. This flight condition will prove to be unacceptable because of tip Mach number limitations and noise considerations, but the performance prediction procedures will be outlined as they are the primary reasons that the aircraft performance specifications were reduced.

6.1.2.1 Determination of Hartzell HC-E5N-3L/8218 operating characteristics

At 400 kts, 45,000 ft, the Hartzell HC-E5N-3L/8218 operates at 1885 RPM with a diameter of

85 in. Accordingly, the helical tip speed is determined to be: $V_{tip} = \sqrt{V_\infty^2 + (\pi n D)^2} = 972$ ft/s.

At 45,000 ft, the speed of sound is 968 ft/s, accordingly, the tip Mach number is 1.01. It should be noted that this tip speed in reality is low because it does not take into account the induced velocity. Still, this tip Mach number is a full 10% higher than is traditionally considered the tip speed Mach limit of 0.90. In conversations with the manufacturer, it was determined that this high tip Mach number causes noise and power losses. From the configuration of the pusher, the noise considerations will only be of great importance to the empennage. For the tip-compressibility power losses, the designers of the HC-E5N-3L/8218 specifically designed the blades to operate in this range. Accordingly the tips of the HC-E5N-3L/8218 use the most advanced transonic airfoil cross sections and three dimensional effects are taken into account for precise tailoring of blade twist. As a result, the manufacturer claims that the tips are lightly loaded and fly at less than 2° angle of attack at this flight condition and as a result, the transonic losses are 75 to 90% lower than a traditionally designed blade.

From conversations with the manufacturer, it was determined that the operational tip Mach number should not be increased further. This means that the product, nD should be fixed at 222.5 ft-rev/s.

From examination of the propeller performance maps and conversations with the manufacturer, the limit on C_p is approximately 0.90. It may be physically possible to operate at higher values of C_p, but excessive losses will occur. The performance maps of the Hartzell HC-E5N-3L/8218 were used to further establish this Cp < 0.90 limit. At the design condition, approximately 350 lbf of thrust is required from the propeller. From section 6.1.2.2 it is seen that 515 hp is available at the design flight condition Accordingly the required efficiency is calculated:

$$\eta = \frac{\left(T_{required\ for\ flight}\left(100\% + \dfrac{T_{blockage} + T_{compressibility} - T_{exhaust}}{T_{required\ for\ flight}}\right)\right)V_{design}}{550 SHP_{av}}$$

$$\eta = \frac{(350\ lbf(0.99))(676\ ft/s)}{\left(550\dfrac{ft\text{-}lbf}{s\text{-}hp}\right)(515\ hp)} = 0.827$$

This propeller efficiency is at the limit of the performance map for a Cp of 0.90 which further validates the requirement that Cp must be less than or equal to 0.90 for this design at the high speed cruise condition. A change in number of blades to 6 will yield only marginal gains in C_{pmax} at a given efficiency. Accordingly, the 5 bladed propeller with a C_{pmax} of 0.90 will be considered.

6.1.2.2 Determination of powerplant characteristics at altitude

To size the propeller, the amount of power that the engine can produce needs to be determined at the design condition. Corrections for temperature, θ, and pressure changes, δ, as well as compressibility due to forward flight speed are taken into account with the following equation:

$$P_{alt} = P_{S.L.}\delta\left(1 + \frac{\gamma-1}{2}M^2\right)^{\frac{\gamma}{\gamma-1}}\sqrt{\theta\left(1 + \frac{\gamma-1}{2}M^2\right)}$$

The following conditions were used to determine the power at altitude:

h = 45,000 ft	humidity = 0.0%	γ = 1.40
V = 400 kts = 676 ft/s	a = 968 ft/s	M = 0.70
T = 390.0°R	θ = 0.752	
p = 2.139 psia	δ = 0.146	

$P_{S.L.}$ = 1645 hp x 2 = 3290 hp

From the above equation, $P_{alt} = 0.184 P_{S.L.}$.

The power at altitude at the design condition without corrections for installation is 606 hp.

From conversations with powerplant expert Dr. Saeed Farokhi, the installation losses for both configurations in the inlet and exit ducting will be (conservatively) 7%.

The gearing losses from the Soloy twin-pac engine were determined to be approximately 4% from discussions with the manufacturer. Current versions of the twin-pac operate with slightly higher losses (4.8%), but Soloy expects this number to drop to less than 3% with improvements. Accordingly, the 4% gearing loss is considered conservative.

The losses from cabin pressurization and accessory drive were not available in precise numbers, but from discussions with Soloy on typical high altitude applications in aircraft of this category, 4% of the power will be lost.

From these estimations, the amount of power that will be available to the propeller is calculated as follows: $SHP_{av} = P_{av}(100\% - P_{ducting} - P_{gearing} - P_{accessory\&cabin\ air})$

$$SHP_{av} = 606\ hp(100\% - 7\% - 4\% - 4\%) = 515\ hp$$

6.1.2.3 Application of power and propeller requirements to propeller resizing

With a tip speed limitation, the product nD must be held constant, with Cp limited to 0.90 and a density of 0.0004601 slugs/ft^3, the equation for Cp is used for determination of the new propeller parameters. Recall that $n_{old}D_{old} = n_{new}D_{new} = 222.5\ \frac{rev\ -\ ft}{s}$ and accordingly,

$$C_P = \frac{550 SHP_{av}}{\rho n_{new}^3 D_{new}^5} = \frac{550 SHP_{av}}{\rho\left(\frac{n_{old}D_{old}}{D_{new}}\right)^3 D_{new}^5} = \frac{550 SHP_{av}}{\rho(n_{old}D_{old})^3 D_{new}^2}$$

from this, $$D_{new} = \sqrt{\frac{550 SHP_{av}}{\rho(n_{old}D_{old})^3 C_{Pdesign}}} = 7.9\ ft = 95\ in.$$

The propeller speed follows: N_{new} = 1687 RPM

6.1.3 Propeller Resizing for Considering New Mission Specifications

From the examination of section 6.1.2, it was decided that the tip Mach number was far too high at the maximum cruise condition. This high tip Mach number would produce an excessive amount of noise and structural fatigue on the booms. Another concern to the design team was that of the ground clearance of the propeller upon rotation.

The design team considered all of the detracting elements of the new propeller diameter and set the new cruise Mach number and altitude lower than the 400 kts at 45,000 ft of the earlier design. Accordingly, it was also decided that the propeller should be the original 85" Hartzell HC-E5N-3L/L8218 and should operate at 1885 RPM. For the determination of the new performance of the propeller, the procedures used will follow those of sections 6.1.2.1 and 6.1.2.2.

6.1.4 Performance of Powerplants and Installed Propeller

Three corrections of the thrust must be determined for the integration of the propeller. The first is due to prop tip Mach effects, the second is due to slipstream blockage and the third is to account for the thrust contribution from the exhaust.

From Figure 7B.1, of Ref. 6.1, the amount of efficiency or thrust loss due to compressibility is approximately 20%. From section 6.1.2.1 it was seen that the design of the propeller reduces this by 75 to 90%. Accordingly, the losses from compressibility are approximately 2 to 5%. Losses of 3% will be used to account for compressibility.

From Figure 7B.3, of Ref. 6.1, approximately 3% of the thrust will be lost due to the effects of a scoop inlet.

From manufacturers data on the TPE331-15, Ref. 6.2, approximately 7% additional thrust can be counted upon at this flight condition from the engine exhaust.

Adding the three contributions above yields a 1% increase in net thrust of the propulsion system as seen in section 6.1.2.1.

From the Hartzell Performance maps of Ref. 6.3, the propeller efficiency was determined at given values of Cp and J. The thrust of the propulsive system was then calculated from:

$$T = 550\eta_{corrected}SHP_{av}/V$$

The fuel flow was calculated according to the SFC at given flight conditions. The results of these calculations are shown in Figures 6.1, 6.2 and 6.3.

The code that was developed for the prediction of the engine performance used all of the assumptions listed in sections 6.1 with respect to installation losses, gearing losses, tip losses, altitude, and flight speed. Not included are estimates for off-design conditions that would induce significantly more fuel flow or cause considerable performance decrements. Among these off-design flight conditions are high humidity, non-standard atmosphere and performance decrements caused by engine wear.

The performance of the TPE331-15 is calculated for various flight conditions considered for the typical mission. The extension of the data to the static thrust range is included so that take-off roll estimates may be performed. These estimates followed the procedures laid out in Chapter 7 of Ref. 6.1 for the propeller and used the engine data of Ref. 6.3.

61
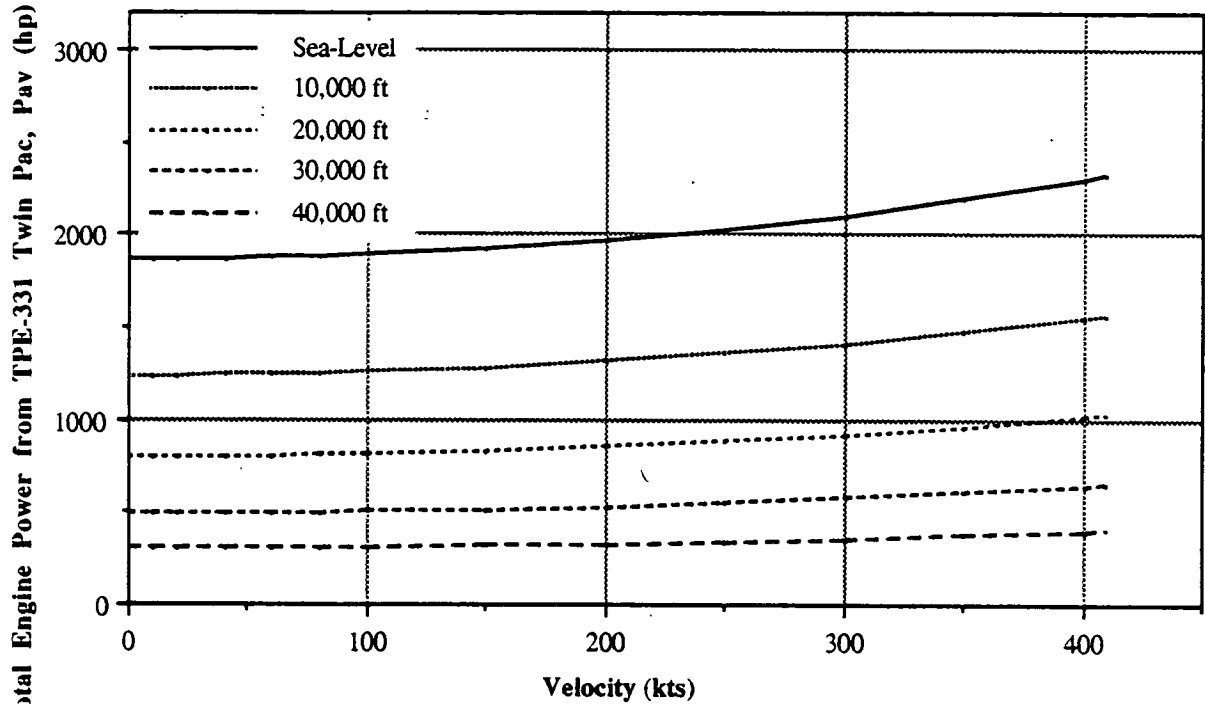
Total Propulsive System Power as a Function of Flight Speed

Figure 6.1: Shaft Power Available to the Propeller
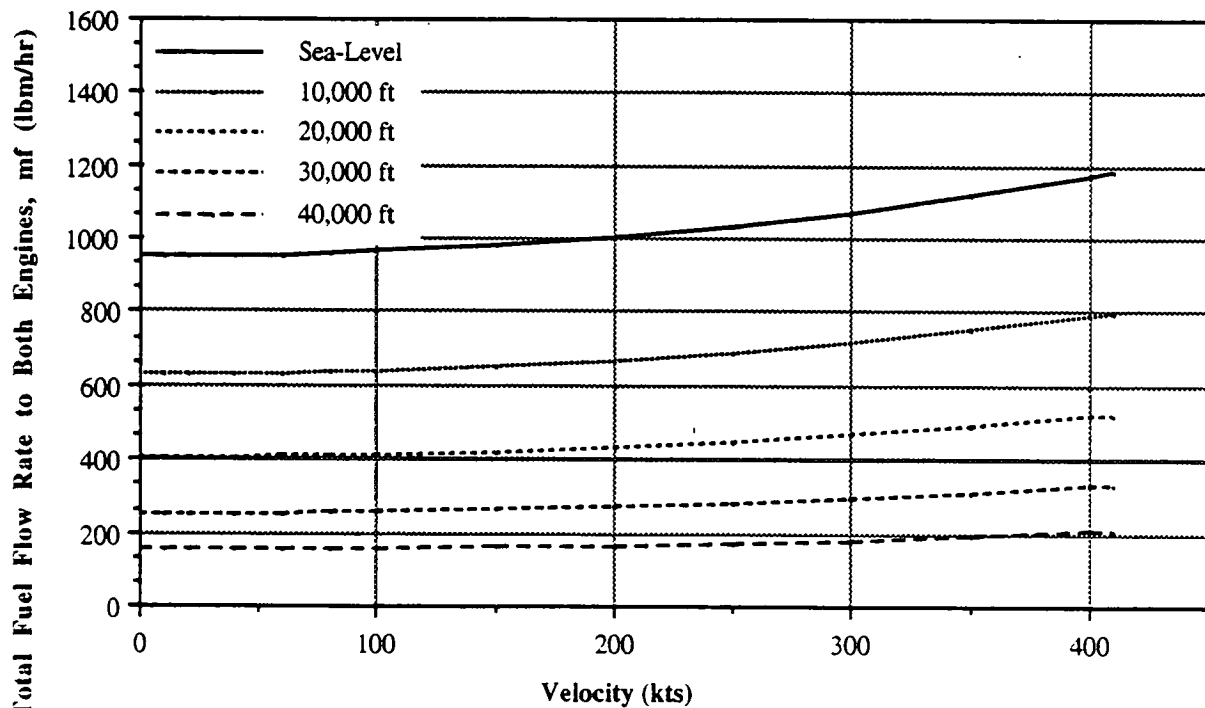
Total Fuel Consumption as a Function of Flight Speed

Figure 6.2: Fuel Flow Rates of Both Engines
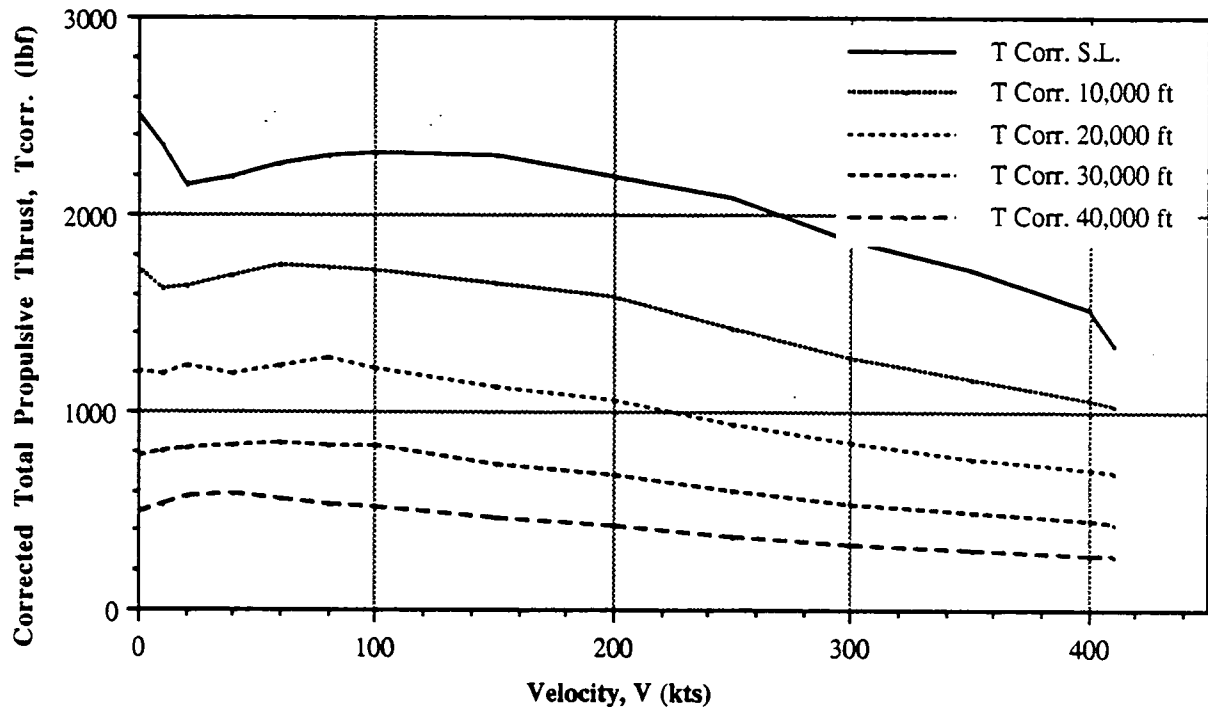
Total Propulsive System Thrust as a Function of Flight Speed

Figure 6.3: Propulsive System Corrected Thrust

6.2 INSTALLATION OF POWERPLANTS AND PROPELLER INTO THE APT AIRFRAME

The two Garrett TPE331-15 engines were integrated in the pusher configuration along with a gearbox joining the engines and combining the powerplants to one shaft. A small shaft extension was added to the gearbox to allow for better faring of the aft end of the aircraft. From conversations with Soloy engineers, several integration considerations should be taken into account.

* Reduce ducting losses to a minimum through gradual bends in short inlet ducts.
* Support both engines in one very rigid support truss to minimize gearing mismatch at the engine power take-off shaft
* Consider an oil cooler for improved reliability and lower maintenance
* Firewall and fire suppression system
* Consider chip count sensors for prognostics/diagnostics
* Consider integration of torque, RPM and fuel flow instruments into the on-board computer

Taking all of the above considerations into account as well as accessibility and maintainability, yields a better picture of the integration scheme as shown in Figures 6.4, 6.5, 6.6 and 6.7.
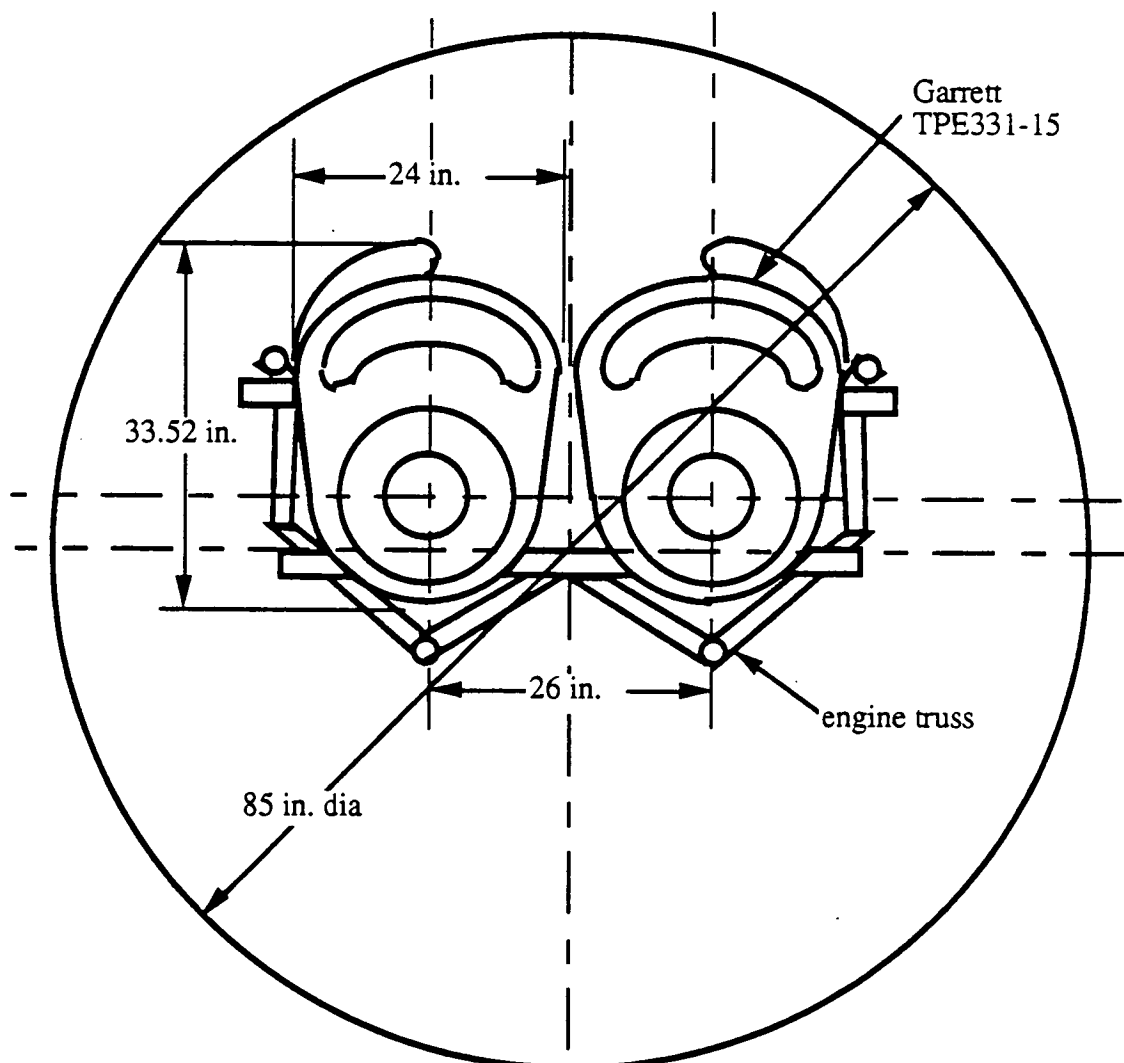
Figure 6.4: Rear View of Powerplants and Propeller Installed in the APT Airframe

inlet

oil cooler inlet

oil cooler exhaust

oil tank

gearbox

engine inlet

engine shaft centerline

prop centerline

engine exhaust

21 in. dia

fire wall

spinner
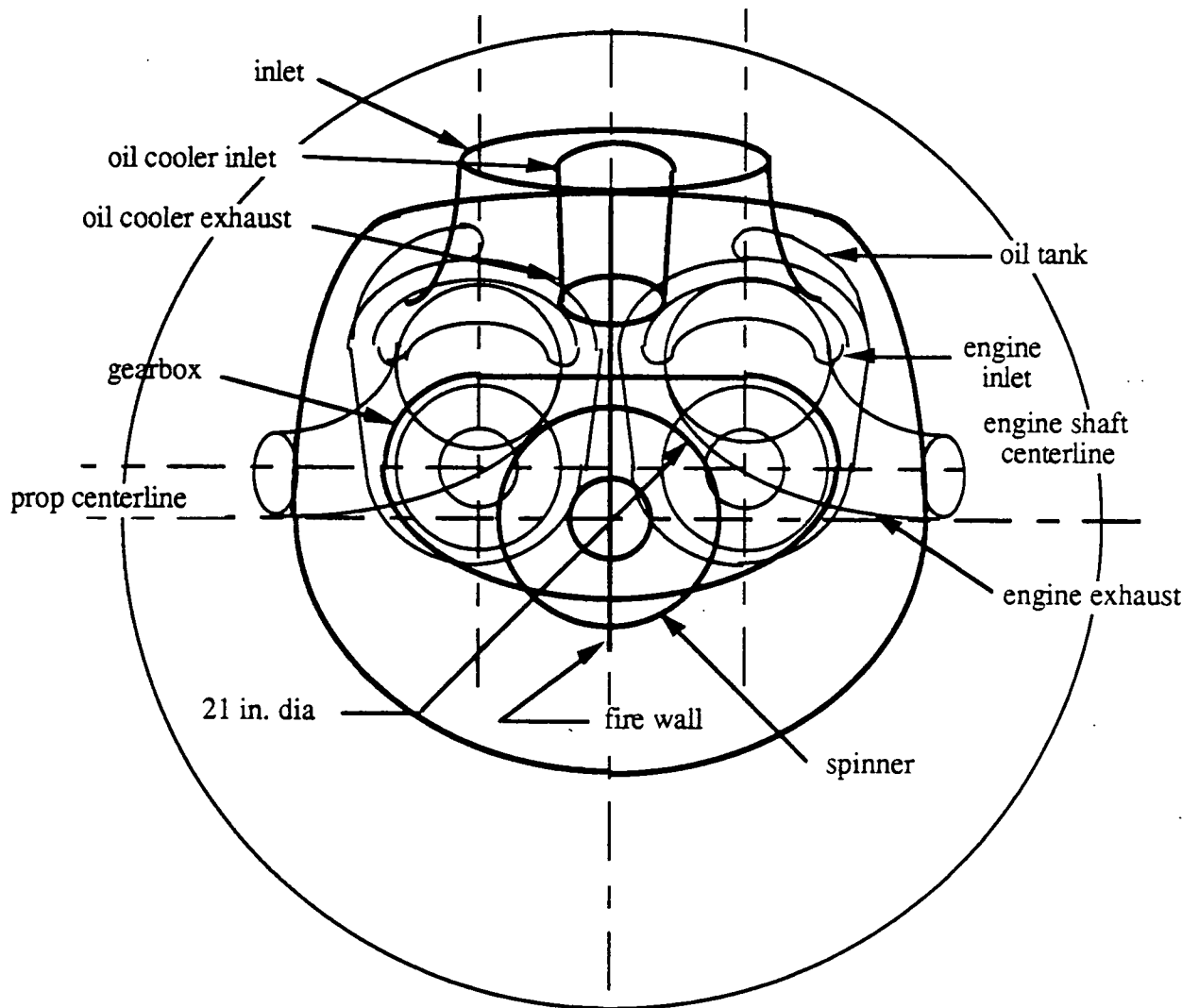
Figure 6.5: Rear View of Powerplants and Propeller Installed in the APT Airframe

ALL DIMENSIONS IN INCHES

417.0

520.7
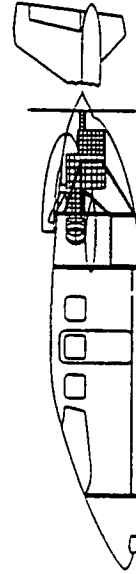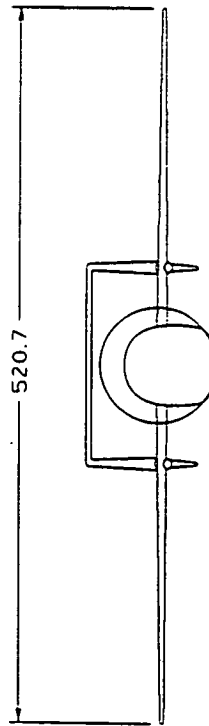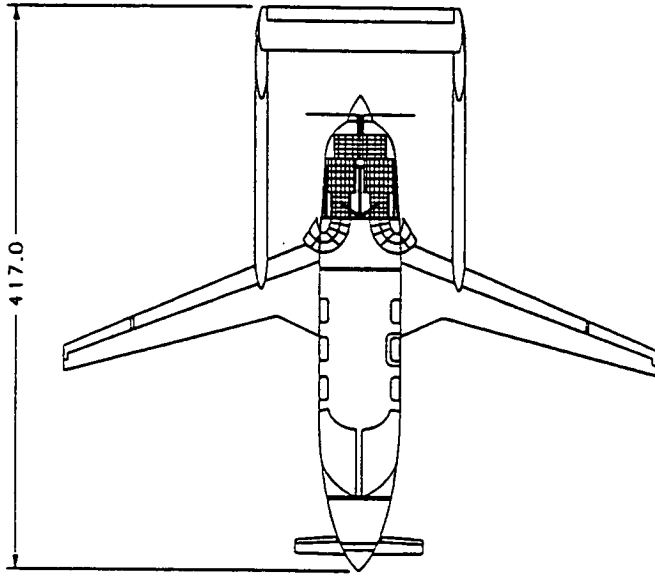
Figure 6.6: TPE331-15/Twin Pac™ General Airframe Installation
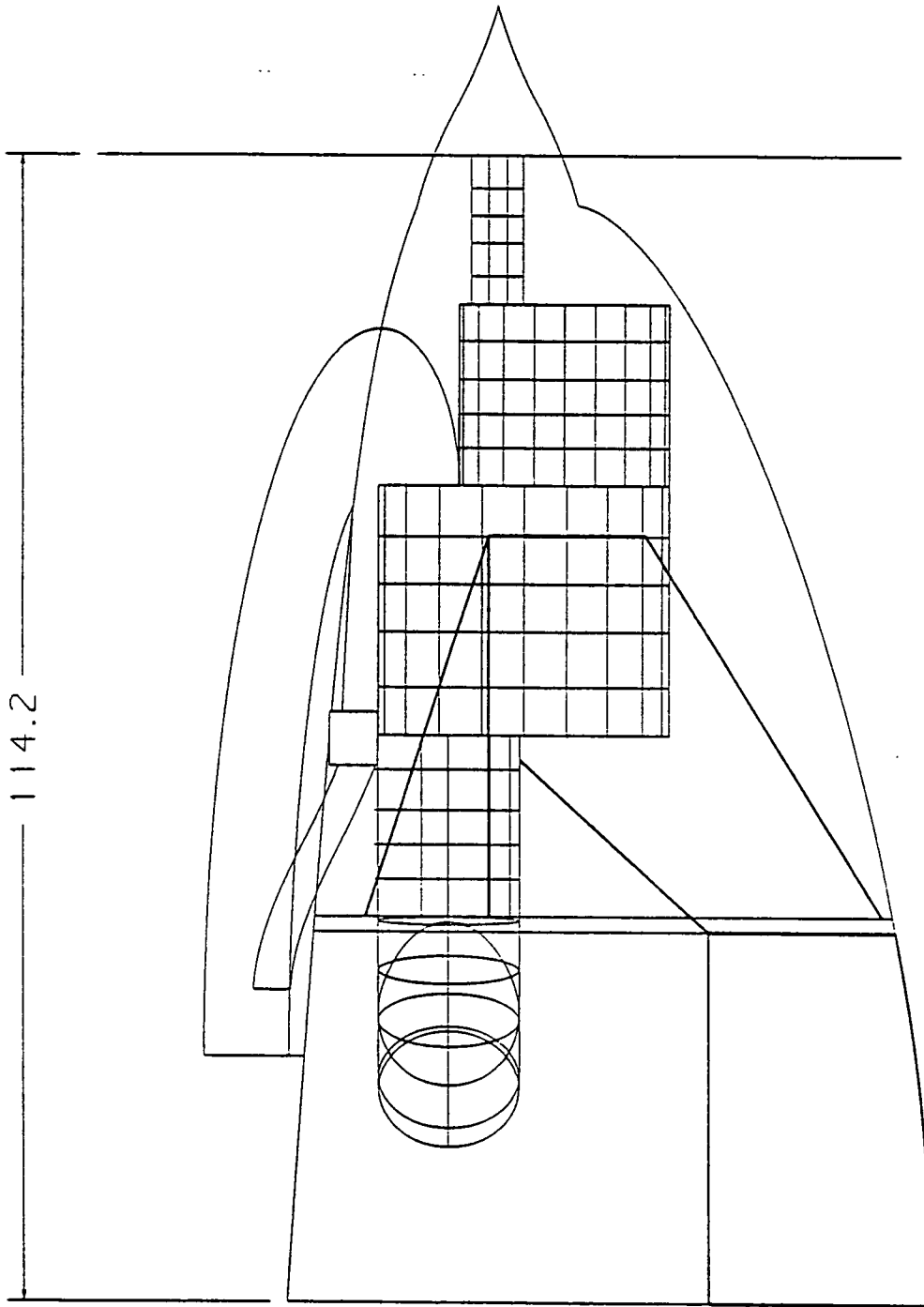
ALL DIMENSIONS IN INCHES

Figure 6.7: TPE331-15/Twin Pac™ Airframe Installation Side View

114.2

6.3 REFERENCES FOR CHAPTER 6

6.1 Lan, C.T., and Roskam, J, "Airplane Aerodynamics and Performance," Roskam Aviation and Engineering Corporation, Ottawa, Kansas, 1980.

6.2 "The Garrett TPE331," Information Brochure published by Garrett Engine Division, Phoenix, Arizona, 1988.

6.3 Chalfant, Wayne et. al., "Hartzell HC-E5N-3L/L8218 Performance Data," performance data sheets published by Hartzell Propeller Inc. Piqua, Ohio 1990.

7. APT SYSTEM LAYOUTS

The purpose of this chapter is to summarize the results of reference 7.1 chapter 5, in presenting the components of the fuel and de-icing systems. Other systems such as: landing gear, pressurization, pneumatic, air conditioning, and avionics were designed during phase 1 and did not require refinement. These systems can be found in reference 7.2. The fuel and de-icing system were studied in more detail due to changes in the basic wing planform. In addition, the initial design choices for the fuel and de-ice system can be found in reference 7.2.

Section 7.1 presents the Electro-Impulse De-Ice, EIDI, system and section 7.2 presents the revised fuel system.

7.1 ELECTRO-IMPULSE DE-ICING SYSTEM

The purpose of this section is to present the de-icing system for the Advanced Personal Transport.

An EIDI system was chosen during phase 1 for the following reasons:

* Electro Impulse coils require only about 300 watts
  for operation, about 1 percent of that required by
  heated wires.

* Electro Impulse coils do not cause delamination in
  composites.

* Electro impulse coils are small: Length - 1 in.
                                     Diameter 2 in.

* There is built in redundancy with a coil located
  approximately every 20 inches.

The EIDI coils are flat wound copper ribbon wire placed just inside the leading edge of the wing's skin with a small gap separating skin and coils. The coils are connected by low resistance, low inductance cables to a high voltage capacitor bank, and energy is discharged through the coil by a remote signal to a silicon-controlled-rectifier. Discharge of the capacitor through the coils creates a rapidly forming and collapsing electro-magnetic field. The fields resulting from current flow in the coils and skin create a repulsive force of several hundred pounds magnitude, but a duration of only a fraction of a millisecond. The small amplitude high acceleration movement of the skin acts to shatter, debond and expel the ice (7.3, 236). Two or three such hits are performed sequentially then the ice is permitted to accumulate until it again approaches an undesirable thickness.

Composite (Non-metallic) leading edges require a doubler, an unalloyed aluminum disc slightly larger than the coils, to be bonded to the leading edge to provide adequate conductance for the eddy currents.

7.1.1 APT Ghost View

The purpose of this section is to present the ghost view for the EIDI system in the Advanced Personal Transport.

Table 7.1 lists the components that make up the de-ice, anti-ice, and de-fog systems.

Table 7.1 Components of the de-ice, anti-ice, and de-fog systems in the APT.

1. Computer
2. Power Distributor
3. From Busbar
4. To Windscreen
5. Inlet
6. Electro-Impulse Coils

Figure 7.1 shows a ghost view of the Advanced Personal Transport with the de-icing, anti-icing, and de-fogging systems included. As a component of the de-icing system, the computer receives information from sensors concerning the ambient temperature and humidity. One of these sensors could be a small wire whose frequency in the airflow is known and when it is not at that frequency for a given flight condition, icing conditions are present. The wire could be heated and the frequency rechecked to determine the amount of icing that is collecting on the plane. Based on these parameters the computer will switch on the de-ice, anti-ice, and de-fog systems. The computer does this by controlling the power distribution box.

The power distribution box switches power to the de-ice, anti-ice, and de-fog systems. The switch is located next to the computer and not next to the wing to allow for landing gear retraction. The power for the coils is supplied by the generator as are most of the aircraft systems.

Item three is the sensor feedbacks used by the computer. Item four is the de-fog for the windshield, this is a heated wire placed within the windshield. Item five is the anti-ice heating element placed on the inlet since ice cannot be allowed to form on the inlet. Notice that at each spanwise location on the canard, wing, and horizontal tail two EIDI coils are employed. This was required because the leading edge radius is relatively small and has nearly straight upper and lower surfaces behind the leading edge.(7.4)

The next logical question for this system is one of fatigue life. A Learfan composite leading edge with a coil pair at each span station was tested, and after 20,000 impulses no damage was visible (7.3). An ultrasonic scan also showed no detectable change. In addition, the tests were performed in a cold box to see the effects of the cold on the bonding agent used to attach the doubler to the skin. Again, no delamination could be detected. From talks with

LEGEND

1 COMPUTER
2 POWER DISTRIBUTOR
3 FROM BUSBAR
4 TO WINDSCREEN
5 INLET
6 ELECTRO IMPULSE COILS
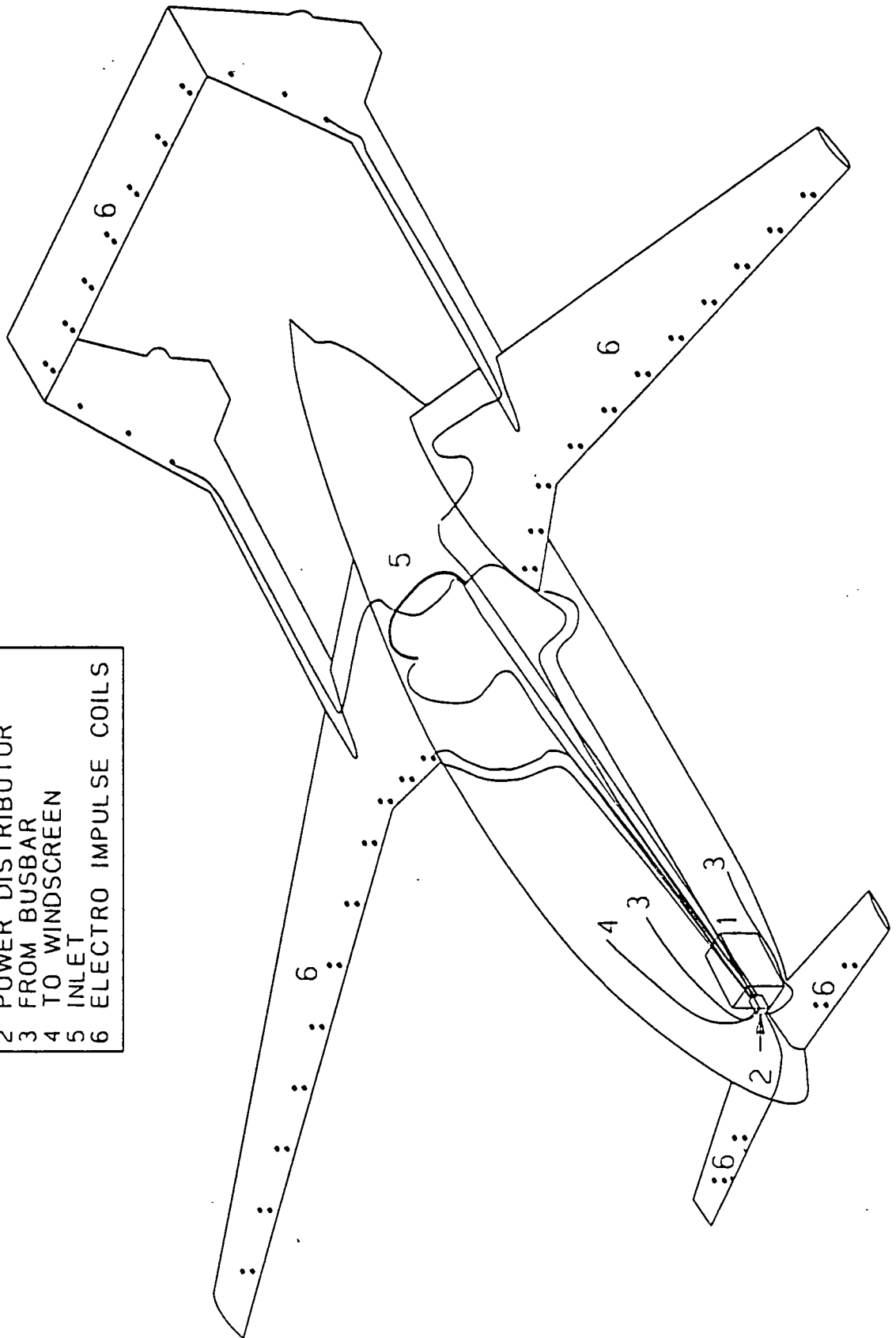
Figure 7.1 : De-Icing, Anti-Icing, De-fog systems in the APT

71

Beechcraft on the Starship 2000, their certification process has shown that the composite bonds are usually the strongest bonds on the entire aircraft. Additional tests were performed by Boeing and these results can be found in reference 7.3.

7.2 APT FUEL SYSTEM

The purpose of this section is to present the fuel system incorporated into the preliminary design of the APT. The purpose of the fuel system is to store and distribute the fuel used by the APT. The fuel system also monitors fuel level and fuel consumption.

7.2.1 Fuel System Functional Diagram

The purpose of this section is to present the fuel system functional diagram. Figure 7.2 on the following page shows the proposed diagram.

The filler caps are located at the tip of each wing. From there the fuel goes through flapper valves into a second wing section. Sumps and vents are located in both sections. The boost pump, is a submerged, constant speed, centrifugal, D.C. powered pump capable of delivering up to 2000 lbm/hr of fuel. The boost pumps operate in the 20-60 psi range, and a failure is registered by the computer when the pressure drops below 3.2 psi. (7.5) From the boost pump the fuel goes into the manifold and through the check valves. From there it passes through the filters and through two separate lines to the engine driven pumps.

The fuel manifold is located inside the center main tank, in the picture it is pulled outside the center line for demonstration purposes only. Included in the manifold is the suction feed valve. In the case of an emergency the suction feed valves allow the engine driven low pressure fuel pumps to draw fuel from the center tank. During normal operations the valve remains closed due to fuel pressure within the manifold.

It is hoped that optical type sensors will be used for measuring the fuel level in the fuel tanks. According to the article USAF Center Solves Communications Avionics Problems with Fiber Optics, in Aviation Week and Space Technology, "..fiber optics are more reliable, more versatile, take up less space, and offer real-time analysis capability... fiber optics will take the lead over other types of sensors..."(7.6). However, at this time not enough factual information is available so a capacitance type sensor will be used. This type of sensor is used on the Beech Starship 2000 and works much the same way as a car battery only now the diodes are used to measure fluid level instead of storing electrical energy.

7.2.2 APT Fuel System Ghost View

The purpose of this section is to describe the ghost view of the fuel system in the APT. Before this is done a summary will be given on the status of available fuel volume.

Table 7.2 lists the components of the APT Fuel System.
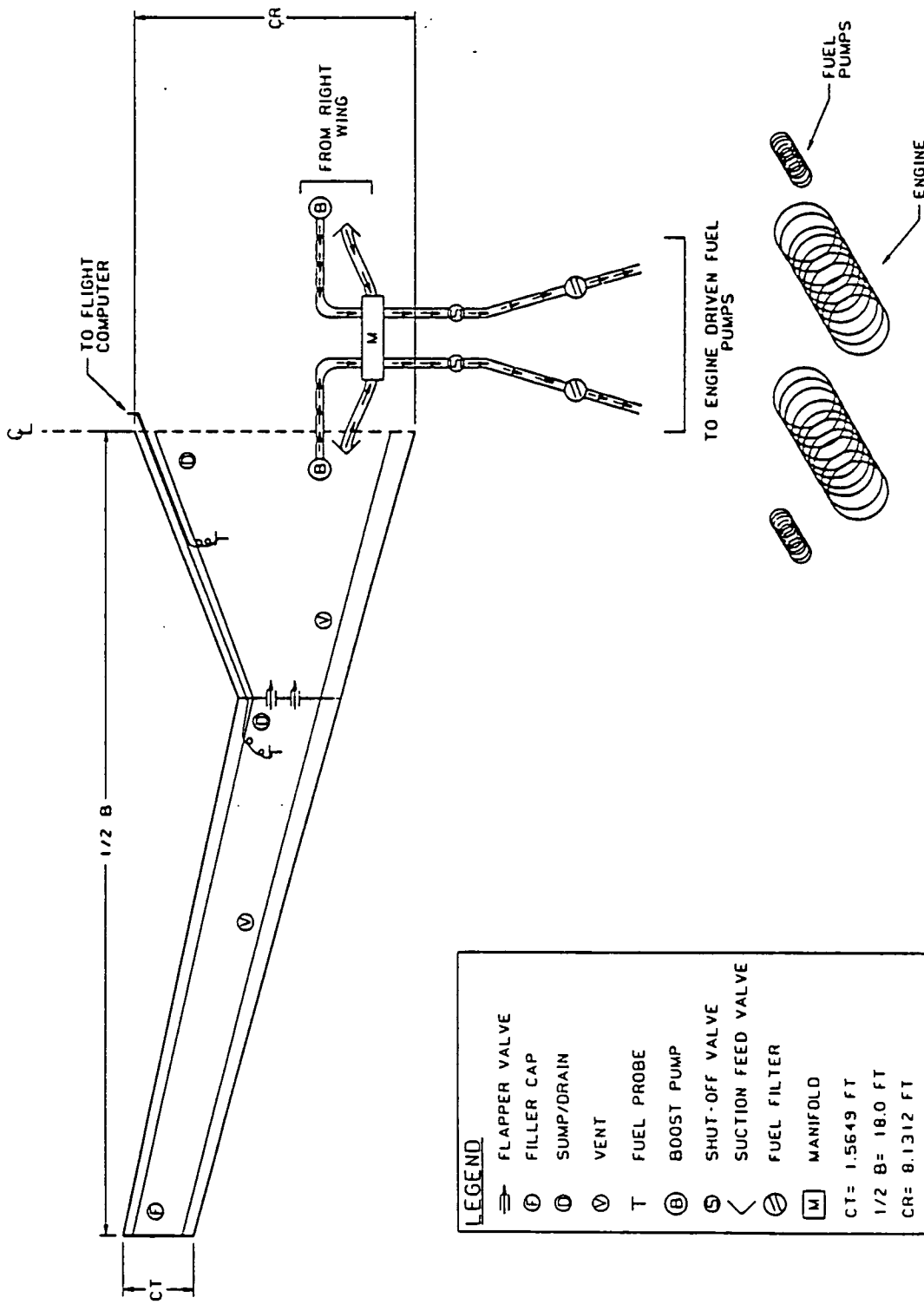
Figure 7.2 : Fuel System Functional Diagram

LEGEND

⇉	FLAPPER VALVE
Ⓕ	FILLER CAP
Ⓓ	SUMP/DRAIN
Ⓥ	VENT
T	FUEL PROBE
Ⓑ	BOOST PUMP
Ⓢ	SHUT-OFF VALVE
∨	SUCTION FEED VALVE
Ⓘ	FUEL FILTER
Ⓜ	MANIFOLD

CT= 1.5649 FT
1/2 B= 18.0 FT
CR= 8.1312 FT

73

Table 7.2 Components of the Fuel System Ghost View

1. Computer
2. Engines (2)
3. Engine Driven Mechanical Pumps
4. Sumps (4)
5. Vents (4)
6. Sensors (6)

Note: The numbers in Table 7.2 correspond to those in Figure 7.3 on the following page.

Figure 7.3 shows a ghost view of the three surface APT configuration including the fuel system layout.

The ghost view shows in a macroscopic view what was presented in the fuel system functional diagram section. However, due to insufficient fuel volume, additional fuel will need to be stored in the tail boom assembly. This is shown in the ghost view by placing circles in the tail booms. This fuel can be accessed through flapper valves like those used between the different fuselage sections.
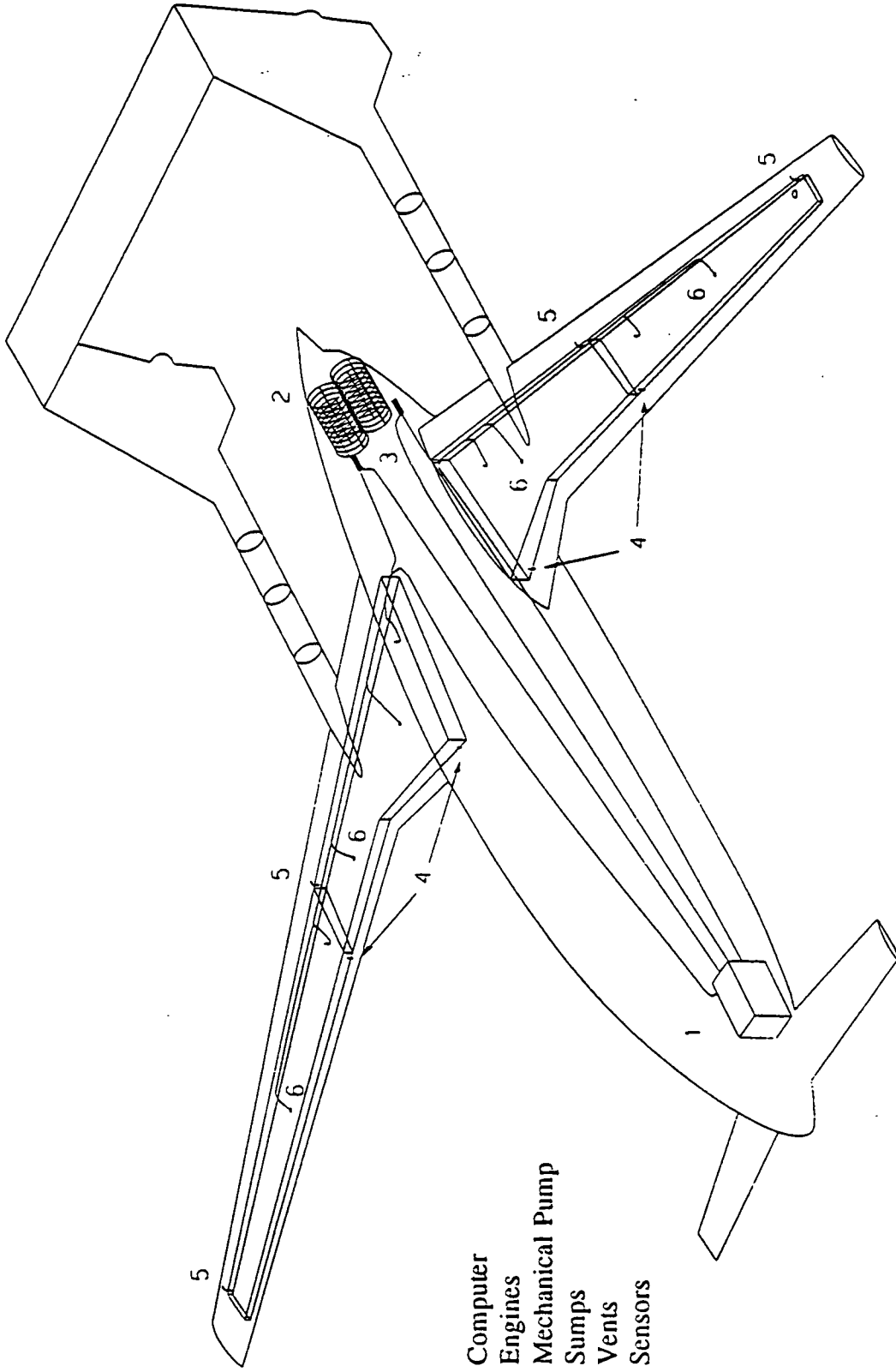
1. Computer
2. Engines
3. Mechanical Pump
4. Sumps
5. Vents
6. Sensors

Figure 7.3: Fuel System Layout of the APT

7.3 REFERENCES FOR THE FINAL REPORT

7.1   APT Airframe Report. University of Kansas, May 1991.

7.2   Axmann, K., Knipp, D. System Layouts for the
      Advanced Personal Transport. 30 November 1990.

7.3   Zumwalt, G.W. Fatigue and Electromagnetic
      Interference Test for Electro-Impulse De-Icing.
      The Wichita State University. SAE 1989, 891062.

7.4   Dirkzwager, A. Natural Laminar Flow Airfoil Design
      for the Advanced Personal Transport. 9 November 1990.

7.5   Mitsubishi MU-2 Training Manual.

7.6   USAF Center Solves Communications Avionics
      Problems with Fiber Optics. 'Aviation Week and
      Space Technology.' Sept. 4, 1989.

7.7   Lan, E., Roskam, J. Airplane Aerodynamics and
      Performance, Roskam Aviation and Engineering
      Corporation, Ottawa, Ks. 1989.

7.8   Roskam, J. Part II: Preliminary Configuration
      Design and Integration of the Propulsion System.
      Roskam Aviation and Engineering Corporation,
      Ottawa, Ks. 1989.

8. PRIMARY FLIGHT CONTROL SYSTEM

8.1 INTRODUCTION

The purpose of this chapter is to review the PFCS study found in Reference 8.1. Simplified block diagrams of the control loops will be presented and explained. The block diagrams will then be used to examine the dynamics of the airplane. This will be accomplished with the use of the root locus method. This analysis will be conducted in the s-plane. After this analysis the study focused on a z-plane analysis and simulation of the system. Finally, some control concepts are investigated for the control of: climb rate, heading rate, and airspeed.

8.2 PFCS CONTROL LOOPS

The APT utilizes a decoupled flight control system. Decoupled flight controls make the the response of the airplane a function of only one input variable. This is different from a conventional control system. A conventional control system will have "side effects" from an input of one controller. For example, if the pilot pulls back on the stick the airplane will start to climb. At the same time the airspeed will begin to fall. Thus to compensate, the pilot must simultaneously add power if he is to maintain the same airspeed. The addition of power is an iterative problem for the pilot. That is he must make an educated guess (based on experience) of the amount of throttle required to compensate for the amount of climb that he desires. After some time, the airplane will respond to the pilot's inputs and reach a new steady state. If this steady state is not the one desired by the pilot he must make another change (or changes) until it does. The decoupled flight control system controls each primary motion variable separately. The three motion variables that are controlled by the pilot are:

- Vertical speed ($\dot{h}$)
- Airspeed (V)
- Heading rate ($\dot{\psi}$)

Using this system the pilot no longer needs to iterate to find the appropriate throttle position. This is because the speed is maintained at the desired value by the airspeed control system. This system has proven to be very easy to fly (Reference 8.2). Making the APT as easy to fly as possible to fly is one of the primary objectives of this design. This makes this control concept the natural choice. The purpose of the following sections is to perform a dynamic analysis of the control loops and make sure that the APT can indeed use this type of control system.

By using the stability derivatives for the APT it was possible to evaluate the dynamic response of the systems by creating root loci for the various loops employed. The following flight conditions were evaluated for the dynamic analysis:

Table 8.1: Flight Conditions Used for Dynamic Analysis

Flight Condition	Mission Segment	Speed (kts)	Altitude (feet)
1	High Speed Cruise	410	20000
2	Power Approach	90	Sea Level

These flight conditions were chosen to represent the two extremes at which the APT will be expected to operate. These two flight conditions represent the largest difference in the stability behavior of the APT. The high speed cruise is conduced at high dynamic pressure while the power approach flight condition represents the lowest levels of dynamic pressure that the airplane will encounter.

8.2.1 Vertical Speed Control Loop

The basic block diagram for this loop was presented in Reference 8.1. It will be repeated here for convenience. This block diagram will be useful for describing the dynamic analysis of the system. For the analysis the full three degree-of-freedom math model was used. This allowed both the short period and phugoid modes to be checked with more accuracy than would be possible by using either the short period or phugoid approximations.
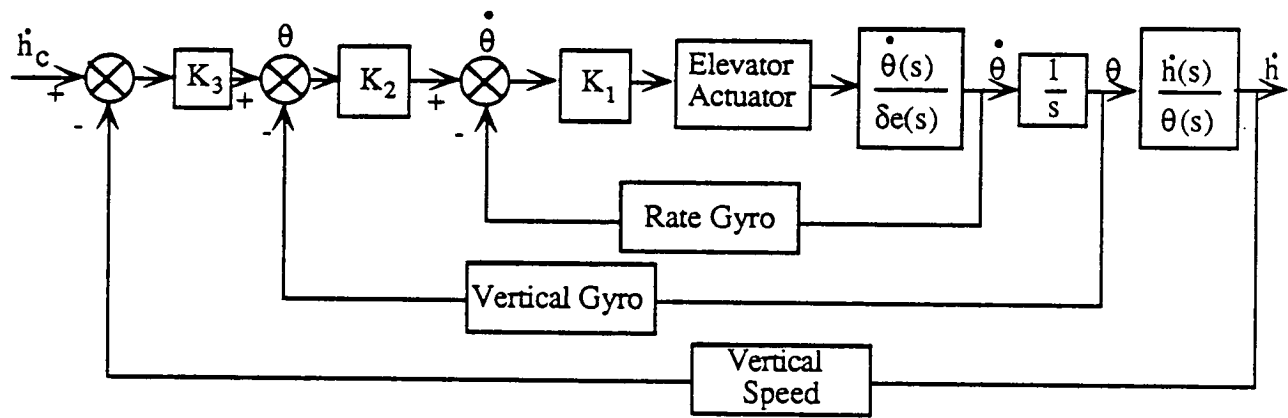

Figure 8.1: Simplified Block Diagram of Vertical Speed Control Loop

The transfer functions are from Reference 8.3 and 8.5. They are repeated in general form here for reference.

$$\frac{\text{Elevator}}{\text{Actuator}} = \frac{a}{s + a}$$

(8.1)

$$\frac{\dot{\theta}}{\delta e} = \frac{K_{\theta \delta e} s (T_{\theta 1} s + 1)(T_{\theta 2} s + 1)}{(s^2 + 2\zeta_{sp}\omega_{nsp} + \omega_{nsp}^2)(s^2 + 2\zeta_p\omega_{np} + \omega_{np}^2)}$$

(8.2)

$$\frac{\dot{h}(s)}{\theta(s)} = \frac{U_1}{57.3}(1 - \frac{\alpha(s)}{\theta(s)})$$

(8.3)

78

Where:

$$\frac{\alpha(s)}{\theta(s)} = \frac{K_{\alpha\delta e}(T_\alpha s + 1)(s^2 + 2\zeta_\alpha\omega_{n\alpha} + \omega_{n\alpha}^2)}{K_{\theta\delta e}(T_{\theta 1}s + 1)(T_{\theta 2}s + 1)}$$

(8.4)

8.2.2 Airspeed Control Loop

This section will discuss the airspeed control loop for the decoupled flight control system. Figure 8.2 shows the block diagram for the auto-throttle control loop used.
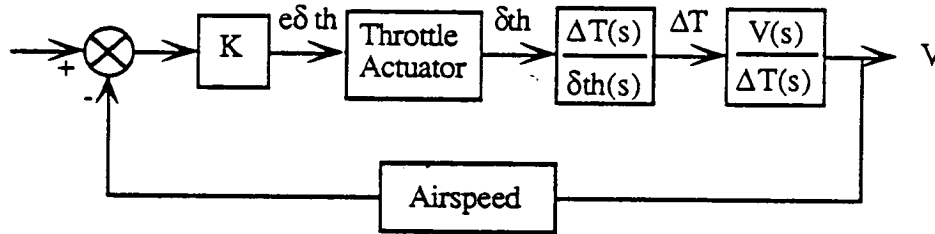

Figure 8.2: Simplified Block Diagram for the Airspeed Control Loop

The transfer functions of this loop are as follows:

$$\frac{\text{Throttle}}{\text{Actuator}} = \frac{a}{s + a}$$

(8.5)

$$\frac{\Delta T(s)}{\delta th(s)} = \frac{b}{s + b}$$

(8.6)

$$\frac{V(s)}{\Delta T(s)} = \frac{K_{u\delta t}/m (T_u s + 1)}{(s^2 + 2\zeta_p\omega_{np} + \omega_{np}^2)}$$

(8.7)

These transfer functions are from Reference 8.3 and 8.5. It can be seen from equation 8.7 that the phugoid approximation is used to determine the transfer function of the airspeed control loop. This is the method used in Reference 8.5 in a similar loop.

The throttle actuator was assumed to be a first order system with a break frequency of 7.5 Hz. The engine transfer function was also assumed to be a first order system but with a break frequency of 10 Hz. This break frequency is reasonable to use for this airplane since it utilizes a direct drive turboprop engine Since the engine and propeller are spinning at a constant speed regardless of power setting increasing power implies that all that has to happen is more fuel be

79

added to the engine. The lack of any appreciable "spool-up" time contributes to the fast response of the engine.

8.2.3 Heading Rate Control Loop

The heading rate control loop is the last loop required to complete the decoupled flight control system. This differs from "normal" lateral-directional control in that heading rate is controlled directly. In a typical airplane the pilot actually controls roll rate. To perform a turn the pilot must first apply aileron in the direction of desired motion. After some period of time the pilot must apply a control input in the opposite direction of the desired motion. This is done to hold the airplane in the desired bank angle. The amount of "cross control" and the time at which it is applied are items which are best determined with the benefit of experience. This is another way in which a conventional airplane is not suitable for the low time or infrequent pilot. To make matters worse the actual heading rate that is obtained with a given bank angle is a function of airspeed. This is due to the following relation:

$$\dot{\psi} = \frac{g \tan\phi}{U_1}$$

(8.8)

It can be seen from the above relation that for a given bank angle the turn rate will increase with a decrease in speed. This further adds to the confusion in terminal flight phases where speed changes are not uncommon. This is not acceptable for the people envisioned to fly the APT so the heading rate control loop of Figure 8.3 is used.
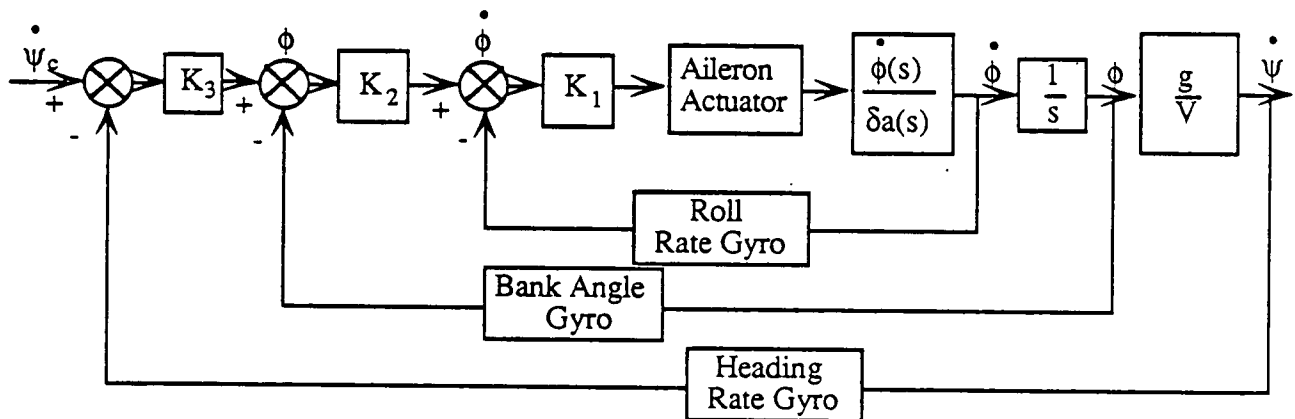

Figure 8.3: Simplified Block Diagram for the Heading Rate Control Loop

The transfer functions of this system have the following form:

$$\frac{\text{Aileron}}{\text{Actuator}} = \frac{a}{s + a}$$

(8.9)

$$\frac{\dot{\theta}}{\delta e} = \frac{K_{\phi\delta a}s(s^2 + 2\zeta_\phi\omega_{n\phi} + \omega_{n\phi}^2)}{(T_S s + 1)(T_R s + 1)(s^2 + 2\zeta_D\omega_{nD} + \omega_{nD}^2)}$$

(8.10)

These transfer functions are from Reference 8.3.

This system will allow the pilot to command a certain turn rate. The control system will determine what bank angle the airplane should be in at the current speed. This system should be much more intuitive to the infrequent pilot. Research at NASA (Reference 8.2) has shown the system to be quite easy and intuitive to fly.

As in the vertical speed loop, the aileron actuator is assumed to be a first order system with a break frequency of 10 Hz. The g/U_1 term is a result of the geometry expressed in equation 8.8.

8.3 CONVERSION FROM S-PLANE TO Z-PLANE

This section discusses the technique used to convert the open loop transfer function (s-plane) of the APT Pusher control system to its equivalent z-plane (discrete) transfer function. Once the equivalent z-plane transfer function has been calculated, a difference equation can be derived.

Since digital controllers are frequently used in control systems, it is necessary to establish equations that relate digital and discrete-time signals. Just as differential equations are used to represent systems with analog signals, difference equations are used for systems with discrete or digital data. Difference equations are also used to approximate differential equations, since the former are more easily programmed on a digital computer, or are generally easier to solve.(Reference 8.3.1)

To calculate the difference equation of the APT Pusher control system, several operations had to be performed. Listed in order they are:

1). separate the transfer function using partial fraction expansion

2). use the cover-up method and/or matrices to solve for the constants

3). determine the equivalent z-plane transfer function

4). simulate the z-plane transfer function using the parallel method

5). determine the difference equations from the parallel diagram

8.3.1 Partial Fraction Expansion

Partial fraction expansion is a helpful tool which can be used to expand the transfer function into simple, recognizable terms. These terms can be converted to the z-domain effortless by the use of z-transform tables. To use the partial fraction technique, the open loop transfer function of the control system has to in factored form. An illustration of this would be:

$$G(s) = \frac{K}{(s+a)\cdot(s+b)\cdot(s+c)\cdot(s+d)} \qquad \text{(eq. 8.3.1)}$$

If any of the roots of the open loop transfer function are complex, they may be combined to form a second order polynomial. An illustration of this would be:

$$G(s) = \frac{K}{(s+a)\cdot(s+b)\cdot(s^2+ds+e)} \qquad \text{(eq. 8.3.2)}$$

82

Where K is the numerator of the transfer function. The reason for the two different techniques for writing a transfer function are to eliminate complex numbers. With the partial fraction expansion in the proper form, the transfer function can be converted to the z-domain by the use of transform tables.

8.3.2 Solving for the Constants of the Partial Fractions

Once the transfer function has been factored into proper form (reference section 8.3.1), it can be expanded into partial fractions. The following is how a fourth order polynomial with two complex roots can be expanded into partial fractions:

$$G(s) = \frac{A1}{s+a} + \frac{A2}{s+b} + \frac{A3(s) + A4}{s^2 + ds + e} \qquad \text{(eq. 8.3.3)}$$

The coefficients can be solved for in two ways. The coefficients over the real roots (A1 and A2) can be solved for using the cover-up method. The least common denominator will need to be found to solve for the coefficients over the polynomial term. The actual process to solve for the constants is not going to be discussed. If further explanation of the technique is requested, reference the Primary Flight Control System Report. (Reference 8.3.4)

By analyzing the control systems for the APT Pusher, it was concluded that unless the control system is small in order, the cover-up method is not recommended due to the truncating error introduced into the coefficients due to rounding. A better technique would involve finding the least common denominator for the partial fraction expansion and then solve for the coefficients using matrices. With the use of matrices, the error from rounding can be reduced since more values are used to determine the solution.

8.3.3 Z-Plane Transfer Function

After all the coefficients of the partial fractions have been solved, a z-transform table can be used to convert the s-plane transfer function into its equivalent z-plane. The first order polynomial terms can be solved directly by finding their equivalent z-transform. However, second order polynomials must be converted into the following form:

$$\frac{s+d}{(s+d)^2 + w^2} \cdot \frac{w}{(s+d)^2 + w^2} \qquad \text{(eq. 8.3.4)}$$

The conversion is done by completing the square on the denominator. Once the desired form is achieved, its equivalent z-transform can also be read directly from a z-transform table.

83

A z-plane root locus plot was done to validate the calculations required to convert the s-plane transfer function into its z-plane equivalent. Reference the Primary Flight Control System Report for the z-plane root locus plots for the speed and longitudinal controls.(Reference 8.3.4)

8.3.4 Simulating Z-Plane Transfer Functions

With the partial fractions now in the z-domain, deriving the difference equations is the next step needed in the conversion process. The parallel method was chosen to handle this task. It was chosen over the direct or cascade method because the mathematical calculations needed to get the difference equation were easier to convert into an algorithm needed for computer simulations.(Reference 8.3.1 and 8.3.3) This can be of top concern when significant figures are important. Refer to the Primary Flight Control System Report, Chapter 3 for an example of parallel simulation.(Reference 8.3.4) The difference equations for each section (one polynomial per section) are added together to get the overall difference equation for the control system.

8.3.5 Difference Equations

There are two basic techniques for solving linear-time-invariant difference equations. The first method, commonly referred to as the classical approach, consists of finding the complementary and the particular parts of the solution, in a manner similar to that used in the classical solution of linear differential equations. (Reference 8.3.2) The second technique, which is a sequential procedure, is the method used in the digital-computer solution of difference equations. The second technique was employed for simulating the APT Pusher.

8.4 DIGITAL CONTROLLER

The purpose of this section is to explain the function and operation of the digital controller and to present an analysis of the computer simulation study. The basic principles for the function of the controller will be discussed along with the application and development of software to analyze the APT Pusher control system.

8.4.1 Digital Controller Principles

A proportional-plus-integral-plus-derivative (PID) controller was chosen for the design of the PFCS controller. Figure 8.4.1 shows a block diagram of a PID controller. The proportional part of the controller increases the low-frequency gain and thus reduces steady-state errors. The derivative portion of the controller adds positive phase angles to the open-loop frequency response and increases the closed-loop response time. This has the effect of improving system stability and increasing the speed of response. The function of the PID controller is then to increase stability margins, decrease response time to transients and/or reduce steady-state errors.

8.4.2 Analog To Digital Transformation

Equation 8.4.1 is the analog version of the PID filter in Figure 8.4.1.

$$m(t) = K_p \cdot e(t) + K_i \quad e(t)dt + K_d \cdot de(t)/dt \qquad \text{(eq. 8.4.1)}$$

Where $e(t)$ is the error input (system input - system output) to the controller and $m(t)$ is the controller output. The time domain error signal $e(t)$ is a real number which represents the error of the system. K_p, K_i, and K_d are the gains associated with the branches of the controller. These are the values which will be determined by computer simulation.

The discrete controller implementation of the integrator is,

$$m_i(k) = T/2[e(k) + e(k-1)] + m_i \cdot (k-1) \qquad \text{(eq. 8.4.2)}$$

The (k-1) expression represents a time delay. This delay is equivalent to the sample time (T) selected for sampling of the output signal. $m_i(k)$ is a function which represents the integral branch of the PID controller.

The implementation for the differentiator was chosen to be,

$$m_d(k) = (1/T)[e(k) - e(k-1)] \qquad \text{(eq. 8.4.3)}$$

This equation approximates differentiation. The difference equation $[e(k) - e(k-1)]$ produces the difference between the present error and the error one sample previous. The sampling period T is the time over which the difference is produced.

The proportional section of the PID controller is represented by $K_p e(k)$. This represents the present error multiplied by a constant.

The discrete controller implementation of equation 8.4.1 is the summation of the integral, derivative, and proportional branches shown in Figure 8.4.1. The discrete time domain equation which represents this controller is ,

$$m(k) = K_p e(k) + K_i m_i(k) + K_d m_d(k) \qquad \text{(eq. 8.4.4)}$$
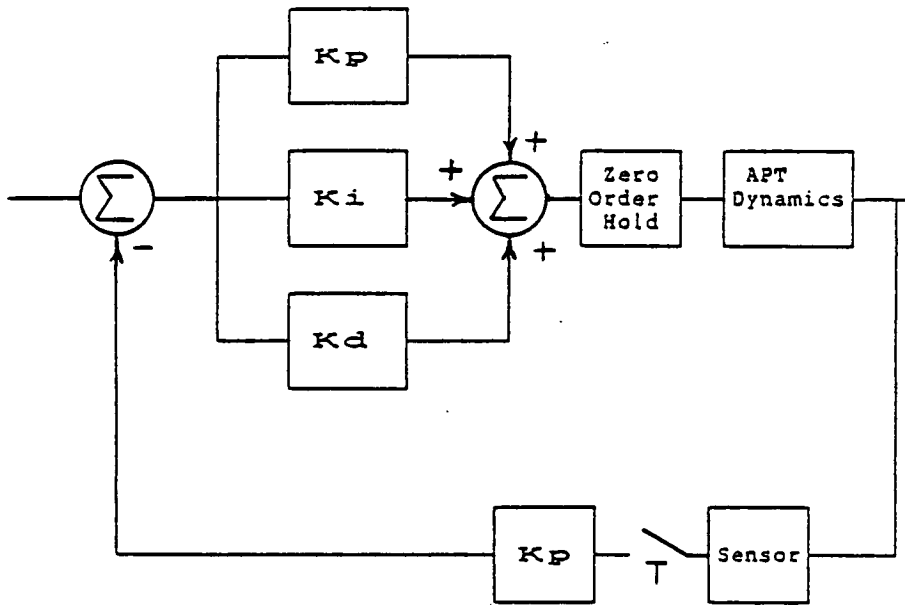
Figure 8.4.1: PID Controller

8.4.3 Primary Flight Control System Software

The Primary Flight Control System (PFCS) software simulates the flight dynamics of the APT pusher. The design of the Primary Flight Controller can be achieved in a timely and cost effective manner by simulating the response which would occur by using mathematical models and computer simulation. The flexibility utilizing software analysis allows for the design (and redesign) of the controller without the costly requirement of constructing a prototype or physical model.

Software to simulate the Lateral and Speed controls of the APT was developed. The software for the speed controller was completed and implemented to determine the gains for the controller. The software for Lateral controller was completed; however, due to time constraints an analysis was not completed.

8.4.4 Analysis Of Computer Simulation

Four parameters in equation 8.4.4 need to be determined: T, K_p, K_i, and K_d. The gains were determined by first implementing a proportional-only controller, and varying K_p (proportional gain). A typical step response is given in Figure 8.4.2. The percent overshoot of 25% shows that proportional only control exhibits poor stability. The steady state error at $T = 20.00$ seconds indicates a poor steady state response. Poor steady state response is represented by the inability of the output to "catch up" to the input leaving a constant error as time goes to infinity. This can be improved with the implementation of integral control.

Next the integral term was added to the controller, and a typical step response is illustrated in Figure 8.4.3. Note the reduction of the steady-state error, as expected.

Finally, the derivative term was added to the controller, resulting in a typical response as shown in Figure 8.4.4. Figures 8.4.3 and 8.4.4 show that derivative control, when used with the proper gain, can yield transient response performance equivalent to proportional only control and simultaneously reduce overshoot dramatically.
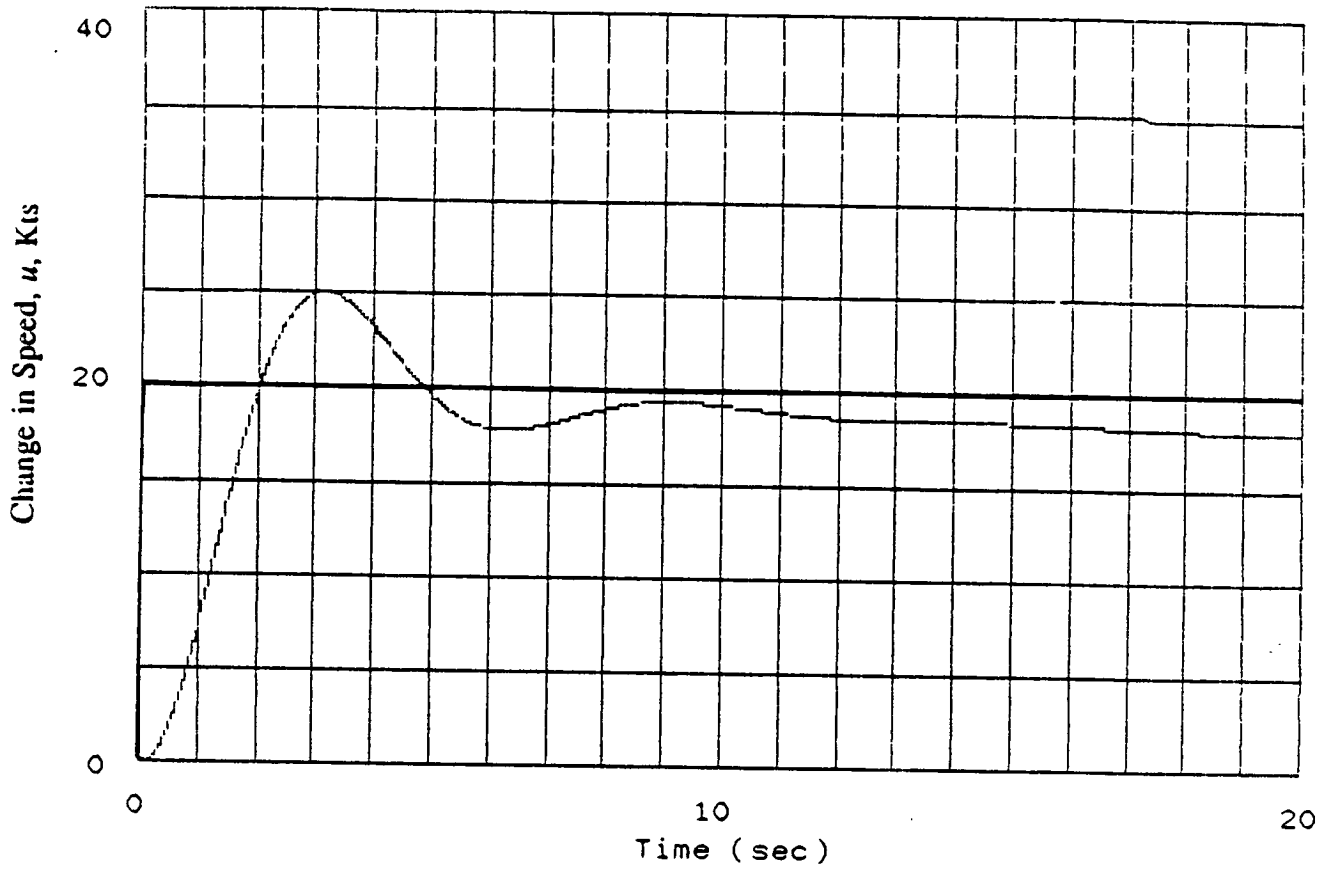
Figure 8.4.2: Speed Control Using Only (Kp)
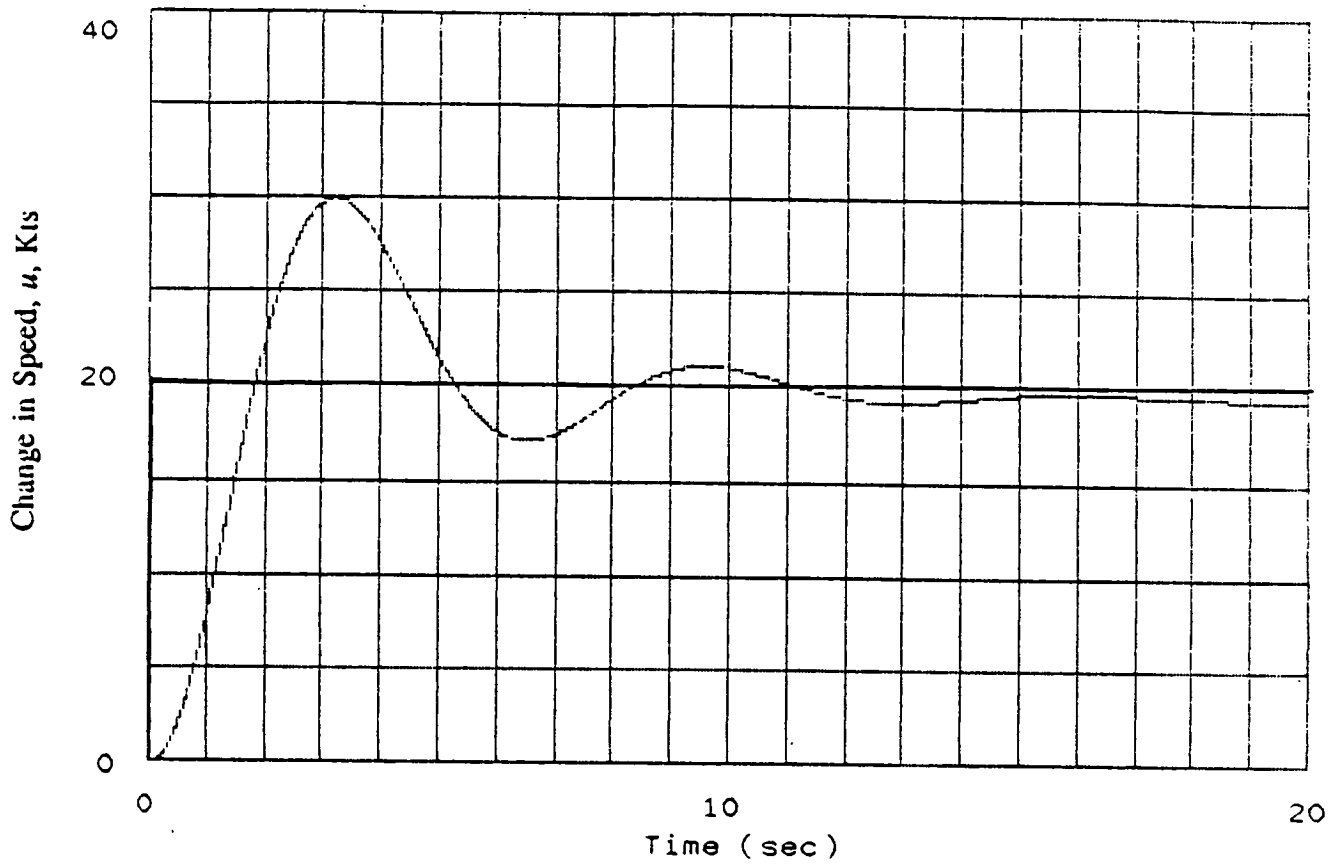
Flight Condition:
>   High Speed Cruise
>   Altitude - 20,000 ft.
> U_1 - 390 Kts

Response to a 20 Kts step increase in speed
$K_p = 20,$ $K_i = 0,$ $K_d = 0$

Flight Condition:
      High Speed Cruise
      Altitude - 20,000 ft.
      U_1 - 390 Kts

Response to a 20 Kts step increase in speed
$K_p = 20,$ $K_i = 2,$ $K_d = 0$

Figure 8.4.3: Speed Control With Ki & Kp
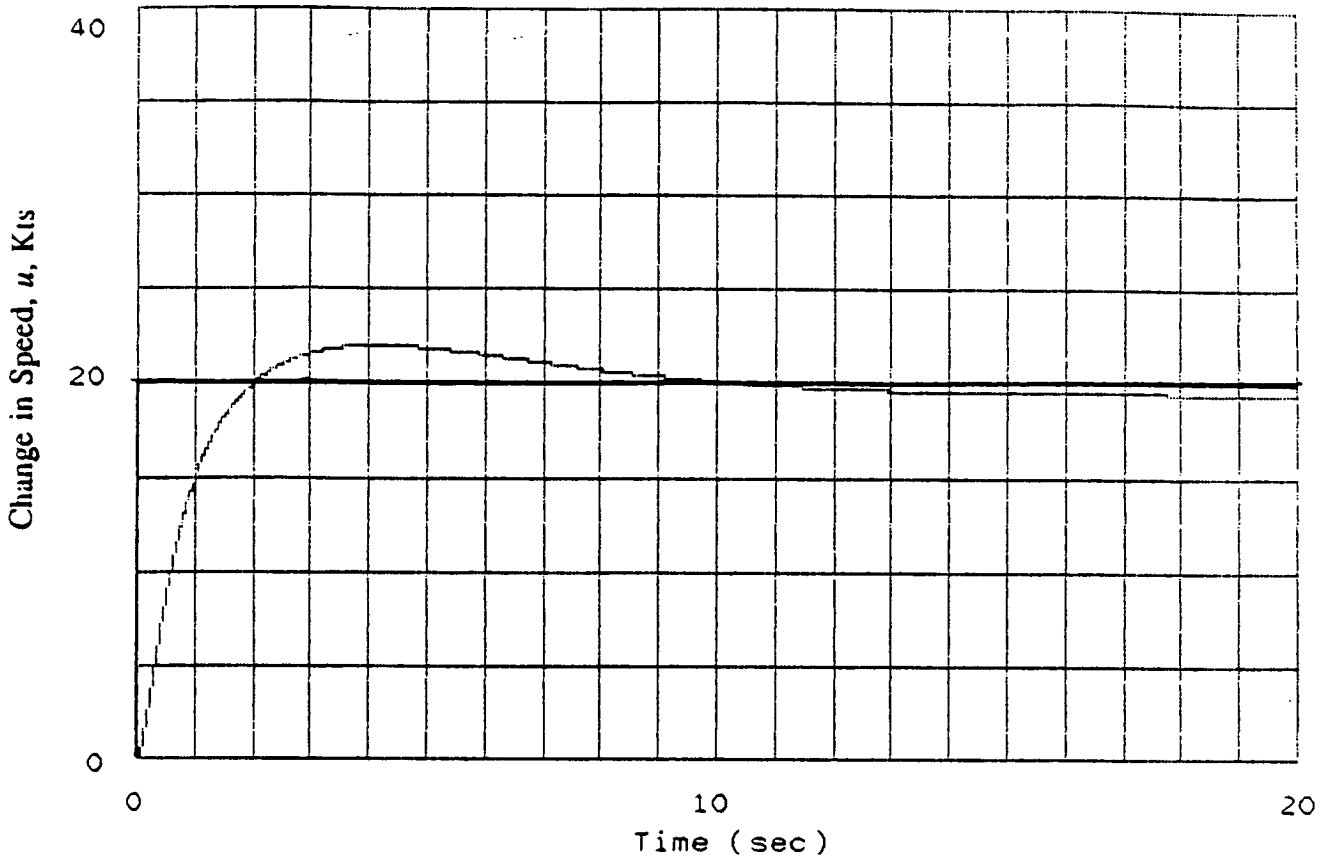
Flight Condition:
    High Speed Cruise
    Altitude - 20,000 ft.
    U_1 - 390 Kts

Response to a 20 Kts step increase in speed
$K_p = 20,$ $K_i = 2,$ $K_d = 20$

Figure 8.4.4: Speed Control With Kp, Ki, & Kd

8.5. PFCS COMPUTER WITH INPUT/OUTPUT BOARDS

The PFCS computer has been designed to handle 30 inputs and 5 outputs at a minimum. However, a computer system with greater capability is suggested to facilitate changes in specifications, redesigns, and any additions.

8.5.1 PFCS Inputs

As referenced, there are a total of 30 inputs into the system. Two inputs (speed control and stick position) come directly from the pilots positioning of the controls. All the remaining inputs are an indirect response to the pilots choice. The inputs to the computer from all the actuators (23) correspond to values of the actuators position potentiometer. These readings are used to verify the response of the actuators in comparison to the position commanded by PFCS for the BITE testing. The actuator inputs are broken down as follows:

* left wing aileron surface	7
* right wing aileron surface	7
* elevator surface	5
* rudders	2
* throttle control	2

The remaining 5 inputs coming from the gyros are used to determine the positioning of the aircraft.

8.5.2 PFCS Outputs

The APT Pusher requirements specify that there will be 5 outputs required from the PFCS computer for controlling flight control surfaces. All the outputs will be for positioning the actuators. The electrical design team has preliminarily specified that only one output would be needed for each control surface of the aircraft. Broken down as follows:

* right wing aileron surface
* left wing aileron surface
* elevator surface
* rudders

The remaining outputs are for throttle control which controls engine speed.

8.5.3 PFCS Computer Design

An IBM 8088 with a 8 MHz crystal was chosen for the Central Processing Unit (CPU). Any compatible system with equivalent or higher quality and performance can be used. The design required the use of 3 input/output (I/O) boards to handle the PFCS immediate needs. Each board has 8 analog to digital (A/D) inputs and 8 digital outputs.

There are many different types of I/O boards that are manufactured. The only requirement specified is that the board be large enough to support the PFCS computer needs. References 8.5.1 and 8.5.2 are catalogs with many I/O board listing with performance specifications to choose from. Model ML-16 was the choice taken for the I/O board. (Reference 8.5.1) The choice was based on three considerations:

1) provided the necessary inputs and outputs
2) compatible with the IBM 8088 CPU
3) economic considerations (cost and availability)

The connection between the CPU and the I/O boards consist of an 8 bit data bus. A ribbon cable with an 8 pin connector will be used.

8.6 OPERATIONAL CONSIDERATIONS

The APT uses a very advanced flight control system compared to other general aviation airplanes. As a result of this the standard input devices of control stick, rudder pedals, and throttle take on new meaning with the decoupled system used in the APT. To illustrate the degree to which the APT is different, consider that the airplane does not even have rudder pedals. This section will discuss the way in which the airplane will be controlled. The following will be covered:

- Vertical speed control
- Heading rate control
- Speed control

8.6.1 Vertical Speed Control

Sidestick controllers were chosen for the APT. The proposed method of longitudinal control of the airplane is illustrated in Figure 8.8.

Increasing vertical speed   Decreasing vertical speed

Front of Airplane

Stick in position
for no vertical speed
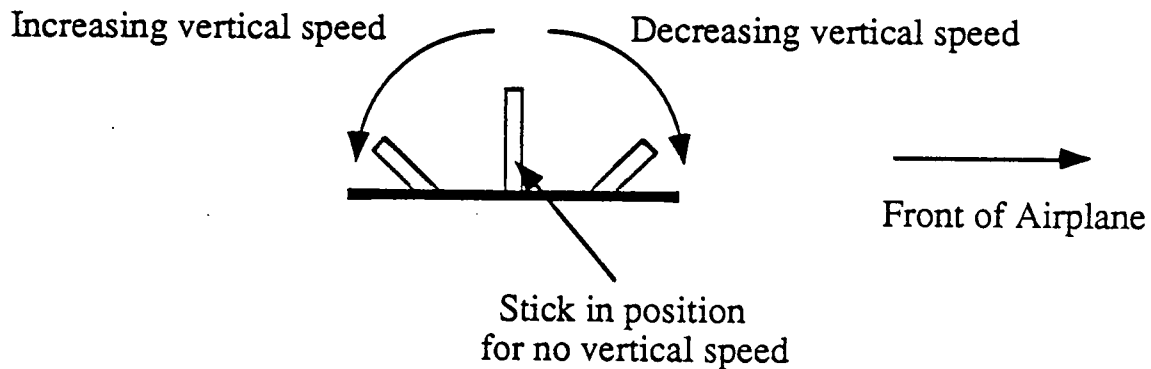
Figure 8.8 Side View of Sidestick Controller

This method would use a control stick that is spring centered to command zero vertical speed. If the pilot wishes to increase the climb rate of the airplane he would simply pull back on the stick. This is very similar to a conventional airplane except that the pilot will not have to iterate the position of the stick to command a given airspeed. This is accomplished through the control loops discussed previously. If the pilot wishes to command a maximum rate of climb (traffic evasion for example) all he would have to do is pull the stick back all the way.

8.6.2 Heading Rate Control

The way in which the pilot controls the lateral-directional movements of the airplane are also different in the APT when compared to a conventional aircraft. The side to side movement of the control stick controls the rate of turn of the airplane. Figure 8.9 shows the effect of the controller when viewed from the rear.

Higher rate of turn to
the left

Higher rate of turn to
the right

Stick in position
for straight and level flight
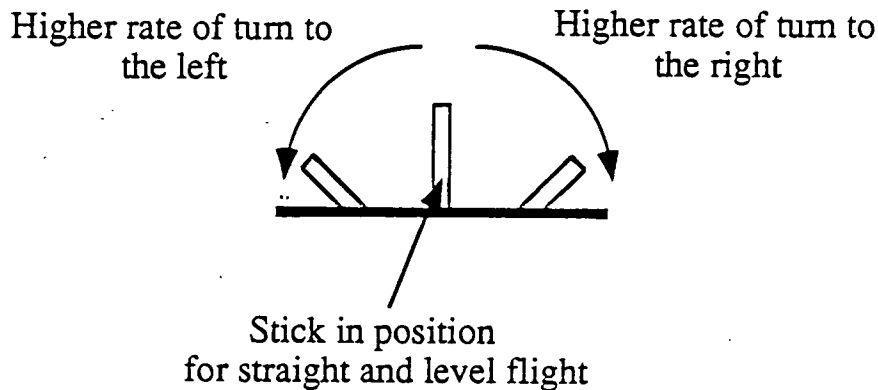
Figure 8.9 Rear View of Sidestick Controller

Like the longitudinal control, this control should not present any difficulties to the pilot. It will reduce the amount of iterations the pilot will have to make to obtain a certain turn rate. He will be able to move the stick to one position and get a given turn rate independent of speed.

8.6.3 Airspeed Control

This controller is the most different from a conventional airplane. This is because a typical airplane controls the amount of power that the engine is producing. Using a pure throttle as a control it is possible to have two different speeds for a given power setting. As a result of this, it is possible to have full power applied in a conventional airplane and the speed will only be a little above stall speed. The phenomenon of "being on the back side of the power curve" as just described is a common cause of general aviation accidents. Using airspeed control will reduce the number of accidents that occur at low speeds.

Speed control in a airplane such as the APT which has a very large speed range (~70 - 410 knots) poses a problem for the controller. Compounding the problem is the fact that conventional throttle throws are limited by cockpit space and pilot ergonomics. The combination of a conventional control and the large speed range results in a control which has a relatively large "gain." A large gain means that for a given handle travel, the increase in speed commanded is quite large. This will make it difficult for the pilot to make small changes in the commanded airspeed.

One possible solution to this problem is shown in Figure 8.10. In this method, the pilot pushes (or pulls) on the speed control handle to increase (or decrease) speed. The commanded airspeed would be displayed on the HUD display. Once the commanded airspeed reached the desired level the pilot would release the handle. The handle would then return to the center position. The center position commands zero increase in speed. Using this method, the speed control handle is "reset" to a new trim speed after the pilot releases the handle. This method effectively eliminates the problems that the conventional method has with a large gain. This method does however bring about a new set of problems. These problems concern the pilot's response to such a system. It may prove to be unnatural and non-intuitive to use such a system.

Position of Speed Control Handle for
No Increase in Command Airspeed

Decrease Speed

Increase Speed

Spring-Centered
Speed Control
Handle

Speed Control Quadrant
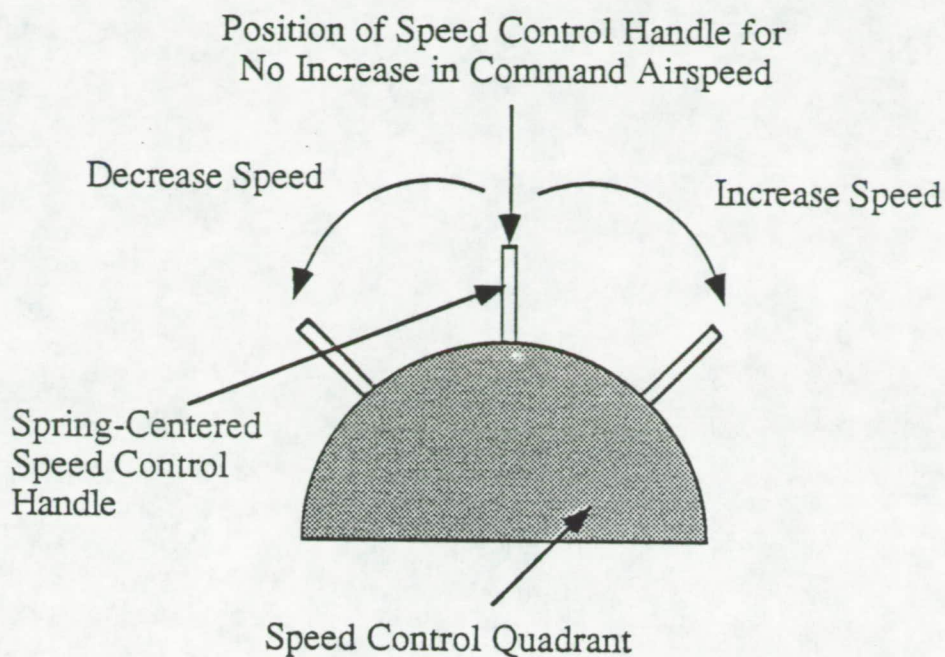
Figure 8.10 Side View of Airspeed Controller

Another possibility to solve the pilot interface problem, it to use a method that is used in Soviet fighters such as the Mig-29 and Su-27. These airplanes use a throttle quadrant which in principle is similar to a conventional throttle. The method that the Soviets use can best be called a "linear throttle control." This idea is presented in Figure 8.11.

Position for Minimum Speed

Position for Maximum Speed

Intermediate Power Setting
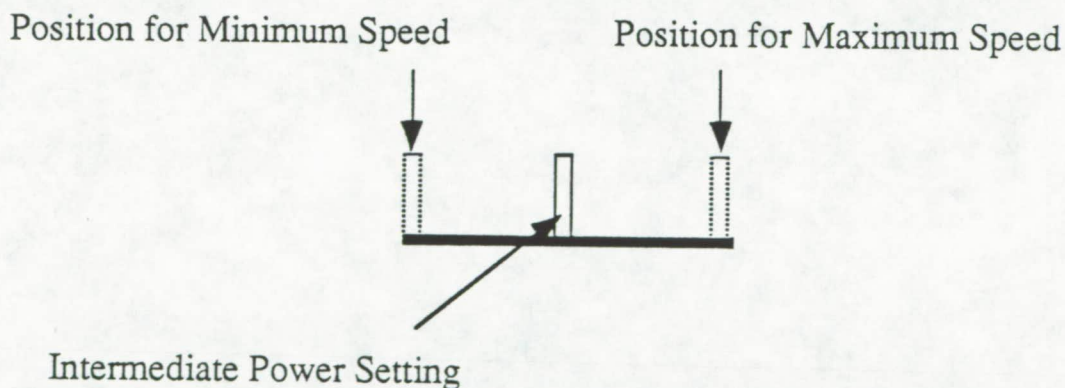
Figure 8.11: Linear Speed Control Handle

By using this type of pilot interface, it is possible to give the pilot a longer travel to work with. Longer travel will reduce the "gain" associated with the conventional method. This in turn should allow the pilot to be able to command small changes in commanded airspeed. Another benefit of this system is that it may be more intuitive to the pilot than the method described above. This is because the pilot will have an indication of the speed potential that remains. For example, if the pilot is flying along with the speed control handle in the $3/4$ position he will immediately have

95

an idea on how much more speed is possible. This can not happen with the previous method since the speed control handle will center to a new trim condition.

The difficulty with this approach is that the travel required to give the pilot adequate resolution may be more than cockpit space will allow. Also, if very large travel is required it may not be ergonomically possible to use this type of system.

It is too early to make a firm decision on what type of method should be used to control airspeed. A much more detailed study of the ergonomic factors as well as pilot in the loop simulations should be performed to best gain an idea of what type of control should be used.

8.7 REFERENCES FOR CHAPTER 8

8.1   Smith, S., et. al., <u>Primary Flight Control System Study</u>, AE 622 Spring 1991, University of Kansas.

8.2   Roskam, J., Airplane Flight Dynamics Part I, 1979, Roskam Aviation and Engineering Corp., Rt 4, Box 274, Ottawa, Kansas, 66067.

8.3   Stewart, E.C. et al., "An Evaluation of Automatic Control System Concepts for General Aviation Airplanes." AIAA Paper number 88-4364

8.4   Barrett, R. et.al., <u>Design Test and Evaluation of the Iron Bird</u>, AE 622 Spring 1991, University of Kansas.

8.5   Roskam, J., Airplane Flight Dynamics Part II, 1979, Roskam Aviation and Engineering Corp., Rt 4, Box 274, Ottawa, Kansas, 66067.

9. ELECTRICAL SYSTEM DESIGN CONSIDERATIONS

Reference 1, the phase I report on the electrical system, discussed most of the preliminary aspects of the APT electrical system. Subjects discussed in detail were load profile analysis, power bus design, power generation, circuit protection, batteries, and voltage regulators. One of the main aspects of the electrical system not addressed in that report is the feasibility of delivering control signals via fiber optic cable versus copper wire. This topic is addressed in this summary. Reference 2 presents a more detailed analysis.

The purpose of this summary is to provide the key results of the analysis. Feasibility will be determined by designing wire and fiber control systems for a control surface, namely the left aileron. Length of wire of fiber and the number of electronic devices required to support each control scheme will be tallied for that particular control surface. The length and number of devices will then be tallied for the other control surfaces (right aileron, elevator, rudder, throttle) based on the totals obtained from the left aileron. This extrapolation is valid due to the similar nature in which control surfaces are controlled.

Once the electronic devices and length of the wire or fiber have been totalled, the control schemes will be compared based on the following criteria:

1. Weight

2. Cost

3. Volume

4. Heat.

The parameters will be totalled for all the aforementioned control surfaces using the wire and fiber control schemes. The parameters will be compared and general conclusions will be drawn concerning all control signals throughout the plane, such as fuel level signaling, temperature signaling, etc.

It should also be noted that the control schemes presented in this report are not to be considered complete designs, i.e. resistors and capacitors required to build filters. Only major components are shown and tallied for the purpose of obtaining a general idea of the total parameter values for each control scheme and the feasibility of wire or fiber in general.

9.1 CONTROL SCHEMES

The purpose of this section is to discuss the three types of control schemes considered in this report. A brief discussion of the parameter contributions to the APT will be provided.

9.1.1 Conventional Copper Wire Control Scheme

The numbers obtained for the comparison parameters for the copper wire control system are as follows:

Weight: 26.28 lbs.

Cost: $330.65

Volume: 364.1 in^3

Heat: 12.5 Watts

About 85% of the total weight of this particular control scheme is made up of copper wire weight. Electronic components needed to realize this system are made up exclusively of operational amplifiers (op amps). Op amps are very small devices that are practically negligible in weight and volume but do contribute all of the heat in this scheme. These devices are relatively reliable (MTBF approx. $3.3\text{x}10^5$ hrs.) for the environment in which the APT is expected to perform. Also included in these totals are printed circuit boards and chip sockets for the op amps.

9.1.2 Individual Fiber Control Scheme

The individual fiber control scheme is obtained by replacing each copper wire in the copper wire control scheme by a plastic fiber. In this scheme we do not utilize the bandwidth capabilities of fiber optic cable, rather we take advantage of the weight savings of plastic over copper. The results for the comparison parameters are as follows:

Weight: 21.37 lbs.

Cost: $396.72

Volume: 362.6 in^3

Heat: 20.4 Watts

The weight of the plastic fiber makes up only 58% of the weight shown above. The cable weight savings over the copper wire is 10.5 lbs. However, additional electronic components are required to realize this scheme. These additional components offset approximately 50% of the cable weight savings making it less attractive than it would have been otherwise. The extra components required are light emitting diodes (LED) and photo detectors (PD). Also required is and extra printed circuit board for a total of two. One is located in the wing and one near the computer equipment under the cockpit. Since the weights of the printed circuit boards, LEDs and PDs were not available, they were estimated conservatively. In reality, it is expected that these devices are lighter than the estimates and therefore will make the individual fiber system more attractive.

The fiber cable was also 57% less expensive than the equivalent length of copper. All of the cost savings were eliminated and surpassed by the cost of the additional electronic devices. In all the individual fiber scheme costs about 20% more than the copper wire control scheme. The additional devices also added 63% more heat to be dissipated and displaced about the same amount of volume.

9.1.3 Amplitude Modulation Control Scheme

In this section, the bandwidth capabilities as well as the weight saving advantage are utilized in an effort to reduce the parameters mentioned at the beginning of this chapter. In this scheme we use a communication method known as amplitude modulation in an effort to transmit all control signals for a particular control surface over single fiber simultaneously. Electronic devices are used to displace the frequency content of feedback signals, transmit, and then filter them to reconstruct the signals. The totals for this scheme are as follows:

Weight: 19.87 lbs.

Cost: $3262.28

Volume: 189.8 in^3

Heat: 24.6 Watts

The fiber cable contributes only 20% to the total weight of this system. However, the electronic components required to realize this scheme offset the cable weight savings of this scheme to a point that makes it only marginally better than the individual fiber scheme. The percentage savings is about 7%.

The money that must be spent to realize the 7% weight reduction presents a 724% cost increase. The bulk of this increase is due to the need for crystal oscillators for modulating the feedback signals. These devices cost approximately $150 apiece greatly increasing the total cost of employing the control scheme.

Also realized with the amplitude modulation system is a 48% decrease in volume over the individual fiber scheme and a 20% increase in heat dissipation.

9.2 CONCLUSIONS AND RECOMMENDATIONS

Since the main concern in comparing parameters is weight reduction, it is obvious that both the amplitude modulation scheme and the individual fiber scheme are advantageous versus the copper wire scheme. The question now is one of cost. Is the extra 1.5 lbs saved by the amplitude modulation scheme over the individual fiber scheme worth the extra $2865 needed to realize it? Is the volume savings of the amplitude modulation scheme a significant part of the decision?

cable and connections in the vibrating environment of a small airplane. If either of the fiber optic control schemes are chosen, they will require extensive testing for reliability. This testing will require manpower and money. Also envisioned is a learning curve to be overcome when installing the fiber optic cable due to the bending radius requirements.

It is recommended here that aerospace engineers examine the data presented in this report and determine if the weight savings proposed by either of the fiber optic control schemes is worth the money required to make them flight worthy.

9.3 REFERENCES

1. Hoffman, Ron, and Wu, Ted, "Electrical System Design Considerations For The Advanced Personal Transport", AE 621, Fall 1991.

2. Evans, Darryl and DeMoss, Shane, "Electrical System Report For The Advanced Personal Transport", AE 622, Spring 1991.

10. STRUCTURAL DESIGN OF THE APT

This chapter presents the structural design of the Advanced Personal Transport Pusher Configuration as discussed in Reference 10.13.

Structural members will be sized for the cabin, the pressurized part of the fuselage, and the wing structure. The structural analysis and member sizing will be based on hand calculations and the result of a finite structural element program. The structural layout of the fuselage behind the aft pressure bulkhead will not be presented.

A preliminary model analysis will be performed by analyzing the natural frequencies for the wing in bending mode for an empty and a fuel loaded configuration.

10.1 FUSELAGE STRUCTURE

The Material selection for the fuselage skin is, as described in Reference 10.4, Glare 3. The reasons for this selection are :
- Glare 3 has a lower weight than aluminum
- Glare 3 offers outstanding fatigue properties
- Glare 3 has better 'fracture toughness properties'

Since the APT fuselage is not circular, which is not very favorable for pressure cabins, the last two mentioned reasons are of great importance.

The structural layout for the APT cabin is shown in Figure 10.1.

The entire fuselage structure could not be used for an finite element calculation because of program limitations. For this reason the structural design of the APT will be based on a part of the fuselage as shown in Figure 10.2.

The forces considered in the calculation will be :
- pressure force due to pressurized fuselage
  [P_{cabin} = 12 psi]
- pressure force on cabin floor
 [P_{floor} = 0.7 psi]
- weight of front part of the fuselage that is not modelled
  [Fy = -760 lb/node, Fz = 84.82*z/node]
- aerodynamic load, assumed to be 33% of fuselage drag at the cruise
  (high) condition [F_{aero} = 45.85 lb/node]

A summary of the forces are given in Figure 10.3. Shear forces at the cross section A-A have not been included in the model because it was impossible to model shear forces.

The maximum stringer and frame forces, calculated with the finite element method, have values far under the maximum allowable values. Since the total fuselage model is not considered in the analysis, good estimation of the effect of the external forces combined with the forces on the

STATION = 1 2 3 4 5 6 7 8 9 10 11 12 13 14 15 16 17 18 19 20

FUSELAGE
STATION   0 8.88 18.06 28.88 40 51.25 60.63 71.38 80.63 90.13 97.5 101.19 110 118.88 121.5 129 138.38 147.75 157.63 168
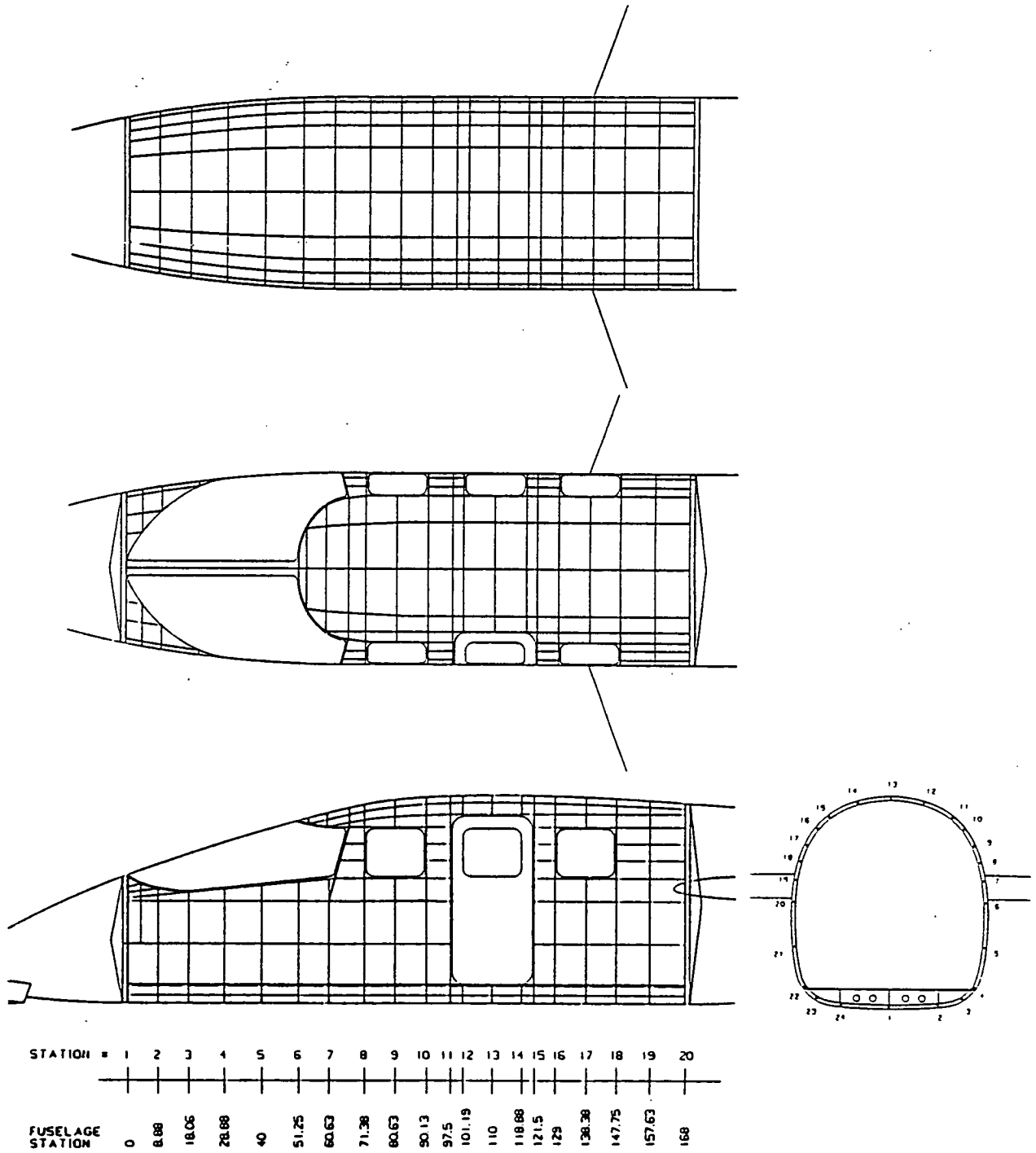
Figure 10.1 : Cabin Structural Layout
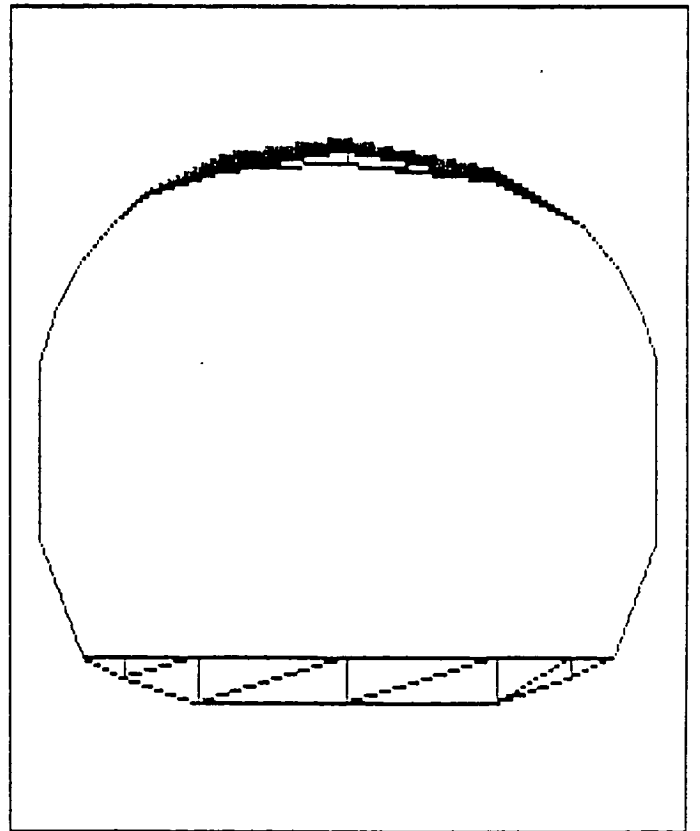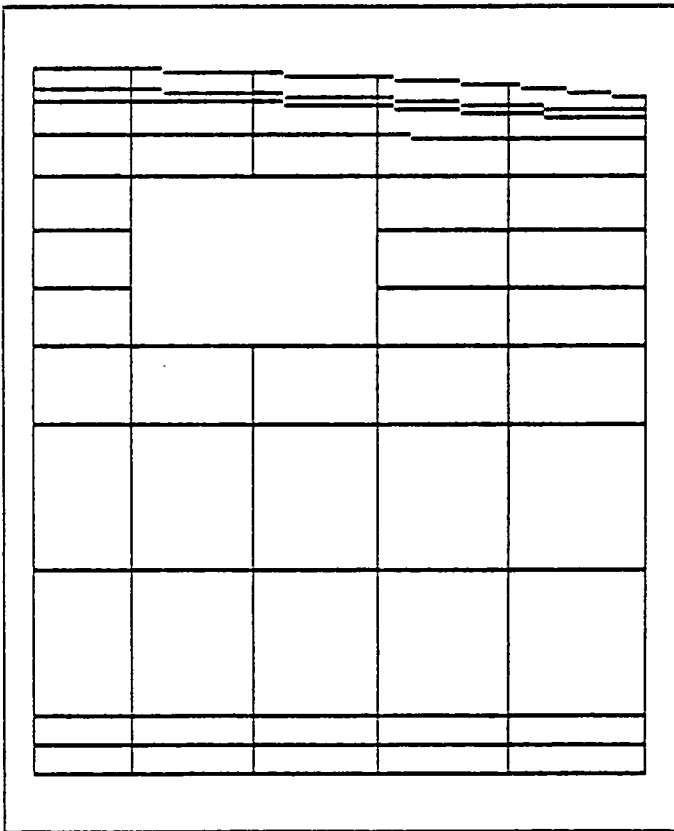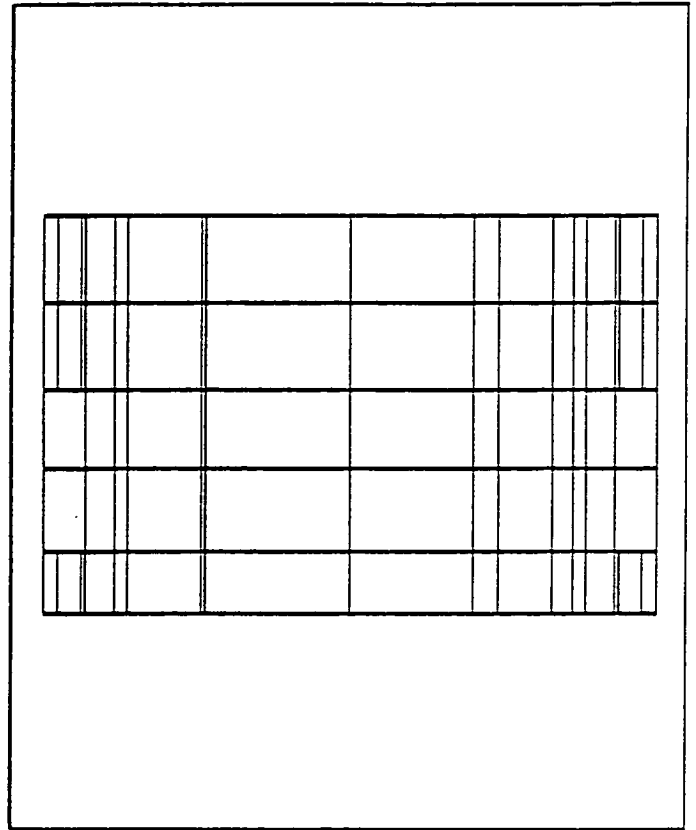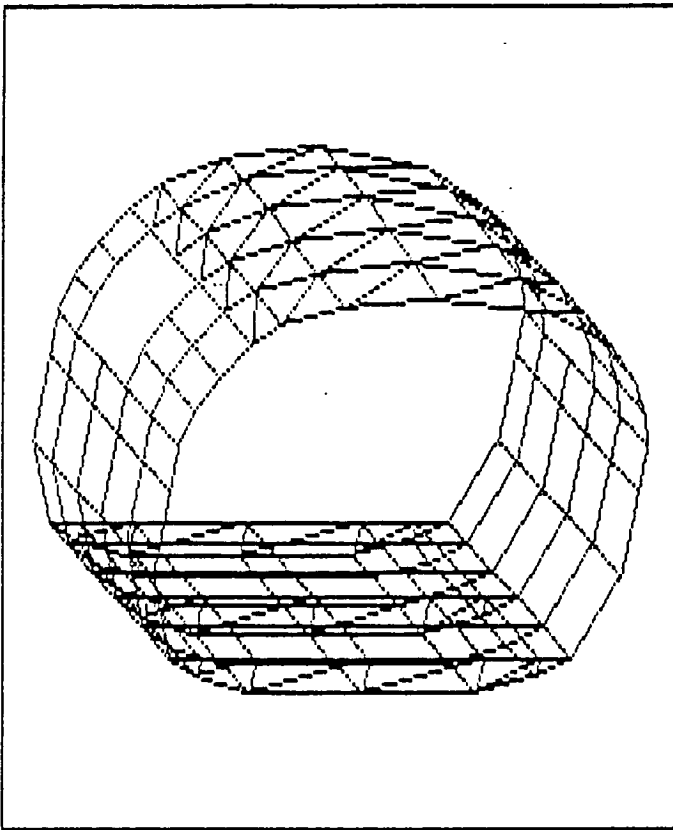
Figure 10.2 : Cabin Part used for Analysis
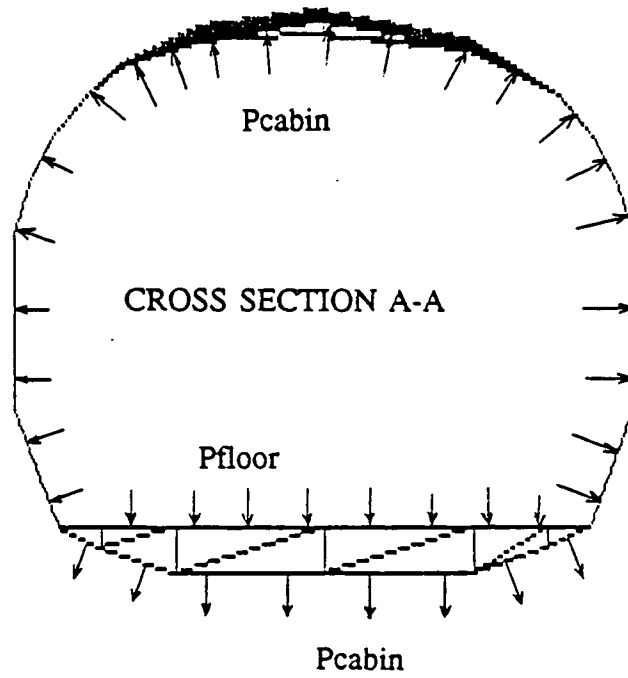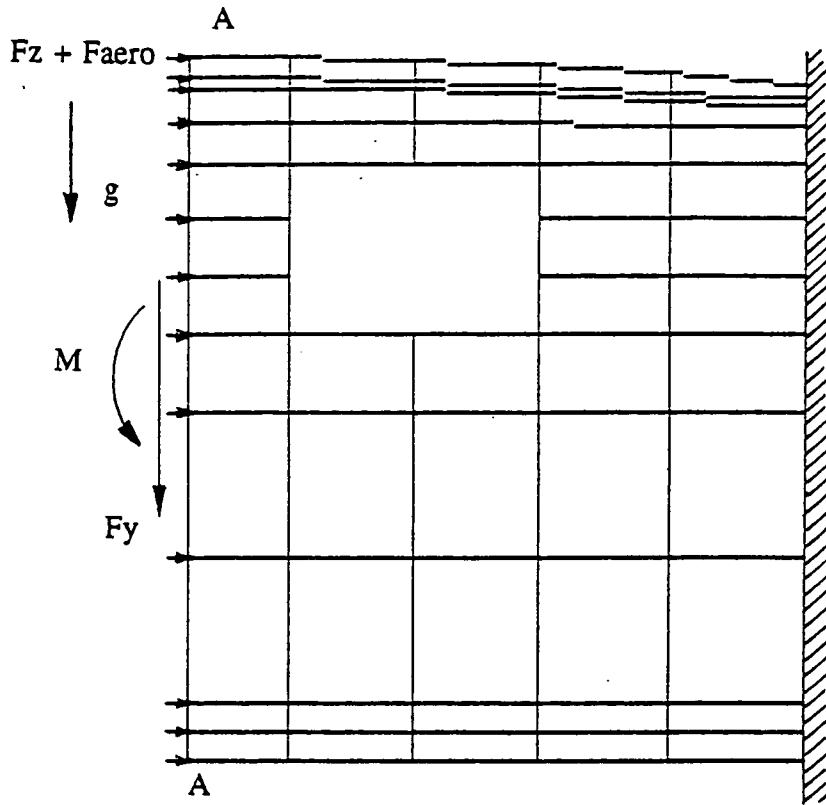
Figure 10.3 : Forces on Cabin considered in Analysis

cabin due to pressurization are not found. For this reason the stringer and frame properties as shown in Figure 10.4 will not be changed to other dimensions.

The stringer and frames will not be manufactured out of Glare. The reason for this is that the bending radius of Glare is approximately three times as big as Aluminum. With small stringer and frames cross sectional areas, the bending radius of Glare will lead to unacceptable shapes of structural members from a stiffness point of view. The skin thickness distribution for the APT cabin is shown in Figure 10.5.

All Dimensions in Inches
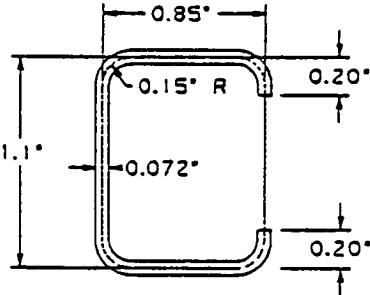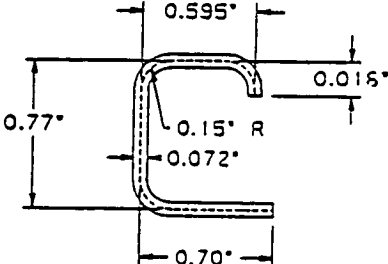
Cabin Frames   Cabin Stringers

[Not the Force Frames around Door Cut-Out]

Figure 10.4 : Cabin Frame/Stringer Size

MATERIAL : GLARE 3

☐ : t = 0.052 "

▨ : t = 0.072 "
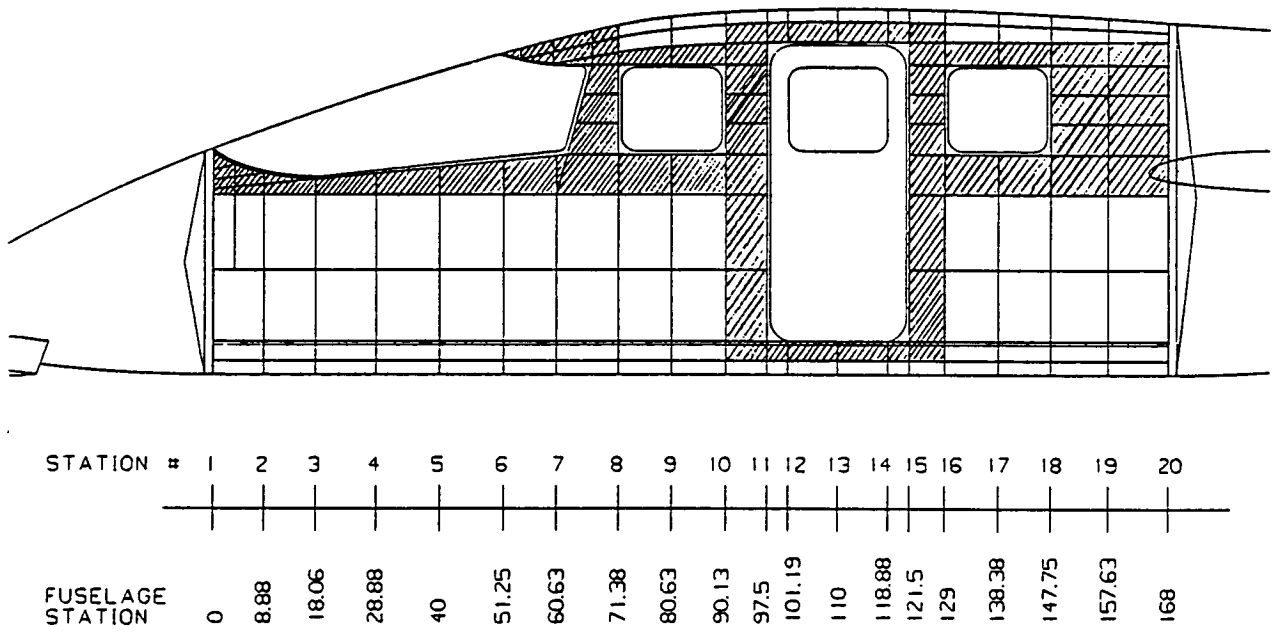
Figure 10.5 : Plate Thickness Distribution of Cabin

10.2 WING STRUCTURE

In this section the structural layout of the APT Pusher wing spar box will be presented.

From Reference 10.2 it is found that GLARE is unacceptable as a structural material for the wing because of lack of strength. The materials used for the wing structure are :
- Al 7075 for the upper wing skin and stringers
- AL 2024 for the lower wing skin and stringers
- AL 2024 for the ribs and spars.

The ultimate load factor for the APT will be 5.4 from gust loading. The forces considered in the calculation will be :
- pressure force due to wing lift
- weight of the wing structure

Not included in forces on the wing in this stage of wing structure design will be :
- Fuel weight
- Weight of mechanic devices, wires, electronic equipment and other equipment in the wing
- Forces introduced due to the horizontal tail transmitted by the tailbooms

The forces on the wing have been modelled as shown in Figure 10.6.

Figure 10.7 shows the Images3D wing spar box input.

From the structural analysis it is found that the forces through the beam members close to the wing root were much too high to prevent the upper wing structure from buckling. Some modification had to be made to the wing structure:
- the stringer size will be increased relatively more for stringer located in the aft swept part of the wing as for the forward swept wing part.
- the number of ribs in the aft swept part of the wing will be increased.
- to decrease the wing plate stresses, the wing skin thickness will be increased in some areas. The modified wing skin thickness distribution is given in Figure 10.8.

The modified wing spar box structure is shown in Figure 10.9.

P1 = 46.923 psi

P2

P3

P4

FRONT VIEW

P2 = 42.23 psi
P3 = 32.85 psi
P4 = 18.77 psi

gravity

50% P

50% P

SIDEVIEW
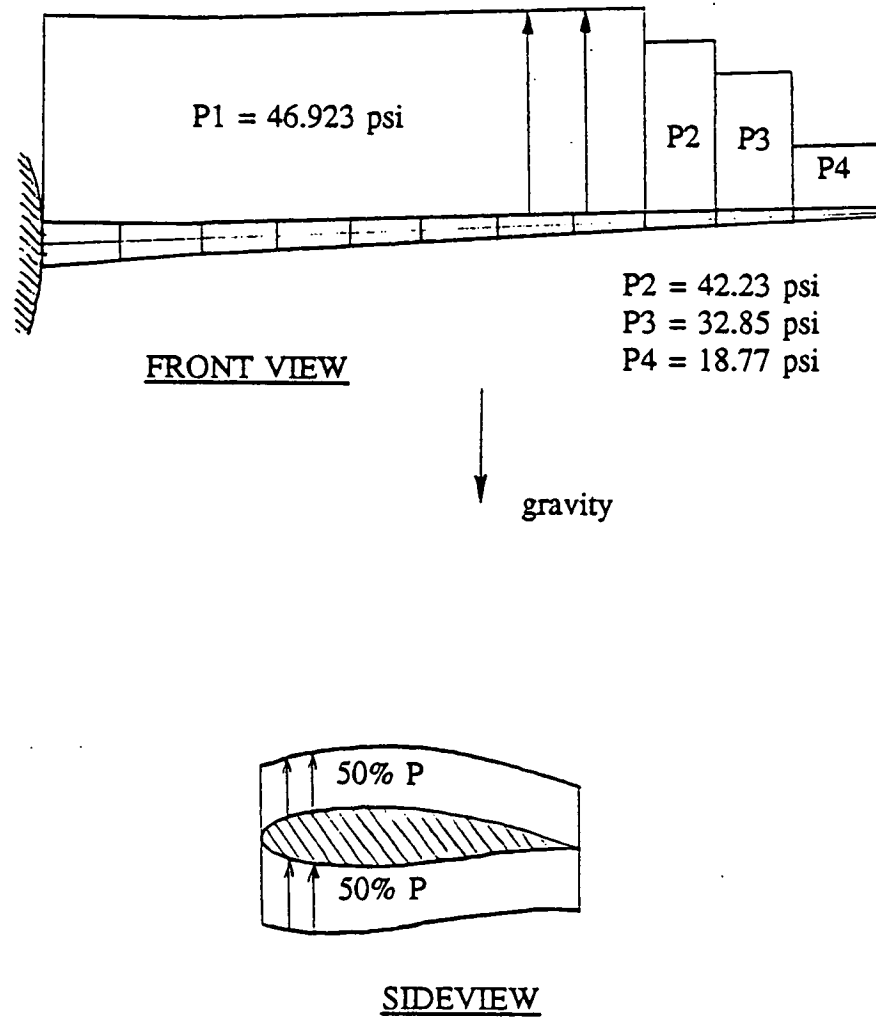
Figure 10.6 : Forces on Wing considered in Analysis
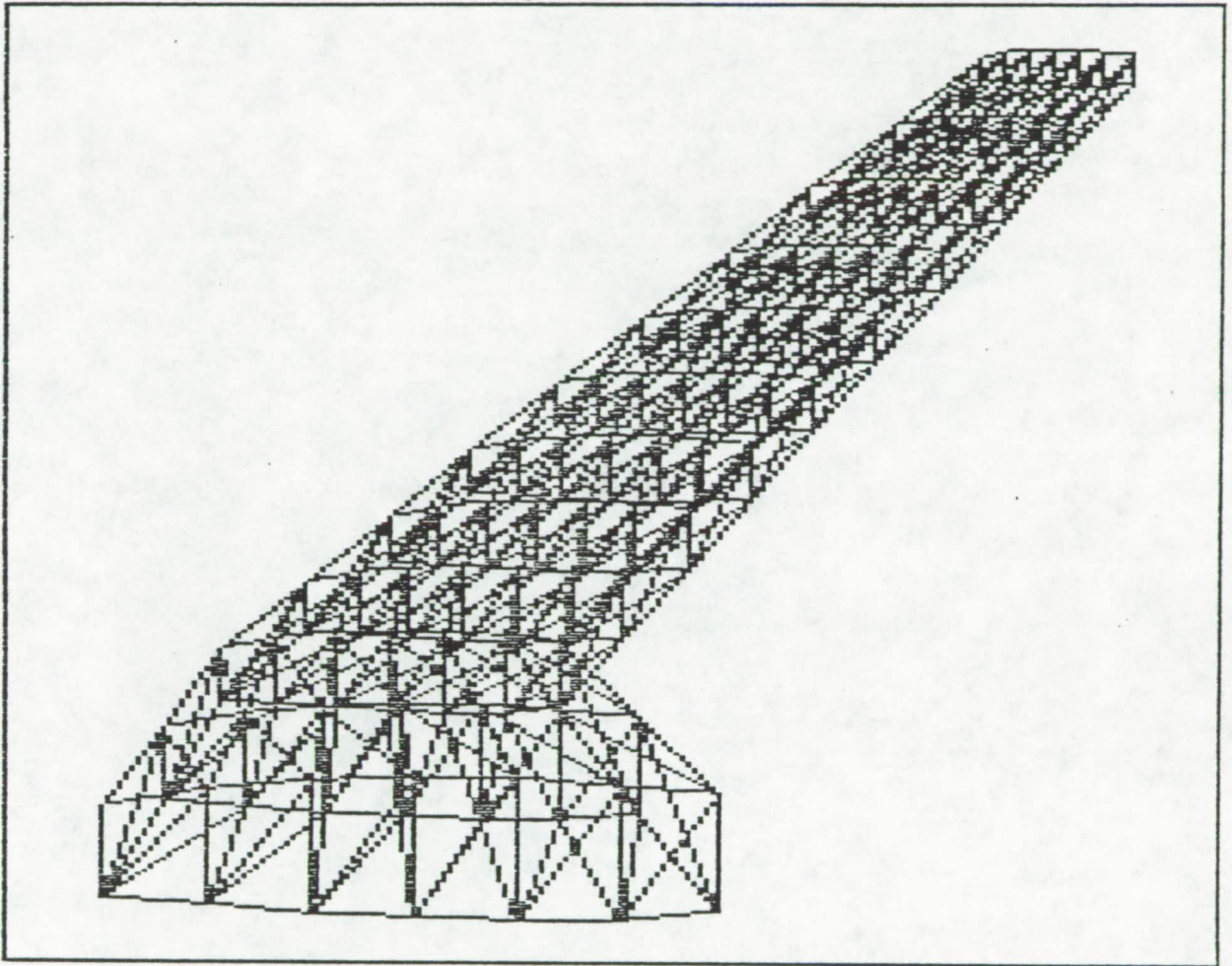
Figure 10.7 : Images3D Spar Box Layout
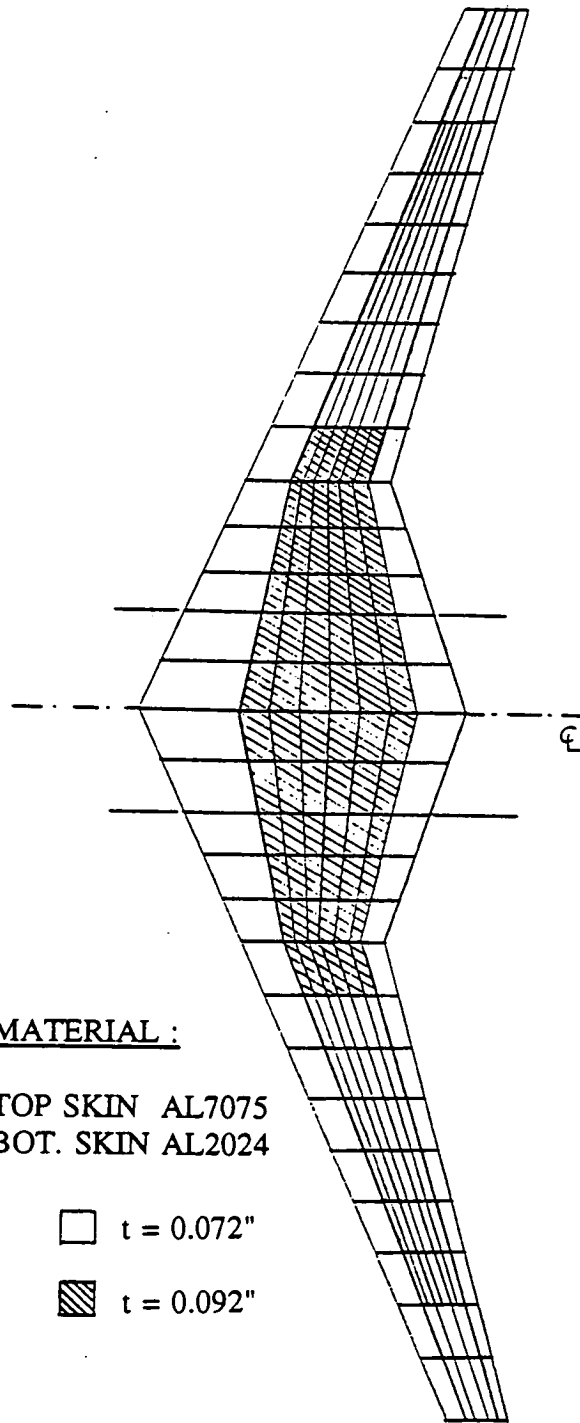
MATERIAL :

TOP SKIN   AL7075
BOT. SKIN AL2024

□ t = 0.072"

▨ t = 0.092"

Figure 10.8 : Wing Plate Thickness Distribution

TYPE A STRINGER

TYPE B STRINGER
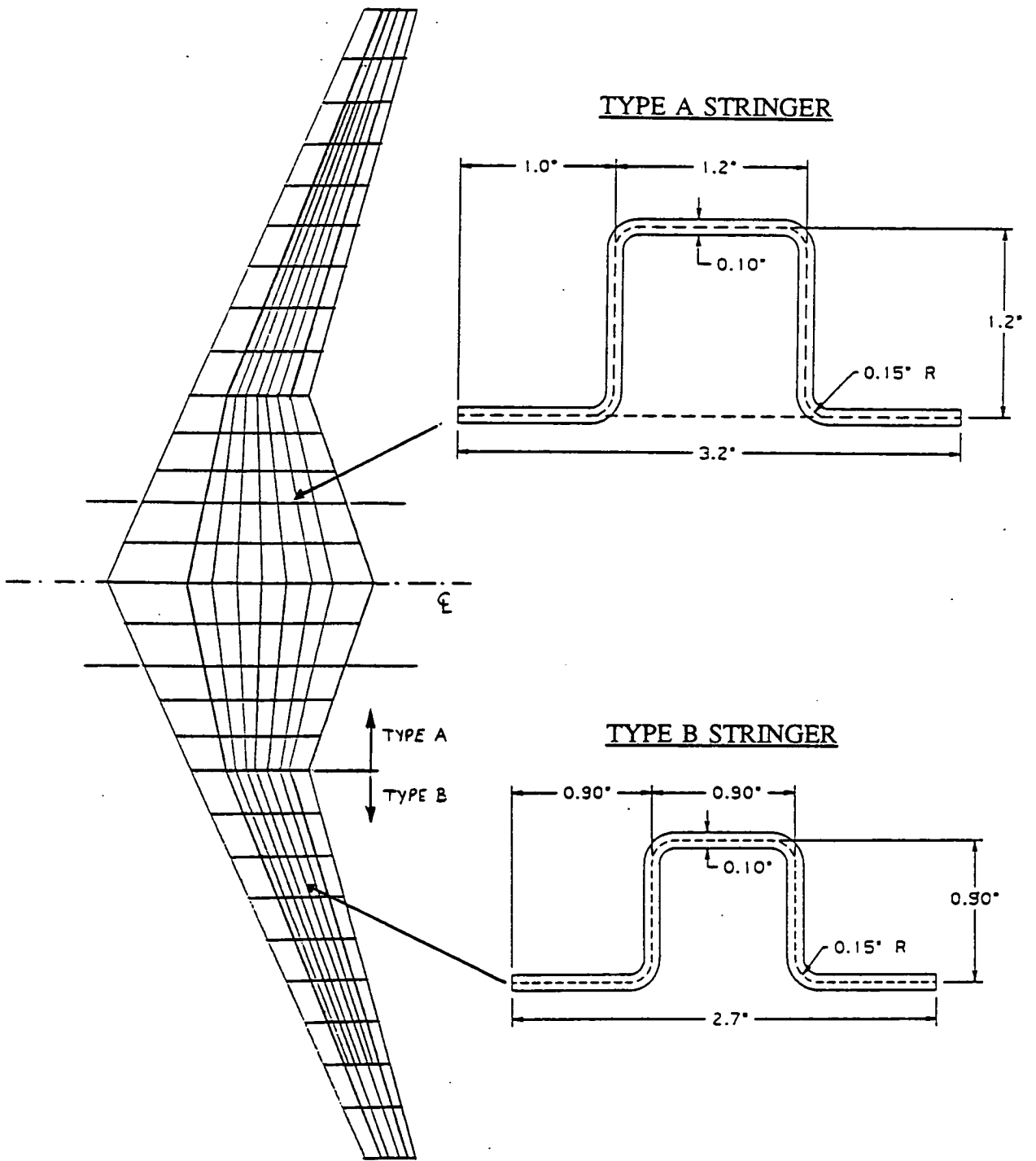
Figure 10.9 : Wing Spar Box Layout

10.3 FLUTTER ANALYSIS

To prevent the wing from flutter, the natural frequencies for the wing for two conditions will be investigated :
- an empty wing
- a fuel loaded wing

The mass distribution used for the computation is given in Reference 10.3 and includes corrections for the increase in wing mass due to the weight of mechanic devices, wires, electronic equipment and other equipment in the wing

The restriction for the evaluation of the wing natural frequencies is that no tail boom weight and/or empennage weight is included in the computation.

Results of the flutter analysis are shown in Figure 10.10.
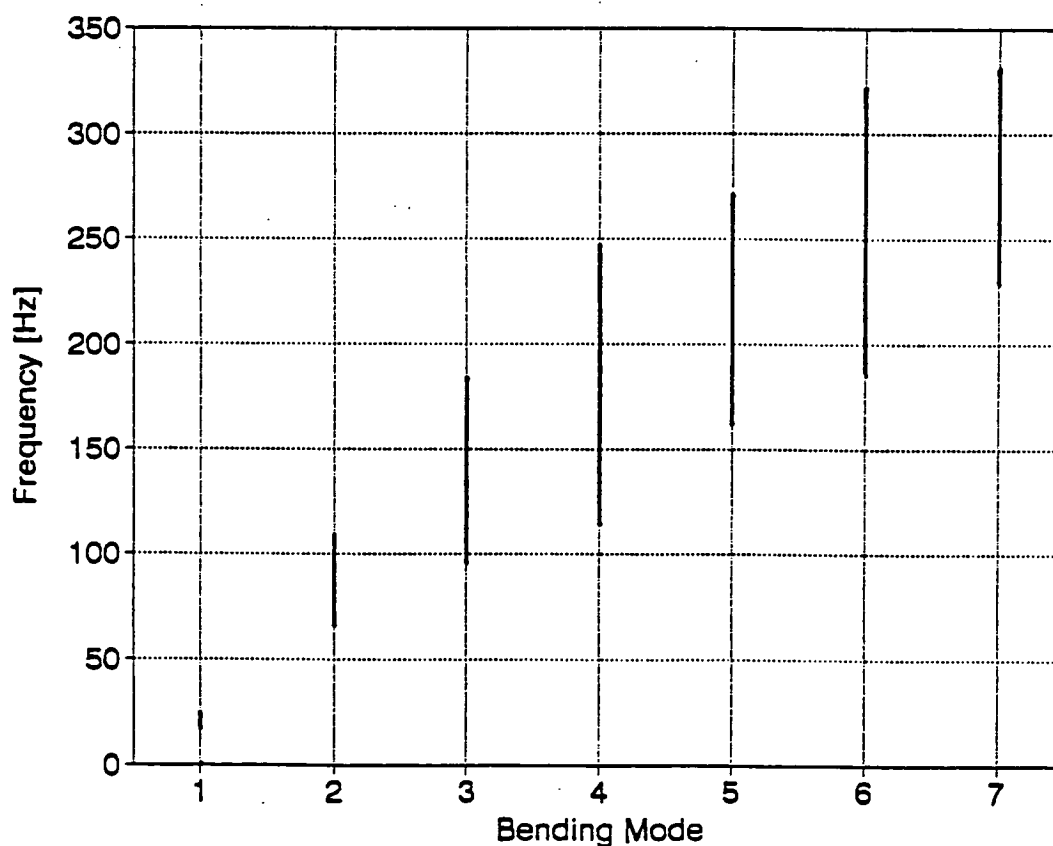
Figure 10.10 : Wing Natural Frequencies

10.4 CONCLUSIONS AND RECOMMENDATIONS

The conclusions of this chapter are :
- The total weight of the Torsion Box is found to be 410 lb.
  This figure does not include bonding, rivets or system component weights and is not corrected for increase in weight due to access panels, reinforcements and weight decrease due to cut outs in ribs.
- To prevent wing flutter, all frequencies occurring in the restricted area in Figure 10.13 should be avoided.
- The tailboom, empennage and aft fuselage structure has not been analyzed, and the shown structure is therefore still very preliminary.
- The stringers and frames will not be made out of GLARE 3. Because the bending radius of GLARE is almost 3 times as big as conventional aluminum, the frame and stringer sizing will lead to, from a stiffness point of view, unacceptable results when small cross sectional areas are allowed.

Recommendations for further structural analysis are :
- With the modified structure a structural analysis should be performed to check if the stress limits are not exceeded.
- For use of the program as described in Reference 8, it is strongly recommended to develop a simple program which will generate the node coordinates, plate and beam definitions and will write these data to a seq. file. This file can be read by the Images program and will save the user lots of work and will provide more accuracy in the calculation. If cut-outs are present they can be defined in a later stage by just deleting the specific plates and/or beams.
- To get a total overview of more accurate flutter frequencies, a model should be developed, including tail and tailbooms.
- The tailboom, empennage and aft fuselage structure should be analyzed more accurately. This has not been done so far because of time constraints/manpower shortage.
- Any structural analysis will lead to more accurate results when the whole structure is considered. With the NASTRAN program this might be possible, however, this program is not as easy to use as Images3D.
- The use of aluminum 7075, which has higher strength but inferior fatigue characteristics compared with Al 2024, for the upper skin of the wing torsion box has to be examined on corrosion characteristics.

10.5 REFERENCES FOR CHAPTER 10

10.1   M. Niu, <u>Airframe Structural Design</u>, Conmilt Press LTD., March 1988.

10.2   J. Anderson and S. Jackson, <u>Preliminary Load and Stress Analysis for the Advanced Personal Transport</u>, University of Kansas, December 1990.

10.3   S. Baugues and J. Weiss, <u>Wing Layout and Manufacturing Tolerances of the Advanced Personal Transport</u>, University of Kansas, December 1990.

10.4   P. Chronister and S. Jackson, <u>Fuselage Design and Manufacturing Study</u>, University of Kansas, December 1990.

10.5   AE 621 Design Team. <u>Preliminary Design Studies of Advanced General Aviation Aircraft</u>, University of Kansas, December 1990.

10.6   E. Torenbeek, <u>Synthesis of Subsonic Airplane Design</u>, Delft University Press, 1982.

10.7   C.Vermeeren, L. Vogelesang and J. Gunnink, <u>New Developments in Fibre Metal Laminates</u>, March 1990.

10.8   Celestrial Software, <u>IMAGES-3D Finite Element User's Manual</u>, Celestial Software Inc., 1990.

10.9   J. Roskam, <u>Airplane Design</u>, Part VI, 1987.

10.10   A. M. Dirkzwager, <u>Natural Laminar Flow Airfoil Design for the Advanced Personal Transport</u>, University of Kansas, December 1990.

10.11   B. Dijkshoorn, <u>Vliegtuigconstructies II</u>, University of Delft Volgnummer 8505 2, October 1977.

10.12   AE 621 Design Team, <u>Preliminary Design of Two Configurations</u>, University of Kansas, December 1990.

10.13   AE 621 A.M.Dirkzwager, <u>Structural Design of the Advanced Personal Transport Pusher Configuration</u>, University of Kansas, December 1990.

11. DEVELOPMENT/MANUFACTURING LAYOUT

The purpose of this chapter is to present the APT facility/department structure and the APT final assembly stages as discussed in Reference 11.6.

11.1 APT DEPARTMENT STRUCTURE

This section will present the department structure for the APT facilities.

The total engineering department, see Figure 11.1, will consist of the following sub-departments:

- Preliminary Design
- Aerodynamics
- Structures
- Certification
- System Integration
- Performance
- Stability/Control
- Electrical System Design
- Cad/Cam Design
- Manufacturing
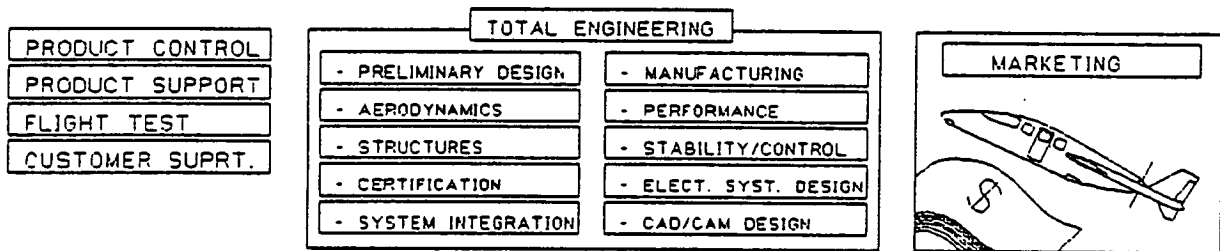
Figure 11.1 : APT Department Structure Layout

Preliminary Design : Even though the APT's market expectations are high, it is not expected that a break even point will be reached in the next ten years. Therefore, APT derivatives have to be developed through constant research by the Preliminary Design Group. In the long term, the company will face financial difficulties if it doesn't look further than the APT. Technological developments together with the experience gained during the APT development should lead to the development of better models in the long term.

Aerodynamics : Detailed design of the wing, empennage and aerodynamic shape of the fuselage will be performed by the Aerodynamic Department. This includes computational flow dynamics, wind tunnel testing and evaluation of flight test data.

Structures : Detailed structural design using finite structural element codes such as Nastran, and flutter and vibration analysis for each aircraft component will be performed by the Structural Design Group.

Certification : Since the APT will charter new areas in which regulations have not yet been defined, new regulations will be jointly developed by the FAA and APT manufacturer. This process was used in the certification process of the Beech Starship 2000. The Certification Department will be concerned with the final certification of the APT; which includes the cooperation with the FAA.

Systems Integration : Since the APT has many different systems, the success of the APT is largely dependent on the performance of this department in effectively integrating all of the systems. In addition to systems integration, this department will be concerned with system maintainability, supportability, and cost.

Performance : This group will be concerned with the determination and improvement of the performance characteristics of the APT.

Stability and Control : Estimation, verification and improvement of the stability and handling qualities of the APT will be the task of this group. This includes the design of the flight control systems.

Electrical System Design : All electrical systems not developed by sub contractors, which includes most of the computer hardware, will be designed in the Electrical System Design Group. This also includes necessary modifications of the hardware provided by sub contractors.

Cad/Cam Design : This group will be responsible for the APT geometry/manufacturing data base. This group forms, like the manufacturing department, a link between engineering and the manufacturing line.

Manufacturing : The Manufacturing Department will be the main link between engineering and the manufacturing lines. It is recommended that this group contain at least one engineer who has a background in all of the major departments and a background in management. This type of personnel should allow for smooth operations between manufacturing and engineering and ultimately a better final product.

All of the APT information will be stored in the host computer in such a manner so that all departments will have access to the latest information. Of course backups will be kept in the case of an emergency. Within the file there will be many different categories, for example CAD/CAM. In some cases, only specific departments will have access to certain areas in the database so that modifications can be made and the database kept current.

Other divisions in the APT manufacturing infrastructure are :

- Marketing
- Product Control
- Product Support
- Flight Test
- Customer Support

11.2 DIFFERENT COMPONENT MANUFACTURING LINES

Recent years have shown that it is very hard for a single airframe manufacturer to successfully start a big project. Most civil as well as military high technology projects these days are a venture between different manufacturers. To make it possible to manufacture the APT with a partner, the manufacturing/storage divisions will consist of the following eight components (see Figure 11.2) :

- Electrical System Manufacturing
- Spare Parts and Supplies
- Frame and Stringer Manufacturing and Plate preparation
- Gear Manufacturing
- Wing Manufacturing
- Empennage Manufacturing
- Tailboom Manufacturing
- Fuselage Manufacturing
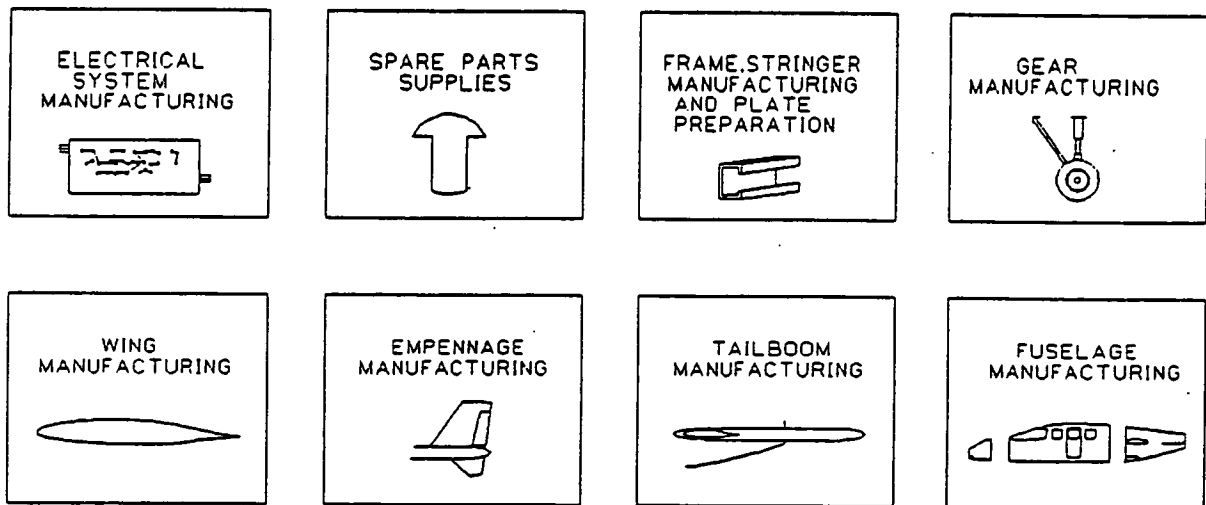
Figure 11.2 : Different Component Manufacturing Lines

Most divisions will be able to use conventional tooling and machinery to manufacture the APT (Reference 11.5). However, the Frame and Stringer Manufacturing Division will use a machine which has to be developed. The machine will be linked with a Cad/Cam network (see Figure 11.3). After a plate has been sized and cut, this machine will form and bend the plate in the shape of the requested stringer or frame. The user only has to select the part number of the stringer or frame and the machine will produce the part. This method of production will give accurate and constant quality once the machine has been calibrated. The general layout of this production system is shown in Figure 11.4.
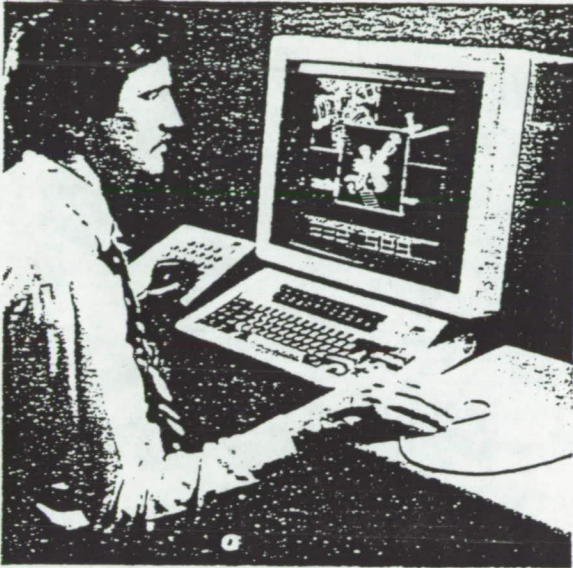
Figure 11.3 :

An Engineer using computer-aided design (CAD). After he is done, his design will be interfaced with computer -aided manufacturing (CAM) to produce the component. (Courtesy Boeing)
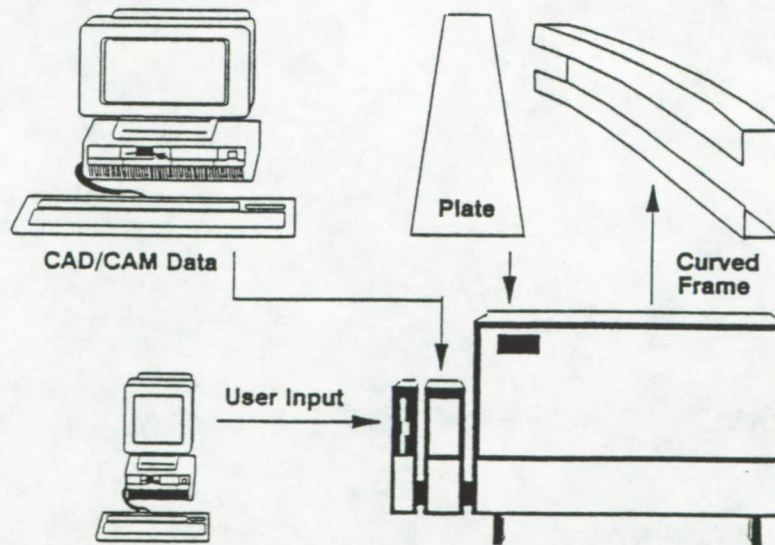
Figure 11.4 : Manufacturing Equipment, stringer and frame bending machine

119

11.3 MANUFACTURING LINE

The production line of the APT is shown in Figure 11.5. The production line is divided into eight steps :

1 - Cabin section will be finished or received from co-manufacturer and prepared for the final production line

2 - Aft fuselage will be attached to the cabin

3 - Main gear and nose gear will be installed, from now on the aircraft must be balanced in the manufacturing process

4 - The wing will be attached to the fuselage

5 - The tailbooms will be attached to the wing

6 - The engine and associated systems will be installed.
The empennage will be attached to the tailboom and the control surfaces will be installed (this includes the wiring)

7 - The spinner/prop will be attached to the engine, the supporting electrical systems will be installed and the wiring will be finished

8 - Cabin furnishings will be installed and the aircraft will be painted
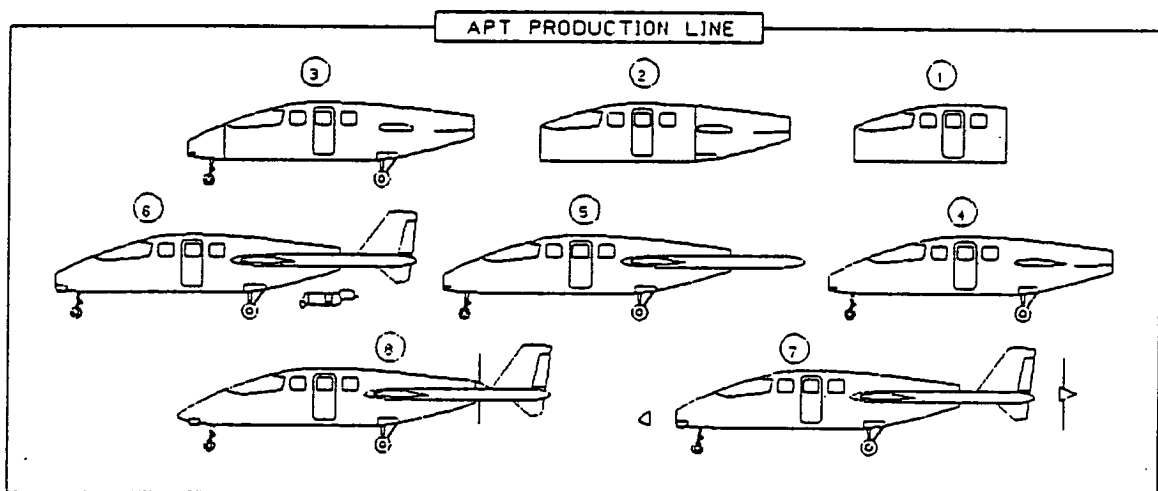
Figure 11.5 : APT Production Line

11.4 REFERENCES FOR CHAPTER 11

11.1   DAR corp, <u>Advanced Aircraft Analysis program</u>, Users Manual 1990.

11.2   J. Roskam, <u>Airplane Design : Part VIII, Airplane Cost Estimation and Optimization : Design, Development, Manufacturing and Operating</u>, Roskam Aviation and Engineering Corporation, Ottawa, KS 66067.

11.3   AE 621, <u>Preliminary Design Study of an Advanced General Aviation Aircraft</u>, University of Kansas, 21 December 1991.

11.4   S. Baugess and J. Weiss, <u>Wing Layout, Design and Manufacturing Tolerances of the Advanced Personal Transport</u>, University of Kansas, December 21 1990.

11.5   P. Cronister, <u>Fuselage Design and Manufacturing Study</u>, University of Kansas, 21 December 1990.

11.6   A. M. Dirkzwager, D. Knipp, <u>Manufacturing Plan and Cost Analysis for the Advanced Personal Transport Pusher Configuration</u>, University of Kansas, December 21 1990.

12. WEIGHT, BALANCE AND INERTIAS

The purpose of this chapter is to present the results from calculations performed to determine the component weights for the APT pusher. These weights will be used to determine the center of gravity of the airplane as well as the c.g. excursion. Finally, the moments of inertia can be calculated using the weight data and the locations of each component. This work is "fine tuning" of the work that was previously accomplished in Reference 12.1.

12.1 WEIGHT ESTIMATION

The methods presented in Reference 12.2 were used to determine the component weights for the APT. The primary inputs to the method are the geometry of the airplane. This is largely unchanged from Reference 12.1 except for the change in wingspan. The wing was re-sized to increase the performance of the airplane. The other inputs to the analysis are values from a V-n diagram and the weights for the passengers and baggage. Both of these inputs are unchanged from Reference 12.1.

Due to the advanced materials and systems used in the airplane, some variation in the weight of some components is to be expected from conventional aircraft. This was accounted for by using "technical factors" multiplied by the various component weights. Most of the assumptions in Reference 12.1 are used again. Some components used different technical factors because it was felt that the old values were a bit to severe. These are listed in Table 12.1.

Table 12.1: Comparison of Technical Factors

Weight Component	Old Tech Factor	New Tech Factor
Flight controls	50% reduction	20% reduction
Electrical system	50% penalty	40% penalty
Instruments & Avionics	20% penalty	30% penalty

It was felt that the 50% reduction assumed for the flight controls was a bit too optimistic for a first generation fly by wire aircraft. This is the reason for the smaller credit taken for technology. Similarly, the 50% increase in the electrical system weight seemed to be too severe and was thus reduced slightly. The instruments and avionics used in the airplane rely extensively on the use of computers and displays. This extensive use of electronics seemed to warrant a little larger penalty than was previously assumed. It is noted that all of these assumptions should be checked as more detailed information is known about the components of the airplane.

The previous information is used in a spreadsheet program to make quick iterations possible. The results from the calculations are summarized in Table 12.2.

Table 12.2: Component Weights for the APT Pusher

STRUCTURE WEIGHT	COMPONENT WEIGHT (lbs.)
Wing	461
Canard	119
Horizontal tail	54
Vertical tail	49
Fuselage	483
Tail booms	94
Landing gear	266
TOTAL:	**1526**

PROPULSION SYSTEM WEIGHTS:	
Engine	860
Air induction sys.	84
Fuel system	179
Propeller	134
Prop. Controls	2
Engine start	34
Engine controls	64
Prop gearbox	150
TOTAL:	**1506**

FIXED EQUIPMENT WEIGHTS:	
Flight Controls	220
Elect. System	316
Instr. & Avionics	192
A/C & Anti-ice	206
Oxygen System	31
Furnishings	203
Aux. Gear	43
Paint	44
TOTAL:	**1254**
EMPTY WEIGHT:	**4286**

12.2 AIRCRAFT BALANCE

The purpose of this section is to describe the balance of the aircraft. This was done using the component weights from the previous section along with the locations of the components to determine the center of gravity of the airplane. The c.g. excursion can also be determined by using different loading and unloading scenarios in the weight and balance spreadsheet. The locations of the components are unchanged from Reference 12.1.

Table 12.3 summarizes the results from the center of gravity analysis.

Table 12.3: Summary of C.G. Locations for the APT

CONDITION	C.G. LOCATION
Gross Weight	245
Empty Weight	246
Most Aft	251
Most Forward	238

It is noted that the most aft c.g. will not be a problem from an airplane stability point of view. This is because this occurs at a point in the loading in which just the wing tanks are filled and no passengers or pilots have entered the airplane. This value will have an impact on the landing gear placement. This will affect the longitudinal tip over considerations of the APT. The furthest that the c.g. will be aft during flight is at the value for gross weight. Using this value the APT has a c.g. travel of 7 inches. With a M.A.C. of 48 inches this corresponds to a 15% shift in center of gravity. From Reference 12.3 it is noted that typical values for this class of airplane are 8-16 inches and 10-21% of M.A.C. Therefore it can be concluded that the APT has acceptable center of gravity travel.

12.3 MOMENTS OF INERTIA

This section will summarize the moments of inertia of the APT. The analysis was conducted for the gross design takeoff weight. The weight and balance spreadsheet of the previous sections was used to obtain the moments of inertia. To check the analysis, the radius of gyration method was also used. The summary of the analysis is given in Table 12.4.

Table 12.4: APT Moments of Inertia

	Components	Radii of Gyration
I_{xx} (slug-ft^2)	4286	4608
I_{yy} (slug-ft^2)	8722	8826
I_{zz} (slug-ft^2)	11205	11881

12.4 REFERENCES FOR CHAPTER 12

12.1 Barrett, R., et al., <u>Preliminary Design of Two Configurations</u>, AE 621, Fall 1990, University of Kansas.

12.2 Roskam, J., <u>Airplane Design: Part V, Component Weight Estimation</u>, Roskam Aviation and Engineering Corporation, Ottawa, KS 66067.

12.3 Roskam, J., <u>Airplane Design: Part II, Preliminary Configuration Design and Integration of the Propulsion System</u>, Roskam Aviation and Engineering Corporation, Ottawa, KS 66067.

13 MAINTENANCE AND REPAIRABILITY STUDY

The goal of the Advanced Personal Transport (APT) maintenance program is to reduced pilot's work load and decrease maintenance Life Cycle Cost (LCC). This is accomplished using Built-In-Test-Equipment (BITE) to provide an advance warning of failures. This maintenance approach will reduce pilot workload while increasing the reliability of the APT by detecting failures prior to their occurrence.

13.1 INTRODUCTION

Many of the maintenance requirements of the APT are similar to other aircraft in its class. However, a distinct feature that the APT employs is its use of Built-In-Test-Equipment to perform maintenance tasks and checks.

The engine section of the APT was designed to simplify repair. All major components may be removed without engine removal. This reduces the LCC and reduces the time required to perform engine repairs. In the event of major engine repair, the entire propulsion unit can be quickly removed.

13.2 APT PUSHER MAINTENANCE SCHEDULE

To provide a comprehensive maintenance program, the APT Pusher maintenance plan includes both scheduled and unscheduled maintenance checks and routines. This maintenance program is based on criteria set by the Federal Aviation Administration (FAA). The maintenance manual of the Beechcraft Starship was used as a guide to develop the maintenance schedule for the APT Pusher.

13.2.1 Scheduled Maintenance

A periodic maintenance schedule was developed based on the FAA requirements. The altimeter instrument and static system and all ATC transponders MUST be tested and inspected in 24-month intervals in compliance with the requirements specified in FAR Part 91. This check must be performed in addition to the inspections included in this schedule. A table detailing the maintenance specifications was developed for the periodic maintenance schedule; However due to its volume, this schedule will not be presented in this report (see reference 13.2).

13.2.2 Unscheduled Maintenance

Unscheduled maintenance procedures are recommended when uncommon incidents occur which may endanger the safety of the aircraft. A table detailing the unscheduled maintenance procedures recommended for the APT Pusher was developed; However due to its volume, this schedule will not be presented in this report (see reference 13.2).

13.3 PRE-FLIGHT BITE TEST SOFTWARE

The focus of this section of the report is software development for the Built In Test Equipment (BITE) testing referred to in Reference 1. The function of this particular software is exclusively to determine the preflight worthiness of flight control surface actuators. The objectives of the test are as follows:

1. Exercise each flight control surface during pre-flight mode of operation.

2. Check each actuator against minimum, unloaded performance criteria.

3. Identify those actuators failing to meet that criteria.

4. Record and store data on each actuator for all previous BITE tests in a file in main computer memory.

5. Upon discovery of faulty actuator(s), abort flight attempt and notify pilot of BITE test failure.

Although a BITE test failure is labeled as a faulty actuator, this may not be the case. A part of this section is devoted to the interpretation as well as the generation of BITE test data.

13.3.1 Generation of Data

This section gives a general description of the process performed by the BITE Test software. The software will perform the following sequence of actions in order:

1. An ample number of successive signals will be transmitted to initialize the actuators of the first control surface to be tested to predetermined "flaps down" angle. This position will be recorded as the minimum start position in the BITE test file.

2. A predetermined number of signals directing the actuators to a "flaps up" position is then transmitted.

3. Once the signals in step 2 have been transmitted to the actuators, their positions are compared to a "flaps up" performance criteria angle as well as recorded in the BITE test file. If any of the actuators fail to meet the performance criteria angle, it is flagged as such in the BITE test file.

4. The actuators are then sent an ample number of signals commanding to initialize at the "flaps up" position. At the end of the transmission the positions of the actuators will be recorded in the BITE test file.

5. A predetermined number of signals corresponding to a "flaps down" position are then sent to the actuators. At the end of the transmission, each actuator position is recorded in the BITE test file as well as compared to the "flaps down" performance criteria angle. Those actuators, if any, not meeting the performance requirement will be flagged in the BITE test file.

6. After completion of the BITE test on that particular control surface, the process is carried out on the next control surface. This process continues until all control surfaces have been tested.

7. If any actuator fails to meet the BITE test criteria, an "abort mission" flag is set. This flag will cause a message to appear on the pilot's CRT indicating that a BITE test failure has occurred.

13.3.2 Interpretation of Data

The purpose of the BITE test is not only to prevent occurrence of flights with faulty equipment but also to be used as a trouble shooting tool to save time and money. By interpreting the data correctly, maintenance time can be greatly reduced.

Examining the BITE test data can direct maintenance personnel toward finding the faulty device that aborts a mission. The data contained in the BITE test file can reveal whether a feedback sensor or amplifier is bad, an open circuit in the power wiring to an actuator has occurred, an open circuit has occurred in the control signal wiring, or an actuator has actually failed.

There are many ways in which to use the data from the BITE test file to greatly reduce trouble shooting time for control surface malfunctions and these are only a few. Since access to the BITE test file will be via a port on the plane's main computer, all maintenance personnel need is a portable computer and cable to obtain the information.

13.3.3 Pre-flight Bite Test Program Code

It is envisioned that this program will be executed before the Primary Flight Controller (PFC) program at the beginning of each flight. Therefore the program will reside in the PFC computer memory. Since the PFC programs were written in the Pascal language, so to was the BITE test program [2]. The BITE test obviously requires communication with the actuator, as does the PFC, and therefore will utilize many of the same communication subroutines as the PFC program.

13.4 ENGINE REMOVAL AND SERVICING

The purpose of this section is to discuss the method in which the APT engine is serviced. Both minor and major servicing of the engine will be discussed. Minor service would include additions of engine oil or changing the oil filter. Other servicing that will be considered to be minor would be the replacement of a Line Replaceable Unit (LRU). These items include but are not limited to the following:

- Starter Generators
- Fuel control units

Major services would include things such as hot section inspections or other repairs that would require the engine to be removed from the airframe. This report will only deal with the engine removal process and not the actual repair.

The APT uses two Garrett TPE331-15 engines mounted to a Soloy Conversions Dual Pack to drive a single propeller. A perspective view of the engine is shown in Figure 13.1.
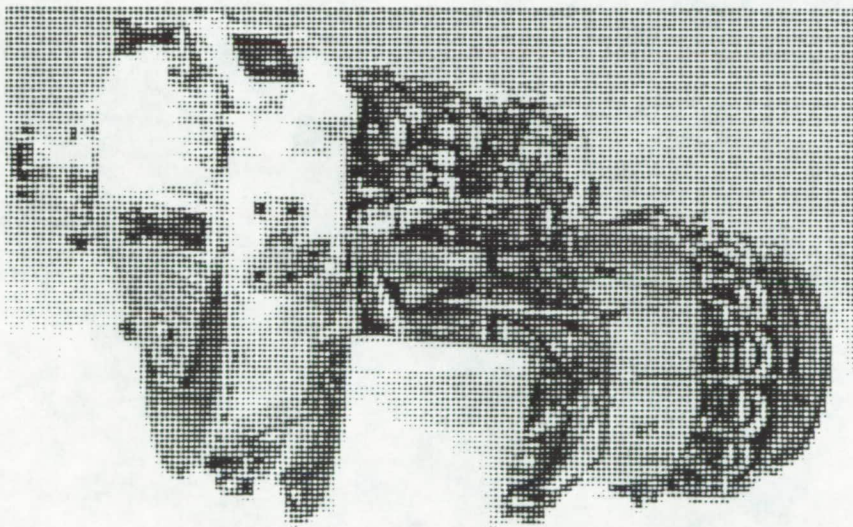
Figure 13.1: Garrett TPE331-15 Turboprop Engine (Copied from Ref. 13.1)

13.4.1 Engine Removal Procedure

This section will cover the procedure used to remove the powerplant unit from the APT. The powerplant was made to be as much of a complete unit as possible. This will allow the entire unit to be removed at once without having to remove a lot of items. This should allow for quick removal times.

The following procedure assumes that the APT is being serviced by an authorized service center. Refer to Figure 13.2 to see how the powerplant unit is attached to the APT airframe.

MAIN ATTACHMENT TRUSS

CENTER TRUSS/ ENGINE BURST SHIELD

PROP SHAFT

GEAR BOX

ENGINE ENVELOPE

ENGINE EXHAUST

SECONDARY ATTACHMENT TRUSS

Figure 13.2: Engine Installation in the APT

130

EXHAUST

INLET

REMOVABLE ENGINE ITEMS

ENGINE TRUSS

LANDING GEAR DOOR
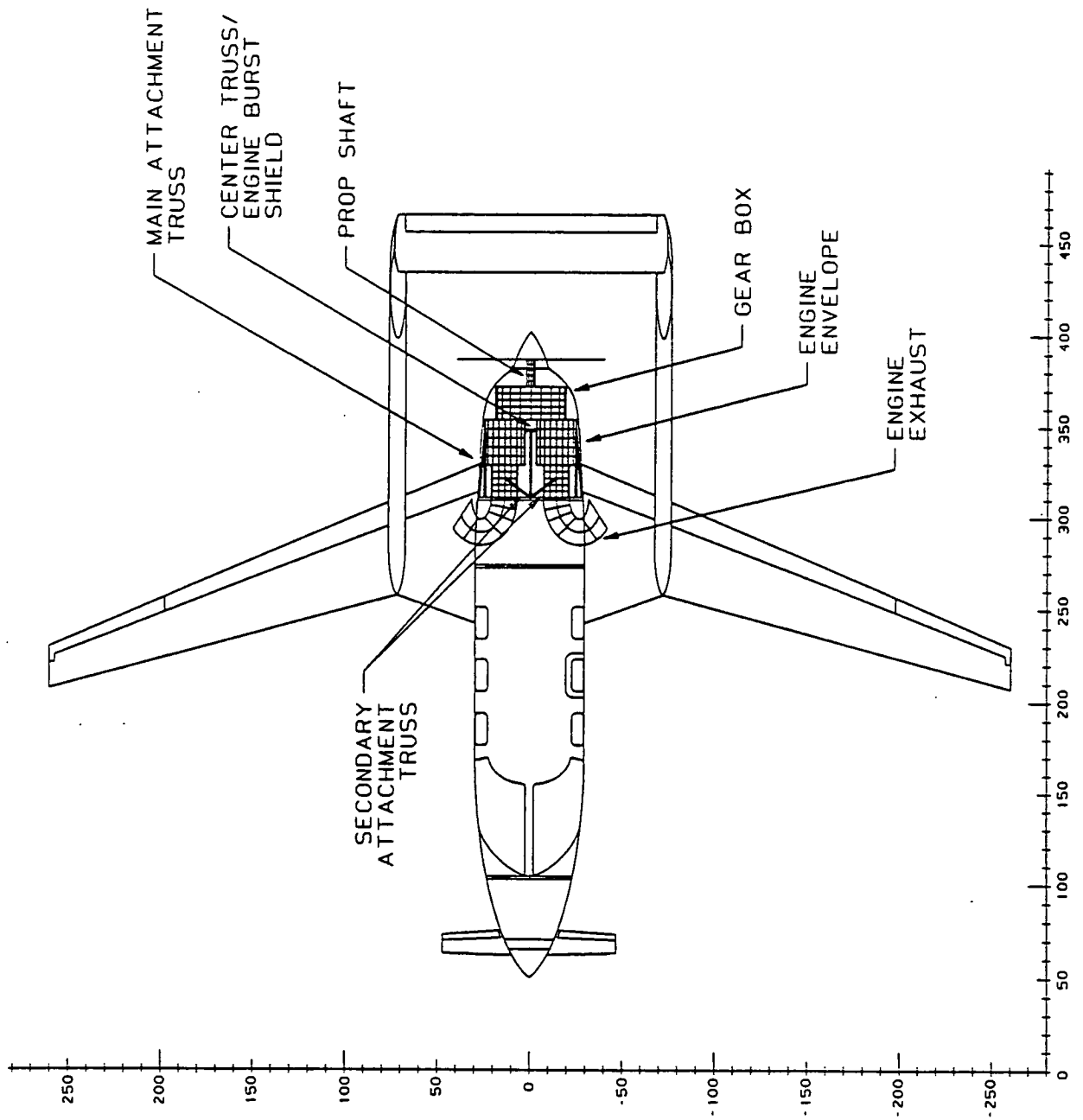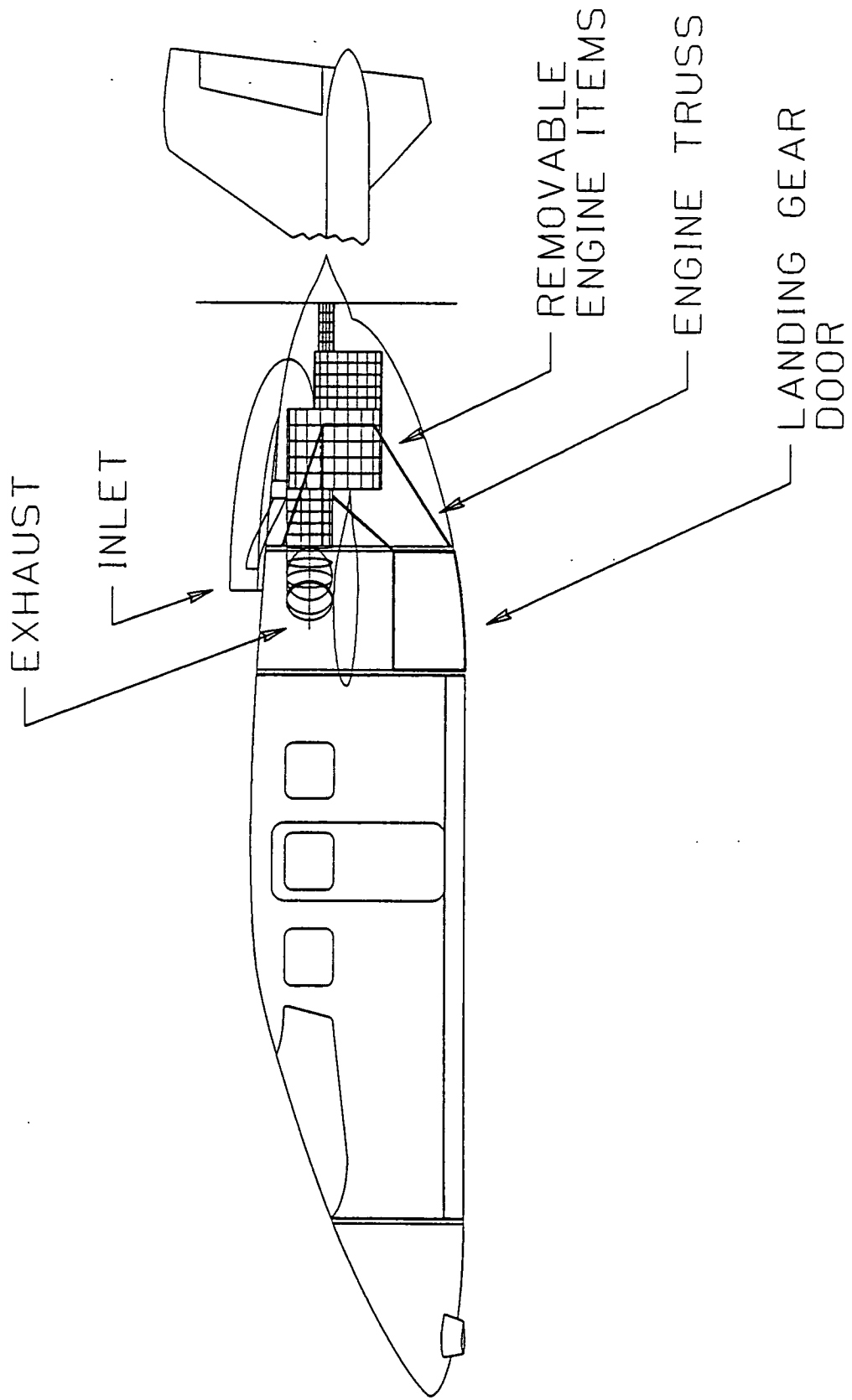
Figure 13.2: **Engine Installation in the APT** (cont.)

131

Table 13.1: Powerplant Removal Procedure

1. Remove upper and lower engine cowlings
2. Disconnect exhaust ducts
3. Disconnect fuel, electrical, and bleed air connections from the engine.
4. Attach engine removal support
5. Relieve engine weight from engine mounting truss by jacking the engine removal tool slightly
6. Remove engine mounting bolts. There are 5 locations on each engine - 10 total
7. Roll entire assembly out from the APT rear fuselage.
8. The propeller may be removed at this time if necessary.
9. At this time the engines may be detached from the gearbox if necessary.

From the above procedure it can be seen that many major components remain attached to the powerplant unit during the removal process. The propeller, engine inlet, and oil cooler all remain attached to the unit. This means that the APT service personnel will not have to remove items that do not need to be fixed. For example, to do a hot section inspection, the preceding procedure would be followed. The inlet and other hardware are not removed because there is no need to. This should save a considerable amount of time when it comes time for major servicing of the powerplant unit. This in turn should reduce the cost of maintenance for the APT.

The Mitsubishi MU-2 series of airplanes also uses Garrett turboprop engines. These engines are mounted in the same manner as is used for the APT. That is they are mounted so that very few items are needed to be disconnected to remove the engine. As a result of this engine removal times are quite low for that airplane. One of the authors has personally witnessed a service center remove a single engine in under 15 minutes. While it is true that the MU-2 does not use two engines mounted together as the APT does, it is reasonable to assume that powerplant removal times for the APT should be in the 20-30 minute time range.

13.4.2 Minor Engine Maintenance Considerations

While the powerplant removal times discussed in the previous section indicates relatively short removal times, it would be nice if the entire propulsive system did not have to be removed for minor maintenance of the system. It is the purpose of the section to demonstrate that it is indeed not necessary to remove the entire system.

Major servicing of the engine such as an overhaul occur quite infrequently. For the Garrett series of engines the minimum time between overhaul (TBO) is 3000 hours. For high use, such as airline service, the interval can be as high as 6000 hours. This time interval is long enough that the 20-30 minutes required to remove the engines is not a great burden. For small items such as starter generators and fuel control units, the mean time between failures (MTBF) is much lower. This

requires more frequent servicing of these type of units. For this reason it is desirable to leave the engines in place and remove only the unit that is faulty.

Figure 13.3 is a two view of the Garrett TPE331-15 engine. It shows the location of the engine driven units that are more likely to fail.
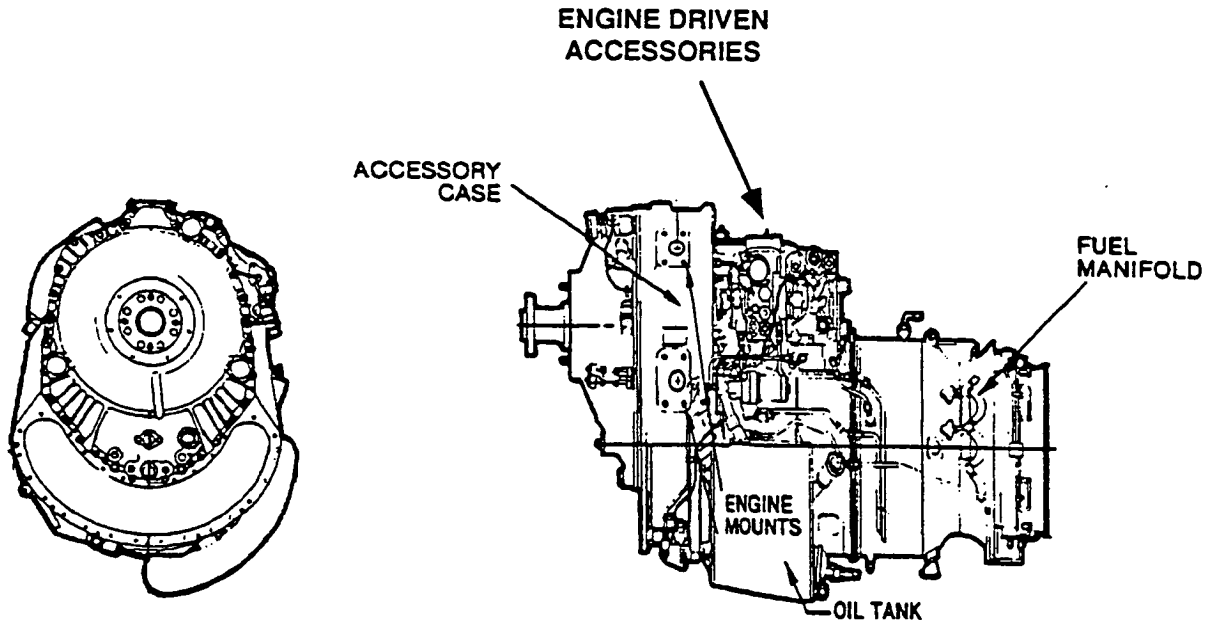

Figure 13.3: Two-view of Garrett engine showing Engine Driven Accessories (From Ref. 13.1)

Figure 13.3 is a picture of a generic TPE331-15. The actual orientation of the engine in the APT airframe can be seen in Figure 13.2. That figure shows the location of the engine driven accessories. As can be seen from the figure, the engine driven accessories are located on the bottom of the engine. It is also apparent from the figure that the engine mounting truss is not blocking access to these items. The location of the engine driven accessories allows them to be accessed from the bottom of the engine area. Table 13.2 gives the procedure for removing a line replaceable unit (LRU).

Table 13.2: Procedure for Replacing a LRU

1. Remove the lower engine cowl.
2. If the left engine is being serviced, work may begin for removing the faulty unit.
3. If the right engine is being serviced, the engine burst guard needs to be removed from between the two engines.
4. Service right engine as required.
5. Installation is in the opposite order.

133

13.5 MISCELLANEOUS SERVICE CONSIDERATIONS

Airplanes are generally quite complex machines with many independent systems that may need to be serviced over the lifetime of the airplane. It is very beneficial from a cost point of view to reduce the amount of work needed to repair the many systems in the airplane. The previous section outlined the procedure for servicing the engine. This section will discuss the servicing techniques envisioned for some of the other systems on the airplane. The systems that will be discussed are:

- De-ice system
- Avionics
- Primary flight controls
- Secondary flight controls
- Air-conditioning system

13.5.1 De-Ice System

The de-icing system chosen for the APT in Reference 13.3 is a somewhat new technology called EIDI (Electro Impulse De-Icing). This system uses many electromagnetic coils which vibrate in such a manner as to actually knock the ice off the surface in the immediate area of the coil. This system was chosen because conventional "boots" are not compatible with obtaining laminar flow and the power losses from bleed air de-icers were considered to be too high. The EIDI coils were not without their problems, however. The main problem was that they present a potential serviceability problem. Since the coils are placed approximately 18" apart a multitude of access panels would be required in the leading edge of the wing to facilitate coil servicing. This again presents a problem for the attainment of laminar flow. This is due to the number of access panels and their location on the leading edge of the wing. To solve the serviceability problem as well as the laminar flow considerations a new method of using EIDI coils was proposed in Reference 13.3.

Basically, the new method mounts the coils to a long, thin strip of metal. This strip of metal is then slid into the wing on tracks which are bonded to the inside of the wing. This can be seen in Figure 13.4. This method allows the leading edge of the wing and canard to be free of laminar flow tripping access panels. From Figure 13.4 it is seen that there are two access panels on the inboard section of the wing. These are used for two reasons

- No laminar flow is assumed to exist at this location due to turbulence from the canard and fuselage
- It would not be possible to bend the track of EIDI coils around the crank in the wing.

The access panels on the inboard section of the wing are also used to disconnect the power wires to the track of coils. The electrical connection could be a simple connector which would allow quick removal of the wires. The wires for the canard coils can be removed from inside the avionics bay access door. It can also be seen that there are access panels to service the EIDI coils located on the

ENGINE AND TRANSMISSION
OIL FILL ACCESS PANEL

ELEVATOR

EIDI ACCESS
PANEL

ENGINE
COWLING

SCALE 1:100

AILERON

FLAPS

ELECTRO-MECHANICAL
ACTUATOR
FOR FLIGHT CONTROL SYSTEM

ELECTRONICS AND AVIONICS

EIDI ACCESS
PANELS

EIDI COIL
TRACK

EIDI COIL
TRACK

REMOVABLE CAPS TO
ALLOW EIDI TRACK
TO BE REMOVED

Figure 13.4: Access Panel Locations

135

Figure 13.4: Access Panel Locations (cont.)

PRESSURIZATION AND AIR CONDITIONING

UPPER ENGINE ACCESS COVER

ENGINE AND TRANSMISSION OIL FILL ACCESS PANEL

LOWER ENGINE ACCESS COVER

MAIN GEAR BAY

AVIONICS BAY ACCESS DOOR

NOSE GEAR BAY

SCALE 1:100

horizontal tail and vertical tail. This is because no laminar flow is assumed to exist on these surfaces of the airplane. It is noted that all of the access panels located on the wing are on the bottom surface of the wing. This is the higher pressure surface of the wing and can maintain a laminar boundary layer better than the top surface. Therefore even though there is a access panel near the leading edge of the wing, this does not necessarily mean that laminar flow is not achievable on these surfaces.

Servicing the EIDI coils would follow the following procedures:

For the wing:

1. Remove inboard access panels
2. Disconnect power wire from the EIDI coil track
3. Remove the cap on the end of the wing
4. Remove attaching bolts of lower EIDI coil track and slide out of wing
5. Repeat step 4 for the upper track of EIDI coils
6. Replace any faulty coils
7. If inboard EIDI coils need to be serviced they are accessed directly through the cut-outs
8. Follow same procedure for other wing, if necessary
9. Installation is in the opposite order

For the canard:

1. Raise avionics bay access door
2. Disconnect power wires to EIDI coils
3. Remove end cap of canard
4. Remove attaching bolts of lower EIDI coil track and slide out of wing
5. Repeat step 4 for the upper track of EIDI coils
6. Replace any faulty coils
7. Repeat for other side of canard if necessary
8. Installation is in the opposite order

For the horizontal tail and vertical tails

1. Remove access panels that are near the faulty coils
2. Remove any faulty coils individually
3. Reinstall new coils
4. Reinstall access panels

13.5.2 Avionics

The APT uses electronic equipment in a way which is normally reserved for much larger airplanes. This is to make the airplane as simple to fly and operate as possible. Luckily, the rapid advances that have been made in digital electronics reduces the number and size of the necessary

computers. It was deemed possible in Reference 13.4 that all of the necessary electronic equipment could be placed in the nose of the airplane. This section will discuss the manner in which the avionics could be serviced in the APT.

The avionics can be serviced through two different locations. The two locations are:

- External access panels on both sides of nose
- Internal access through cabin

The majority of the computer will be located in the nose. The access panel shown in Figure 13.4 will be used to remove the components of the avionics system. The displays, keyboards and other interface equipment is located in the cabin and can be serviced from in the cabin.

13.5.3 Primary Flight Controls

The APT utilizes a novel control scheme in which the control surfaces are driven by multiple actuators as opposed to the conventional method of using a single actuator. Single actuators must carry all of the loads and consequently are typically heavy and expensive. The APT is shown to have a considerable weight advantage by using more, but smaller actuators (Reference 13.5). This control concept has been tested for a short period of time. In Reference 13.5 the servo-actuators envisioned for use in the APT have undergone 38 hours of testing with no failures. The testing is continuing and with some more simulation time more accurate reliability statements can be determined for the actuators.

The one conclusion that can be made about the aileron-servotab system is that the system will perform for at least 38 hours, and be free of failures. From this, an estimate of the reliability of the system can be made. For a catastrophic failure, a hard-over failure in the same direction of five of the ten actuators will occur. Using 38 hours as the probability of failure in one direction, once every 76 hours, a servotab will fail in a particular direction. Accordingly, for five servotab actuators to fail in the same direction, this will occur every 76^5 hours = 2.53×10^9 hours. Since this is less than one catastrophic occurrence in 10^9 hours, this system from a safety point of view is acceptable. The other major issue of reliability is the frequency of actuator changes. If an actuator has an MTBF of 1000 hours and there are 20 actuators on the aircraft, the operator is required to change an actuator every 50 hours. This may be unacceptable from an owner-operator point of view. No clearly established guidelines have been published on this matter, but is should be conservative to suggest that the higher the MTBF, the greater the customer satisfaction. If it turns out that the MTBF is such that servo-actuators must be frequently replaced, then the operator will want to be able to do this quickly. This section deals with the maintainability issue.

The principal issue as far as the maintainability of the servo-actuator system is concerned, is the accessibility and speed of replacement of each servo-actuator. The bottom of the servo-actuator is bonded to the access panel which is attached to the bottom skin of the aileron with four nylon-head self-locking nuts. The removal and installation time is estimated to be approximately 5 minutes. The servo-actuator will be connected with four screws, one pushrod, and one electrical umbilical. Each component can be easily accessed and removed by ground crews. It should be

noted that all flight control surfaces including the elevator, the rudder and the ailerons will be actuated by the same servo-actuators and will be installed and removed in the same manner. This will facilitate fast and professional maintenance. Figure 13.5 shows the procedure that will be used for removal and installation of a new servo-actuator. The access panel on the bottom side (pressure surface) of the aileron will be removed. The servo-actuator is than rotated and slid out of the access port. The push-rod is then removed along with the electrical umbilical. A simple locking clevis pin is used to join the push-rod to the actuator head. Currently, stamped nylon is used for the actuator head. For flight hardware, either a change of material to aluminum should be implemented, or Teflon bushings should be swaged into place.

1. Access panel on bottom is removed by four locking screws

2. Servo is lowered, linkage and umbilical are disconnected

3. New servo is installed
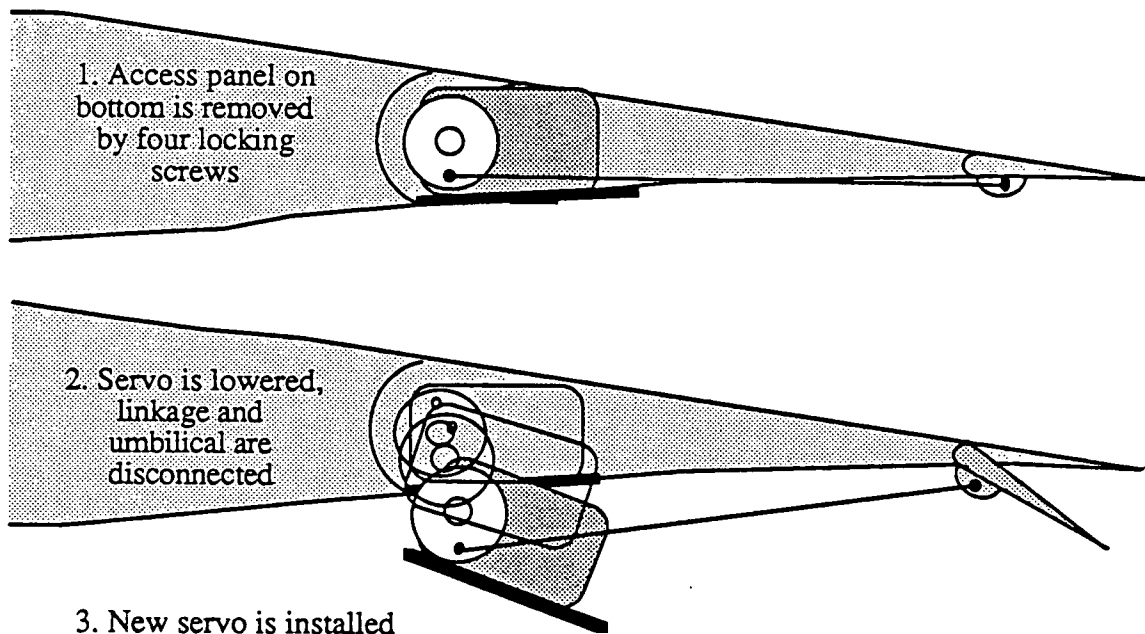
Figure 13.5 Servo-actuator Removal and Installation Procedure

This procedure will be used on all surfaces that use servo-actuators for actuation. For the rudders which do not have a pressure surface, the inboard sides of the rudders will have the access panels for the actuators. The reason for placing the access panels on the inboard portions of the rudders is that the mechanics can access all of the actuators on the elevator and rudder without changing position of the work stand. This will decrease the time required for inspection and removal. Also, the appearance of the aircraft will not be decreased in the profile with the sight of access panels and linkages.

13.5.4 Secondary Flight Controls

The secondary flight controls that will be discussed in this section are:

- Main wing flaps
- Canard flaps
- Landing gear actuation

As found in Reference 13.4, the APT uses electrical motors for all of these functions. It will therefore be necessary to have access to the electric motors and drive-shafts that are required to move the above items.

13.5.4.1 Main wing flaps

The main wing flaps on the APT are electrically actuated fowler flaps. The method of actuation was chosen in Reference 13.4 to consist of a centrally located electric motor and drive shafts to drive the outboard sections of the flap. This is the same method that is used in the Mitsubishi MU-2. The electric motor may be accessed through the landing gear bay. The drive shafts and jackscrews can be actuated through the access panels located in the wing. These cut-outs can be seen in Figure 13.4.

13.5.4.2 Canard flaps

The canard flaps on the APT are also electrically actuated but the are plain flaps instead of fowler flaps. This allows the the flaps to be actuated by using a torque tube mounted inside the flap. The torque tube in turn is acted upon by a electric motor driving a jackscrew. The only service that will be required of the canard flap is the inspection, repair, and replacement of the electric actuator. This can be accomplished through the nose landing gear door bay.

13.5.4.3 Landing gear

The landing gear is actuated by two electric actuators, one for the nose gear and one that drives both main gear. Both of these actuators are accessible from the landing gear bays.

13.5.5 Air Conditioning System

The APT uses an air-cycle machine for heating and cooling the cabin air. These units have proven to be quite reliable in service and should not require frequent service. When service is required it would be beneficial to have easy access to the air-cycle unit for quick service. This section will discuss the maintenance of this unit.

As can be seen from Figure 13.4, there is an access panel directly above the location of the air-cycle machine. This panel will allow the unit to be serviced or removed.

13.6 REFERENCES FOR CHAPTER 13

13.1   Bauguess, S., et. al., Maintenance and Repairability Study for the Advanced Personal Transport, AE 621, Fall 1990, University of Kansas.

13.2   Evans, D., et. al., Maintenance and Repairability Study for the Advanced Personal Transport, AE 622, Spring 1991, University of Kansas

13.3   Gomer, et.al., Airframe Design Report, AE 622, Spring 1991, University of Kansas.

13.4   Gomer, et.al., Summary of the Design of an Advanced Personal Transport, AE621, December 1990, University of Kansas.

13.5   Barrett, R., et. al., <u>Design Test and Evaluation of the Iron Bird</u>, AE 622, Spring 1991, University of Kansas.

14. STABILITY AND CONTROL

The purpose of this chapter is to derive and discuss the static stability characteristics of the APT pusher configuration.

To satisfy level 1 requirements as defined in Reference 14.1, a sensitivity study is performed for the lateral/directional stability characteristics.

14.1 FLIGHT CONDITIONS

For the calculations of the stability and control derivatives and open loop handling qualities, three flight conditions are selected :

-	Power Approach	Altitude= Sea Level
		Speed = 90 kts
-	Economic Cruise	Altitude= 40000 ft
		Speed = 310 kts
-	Max. Speed Cruise	Altitude= 20000 ft
		Speed = 410 kts

In all three conditions the most aft center of gravity is considered.

The APT steady state and other characteristics for the three flight conditions are shown in Table 14.1.

Table 14.1 : Characteristics for the Three Flight Conditions

Flight Condition		1	2	3
		Power Approach	Economic Cruise	Max. Speed Cruise
Altitude	(ft)	sea level	40000	20000
Air Density	(slugs/ft^3)	2.377×10^{-3}	0.5851×10^{-3}	1.2664×10^{-3}
Speed	(kts)	90	310	410
Center of Gravity *	(ft)	17*	17*	17*
Initial Attitude	(deg)	0	0	0
Geometry and Inertias				
Wing Area	(ft^2)	130	130	130
Wing Span	(ft)	36	36	36
Wing Mean Geom. Chord (ft)		3.99	3.99	3.99
Weight	(lbs)	5500	6250	7000
Ixx	(slug ft^2)	8474	9211	9496
Iyy	(slug ft^2)	7298	7933	8178
Izz	(slug ft^2)	15409	16749	17267
Ixz	(slug ft^2)	717	779	803
Steady State Coefficients				
C_L		1.5406	0.5790	0.1773
C_D		0.2337	0.0323	0.0168
C_{Tx}		0.2337	0.0323	0.0168
Cm		0.0	0.0	0.0
Cm_T		0.0	0.0	0.0

* Center of Gravity is measured from Fuselage Nose Apex

14.2 STABILITY AND CONTROL DERIVATIVES

In this section the stability and control derivatives for the above mentioned three flight conditions are presented. The derivatives are obtained from the Advanced Aircraft Analysis program (Reference 14.3). The theory of this program is based on theory as provided in Reference 14.2.

The longitudinal derivatives for the APT in the three flight conditions are shown in Table 14.2.

Table 14.2 : Longitudinal Derivatives for the APT

Longitudinal Derivatives		1	2	3
Cm_u		0.0741	0.1738	0.0872
Cm_α	(rad^{-1})	-0.8356	-0.6042	-0.2838
Cm_α	(rad^{-1})	-7.703	-11.9600	-15.8857
Cm_q		-40.10	-48.9117	-55.4800
Cm_{Tu}		0.0895	0.0093	0.0073
$Cm_{T\alpha}$	(rad^{-1})	0.0	0.0	0.0
CL_u		0.0272	0.2187	0.1274
CL_α	(rad^{-1})	6.1038	7.6243	8.8385
CL_α	(rad^{-1})	2.1892	3.3349	4.3840
CL_q		10.1879	11.7972	12.9373
CD_α	(rad^{-1})	0.7137	0.3350	0.1189
CD_u		0.0	0.0	0.0
CT_{Xu}		-0.7011	-0.0969	-0.0504
$CL\delta_E$	(rad^{-1})	0.4686	0.4816	0.4793
$CD\delta_E$	(rad^{-1})	0.0	0.0	0.0
$Cm\delta_E$	(rad^{-1})	-1.8405	-1.9816	-1.8825

144

The lateral/directional derivatives for the APT in the three flight conditions are shown in Table 14.3.

Table 14.3 : Lateral/Directional Derivatives of the APT

Lateral-Directional Derivatives		1	2	3
Cl_β	(rad^{-1})	-0.1283	-0.1520	-0.1563
Cl_p	(rad^{-1})	-0.4414	-0.3858	-0.3678
Cl_r	(rad^{-1})	0.3816	0.2104	0.1253
Cl_β	(rad^{-1})	0.0029	0.0032	-0.0033
$Cl\delta_A$	(rad^{-1})	0.1152	0.1495	0.1686
$Cl\delta_R$	(rad^{-1})	0.0119	0.0110	0.0103
Cn_β	(rad^{-1})	0.1110	0.1086	0.0868
Cn_p	(rad^{-1})	-0.1889	-0.0692	-0.0218
Cn_r	(rad^{-1})	-0.2845	-0.2658	-0.2631
Cn_β	(rad^{-1})	0.0256	0.0282	0.0295
$Cn\delta_A$	(rad^{-1})	-0.0248	-0.0121	-0.0042
$Cn\delta_R$	(rad^{-1})	-0.0815	-0.0756	-0.0701
Cy_β	(rad^{-1})	-0.9909	-0.9909	-0.9909
Cy_p	(rad^{-1})	-0.0910	-0.0910	-0.0910
Cy_r	(rad^{-1})	0.6198	0.6198	0.6198
Cy_β	(rad^{-1})	0.0663	0.0730	0.0763
$Cy\delta_A$	(rad^{-1})	0.0	0.0	0.0
$Cy\delta_R$	(rad^{-1})	0.1992	0.1852	0.1715

14.3 OPEN-LOOP HANDLING QUALITY ANALYSIS

It is important to the pilot that certain modes of motion of the airplane are well behaved. The purpose of this section is to present the handling quality characteristics of the APT in terms of mode and mode shape characteristics.

The longitudinal and lateral/directional characteristics are calculated with the Advanced Aircraft Analysis program (Reference 14.3). The following sections will present the results for three flight conditions.

14.3.1 Dynamic Longitudinal Stability

PHUGOID :   Table 14.4 shows the phugoid characteristics for the APT. The APT satisfies the requirements for level 1 flights in flight condition 1. In the other two flight conditions it can be seen that the characteristics are very close to the level 1 flight requirements ($\zeta_{PH} > 0.04$).

SHORT PERIOD : The APT satisfies in all three flight conditions the requirements set for level 1 flights (see table 14.4).

Table 14.4 : Longitudinal Mode Shapes for the APT

Longitudinal Dynamic Analysis Phugoid and Short Period	1	2	3
ω_{PH} (rad/sec)	0.2854	0.1380	0.1342
ζ_{PH}	0.1148	0.0385	0.0354
ω_{SP} (rad/sec)	1.5965	2.0147	3.5343
ζ_{SP}	0.6735	0.5118	0.8849

14.3.2 Dynamic Lateral/Directional Stability and Roll Response

SPIRAL : Table 14.5 shows the APT spiral characteristics for the three flight conditions. The requirements for level 1 flights are satisfied for flight condition 1 but the spiral mode is too stable.

DUTCH ROLL : The requirements for level 1 flying qualities are not satisfied for flight condition 2 and 3 ($\zeta_D > 0.08$). In section 14.4 it will be shown that this can be solved by changing the wing dihedral.

ROLL : The APT satisfies the requirements set for level 1 flying qualities in all three flight conditions.

Table 14.5 : Lateral/Directional Mode Shapes for the APT

Lateral-Directional Dynamic Analysis Spiral, Dutch Roll and Roll		1	2	3
T_S	(sec)	-83.210	58.069	27.417
T_{2S}	(sec)	-57.676	40.250	19.004
ω_D	(rad/sec)	1.144	1.630	2.579
ζ_D		0.011	-0.005	0.069
T_R	(sec)	0.844	1.152	0.540

14.4 SENSITIVITY ANALYSIS

In this section a sensitivity analysis will be performed. The purpose of this analysis is to change the lateral/directional handling qualities of the APT by changing the wing dihedral or vertical tail area. The effect of the lateral derivatives Cy_β, Cl_β and Cn_β on the lateral/directional handling quality characteristics are shown in Figure 14.1 to Figure 14.15 for the three flight conditions. To satisfy level 1 flying quality requirements, it is obvious from these figures that conflicting requirements concerning the selection of Cl_β are found.

The effect of the wing dihedral and the vertical tail area on the Cy_β, Cl_β and Cn_β are shown in Figure 14.16 to Figure 14.21. To satisfy the level 1 requirements for the dutch roll ($\zeta_D > 0.08$), the dihedral of the wing has to be decreased to -2 degrees. Unfortunately this modification will make the spiral mode too stable in all three flight conditions. The lateral/directional mode shapes for the dihedral of -2 degrees are shown in table 14.6.

Table 14.6 : Modified Lateral/Directional Mode Shapes for the APT

Lateral-Directional Dynamic Analysis Spiral, Dutch Roll and Roll	1	2	3
T_S (sec)	-8.434	-51.790	-100.000
T_{2S} (sec)	-5.846	-35.898	-69.310
ω_D (rad/sec)	1.085	1.592	2.674
ζ_D	0.202	0.080	0.133
T_R (sec)	1.142	1.574	0.655
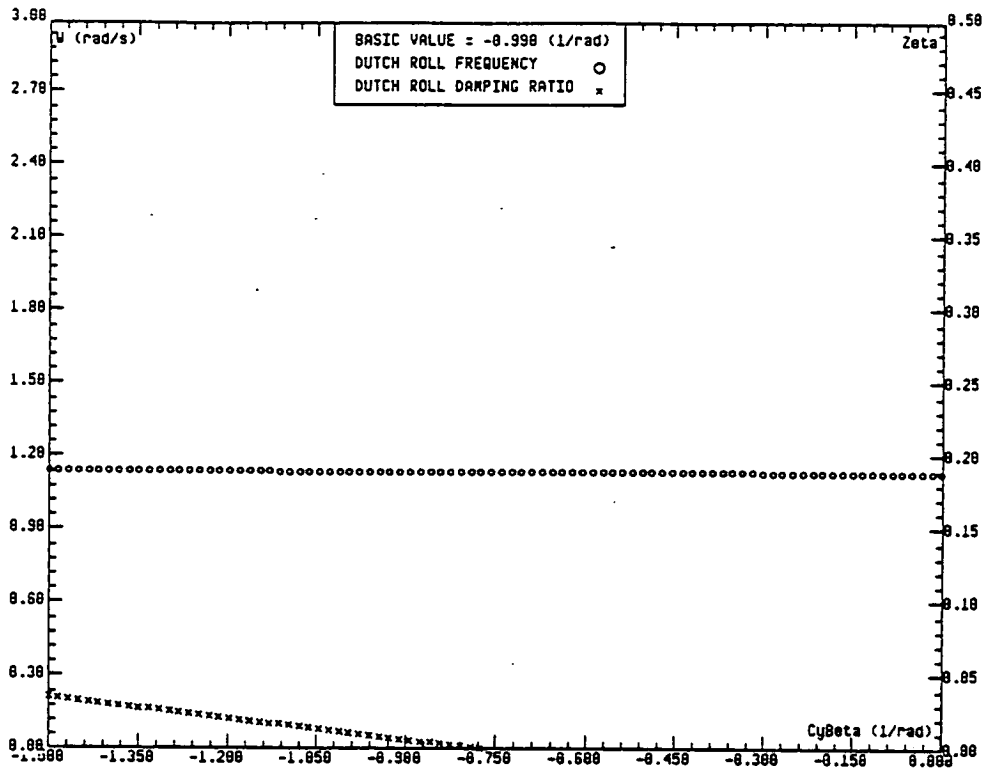
Figure 14.1 : Dutch Roll Natural Frequency and Damping Ratio as a Function of Cy_β
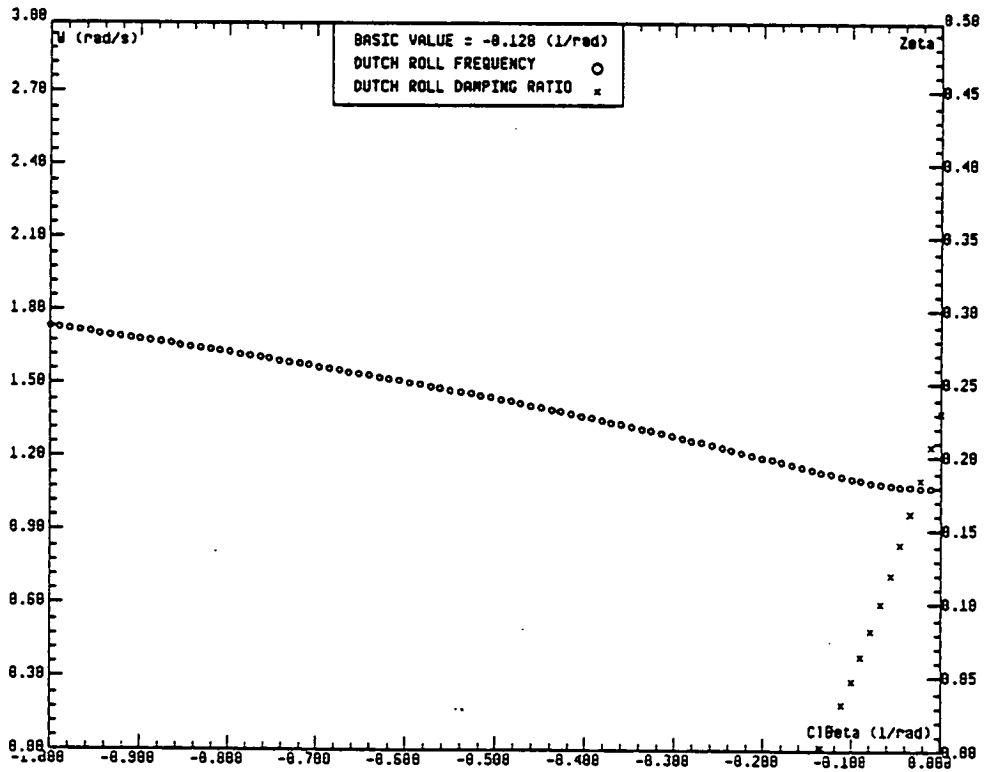
Flight Condition 1

Figure 14.2 : Dutch Roll Natural Frequency and Damping Ratio as a Function of Cl_β

Flight Condition 1

149
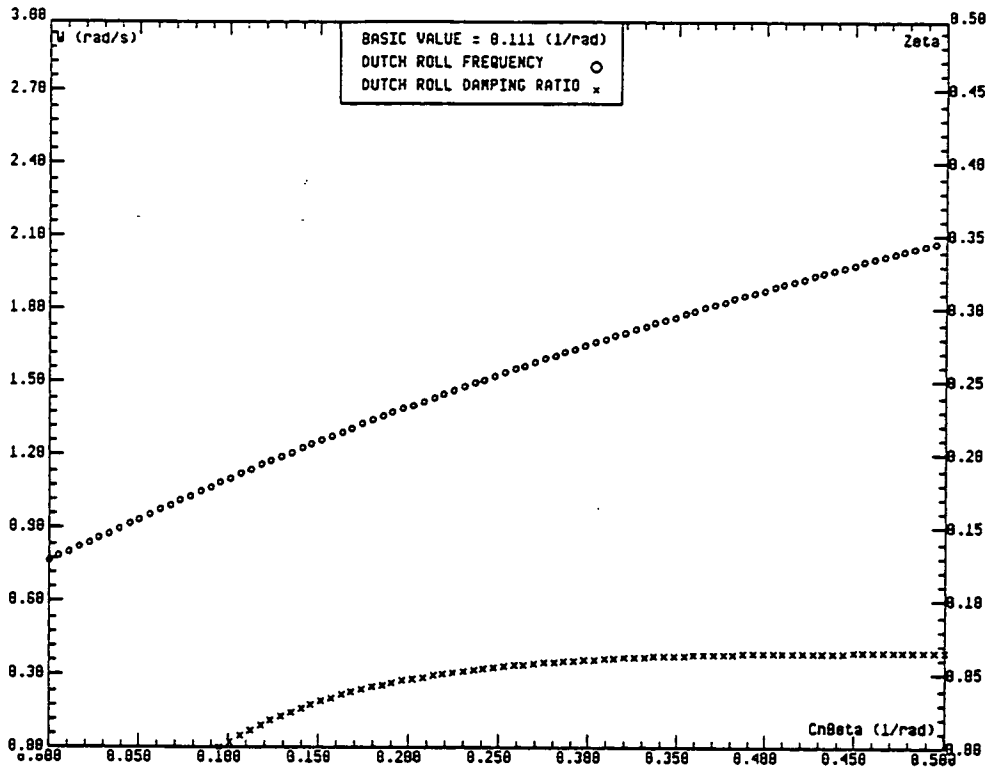
Figure 14.3 : Dutch Roll Natural Frequency and Damping Ratio as a Function of Cn_β
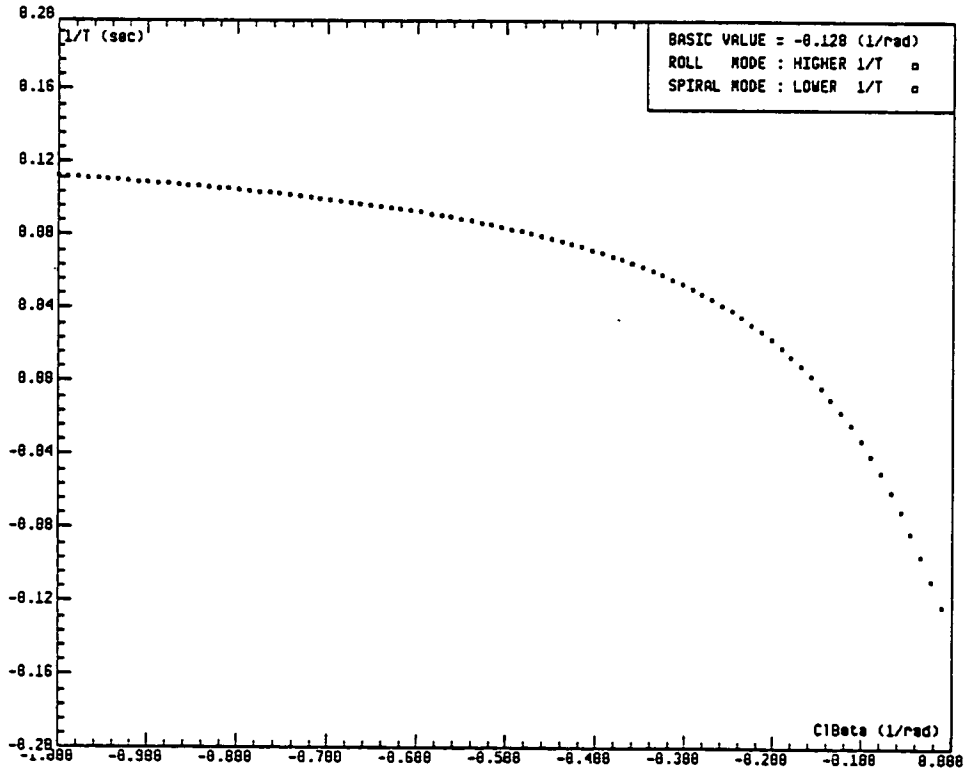
Flight Condition 1

Figure 14.4 : Spiral Time Constant as a function of Cl_β

Flight Condition 1

150
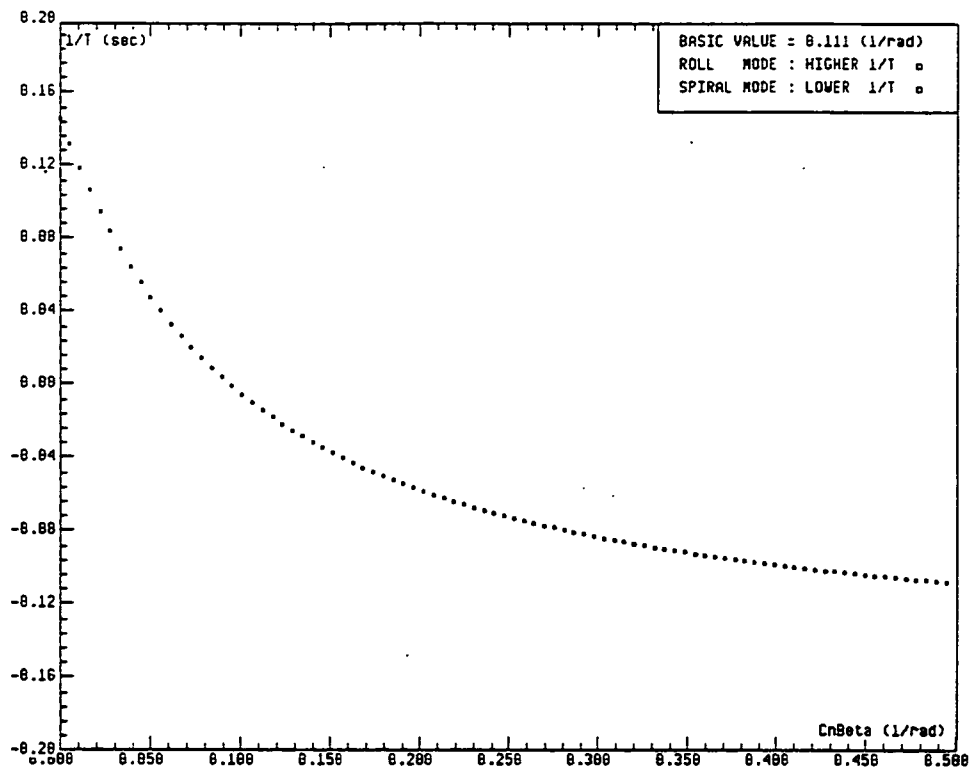
Figure 14.5 : Spiral Time Constant as a function of Cn_β
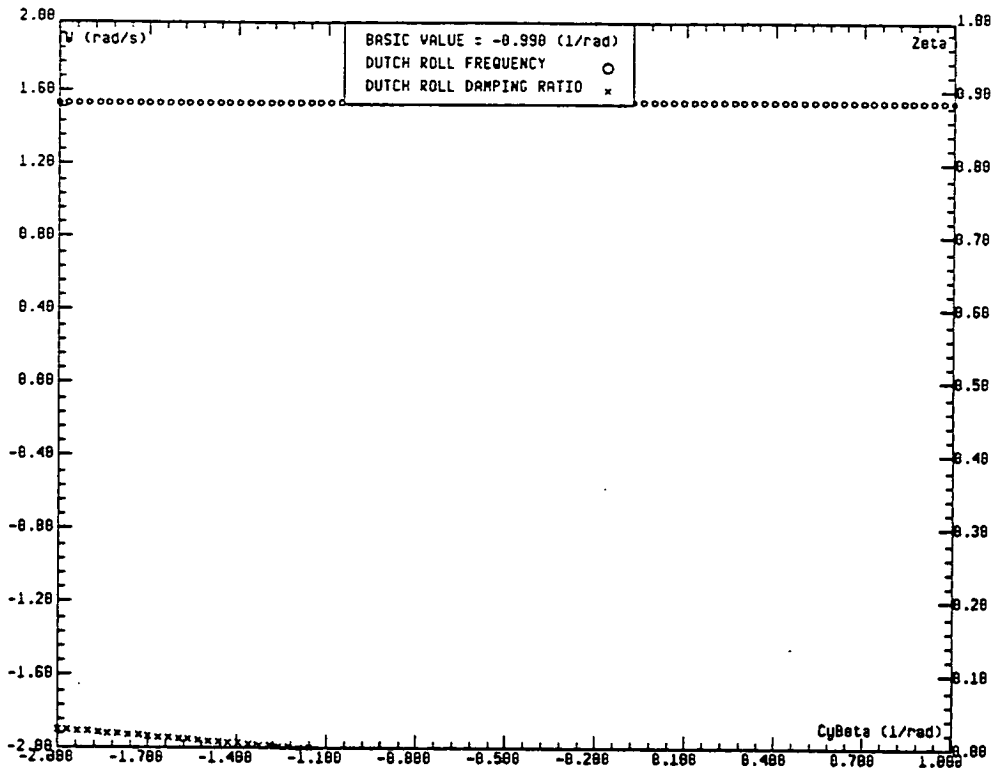
Flight Condition 1

Figure 14.6 : Dutch Roll Natural Frequency and Damping Ratio as a Function of Cy_β .
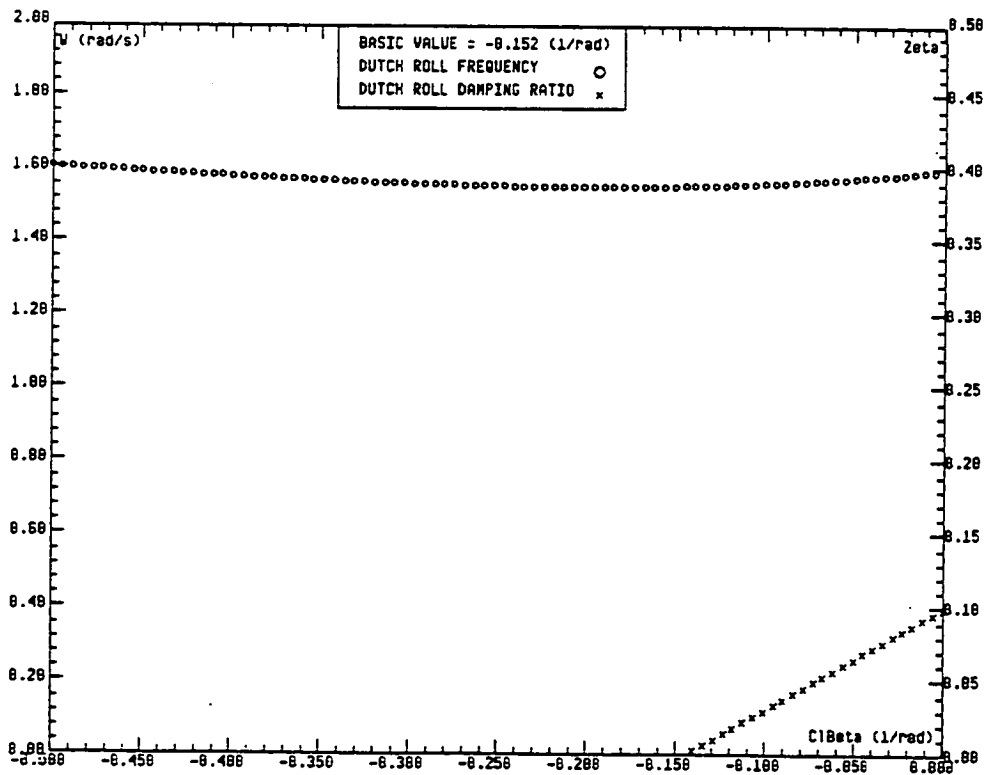
Flight Condition 2

Figure 14.7 : Dutch Roll Natural Frequency and Damping Ratio as a Function of Cl_β
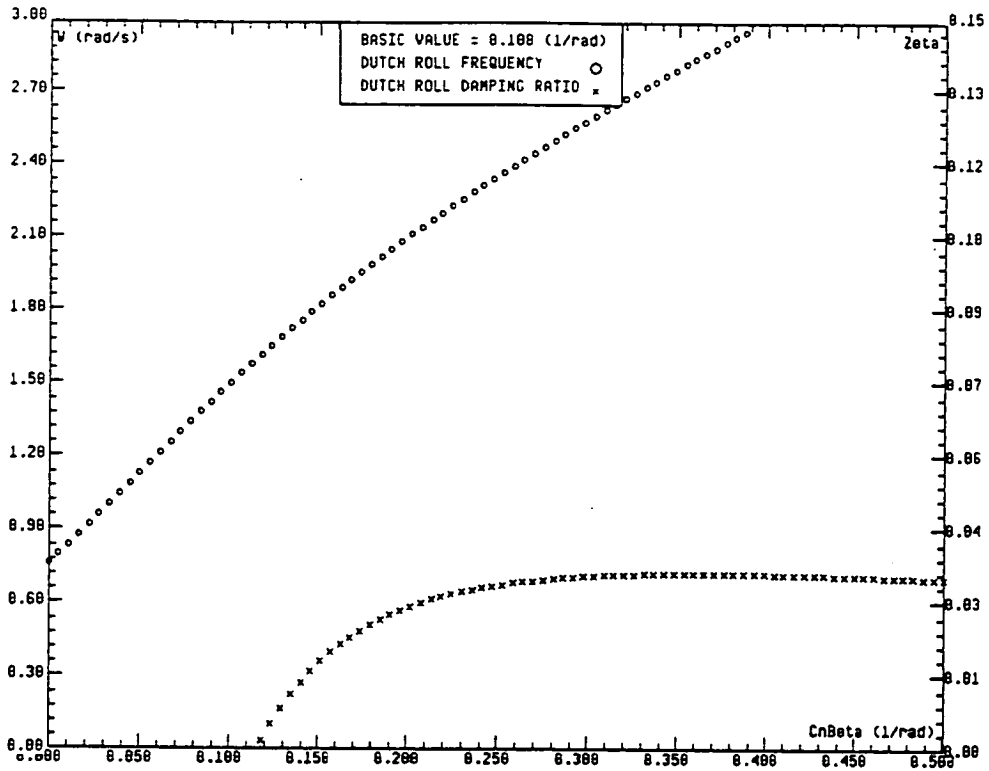
Flight Condition 2

Figure 14.8 : Dutch Roll Natural Frequency and Damping Ratio as a Function of Cn_β
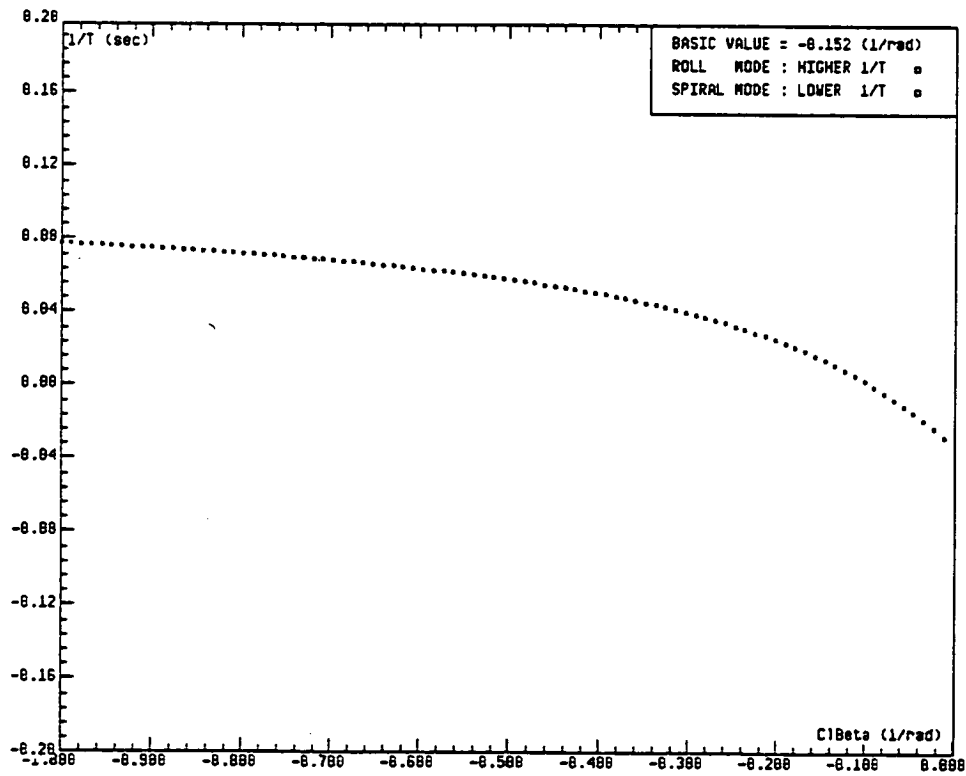
Flight Condition 2

Figure 14.9 : Spiral Time Constant as a function of Cl_β

Flight Condition 2

153
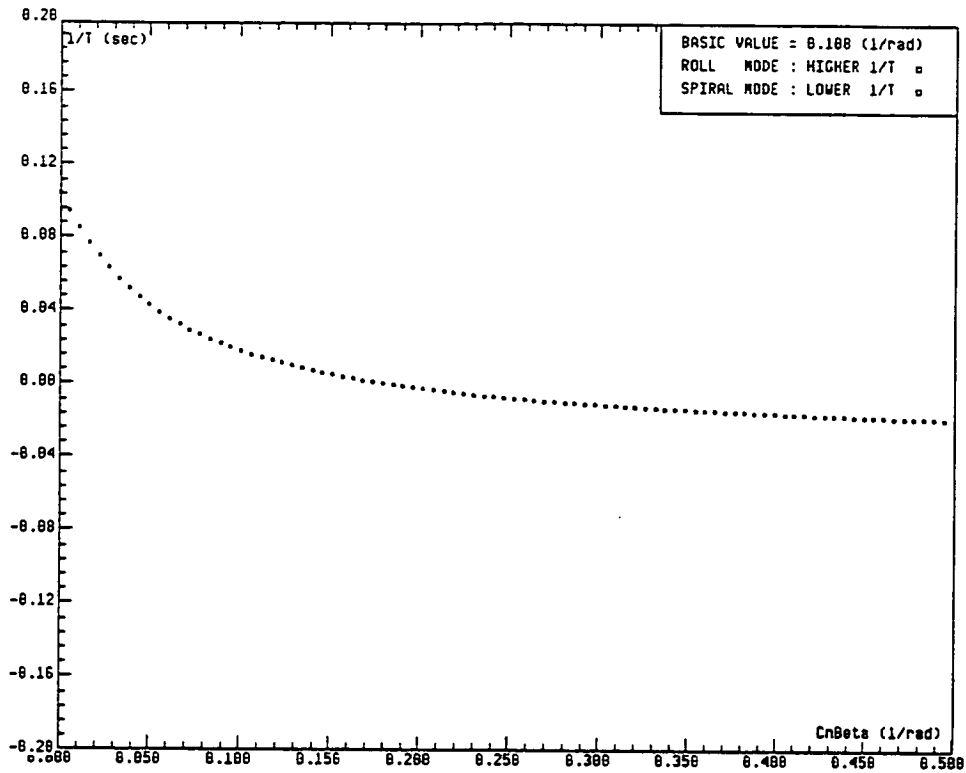
Figure 14.10 : Spiral Time Constant as a function of Cn_β
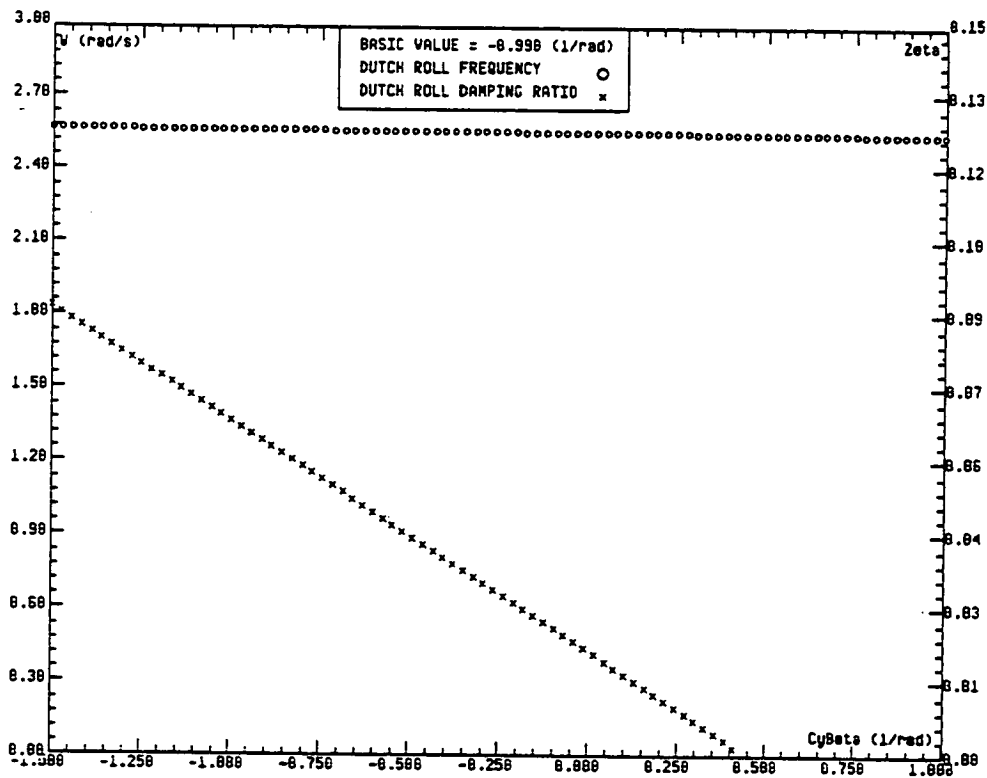
Flight Condition 2

Figure 14.11 : Dutch Roll Natural Frequency and Damping Ratio as a Function of Cy_β

Flight Condition 3

154
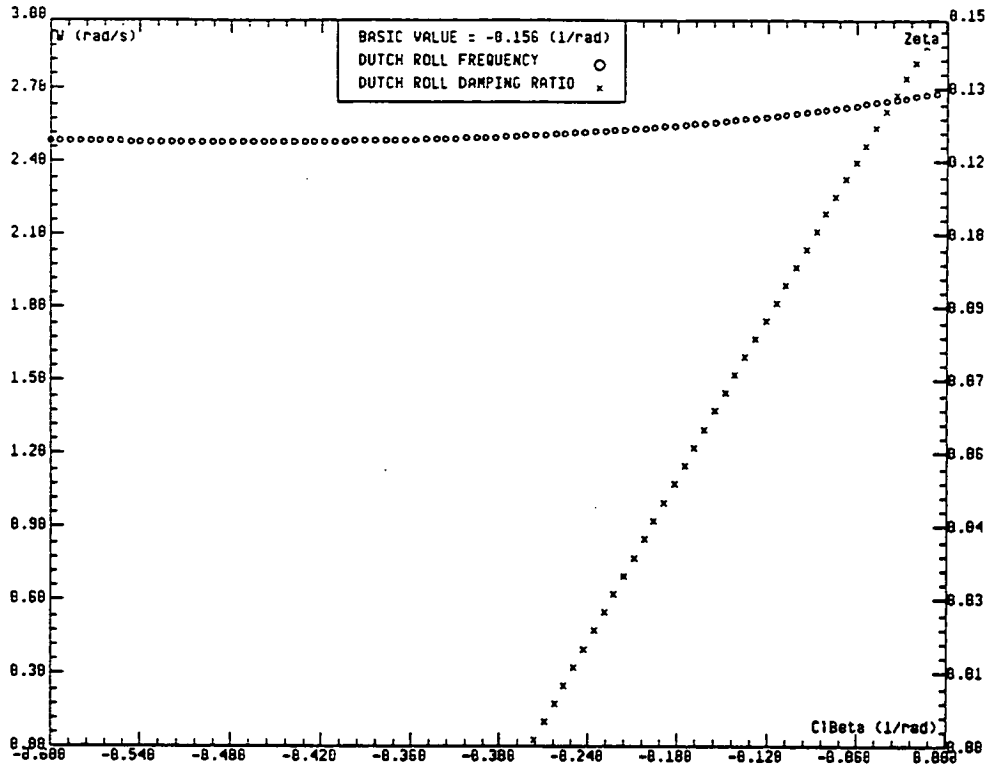
Figure 14.12 : Dutch Roll Natural Frequency and Damping Ratio as a Function of Cl_β
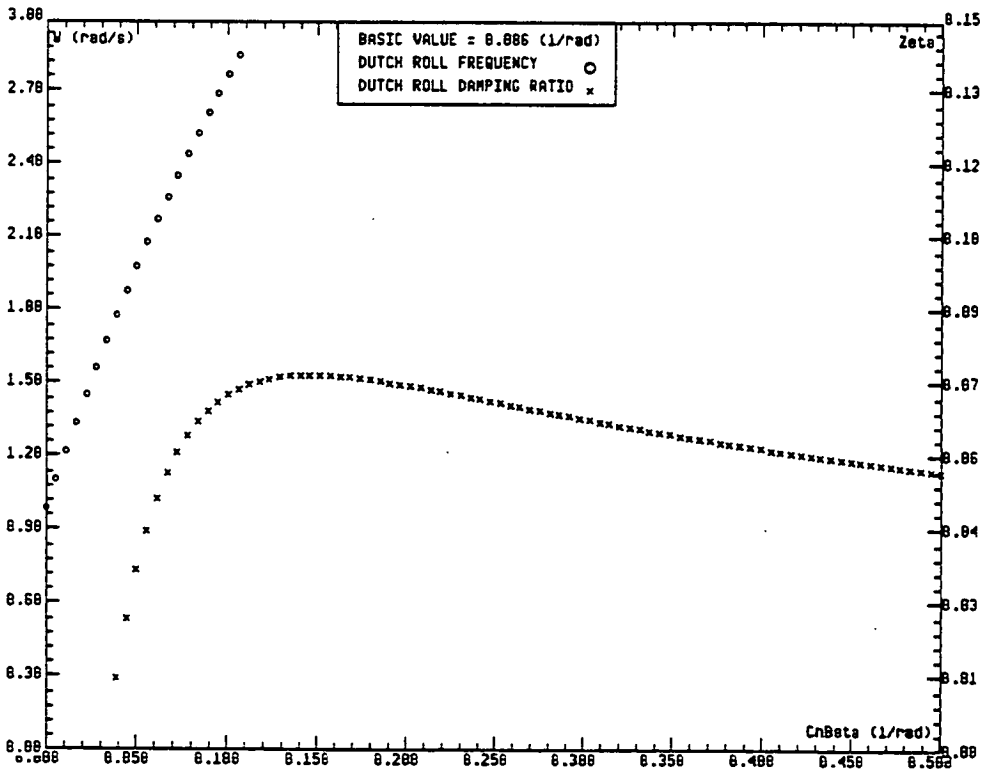
Flight Condition 3

Figure 14.13 : Dutch Roll Natural Frequency and Damping Ratio as a Function of Cn_β

Flight Condition 3

155
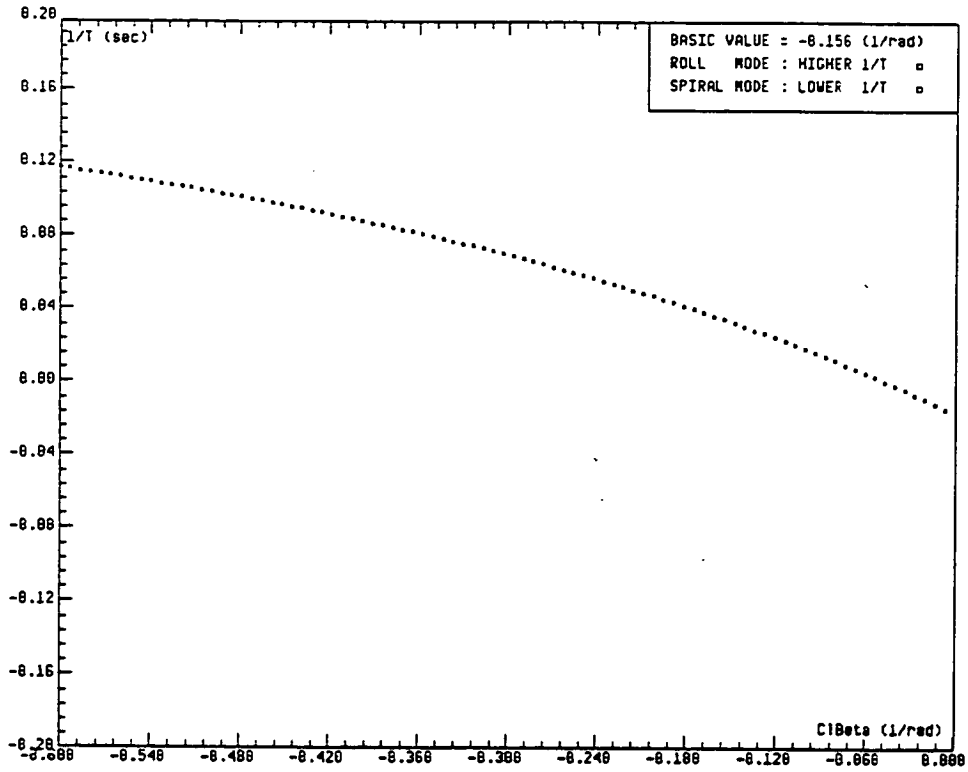
Figure 14.14 : Spiral Time Constant as a function of Cl_β
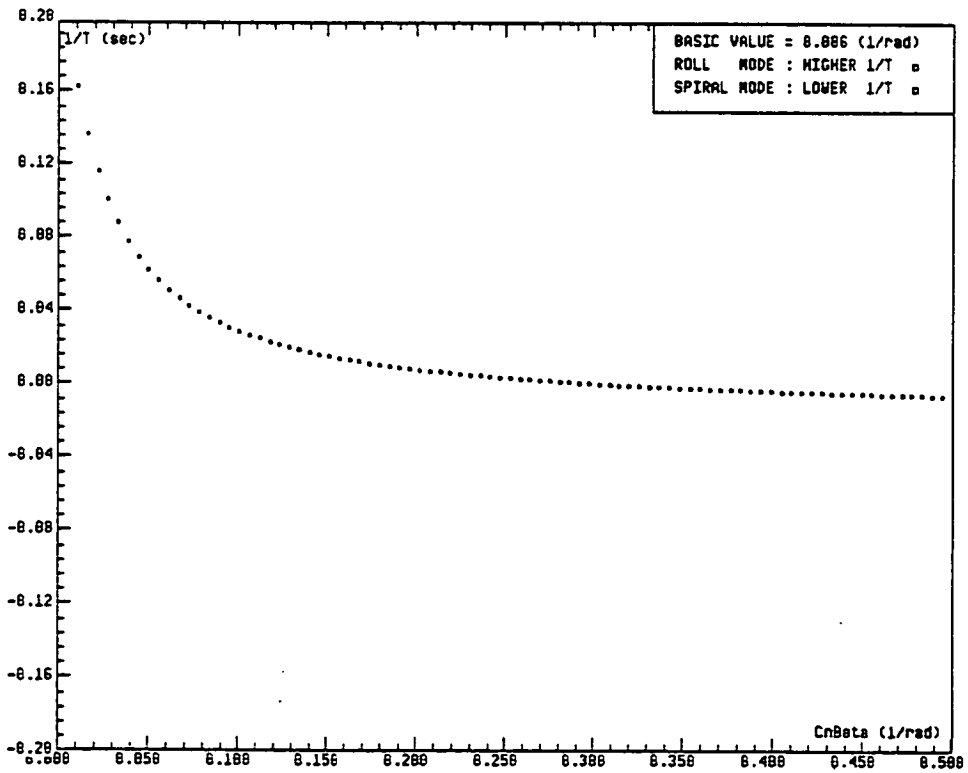
Flight Condition 3

Figure 14.15 : Spiral Time Constant as a function of Cn_β

Flight Condition 3

156
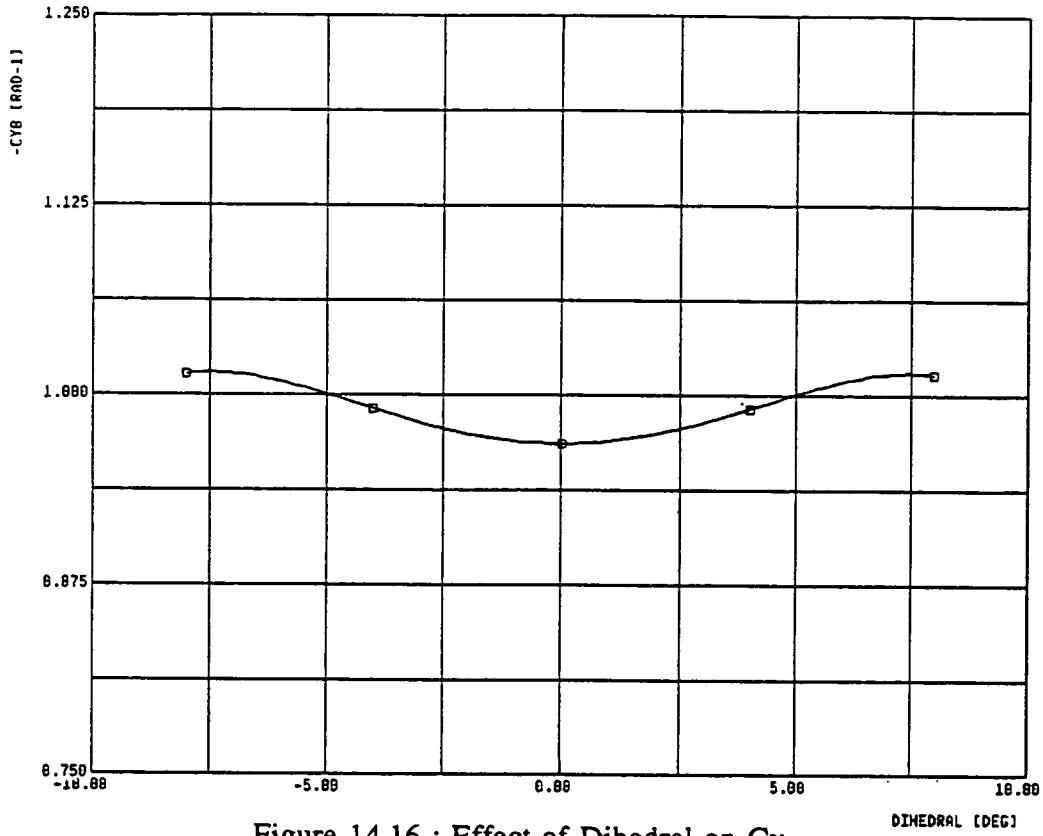
Figure 14.16 : Effect of Dihedral on Cy_β
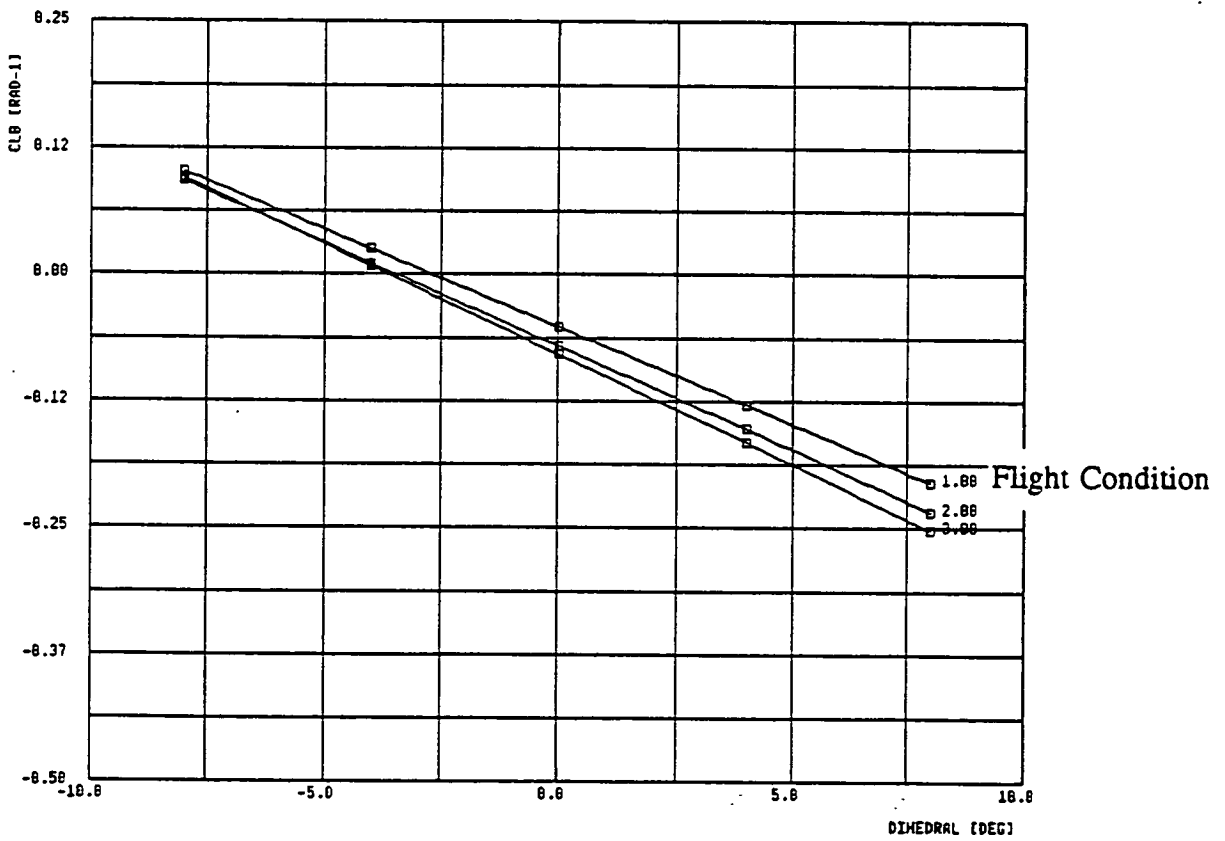
Figure 14.17 : Effect of Dihedral on Cl_β

157
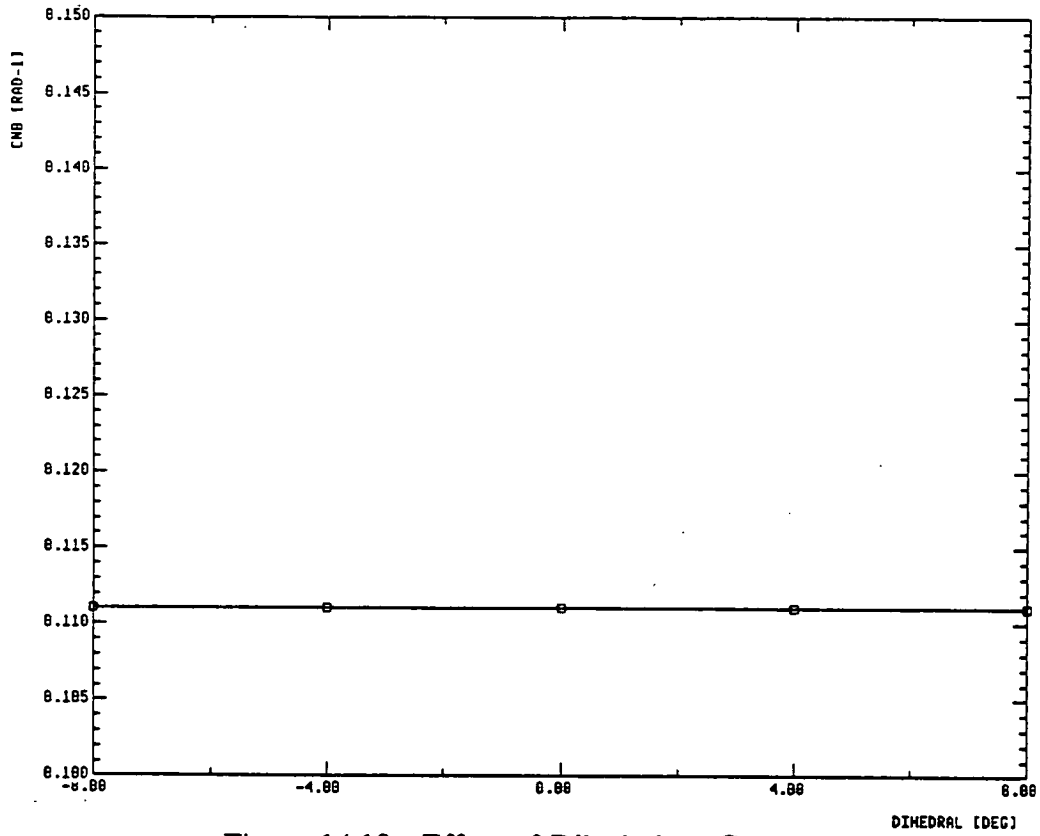
Figure 14.18 : Effect of Dihedral on Cn_β

Sv [ft]
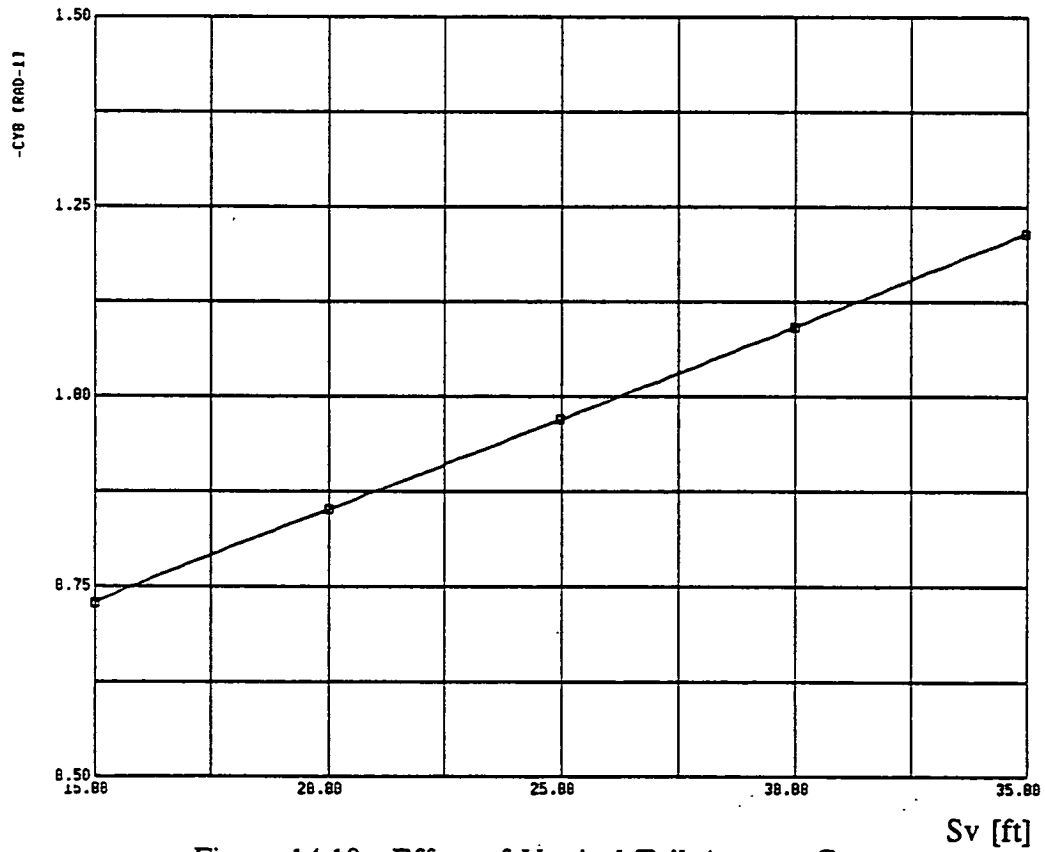
Figure 14.19 : Effect of Vertical Tail Area on Cy_β

158
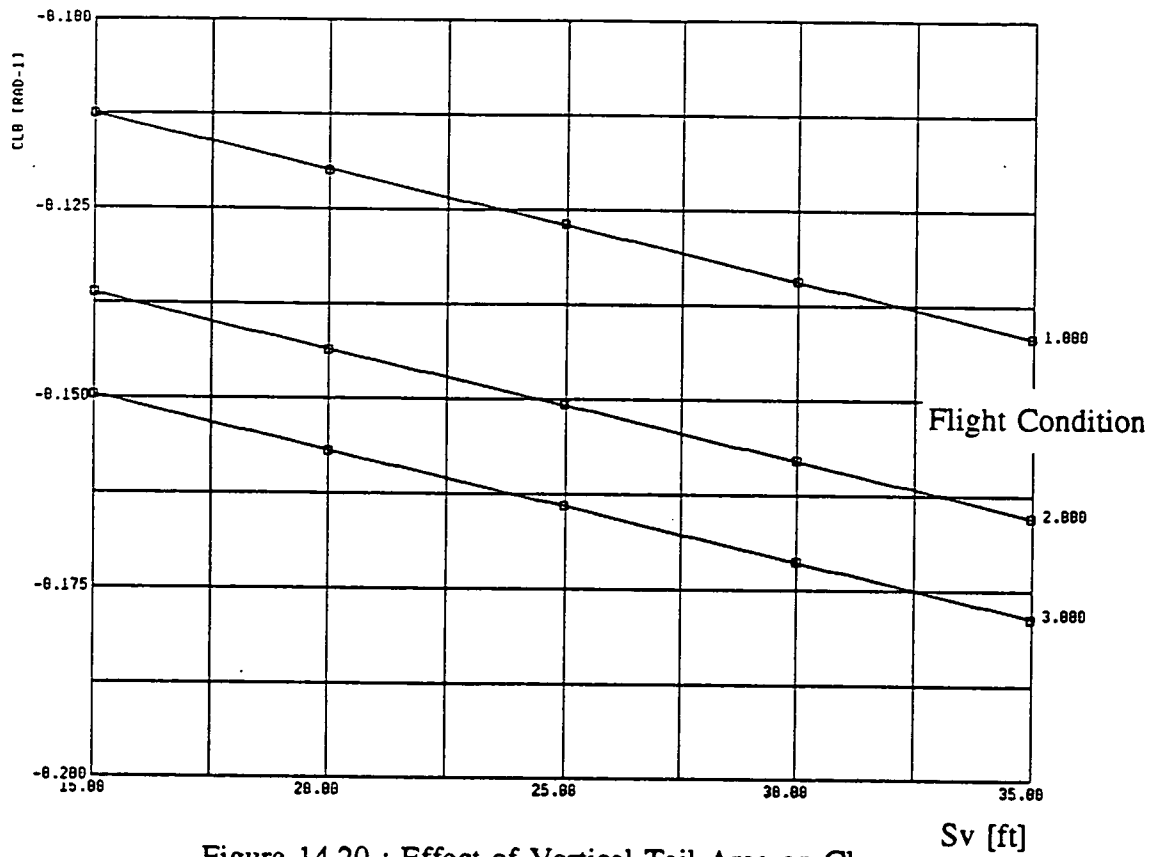
Figure 14.20 : Effect of Vertical Tail Area on Cl_β
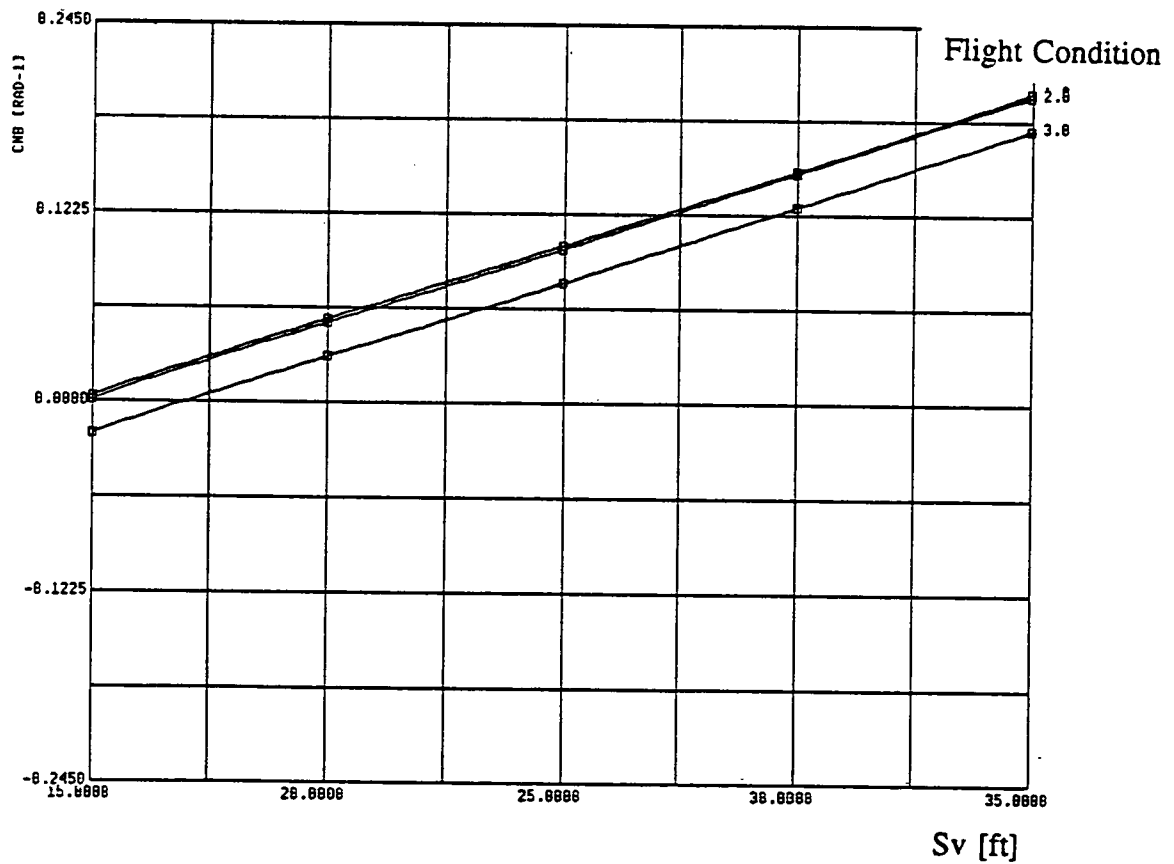
Figure 14.21 : Effect of Vertical Tail Area on Cn_β

159

14.5 CONCLUSIONS

To satisfy the level 1 handling quality requirements, conflicting requirements are met. Though the APT will still have some unsatisfying spiral characteristics (too stable) it is found that the dutch roll characteristics are satisfied when changing the wing dihedral to -2 degrees.

14.6 REFERENCES FOR CHAPTER 14

14.1   Roskam J., Airplane Flight Dynamics and Automatic Flight Control PART I, Roskam Aviation and Engineering Corporation, 1982.

14.2   Roskam J., Airplane Design PART VI, Preliminary Calculation of the Aerodynamic Thrust and Power Characteristics, Roskam Aviation and Engineering Corporation, 1989.

14.3   DAR Corparation, Advanced Aircraft Analysis (AAA), 120 East Ninth (second Floor West), Lawrence, KS 66044, USA, 1991.

15. PERFORMANCE

This Chapter will present the performance capabilities of the APT. The wing of the APT was re-sized in an attempt to increase the cruise speed and range of the airplane. Both of these quantities were found to be lacking in Reference 15.1. To further add to the performance problems the installed thrust has decreased from the levels in Reference 15.1. The loss of thrust has already been discussed in Chapter 6. Next a discussion of the mission capability with respect to the mission specification will be made.

15.1 WING RE-SIZING

As mentioned above, the performance characteristics of the airplane did not meet all of the mission requirements. To remedy this the wing was decreased in area. This was done to increase the wing loading and to reduce the drag contribution from the wing by having less wetted area. A spreadsheet program was used to calculate the drag from the wing. This allowed for quick iteration of wing area until the drag was reduced enough to permit the maximum cruise speed. The new wing area as a result of the calculations is:

$$S = 130 \text{ ft}^2$$

This corresponds to a take-off wing loading of 55.8 psf. This compares with a wing loading for the Piaggio P.180 of 62 psf and 51.3 psf for the Beech Starship.

15.2 MISSION CAPABILITY

The purpose of this section is to present the performance capabilities of the APT. This is done using the thrust data from Chapter 4 and the methods of References 15.2 and 15.3. The performance capabilities are compared with the mission specification defined in Reference 15.4. The requirements of the mission specification pertaining to performance are listed below in Table 15.1.

Table 15.1: Performance Constraints for the APT

Take-off field length (ft.)	2000 ft
Landing distance over 50 ft. obstacle (ft.)	2500 ft
Max. rate of climb ($^{ft}/_{min}$)	4000 $^{ft}/_{min}$
High speed cruise (kts.)	420 kts
Maximum range (nm)	1200 nm

The performance abilities of the APT will now be discussed.

TAKE-OFF:

From Table 15.1 it is seen that the APT needs to have a take-off ground run of 2000 feet. The actual distance required for take-off was calculated to be:

$$S_g = 1961 \text{ ft}$$

It is seen that the take-off distance requirements are met. This is with a maximum take-off lift coefficient of 2.0.

RATE OF CLIMB:

From Table 15.1 it is seen that the APT needs to have a maximum rate of climb of 4000 $^{ft}/_{min}$. The actual rate of climb that the APT is capable of is:

$$(RC)_{max} = 4000 \; (^{ft}/_{min})$$

It is seen that the rate of climb requirements are met.

CRUISE:

The APT is required to cruise at high speeds. The maximum level cruise speed is useful to know. Also, the speed for long range cruise is also helpful for mission planning. The performance calculations indicated that the APT has the following cruise speed capabilities:

$$V_{Cmax} = 415 \text{ kts. @ } 20000 \text{ ft}$$
$$V_{C \text{ max range}} = 310 \text{ kts @ } 40000 \text{ ft}$$

RANGE:

The maximum range for the APT is found using the long range cruise speed from above. The maximum range for the APT is:

$$R_{max} = 1300 \text{ nm}$$

Meeting the range requirement was possible because of two changes. First, the reduced wing area and increased wing loading resulted in higher values of $^L/_D$. Second, an increase in the amount of fuel carried was also necessary.

15.3 REFERENCES

15.1 Barrett, R., et al., <u>Preliminary Design of Two Configurations</u>, AE 621, Fall 1990, University of Kansas.

15.2 Roskam, J., Airplane Design Part VII: Determination of Stability, Control and Performance Characteristics: FAR and Military Requirements. Published by Roskam Aviation and Engineering Corp., Rt.4, Box 274, Ottawa, Kansas, 66067

15.3 Lan, E.T, and Roskam, J., Airplane Aerodynamics and Performance. Published by Roskam Aviation and Engineering Corp., Rt.4, Box 274, Ottawa, Kansas, 66067

15.4 Burgstahler, D. and Huffman, D. AE 621 Task Number 5: Mission Specification. Fall 1990.

16. COST ANALYSIS

The purpose of this chapter is to present the different cost components for the APT. The following cost components are estimated for the year 2000 :

- research, development, testing and evaluation cost
- manufacturing and acquisition cost
- direct and indirect operation cost
- life cycle cost
- disposal cost
- airplane estimated price

The **Research, Development, Testing and Evaluation Cost** (RDTE) consists of the following components:

- Airframe engineering and design cost : covers all expenses associated with the preliminary design and engineering work.
- Development support and testing cost : covers the cost of fixing problems found after the preliminary design and testing of the aircraft.
- Flight test aircraft cost : accounts for any special test and simulations that have to be performed for complex programs.
- Flight test operation cost
- Test and simulation facility cost
- RDTE profit
- RDTE financing cost

The **Manufacturing and Acquisition Cost** (C_ACQ) includes the following cost components:

- Airframe engineering and design
- Airplane program production cost
- Flight test operation cost
- Financing cost for manufacturing phase
- Manufacturing profit

The **Operating Cost** (C_OPS) includes the following items :

- Fuel and insurance cost
- Maintenance cost
- Depreciation cost
- Landing fees and taxes
- Financing cost

The **Life Cycle Cost** (LCC) includes the following items :

- This cost is the sum of the other costs.

The **Disposal** Cost (C_DISP) includes any cost made for disposal of materials and fluids of the APT.

Reference 16.1 provides labor fees, fudge factors, hardware prices and other parameters for the APT cost estimation for a fixed production of a total of 200 airplanes.

16.1 COST PER AIRCRAFT

The purpose of this section is to present the year 2000 cost parameters of the APT per aircraft produced. Dividing by the number of aircraft gives a reference on which comparisons can be developed.

Figure 16.1 shows how the relative RDTE cost per number of aircraft decreases with the more aircraft that are produced. However, it is during the RDTE phase that approximately 85% of the final design is determined. Obviously, this is probably the most critical phase of aircraft design since the final design predicated the associeated cost for the aircraft. Looking at Table 16.1, it is clear that the cumulative RDTE cost is constant no matter how many planes are produced.

Figure 16.1 also provides insight into how the relative C_ACQ and C_DISP decrase with the number of planes produced. Physically, this relates to the fact that once all of the equipment, methods, and management have been developed for the first plane it does not have to be done again, therefore, the relative C_ACQ is inversely proportional to the number of aircraft produced.
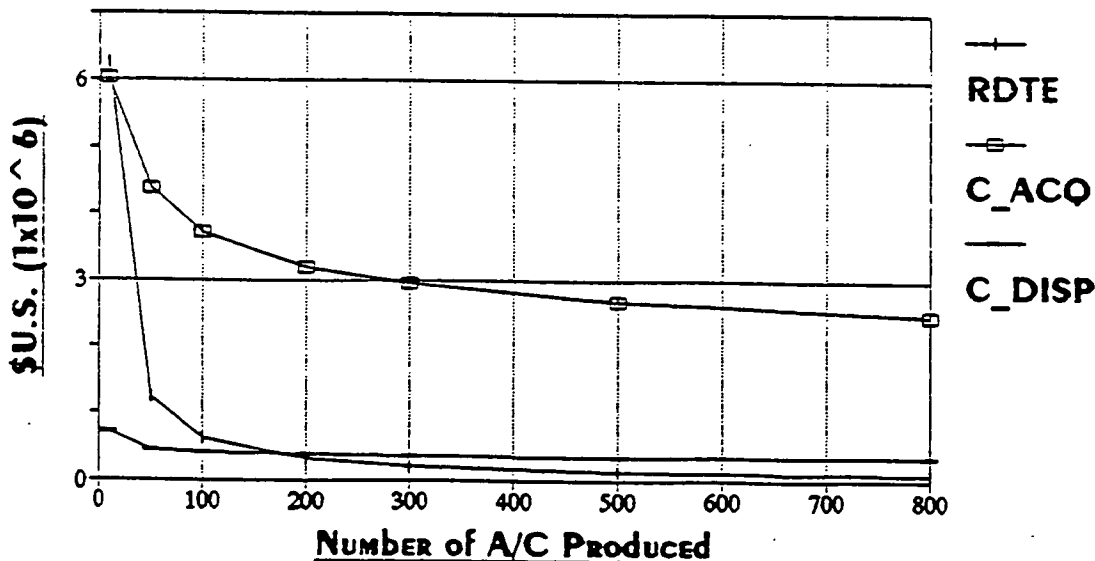
Figure 16.1: Program Cost Per Number of Aircraft

165

The data in Figure 16.2 shows how the Operating Cost, C_OPS, and Life Cycle Cost, LCC, decrease with the number of planes that are produced.

In all of the graphs, it is clear that if less than 100 APT aircrft are produced, then the cost will be extremely high. All of the cost parameters show a dramatic decrease within the first 100 planes produced. After 100 planes are produced the relative change in price is not so dramatic.

The Airplane Estimated Price (AEP), shown in Figure 16.3, supports the previous argument. From 10 to 100 planes the AEP decreases by eight million dollars. Clearly, if there is no a market for at least 100 APT aircraft it is unwise to produce even a single one because so much of the cost is already fixed by the time a single plane is produced. The AEP for a production run of 200 Advance Personal Transports is 3.516 million dollars.
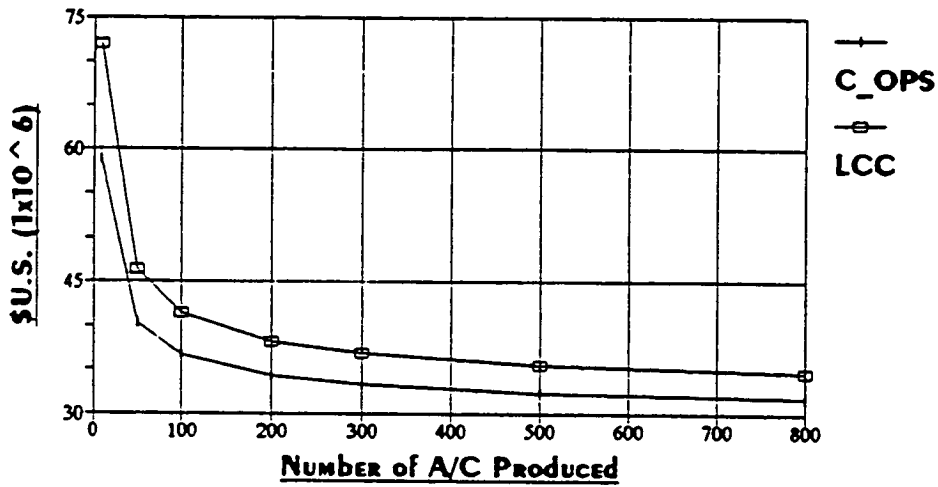
Figure 16.2: Program Cost Per Number of Aircraft
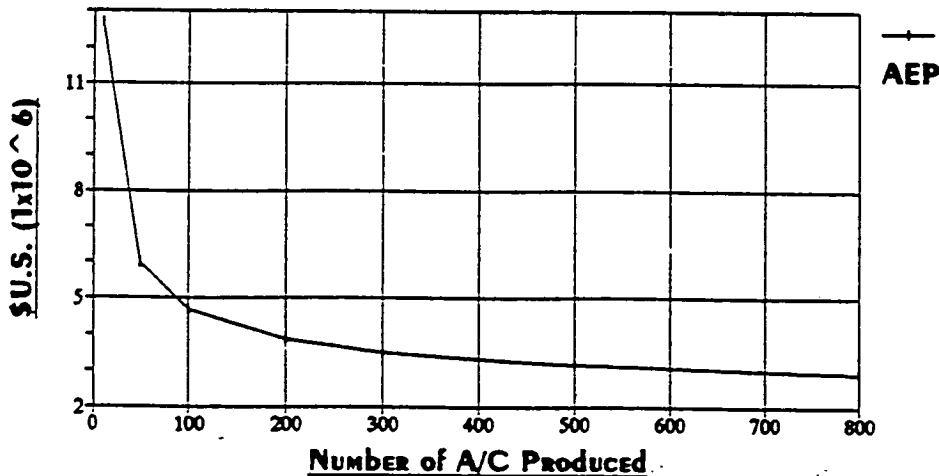
Figure 16.3: Airplane Estimated Price

16.2 CUMULATIVE COST

The purpose of this section is to present the cumulative cost parameters of the APT.

All of the cumulative cost parameters increased as the number of planes produced. Clearly, the more planes produced the greater the total cost. However, the RDTE cost remained constant since this money is spent regardless of how many planes are produced. The primary purpose for this information is to give an idea of just how expensive it is to produce a plane.

16.3 AVIONICS PRICE TRADE STUDY

The purpose of this section is to look at how a change in the base suite avionics price, from the assumed 1 million dollar price to 1.5 million, affects the outcome of the various cost parameters. The data for this study can be seen in Table 16.1, Airplane Cost Data.

Looking at the RDTE cost, one can see that the relative RDTE cost is slightly higher for the more costly avionics suite both for 200 and 500 aircraft. Physically this means that it takes a little more money to develop and test the more expensive, and one can assume, more advanced avionics package.

The acquisition, operating, disposal and life cycle cost all increased with the increased avionics price. An interpretation of this could be that as the avionics become more complex, it does not necessarily mean that less maintenance will be required. In the future, this will more than likely be the case. However, with today's technology this is not always true. Furthermore, since the avionics are more expensive and advanced it will cost more to acquire and dispose of the materials used in the avionics.

The airplane estimated price, AEP, shows an increase of about 300,000 dollars for the 500,000 dollars worth of extra avionics on board. One should not expect a dollar for dollar increase since putting more advanced avionics on the plane could reduce the cost in some areas, and increase the cost in other areas.

Cost/Number of Aircraft Produced $(x10^6)$ Avionics $1x10^6$						
#	RDTE	C_ACQ	C_OPS	C_DISP	LCC	AEP
10	6.2658	6.0349	58.9257	0.719	71.9459	12.68
50	1.25316	4.38198	40.2832	0.46382	46.3824	5.98
100	0.62658	3.728	36.701	0.41471	41.471	4.695
200	0.31329	3.203	34.357	0.38255	38.2555	3.855
300	0.20886	2.952	33.363	0.368927	36.89267	3.499
500	0.125316	2.68736	32.3892	0.355574	35.5574	3.15
800	0.078323	2.487313	31.69863	0.3451	34.61	2.903

Cumulative Cost for # of A/C Produced $(x10^6)$ Avionics $1x10^6$						
#	RDTE	C_ACQ	C_OPS	C_DISP	LCC	AEP
10	62.658	60.349	589.257	7.19	719.459	12.301
50	62.658	219.099	2014.16	23.191	2319.12	5.635
100	62.658	372.8	3670.1	41.471	4147.1	4.355
200	62.658	640.6	6871.4	76.51	7651.1	3.516
300	62.658	885.6	10008.9	110.678	11067.8	3.161
500	62.658	1343.68	16194.6	177.787	17778.7	2.813
800	62.658	1989.85	25358.9	276.08	27688	2.566

Cost/Number of Aircraft Produced $(x10^6)$ Avionics $1.5x10^6$						
#	RDTE	C_ACQ	C_OPS	C_DISP	LCC	AEP
200	0.317455	3.8499	36.178	0.40755	40.753	4.167
500	0.126982	3.3344	34.2036	0.380454	38.0454	3.461

16.4 REFERENCES FOR CHAPTER 16

16.1 Dirkzwager, A., Knipp, D., <u>Manufacturing Plan and Cost Analysis for the Advanced Personal Transport Pusher Configuration.</u> University of Kansas, May 1991.

17. CONCLUSIONS AND RECOMMENDATIONS

The following conclusions and recommendations are for both Phase I and Phase II design studies.

17.1 CONCLUSIONS

The Advanced Personal Transport will use a differential GPS with an INS interface to achieve CAT II approaches and zero visibility ground operations without use of ground based equipment.

Through the use of a heads up display unit and a multi-function touch-screen display, all other flight instrumentation can be excluded. It was determined that an IGG equipped airplane can lead to a 70% reduction in pilot workload.

The APT will have a fly-by-wire, decoupled response flight control system that will provide control system operations that should greatly improve flying qualities.

The airframe of the Advanced Personal Transport pusher configuration has been redesigned to reach the performance requirements stated in the mission specification. All of the performance requirements are satisfied. The primary requirements are listed below:

S_g = 1961 ft

RC_{max} = 4000 ft/min

V_{max_cruise} = 415 kts @ 20000 ft

$V_{max\_cruise\ range}$ = 310 kts @ 40000 ft

R_{max} = 1300 nm

The estimated airplane price of the APT is 3.52 million dollars.

The center of gravity travel of the APT is well within the expected limits of similar aircraft. Also, the calculated moments of inertia compare well with the values obtained using the radius of gyration method.

It was determined that if the wing dihedral is changed to -2°, Level 1 dutch roll handling characteristics are satisfied. This would, however, also create the spiral mode of the aircraft to be too stable.

An electro-impulse de-icing system will be used on the leading edge of the wing. A maintenance and repairability scheme was devised to keep surface tolerances within levels required for natural laminar flow. With the downsizing of the wing, there was determined to be inadequate room in the wing for all of the mission fuel required. Some fuel will then have to be stored in the tail booms.

The final three-view of the APT, which also displays the propulsion system integration, is shown in Figure 6.6.

17.2 RECOMMENDATIONS

The amount of laminar flow obtainable on the forward fuselage is still unknown. A more detailed analysis should be conducted using wind tunnel tests and computer panel codes to more accurately determine a fuselage shape that obtains as much laminar flow as practical.

The spiral mode of the aircraft needs to be altered to a more favorable, less stable, state. Further trade studies should be conducted to determine if this is possible.

Appendix A

Garrett TPE331-15/Twin Pac™ Performance Prediction Code Runs at Various Flight Conditions

This appendix will deliver the computer data generated for the prediction of the performance of the Garrett TPE331-15 engines as they are installed in the Soloy Twin-Pac™. This Twin-Pac™ was integrated into the fuselage of the Advanced Personal Transport (APT). Accordingly, the code included performance increments and decrements caused by installation, gearing, tip-losses, ducting, altitude and airspeed.

2184 Performance of Modified Hartzell HC-E5N-3L/L8218 on TPE-331-15 at Sea-Level

hpo = 2186 Theta = 1.00058 Delta = 1.0006
hp av. =

V (kts)	B	D (ft)	Pav (hp)	BSFC lbm/(hp-hr)	N (RPM)	T (°R)	Rho (sl/ft3)	CLi	AF	CP	J	EtaP at Cp, J	T (lbf)	T corr. (lbf)	Pav (hp)	mf lbm/hr
0	5	7.08	1858	0.510	1885	518.9	.0023780	0.53	154	0.777	0.549	0.265	2215	2508	1858	948
10	5	7.083	1858	0.510	1885	518.9	.0023780	0.533	154	0.777	0.589	0.28	2184	2346	1858	948
20	5	7.083	1859	0.510	1885	518.9	.0023780	0.533	154	0.778	0.631	0.292	2127	2149	1859	948
40	5	7.083	1862	0.510	1885	518.9	.0023780	0.533	154	0.779	0.722	0.341	2173	2194	1862	950
60	5	7.083	1867	0.510	1885	518.9	.0023780	0.533	154	0.781	0.824	0.398	2230	2252	1867	952
80	5	7.083	1874	0.510	1885	518.9	.0023780	0.533	154	0.784	0.933	0.465	2308	2331	1874	956
100	5	7.083	1884	0.510	1885	518.9	.0023780	0.533	154	0.788	1.05	0.509	2256	2279	1884	961
150	5	7.083	1916	0.510	1885	518.9	.0023780	0.533	154	0.802	1.366	0.657	2277	2300	1916	977
200	5	7.083	1962	0.510	1885	518.9	.0023780	0.533	154	0.821	1.518	0.718	2294	2317	1962	1001
250	5	7.083	2022	0.510	1885	518.9	.0023780	0.533	154	0.846	1.897	0.78	2055	2075	2022	1031
300	5	7.083	2097	0.510	1885	518.9	.0023780	0.533	154	0.877	2.277	0.812	1849	1867	2097	1070
350	5	7.083	2188	0.510	1885	518.9	.0023780	0.533	154	0.915	2.656	0.834	1698	1715	2188	1116
400	5	7.083	2297	0.510	1885	518.9	.0023780	0.533	154	0.961	3.036	0.805	1505	1520	2297	1171
410	5	7.083	2321	0.510	1885	518.9	.0023780	0.533	154	0.971	3.112	0.721	1329	1342	2321	1184

hpo =   1449   **2184** Performance of Modified Hartzell HC-E5N-3L/L8218 on TPE-331-15 at 10,000 ft.
hp av. = 1449   Theta = 0.93135   Delta = 0.6875

V (kts)	B	D (ft)	Pav (hp)	BSFC ɔm/(hp-hr)	N (RPM)	T (°R)	Rho (sl/ft3)	CLi	AF	CP	J	EtaP at Cp, J	T (lbf)	T corr. (lbf)	Pav (hp)	mf lbm/hr
0	5	7.08	1232	0.510	1885	483	.0017553	0.53	154	0.698	0.521	0.272	1590	1724	1232	628
10	5	7.083	1232	0.510	1885	483	.0017553	0.533	154	0.698	0.56	0.279	1517	1620	1232	628
20	5	7.083	1232	0.510	1885	483	.0017553	0.533	154	0.698	0.602	0.319	1613	1630	1232	629
40	5	7.083	1235	0.510	1885	483	.0017553	0.533	154	0.7	0.695	0.381	1673	1690	1235	630
60	5	7.083	1238	0.510	1885	483	.0017553	0.533	154	0.702	0.797	0.448	1720	1737	1238	631
80	5	7.083	1243	0.510	1885	483	.0017553	0.533	154	0.705	0.908	0.508	1718	1736	1243	634
100	5	7.083	1250	0.510	1885	483	.0017553	0.533	154	0.708	1.027	0.565	1700	1717	1250	637
150	5	7.083	1273	0.510	1885	483	.0017553	0.533	154	0.721	1.346	0.698	1631	1647	1273	649
200	5	7.083	1306	0.510	1885	483	.0017553	0.533	154	0.74	1.518	0.739	1571	1587	1306	666
250	5	7.083	1349	0.510	1885	483	.0017553	0.533	154	0.764	1.897	0.797	1400	1414	1349	688
300	5	7.083	1402	0.510	1885	483	.0017553	0.533	154	0.795	2.277	0.824	1254	1267	1402	715
350	5	7.083	1468	0.510	1885	483	.0017553	0.533	154	0.832	2.656	0.841	1149	1160	1468	749
400	5	7.083	1546	0.510	1885	483	.0017553	0.533	154	0.876	3.036	0.831	1046	1056	1546	788
410	5	7.083	1563	0.510	1885	483	.0017553	0.533	154	0.886	3.112	0.821	1019	1029	1563	797

hpo =
hp av. = 931.7

2184 Performance of Modified Hartzell HC-E5N-3L/L8218 on TPE-331-15 at 20,000 ft.

Theta = 0.86251 Delta = 0.4593

V (kts)	B	D (ft)	Pav (hp)	BSFC lbm/(hp-hr)	N (RPM)	T (°R)	Rho (sl/ft3)	CLi	AF	CP	J	EtaP at Cp, J	T (lbf)	T corr. (lbf)	Pav (hp)	mf lbm/hr
0	5	7.08	791.9	0.510	1885	447.3	.0012664	0.53	154	0.622	0.492	0.306	1219	1206	791.9	404
10	5	7.083	792	0.510	1885	447.3	.0012664	0.533	154	0.622	0.531	0.321	1183	1195	792	404
20	5	7.083	792.4	0.510	1885	447.3	.0012664	0.533	154	0.622	0.573	0.358	1223	1235	792.4	404
40	5	7.083	793.9	0.510	1885	447.3	.0012664	0.533	154	0.624	0.667	0.402	1183	1195	793.9	405
60	5	7.083	796.5	0.510	1885	447.3	.0012664	0.533	154	0.626	0.771	0.479	1224	1236	796.5	406
80	5	7.083	800	0.510	1885	447.3	.0012664	0.533	154	0.628	0.883	0.562	1258	1270	800	408
100	5	7.083	804.6	0.510	1885	447.3	.0012664	0.533	154	0.632	1.004	0.608	1205	1217	804.6	410
150	5	7.083	820.6	0.510	1885	447.3	.0012664	0.533	154	0.645	1.327	0.731	1117	1128	820.6	419
200	5	7.083	843.5	0.510	1885	447.3	.0012664	0.533	154	0.663	1.518	0.758	1041	1051	843.5	430
250	5	7.083	873.4	0.510	1885	447.3	.0012664	0.533	154	0.686	1.897	0.812	924	933	873.4	445
300	5	7.083	911	0.510	1885	447.3	.0012664	0.533	154	0.716	2.277	0.837	828	836	911	465
350	5	7.083	956.7	0.510	1885	447.3	.0012664	0.533	154	0.752	2.656	0.848	755	762	956.7	488
400	5	7.083	1011	0.510	1885	447.3	.0012664	0.533	154	0.794	3.036	0.842	693	700	1011	516
410	5	7.083	1023	0.510	1885	447.3	.0012664	0.533	154	0.804	3.112	0.836	680	686	1023	522

hpo =
hp av. = 577.7 Theta = 0.79387 Delta = 0.2969

2184 Performance of Modified Hartzell HC-E5N-3L/L8218 on TPE-331-15 at 30,000 ft.

V (kts)	B	D (ft)	Pav (hp)	BSFC om/(hp-hr)	N (RPM)	T (°R)	Rho (sl/ft3)	CLi	AF	CP	J	EtaP at Cp, J	T (lbf)	T corr. (lbf)	Pav (hp)	mf lbm/hr
0	5	7.08	491.1	0.510	1885	411.7	.0008893	0.53	154	0.549	0.462	0.302	794	767	491.1	250
10	5	7.083	491.1	0.510	1885	411.7	.0008893	0.533	154	0.549	0.501	0.346	838	802	491.1	250
20	5	7.083	491.4	0.510	1885	411.7	.0008893	0.533	154	0.55	0.544	0.362	808	816	491.4	251
40	5	7.083	492.4	0.510	1885	411.7	.0008893	0.533	154	0.551	0.639	0.429	818	826	492.4	251
60	5	7.083	494.1	0.510	1885	411.7	.0008893	0.533	154	0.553	0.744	0.503	826	834	494.1	252
80	5	7.083	496.5	0.510	1885	411.7	.0008893	0.533	154	0.555	0.858	0.569	813	822	496.5	253
100	5	7.083	499.6	0.510	1885	411.7	.0008893	0.533	154	0.559	0.98	0.648	816	824	499.6	255
150	5	7.083	510.4	0.510	1885	411.7	.0008893	0.533	154	0.571	1.308	0.742	716	723	510.4	260
200	5	7.083	525.8	0.510	1885	411.7	.0008893	0.533	154	0.588	1.518	0.784	671	678	525.8	268
250	5	7.083	546.1	0.510	1885	411.7	.0008893	0.533	154	0.611	1.897	0.824	586	592	546.1	279
300	5	7.083	571.6	0.510	1885	411.7	.0008893	0.533	154	0.639	2.277	0.846	525	530	571.6	292
350	5	7.083	602.7	0.510	1885	411.7	.0008893	0.533	154	0.674	2.656	0.854	479	484	602.7	307
400	5	7.083	640	0.510	1885	411.7	.0008893	0.533	154	0.716	3.036	0.842	439	443	640	326
410	5	7.083	648.2	0.510	1885	411.7	.0008893	0.533	154	0.725	3.112	0.825	425	429	648.2	331

hpo =
hp av. = 350.4   Theta = 0.75202   Delta = 0.185

2184 Performance of Modified Hartzell HC-E5N-3L/L8218 on TPE-331-15 at 40,000 ft.

V (kts)	B	D (ft)	Pav (hp)	BSFC ɔm/(hp-hr)	N (RPM)	T (°R)	Rho (sl/ft3)	CLi	AF	CP	J	EtaP at Cp, J	T (lbf)	T corr. (lbf)	Pav (hp)	mf lbm/hr
0	5	7.08	297.9	0.510	1885	390	.0005851	0.53	154	0.506	0.443	0.322	535	492	297.9	152
10	5	7.083	297.9	0.510	1885	390	.0005851	0.533	154	0.507	0.483	0.361	550	521	297.9	152
20	5	7.083	298.1	0.510	1885	390	.0005851	0.533	154	0.507	0.526	0.401	562	567	298.1	152
40	5	7.083	298.7	0.510	1885	390	.0005851	0.533	154	0.508	0.621	0.481	572	577	298.7	152
60	5	7.083	299.8	0.510	1885	390	.0005851	0.533	154	0.51	0.727	0.539	549	555	299.8	153
80	5	7.083	301.4	0.510	1885	390	.0005851	0.533	154	0.512	0.843	0.591	522	527	301.4	154
100	5	7.083	303.4	0.510	1885	390	.0005851	0.533	154	0.516	0.966	0.659	511	516	303.4	155
150	5	7.083	310.3	0.510	1885	390	.0005851	0.533	154	0.528	1.296	0.758	448	453	310.3	158
200	5	7.083	320.2	0.510	1885	390	.0005851	0.533	154	0.544	1.518	0.794	414	418	320.2	163
250	5	7.083	333.2	0.510	1885	390	.0005851	0.533	154	0.567	1.897	0.831	361	364	333.2	170
300	5	7.083	349.6	0.510	1885	390	.0005851	0.533	154	0.594	2.277	0.85	323	326	349.6	178
350	5	7.083	369.6	0.510	1885	390	.0005851	0.533	154	0.628	2.656	0.857	295	298	369.6	189
400	5	7.083	393.7	0.510	1885	390	.0005851	0.533	154	0.669	3.036	0.851	273	276	393.7	201
410	5	7.083	399	0.510	1885	390	.0005851	0.533	154	0.678	3.112	0.831	263	266	399	204

A-5

622 Pro, Thrust Data

	mf 20,000 ft	T Corr.	Pav 30,000 ft	mf 30,000 ft	T Corr.	Pav 40,000 ft	mf 40,000 ft
1	404.000	767.000	491.100	250.000	492.000	297.900	152.000
2	404.000	802.000	491.100	250.000	521.000	297.900	152.000
3	404.000	816.000	491.400	251.000	567.000	298.100	152.000
4	405.000	826.000	492.400	251.000	577.000	298.700	152.000
5	406.000	834.000	494.100	252.000	555.000	299.800	153.000
6	408.000	822.000	496.500	253.000	527.000	301.400	154.000
7	410.000	824.000	499.600	255.000	516.000	303.400	155.000
8	419.000	723.000	510.400	260.000	453.000	310.300	158.000
9	430.000	678.000	525.800	268.000	418.000	320.200	163.000
10	445.000	592.000	546.100	279.000	364.000	333.200	170.000
11	465.000	530.000	571.600	292.000	326.000	349.600	178.000
12	488.000	484.000	602.700	307.000	298.000	369.600	189.000
13	516.000	443.000	640.000	326.000	276.000	393.700	201.000
14	522.000	429.000	648.200	331.000	266.000	399.000	204.000

ERRT 2/15/91   PROPULSION   AFT FUSLEE

622 Prop hrust Data

Tue, Feb 5, /91 8:53 PM

	Velocity (kts)	T Corr. S.L.	P av S.L.	mf S.L.	T Corr. 10,000 ft	Pav 10,000 ft	mf 10,000 ft	T Corr. 20,000	Pav 20,000 ft
1	0.000	2508.000	1858.000	948.000	1724.000	1232.000	628.000	1206.000	791.900
2	10.000	2346.000	1858.000	948.000	1620.000	1232.000	628.000	1195.000	792.000
3	20.000	2149.000	1859.000	948.000	1630.000	1232.000	629.000	1235.000	792.400
4	40.000	2194.000	1862.000	950.000	1690.000	1235.000	630.000	1195.000	793.900
5	60.000	2252.000	1867.000	952.000	1737.000	1238.000	631.000	1236.000	796.500
6	80.000	2304.000	1874.000	956.000	1736.000	1243.000	634.000	1270.000	800.000
7	100.000	2308.000	1884.000	961.000	1717.000	1250.000	637.000	1217.000	804.600
8	150.000	2300.000	1916.000	977.000	1647.000	1273.000	649.000	1128.000	820.600
9	200.000	2190.000	1962.000	1001.000	1587.000	1306.000	666.000	1051.000	843.500
10	250.000	2075.000	2022.000	1031.000	1414.000	1349.000	688.000	933.000	873.400
11	300.000	1867.000	2097.000	1070.000	1267.000	1402.000	715.000	836.000	911.000
12	350.000	1715.000	2188.000	1116.000	1160.000	1468.000	749.000	762.000	956.700
13	400.000	1520.000	2297.000	1171.000	1056.000	1546.000	788.000	700.000	1011.000
14	410.000	1342.000	2321.000	1184.000	1029.000	1563.000	797.000	686.000	1023.000
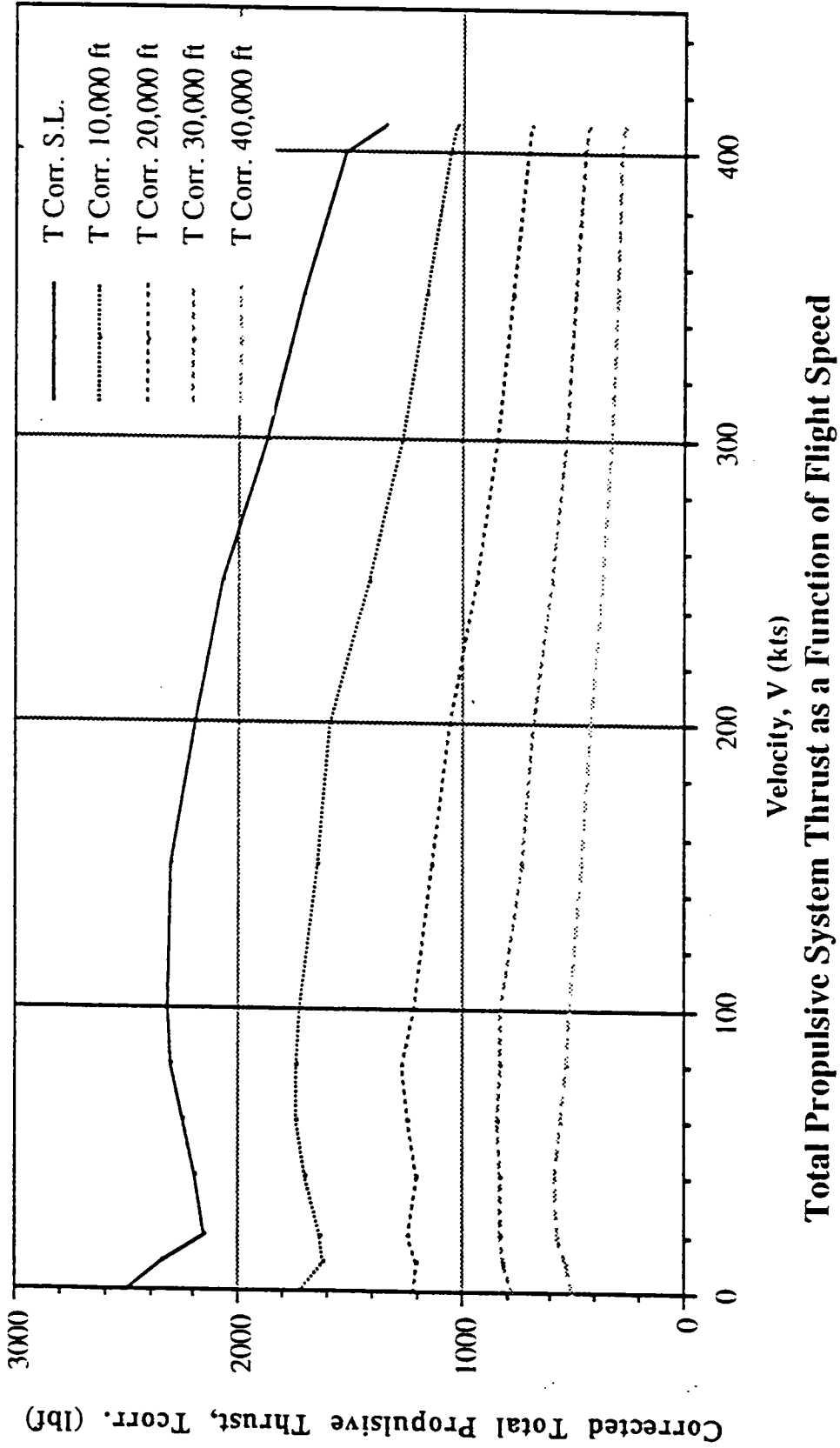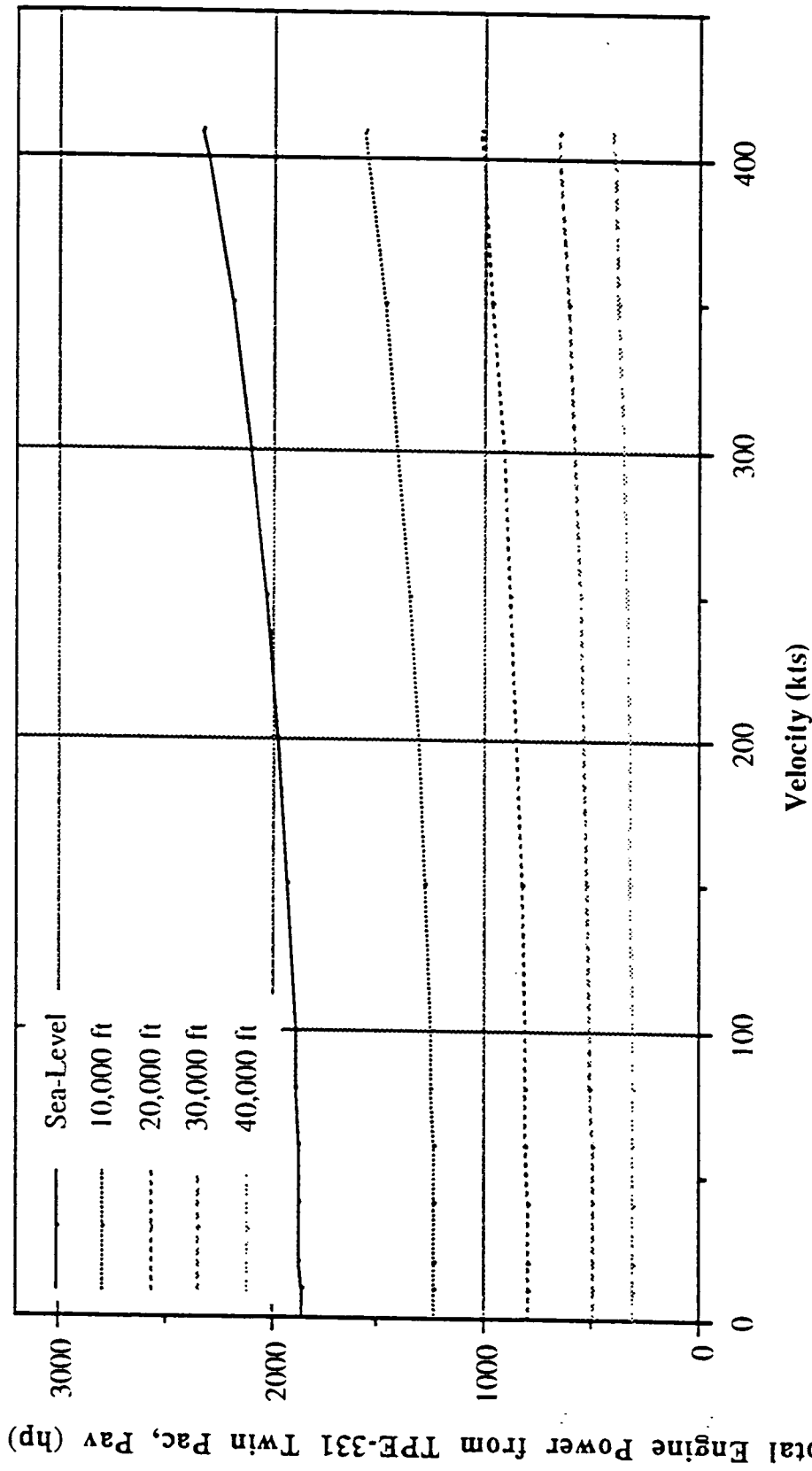
A-7

Total Propulsive System Thrust as a Function of Flight Speed

Velocity, V (kts)

Corrected Total Propulsive Thrust, Tcorr. (lbf)

Legend:
- T Corr. S.L.
- T Corr. 10,000 ft
- T Corr. 20,000 ft
- T Corr. 30,000 ft
- T Corr. 40,000 ft

Total Propulsive System Power as a Function of Flight Speed

A-9

Total Fuel Consumption as a Function of Flight Speed

Velocity (kts)

Total Fuel Flow Rate to Both Engines, mf (lbm/hr)

Legend:
- Sea-Level
- 10,000 ft
- 20,000 ft
- 30,000 ft
- 40,000 ft

182

A-10
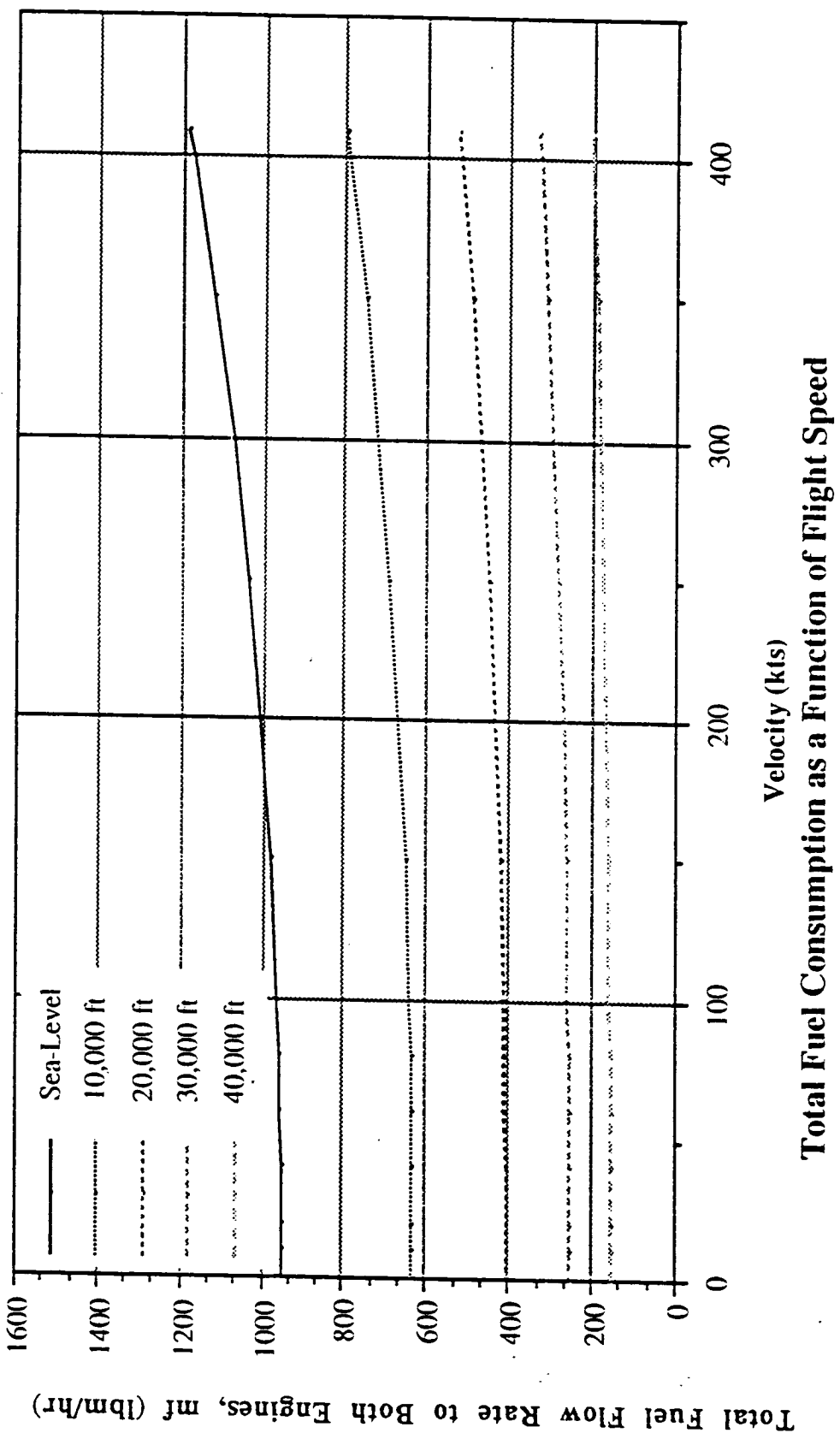
Appendix B

APT Fuel Volume Calculation

The purpose of this section is to present the calculated APT fuel volume.

APT Pusher Fuel Volume Calculation				
Span Loc (inches)	Y1 (inches)	Y2 (inches)	Chord (feet)	Fuel Vol (feet ^ 3)
0	43.92	53.65	8.130833	0
6	40.15521	52.67972	7.736245	1.068313 **
12	36.39043	51.70944	7.341656	1.924227
18	32.62564	50.73917	6.947067	1.722944
24	28.86085	49.76889	6.552479	1.532779
30	25.09607	48.79861	6.15789	1.35373
36	21.33128	47.82833	5.763301	1.185798
42	17.56649	46.85806	5.368712	1.028984
48	13.80171	45.88778	4.974124	0.883286
54	10.03692	44.9175	4.579535	0.748705
60	6.272134	43.94722	4.184946	0.625242
66	2.507348	42.97694	3.790358	0.512895
72	0	42.00667	3.500556	0.437464
78	0	41.03639	3.419699	0.417488
84	0	40.06611	3.338843	0.397979
90	0	39.09583	3.257986	0.378937
96	0	38.12556	3.17713	0.360361
102	0	37.15528	3.096273	0.342253
108	0	36.185	3.015417	0.324611
114	0	35.21472	2.93456	0.307436
120	0	34.24444	2.853704	0.290727
126	0	33.27417	2.772847	0.274486
132	0	32.30389	2.691991	0.258711
138	0	31.33361	2.611134	0.243403
144	0	30.36333	2.530278	0.228562
150	0	29.39306	2.449421	0.214188
156	0	28.42278	2.368565	0.200281
162	0	27.4525	2.287708	0.18684
168	0	26.48222	2.206852	0.173866
174	0	25.51194	2.125995	0.161359
180	0	24.54167	2.045139	0.149319
186	0	23.57139	1.964282	0.137745
192	0	22.60111	1.883426	0.126638
198	0	21.63083	1.802569	0.115998
204	0	20.66056	1.721713	0.105825
210	0	19.69028	1.640856	0.096119
216	0	18.72	1.56	0.08688
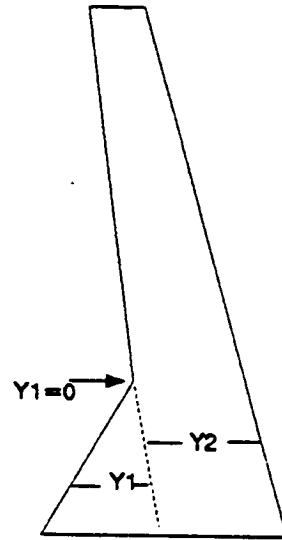
Equation Summary

Fuel Volume =
$(.70c-.105c)*.(13-.01)c*(dspan/12)$

$t/c = .13$

$Y1 = 3.66' - (spanloc/5.833')/3.66'$
for $0 < Span\_loc < 5.833'$

$Y2 = 4.4712' - ((4.4712'-1.56')/18')*sp\_loc$
for $0 < Sp\_loc < 18'$

** 3" taken from span location to
account inboard spar location -
fuselage attachment

Total Fuel Volume Both Wings (ft ^ 3)

32.53125

.15b for lightning strike
.9 scaling factor for pumps/bays/ribs

APPENDIX C: WEIGHT AND BALANCE SPREADSHEET

This Appendix contains the spreadsheet used to determine the component weights for the APT. It is a spreadsheet developed for General Aviation airplanes. It also calculates the center of gravity of the airplane as well as the moments of inertia.

CLASS II WEIGHT AND BALANCE SPREADSHEET FOR GENERAL AVIATION

Written by: Ed Wenninger
Revision: 5/10/91
Current data: APT Pusher Configuration

LIST OF RESULTS

WE =	4286	pounds	WTO =	7264	pounds
Xcg WE =	246.1	inches	Xcg WTO =	244.6	inches
Ycg WE =	0.0	inches	Ycg WTO =	0.0	inches
Zcg WE =	73.1	inches	Zcg WTO =	75.6	inches
Ixx TO =	4553	slug-ft^2	Izz TO =	11205	slug-ft^2
Iyy TO =	8722	slug-ft^2	Ixz TO =	809	slug-ft^2

REQUIRED INPUT DATA AND GEOMETRY

WING TERMS
- Sw = 130
- ARw = 10.03
- b = 36.11
- 0.5c Sweep = 17.5
- 0.25c Sweep = 14.51
- lambda wing = 0.2766
- GW guess = 7264
- n_ult = 5.3
- trw = 0.71
- t/c max = 0.13
- VH = 224.5
- We guess = 4286

CANARD TERMS
- Sc = 19.7
- ARc = 7
- bc = 11.8
- 0.5c Sweep = 0
- trc = 0.2
- 0.25c Sweep = 0
- lambda = 0.7
- t/c max = 0.1

LANDING GEAR TERMS
- lsm = 6
- lsn = 3

HORIZ. TAIL
- S_h = 32.9
- b_h = 12.2
- trh = 0.24
- lh = 16.8
- M.A.C. h = 2.64
- 0.5c Sweep = 0
- VD = 250

TECH FACTORS:
- Wing 0.95
- Fuselage 0.9
- Horizontal tail 0.85
- Vertical tail 0.85
- Canard 0.8

FUSELAGE TERMS:
- lf = 27.3
- hf = 5.3
- wf = 5
- VC = 202.1
- Sfgs = 353.7
- h - boom = 0.83
- w - boom = 0.75
- S - boom = 26.9
- L-boom = 20
- N row = 3

VERTICAL TAIL TERMS
- Sv = 20.2
- 0.5c Sweep = 15
- bv = 5
- trv = 0.44
- # of surfaces = 2

MISCELEANEOUS TERMS:
- Mff = 0.728
- Np = 1
- Nbl = 5
- Dp = 6.7
- PTO = 700
- Ne = 2
- Nt = 2
- Wtfo = 35
- Npax = 6
- MD = 0.7
- lcabin = 13.8
- (W/S) max = 43
- q bar dive = 211.7

INLET TERMS:
- Ninl = 2
- Ld = 4
- Ainl = 2

ESTIMATE STRUCTURAL WEIGHT

COMPONENT:	USAF	Torenbeek	AVERAGE	Avg*Tech	Wgt. Fraction
Wing	489	482	485	461	0.063
Canard	152	144	148	119	0.016
Horizontal tail	74	54	64	54	0.007
Vertical tail	55	60	58	49	0.007
Fuselage	512	561	536	483	0.066
Tail booms	97	113	105	94	0.013
Landing gear	256	276	266	266	0.037
		Estimated main gear weight:		186	0.026
		Estimated nose gear weight:		80	0.011

Wstr = 1526 pounds   Wstr/Wto = 0.247

ESTIMATION OF PROPULSION SYSTEM WEIGHTS

COMPONENT:	METHOD 1:	METHOD 2:	AVERAGE	VALUE USED	Wgt. Fraction
Engine	430	-	430	860	0.118
Air induction sys.	84		84	84	0.012
Fuel system	158	199	179	179	0.025
Propeller	117	151	134	134	0.018
Prop. Controls	2		2	2	0.000
Engine start	34		34	34	0.005
Engine controls	64		64	64	0.009
Prop gearbox	150	-	150	150	0.021

Wprop. = 1506 pounds   Wprop/Wto = 0.207

ESTIMATE FIXED EQUIPMENT WEIGHT

COMPONENT:	METHOD 1:	METHOD 2:	AVERAGE	VALUE USED	Wgt. Fraction
Flight Controls	279	270	274	220	0.030
Elect. System	257	195	226	316	0.044
Hydraulic System	N.A.	N.A.	N.A.		0.000
Instr. & Avionics	198	98	148	192	0.026
A/C & Anti-ice	217	194	206	206	0.028
Oxygen System	25	37	31	31	0.004
Furnishings	248	158	203	203	0.028
Aux. Gear	43	-	43	43	0.006
Paint	44		44	44	0.006
Ballast	0	-	0	0	0.000

Wfe = 1254 pounds   Wfe/Wto = 0.173

ENTER PASSENGER, BAGGAGE, AND FUEL WEIGHTS

ITEM	WEIGHT	QUANTITY	TOTAL WEIGHT		
Pass. group 1	175	1	175		
Pass. group 2	175	2	350	Pax. Total =	875
Pass. group 3	175	2	350		
Pass. group 4	0	2	0		
Baggage 1	30	4	120		
Baggage 2	30	2	60	Baggage Total=	180
Baggage 3	0		0	Wpayload =	1055
Fuel Tank 1	1923	1	1923		
Fuel Tank 2	0	1	0	Wfuel =	1923
Fuel Tank 3	0	1	0		
Fuel Tank 4	0	1	0		

188

Component	X (F.S) in.	Y (B.L.) in.	Z (W.L.) in.	X - Moment	Y - Moment	Z - Moment
Flight Controls	180.0	0.0	65.0	39518.8	0.0	14270.7
Elcet. System	150.0	0.0	65.0	47420.3	0.0	20548.8
Hydraulic Sys.	0.0	0.0	0.0	0.0	0.0	0.0
Instr & Avionics	90.0	0.0	70.0	17322.7	0.0	13473.2
A/C & Press.	200.0	0.0	70.0	41109.6	0.0	14388.4
Oxygen System	140.0	0.0	60.0	4327.7	0.0	1854.7
Furnishings	180.0	0.0	70.0	36517.1	0.0	14201.1
Aux. Gear	80.0	0.0	60.0	3429.1	0.0	2571.8
Paint	255.0	0.0	80.0	11114.4	0.0	3486.9
Ballast	0.0	0.0	0.0	0.0	0.0	0.0

Xcg FE = 160.1 inches
Ycg FE = 0.0 inches
Zcg FE = 67.6 inches

Component	X (F.S) in.	Y (B.L.) in.	Z (W.L.) in.	X - Moment	Y - Moment	Z - Moment
Fuselage	195.0	0.0	72.0	94140.0	0.0	34759.4
Tail Booms	360.0	0.0	82.0	33971.7	0.0	7738.0
Wing	260.0	0.0	85.0	119916.1	0.0	39203.3
Canard	70.0	0.0	47.0	8304.8	0.0	5576.1
Horizontal Tail	440.0	0.0	135.0	23784.2	0.0	7297.4
Vertical Tail	425.0	0.0	105.0	20785.9	0.0	5135.3
Main Gear	275.0	0.0	35.0	51270.1	0.0	6525.3
Nose Gear	98.0	0.0	35.0	7830.3	0.0	2796.5
Engines	328.0	0.0	75.0	282080.0	0.0	64500.0
Air Induct. Sys.	290.0	0.0	65.0	24232.4	0.0	5431.4
Fuel System	280.0	0.0	82.0	50004.4	0.0	14644.1
Propeller	386.0	0.0	87.0	51559.0	0.0	11620.8
Prop. Controls	180.0	0.0	70.0	408.2	0.0	158.7
Engine Start	335.0	0.0	90.0	11355.3	0.0	3050.7
Engine Control	180.0	0.0	70.0	11560.2	0.0	4495.6
Prop. Gearbox	355.0	0.0	85.0	53250.0	0.0	12750.0
Trapped fuel/oil	280.0	0.0	82.0	9800.0	0.0	2870.0
Fixed Equip.	160.1	0.0	67.6	200759.6	0.0	84795.5
Pass. group 1	158.0	0.0	70.0	27650.0	0.0	12250.0
Pass. group 2	187.0	0.0	70.0	65450.0	0.0	24500.0
Pass. group 3	240.0	0.0	70.0	84000.0	0.0	24500.0
Pass. group 4	0.0	0.0	0.0	0.0	0.0	0.0
Baggage grp. 1	258.0	0.0	61.0	30960.0	0.0	7320.0
Baggage grp. 2	172.0	0.0	63.0	10320.0	0.0	3780.0
Baggage grp. 3	0.0	0.0	0.0	0.0	0.0	0.0
Fuel Tank 1	262.0	0.0	85.0	503826.0	0.0	163455.0
Fuel Tank 2	0.0	0.0	0.0	0.0	0.0	0.0
Fuel Tank 3	0.0	0.0	0.0	0.0	0.0	0.0
Fuel Tank 4	0.0	0.0	0.0	0.0	0.0	0.0

Component	Mass (slug)	Ixx (s - ft^2)	Iyy (s - ft^2)	Izz (s - ft^2)	Ixz (s - ft^2)
Fuselage	15.0	1.3	258.2	256.9	18.6
Tail Booms	2.9	115.4	271.9	271.0	15.0
Wing	14.3	8.8	32.3	23.5	14.4
Canard	3.7	20.9	802.1	781.2	127.9
Horizontal Tail	1.7	41.2	486.5	445.3	135.4
Vertical Tail	1.5	9.1	352.5	343.4	56.0
Main Gear	5.8	118.5	103.4	37.1	-49.6
Nose Gear	2.5	28.4	399.4	370.9	102.7
Engines	26.7	0.1	1289.8	1289.7	-9.2
Air Induct. Sys.	2.6	2.0	39.1	37.1	-8.7
Fuel System	5.6	1.6	49.8	48.2	8.7
Propeller	4.2	3.8	579.8	576.1	46.5
Prop. Controls	0.1	0.0	2.1	2.0	0.2
Engine Start	1.1	1.5	61.2	59.7	9.5
Engine Control	2.0	0.4	58.4	57.9	5.0
Prop. Gearbox	4.7	2.9	397.2	394.3	33.6
Trapped fuel/oil	1.1	0.3	9.8	9.4	1.7
Fixed Equip.	39.0	17.2	1952.1	1934.9	182.5
Pass. group 1	5.4	1.2	284.8	283.6	18.3
Pass. group 2	10.9	2.4	253.5	251.1	24.4
Pass. group 3	10.9	2.4	4.0	1.6	2.0
Pass. group 4	0.0	0.0	0.0	0.0	0.0
Baggage grp. 1	3.7	5.5	10.1	4.6	-5.0
Baggage grp. 2	1.9	2.1	70.4	68.4	11.9
Baggage grp. 3	0.0	0.0	0.0	0.0	0.0
Fuel Tank 1	59.8	36.7	161.7	125.0	67.7
Fuel Tank 2	0.0	0.0	0.0	0.0	0.0
Fuel Tank 3	0.0	0.0	0.0	0.0	0.0
Fuel Tank 4	0.0	0.0	0.0	0.0	0.0

Component	Avg. length	Avg. hgt.	Avg. Width	Ixx (s-ft^2)	Iyy (s-ft^2)	Izz (s-ft^2)
Fuselage	327	52	52	70	700	700
Wing	60	7	533	2546	22	1768
Engine	37	21	40	19	17	24
Fuel 1	45	5	200	1494	53	1039
Fuel 2	0	0	0	0	0	0
Fuel 3	0	0	0	0	0	0
Fuel 4	0	0	0	0	0	0

Loading Seq.	We + ΣWi	X moment	Xcg (in.)	Z moment	Zcg (in.)
Fuel Tank 1	6209.3396	1558838.22	251.047344		
Pass. group 1	6384.3396	1586488.22	248.49684		
Pass. group 2	6734.3396	1651938.22	245.3007		
Pass. group 3	7084.3396	1735938.22	245.03882		
Baggage 1	7204.3396	1766898.22	245.25471		
Baggage 2	7264.3396	1777218.22	244.64966		
Fuel Tank 1	6209.3396	1558838.22	251.047344		
Pass. group 1	6384.3396	1586488.22	248.49684		
Pass. group 2	6734.3396	1651938.22	245.3007		
Pass. group 3	7084.3396	1735938.22	245.03882		
Baggage 2	7144.3396	1746258.22	244.425421		
Baggage 1	7264.3396	1777218.22	244.64966		
Fuel Tank 1	6209.3396	1558838.22	251.047344		
Baggage 1	6329.3396	1589798.22	251.179162		
Pass. group 3	6679.3396	1673798.22	250.593369		
Pass. group 2	7029.3396	1739248.22	247.426972		
Pass. group 1	7204.3396	1766898.22	245.25471		
Baggage 2	7264.3396	1777218.22	244.64966		

Unloading	Wto - ΣWi	X moment	Xcg (in.)	Z moment	Zcg (in.)
Fuel Tank 1					
Pass. group 1					
Pass. group 2					
Pass. group 3					
Baggage 1					
Baggage 2					
Fuel Tank 1	5341.3396	1273392.22	238.403156		
Baggage 1	5221.3396	1242432.22	237.952769		
Pass. group 3	4871.3396	1158432.22	237.805678		
Pass. group 2	4521.3396	1092982.22	241.73858		
Pass. group 1	4346.3396	1065332.22	245.110211		
Baggage 2	4286.3396	1055012.22	246.133604		
Fuel Tank 1					
Pass. group 1					
Pass. group 3					
Pass. group 2					
Baggage 2					
Baggage 1					

191